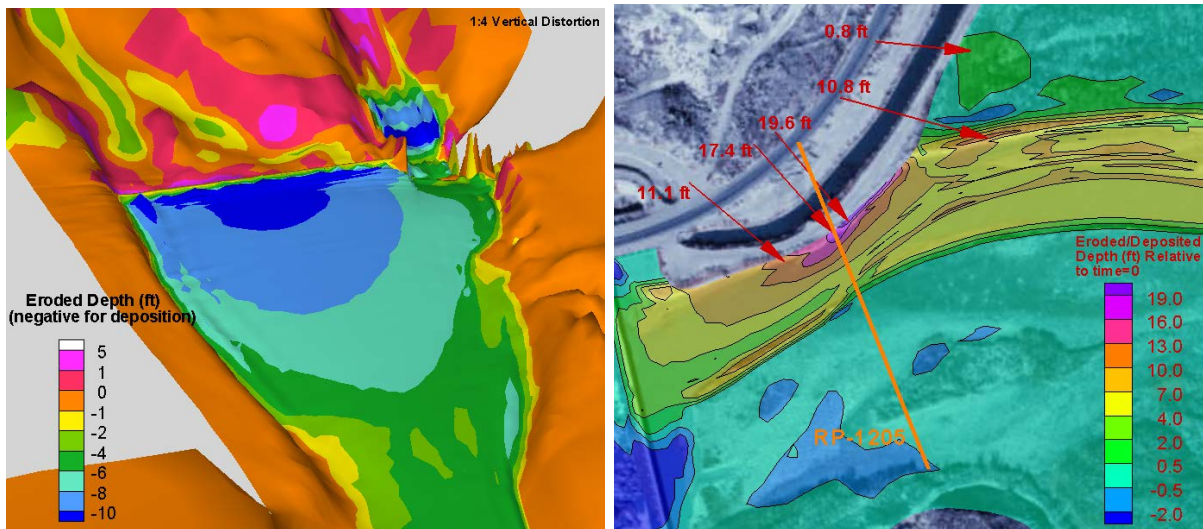




— BUREAU OF —
RECLAMATION

SRH-2D User's Manual: Sediment Transport and Mobile-Bed Modeling



Mission Statements

The Department of the Interior (DOI) conserves and manages the Nation's natural resources and cultural heritage for the benefit and enjoyment of the American people, provides scientific and other information about natural resources and natural hazards to address societal challenges and create opportunities for the American people, and honors the Nation's trust responsibilities or special commitments to American Indians, Alaska Natives, and affiliated island communities to help them prosper.

The mission of the Bureau of Reclamation is to manage, develop, and protect water and related resources in an environmentally and economically sound manner in the interest of the American public.

Acknowledgments

Many internal and external engineers and scientists have made contributions to the review and testing of the SRH-2D version 3 model. Their efforts have greatly enhanced the quality of the work documented here. It is acknowledged that David Gaeuman at the Trinity River Division, Yurok Tribe Fisheries Department, has contributed to Section 8.2 along with a peer review of the document. Deena Larsen at the Technical Service Center, Bureau of Reclamation, has edited and formatted the document.

The sediment module development reported has been funded through many Reclamation projects. Additional funding sources include the Reclamation's Science and Technology Program and Taiwan Water Resources Agency under the Technical Assistance Cooperation Agreement.

Disclaimer

No warranty is expressed or implied regarding the usefulness or completeness of the information contained in this report. References to commercial products do not imply endorsement by the Bureau of Reclamation and may not be used for advertising or promotional purposes.

SRH-2D User's Manual: Sediment Transport and Mobile-Bed Modeling

Prepared by:

**Yong G. Lai, Ph.D., Project Management
Technical Service Center**

Reviewed by:

**David Gaeuman, Ph.D.
Yurok Tribe Fisheries Department
Trinity River Division**

Cover Photo: Screenshot of SRH-2D model results (Reclamation).

Acronyms and Abbreviations

°C	degrees Celsius
1D	one-dimensional
2D	two-dimensional
2DM	2D generic Mesh
AAO	Albuquerque Area Office
ADCP	Acoustic Doppler Current Profiler
DEM	Digital Elevation Model
DHL	Delft Hydraulics Laboratory
DIP	dynamic input
EB-26	channel cross line used specifically for Rio Grande, AAO Office.
ID	Identification
EH	Engelund-Hansen
GEC	Gathard Engineering Consulting
HEC-RAS	Hydrologic Engineering Center's River Analysis System
LiDAR	light ranging and detection
MPM	Meyer-Peter-Muller
NID	National Inventory of Dams
PWA	Phillip Williams and Associates, Ltd.
Q_and_A	question and answer
Reclamation	Bureau of Reclamation
RM	river mile
RP-1205	channel cross line used specifically for Rio Grande
RST	restart
SI	International System of Units
SMS	Surface-Water Modeling System
SOF	Script Output File
SRH-2D	Sedimentation and River Hydraulics – Two-Dimensions
SRHGEOM	Sedimentation and River Hydraulics Geometric Mesh
USGS	U.S. Geological Survey

Measurements

cm	centimeter
ft/ft	foot per foot
ft/day	feet per day
g/L	grams per liter
kg/m ² /hr	kilograms per square meter per hour
kg/m ³	kilograms per cubic meter
lb/ft ²	pounds per square foot
lb/ft ² /hr	pounds per square feet per hour
lb/ft ³	pounds per cubic foot
lbm	pound mass
l/s	liters per second
m	meter
mg/L	milligrams per liter
m/s	meters per second
m ³	cubic meter
m ³ /s	cubic meters per second
mm	millimeter
mm/s	millimeters per second
N/m ²	newtons per square meter
Pa	pascal
ppm	parts per million
yd ³	cubic yards

Contents

Acronyms and Abbreviations	v
Measurements	vi
Contents	vii
Summary	1
Chapter 1. Introduction.....	3
1.1. Software and Hardware Requirement.....	3
1.2. SRH-2D Package	4
1.3. About the Mobile-Bed Module.....	4
1.4. Limitations	5
1.5. Disclaimer	6
Chapter 2. Pre-Processing with Partial-Interface Mode.....	7
2.1. General Inputs.....	7
2.2. Bed Layer Properties	16
Chapter 3. Tutorial Cases	19
3.1. Non-Cohesive Sediment Degradation Modeling	19
3.1.1. Model Domain, Mesh, and Model Inputs.....	19
3.1.2. Running SRH-2D Preprocessor.....	19
3.1.3. Pre-Processing Summary.....	25
3.2. Cohesive Sediment Modeling of Rio Grande	27
3.2.1. Model Domain, Mesh and Other Conditions	27
3.2.2. Running the SRH-2D Preprocessor.....	28
3.2.3. Pre-Processing Summary.....	36
3.2.4. Flow-Only Simulation Option	39
3.2.5. Mobile-Bed Simulation.....	40
3.2.6. Results	42
Chapter 4. Mathematical Equations.....	45
4.1. Flow Equations.....	45
4.1.1. Flow Solver.....	45
4.1.2. Bed Stresses.....	46
4.1.3. Turbulence Model.....	46
4.2. Shear Stress Partition.....	46
4.3. Representation of Vertical Layers	48
4.4. Sediment Transport Equations.....	49
4.4.1. Introduction.....	49
4.4.2. Variable-Load Equation.....	50
4.4.3. Sediment Transport Mode Parameter	51
4.4.4. Currents and Gravity Force	51
4.4.5. Sediment Movement Velocity.....	52
4.4.6. Sediment Exchange Between Water Column and Bed	52
4.4.7. Sediment Mixing and Dispersion.....	53
4.4.8. Equilibrium Sediment Transport Equations	54
4.5. Bed Dynamics	56
4.6. Cohesive Sediment Equations	58

Chapter 5. Initial and Boundary Conditions	63
5.1. Initial Conditions.....	63
5.2. Inlet Boundary	63
5.3. Exit Boundary	63
Chapter 6. Numerical Methods	65
6.1. Sediment Transport Equation Discretization.....	65
6.2. Bed Dynamics	67
6.3. Time Integration	69
Chapter 7. Model Verification	71
7.1. Aggradation in a Straight Channel.....	71
7.2. Degradation in a Straight Channel.....	72
7.3. Contraction Scour Simulation.....	75
7.3.1. Introduction.....	75
7.3.2. Flume Case Description.....	75
7.3.3. Numerical Model Details	76
7.3.4. Calibration Simulation	77
7.3.5. Erosion and Deposition Simulation Results.....	79
7.3.6. Concluding Remarks	81
7.4. Alternate Bar Formation Downstream of a Dike.....	81
7.4.1. Introduction.....	81
7.4.2. Numerical Modeling and Comparison	83
7.4.3. Sensitivity Study.....	85
7.5. Pool and Bar Formation in Channel Bends	88
7.5.1. Introduction.....	88
7.5.2. A Bend with Uniform Bed.....	89
7.5.3. A Bend with Non-Uniform Bed	92
Chapter 8. Model Applications	95
8.1. Scour Analysis along an Outer Bank of a Section of the Rio Grande	95
8.1.1. Background.....	95
8.1.2. Empirical Analysis.....	96
8.1.3. Numerical Model Description.....	97
8.1.4. Boundary Conditions and Other Parameters	99
8.1.5. Results and Discussion	99
8.1.6. Concluding Remarks	101
8.2. Trinity River Gravel Injection Study	102
8.2.1. Purpose of the Simulation.....	102
8.2.2. The Solution Domain	102
8.2.3. Initial Calibration and Parameter Selection.....	104
8.2.4. Initial Conditions.....	106
8.2.5. Water and Sediment Boundary Conditions	108
8.2.6. Pre-Processor Interactive Input.....	114
8.2.7. Dynamic Input	124
8.2.8. Model Results	125
8.2.9. Recommendations for Implementation	129
8.2.10. Implementation and Validation	129
8.3. Channel Formation Due to Reservoir Drawdown.....	130
8.3.1. Background.....	130
8.3.2. About the Study Site.....	131
8.3.3. Model Details.....	133
8.3.4. Scenarios and Other Model Inputs.....	134
8.3.5. Results and Discussion	136

8.3.6. Remarks about the Modeling	140
8.4. Channel Morphology Prediction Upstream of the Elephant Butte Reservoir	140
8.4.1. Background.....	140
8.4.2. Data and Parameters.....	141
8.4.3. Results and Discussion	143
8.4.4. Remarks about the Modeling	147
Appendix A. Other Sediment Equations and Their Assessment.....	148
A.1. Wu Equation	148
A.2. Bagnold Equation.....	149
A.3. Ackers and White Equation.....	150
A.4. van Rijn Equation	150
A.5. Yang Transport Equations	151
A.6. Comparative Study with Flume Cases	153
A.6.1. Aggradation in a Straight Channel	153
A.6.2. Degradation in a Straight Channel	158
A.7 Comparative Study with a Chosui River Reach	165
References	171

Summary

Sedimentation and River Hydraulics-Two-Dimensions (SRH-2D), is a two-dimensional (2D), depth-averaged, hydraulic and sediment transport mobile-bed model for simulating shallow waterways. The Bureau of Reclamation (Reclamation) has been developing this model since 2003 and is continuously improving the model. See <https://www.usbr.gov/tsc/techreferences/computer%20software/models/srh2d/index.html> for its future updated models. This document is the User's Manual for the SRH-2D sediment transport mobile-bed modeling; it should be used together with the User's Manual for flow modeling by Lai (2008).

SRH Model History. The hydraulic flow model, SRH-2D Version 1, was first released in 2006 (Lai 2006); Version 2 was released in 2008 (Lai 2008). The flow modeling theory and model verifications were scientifically documented in a journal paper (Lai 2010). The sediment transport mobile-bed module has been developed and coupled with the flow solver since 2008. The new sediment modeling capability, SRH-2D Version 3, was distributed for public use in 2010. The sediment module can simulate fractional sediment transport, changes in the particle size distribution of the bed, and local changes in bed elevation (scour and deposition) over time. Although Version 3 has been widely used for sediment modeling, a user's manual describing its sediment modeling functionality has not previously been distributed. Recently, it was documented in a journal paper (Lai 2020).

Sediment transport mobile-bed module. Reclamation has been researching and developing the sediment transport mobile-bed module for many years. SRH-2D incorporates the current state-of-the-art in its category and is based on a relatively general and proven set of mathematical governing equations. SRH-2D version 3 has so far been tested and verified by an extensive number of laboratory and field cases; some of them are discussed in this document. Further, the sediment model has already been applied, with great success, to an extensive number of projects at Reclamation and by external institutions and consulting companies. Some of the model verifications and project applications have been documented in the form of reports and scientific papers and are distributed along with the model.

The philosophy in selecting the governing equations is that the fewest assumptions are made with regard to the sediment transport modeling, but the model remains relatively simple to apply with minimal model inputs. Key sediment transport mobile-bed features are:

- Multi-Size Sediment Transport: the so-called non-uniform approach
- Variable-Load Approach: simultaneous suspended-, bed-, and mixed-loads
- Non-Equilibrium Transport: more general and accurate than the Exner-equation approach
- Multi-Layer Bed Dynamics: subsurface layer stratigraphy is taken into consideration

SRH-2D User's Manual: Sediment Transport and Mobile-Bed Modeling

- Sorting/Armoring Simulation
- Non-Cohesive, Cohesive, or Mixed Sediments
- Sediment Transport Capacity Equations: a wide range of selections
- Effects of Secondary Flow and Gravity: important to simulate erosion along the outer bends

With SRH-2D, sediment transport mobile-bed modeling is configured to be a time-accurate unsteady bed evolution simulation—even if the flow is constant.

This manual provides instructions only for the SRH-2D sediment transport mobile-bed capabilities only. The SRH-2D flow model User's Manual (Lai, 2008) should be consulted to learn and understand the basics of the model. The two manuals are meant to be used together to perform a sediment transport mobile-bed numerical simulation. The manuals themselves are usually sufficient to get a basic training on how to use SRH-2D.

Chapter 1. Introduction

See the Introduction section of the User's Manual by Lai (2008) to gain a general overview of the flow modeling with SRH-2D at: <https://www.usbr.gov/tsc/techreferences/computer%20software/models/srh2d/index.html>.

1.1. Software and Hardware Requirement

Three software programs are needed for a complete analysis with SRH-2D:

- 1) mesh generation software;
- 2) the SRH-2D package; and
- 3) post-processing graphical software.

SRH-2D uses Surface-Water Modeling System (SMS), for mesh generation and post-processing (items 1 and 3). 2D meshes may be generated using the older versions of SMS (version 12 and earlier) which produce the generic mesh format called 2DM. The newer versions 13 and above create 2D meshes in a new format named SRHGEOM¹. SRH-2D can take either 2DM or SRHGEOM as its mesh input. The advantages of SMS 13 and above are: (a) SRH-2D has been fully integrated with SMS so that SMS is the only “software” visible to users and the entire modeling process can be done within SMS; (b) a community version of SMS is available and free to users. Go to www.aquaveo.com for SMS download.

SRH-2D may be operated in one of two modes:

- **Partial-Interface** mode allows a user to generate a 2D mesh, run SRH-2D model, and post-process results separately. For beginners or those who do research, Partial-Interface is recommended as it is the quickest way to learn SRH-2D. Further, users may have more freedom and fuller control of the modeling process. Some examples include the following. Users may generate the mesh or post-process the results with software other than SMS. Users may have already been familiar with other software for post-processing model results and do not want to learn a new one. The SRH-2D input file is simple and can be edited to change the model inputs quickly for sensitivity/parametric studies. Users may create their own Python script to automate the preparation and submission of large number of cases. Users may also use other mesh generators such as SRH-Mesh developed at Reclamation or other graphical software for post-processing such as GIS, Paraview and TECPLOT.
- **SMS-Interface** mode is more appropriate to application-oriented users. The free community SMS versions have all the capabilities required to conduct a modeling

¹ SRHGEOM is a special file format used by the commercial code SMS and stands for Sedimentation and River Hydraulics Geometric Mesh.

project. The fee-based SMS provides a wider range of capabilities for post-processing the results and organizing modeling scenarios/alternatives.

This manual is limited to the Partial-Interface training only. Users who want to use the SMS-Interface mode should take a training class which is regularly offered through Federal Highway Administration (FHWA) by Scott Hogan (Scott.Hogan@dot.gov) or by Aquaveo, LLC (www.aquaveo.com).

SRH-2D can be run on any laptop or desktop PC with the Window-based operating system. SRH-2D does not yet support the Linux-based platforms.

1.2. SRH-2D Package

SRH-2D version 3 release package consists of two programs:

- *Srh2d_pre* is a preprocessor that generates an input file needed to run *srh2d*. The preprocessing interface is in the form of Q-and-A designed such that users do not need to memorize most input commands. The Q-and-A session usually provides instructions and guidelines on how to select appropriate inputs.
- *Srh2d* is the main flow and sediment solver that reads the input data generated by *srh2d_pre*, carries out the simulation, and outputs the results to data files. The output results files may be viewed and processed using graphic software such as SMS, GIS, Excel, Paraview and TECPLOT.

SRH-2D solves all governing equations in International System of Units (SI) (e.g., distance and mesh coordinates are in meters, elevation and water depth in meters, velocity in meters per second [m/s], stress in newtons per square meter [N/m²] or pascal [Pa], etc.). Users, however, can use either SI or English units in model inputs or outputs. The specific unit used is clearly indicated during the running of *srh2d_pre*. Units are also appended to the variable names in the output files.

A typical modeling session consists of four steps: mesh generation and boundary identification, preprocessing with *srh2d_pre*, model execution with *srh2d*, and results post-processing. These steps have been described in the version 2 manual of Lai (2008) and not repeated in this manual.

1.3. About the Mobile-Bed Module

The SRH-2D version 3 mobile-bed module has these general features:

- **Multi-Size Sediment Representation:** All sediments in the model domain may be divided into a number of sediment size classes. Each size class is transported and tracked by the model (non-uniform representation). Cohesive sediments are lumped into one size class and represented by the size class number one.

- **Variable-Load:** Each sediment size class may be transported as suspended load, bedload, or mixed load. User may also specify the type of load. If the load type is left unspecified, then SRH-2D will determine the load type automatically according to the local flow variables using empirically developed equations.
- **Non-Equilibrium Transport:** Transport of each sediment size class is governed by a partial differential equation of the convection-diffusion type so that mass conservation may be conserved. The source/sink terms of the equation are governed by the sediment transport capacity, fall velocity, and/or cohesive sediment erosion-deposition properties. So, the computed sediment flux is not in general the same as the sediment capacity—allowing the transport rate in a non-equilibrium state.
- **Multi-Layer Bed Dynamics:** Riverbed subsurface may consist of multiple layers (vertical stratigraphy). Each layer may have different sediment properties such as the thickness, porosity, and gradation. During sediment transport, the top layer properties may change in time according to the mass conservation principle. The procedure allows the simulation of bed armoring and sorting.
- **Sediment Transport Capacity Equation:** A number of popular sediment transport capacity equations are available to use. Recommendations are given for each type of river when *srh2d_pre* is run.
- **Effects of Secondary Flow and Gravity:** Sediment size class movement direction does not have to coincide with the depth-averaged flow velocity vector. The sediment velocity may deviate from the flow in practice due to secondary flows in bends and gravity force on sloping surfaces.
- **Cohesive Sediment:** In addition to the non-cohesive sediments, cohesive sediment is also modeled. The cohesive sediments are lumped into one unit and represented by sediment size class number one. The cohesive sediment may assume its own properties such as porosity and erosion-deposition properties and characteristics. A mixture of cohesive and non-cohesive sediments is allowed, and the amount of cohesive sediment is determined by the bed layer gradation input.

1.4. Limitations

SRH-2D version 3 has the following limitations:

- **Local scours.** This version is a depth-averaged model, so local scours may not be predicted correctly. For example, scours immediately downstream of weirs and around the bridge piers and abutments may not be predicted adequately. However, contraction and bend scours have been simulated well by SRH-2D in the past (see further discussion later in the document).

- **Lateral erosion.** Only vertical erosion and deposition are simulated; lateral erosion (e.g., near a bank) is not considered. A bank erosion module is still under research and development and unavailable in the current release.
- **Windows platform.** Only personal computers with the Windows Operating System are supported.

1.5. Disclaimer

SRH-2D and information provided in this manual are developed for Reclamation's use. Despite many successful applications of SRH-2D, Reclamation does not guarantee the performance of the program. SRH-2D is a program that requires engineering expertise to use and to interpret the results. Like other computer programs, SRH-2D is potentially fallible. All results obtained from the use of the program should be carefully examined and peer-reviewed by an experienced engineer to determine if they are reasonable and accurate. Reclamation assumes no responsibility for the misuse of SRH-2D and misinterpretation of the model results and makes no warranties concerning the accuracy, completeness, reliability, usability, or suitability for any particular purpose of the software or the information in this manual. Reclamation will not be liable for any special, collateral, incidental, or consequential damages in connection with the use of the software.

Chapter 2. Pre-Processing with Partial-Interface Mode

The Partial-Interface mode of SRH-2D is designed to perform mesh generation, simulation, and result post-processing separately. This way, each step can be done using different software, leading to increased freedom and control in the modeling process. The pre-processor of SRH-2D's question and answer (Q_and_A) session offers guidelines on how to enter various model input parameters and can be handy for occasional users. Although any 2D mesh generation program may be used, only 2D generic mesh (2DM) or SRHGEOM meshes generated by SMS are discussed in this manual and later for model training.

A 2D mesh contains at least two pieces of information: the 2D mesh itself (collection of cells, nodes, and connectivity information) and a list of “nodestrings” specifying the model boundaries. Further, a material ID is assigned to each mesh cell so that spatially varying properties such as the Manning's roughness coefficient and bed sediment properties can be assigned to cells. Both 2DM and SRHGEOM meshes may be used even if they are generated using the SMS-Interface mode.

The *srh2d_pre* is an interactive program that asks a question to prompt users to provide an answer so that all input parameters may be collected and processed. This manual only explains the questions related to the sediment transport mobile-bed module. Other inputs in this interactive program are mostly relevant to the flow-only simulation and have been explained in the 2008 Users' Manual (Lai, 2008). Not all commands/questions will appear in an actual preprocessing session as only relevant questions will appear.

Note that some input parameters are mandatory while others are optional. Optional input parameters appear in brackets, e.g., [PARAM]; default values are assigned if users do not enter the values of the optional parameters.

A list of input commands/questions relevant to sediment modeling are discussed in the following subsections, along with possible answers/inputs to run SRH-2D. It is used with the Partial-Interface mode.

2.1. General Inputs

==> SELECT-INPUT-METHOD

After starting *srh2d_pre*, users are prompted to select the “**Input Method.**”

- **For a new modeling case** when the Script Input File, *_SIF.dat*, does not exist, enter the number 1

- **For an existing modeling case** when the `_SIF.dat` has been created before and already exists, enter the number 2

As the *srh2d_pre* session progresses, a new Script Output File (SOF), `_SOF.dat`, is continuously created to document all user inputs/entries. After a successful run of *srh2d_pre* with option 1, save the `_SOF.dat` file by renaming it as `_SIF.dat`.

The SIF file is the main input file that may be used to repeat the SRH-2D run by using option 2 of the input method. The SIF file is a text file which may be edited to change the model inputs/entries using any text editor. SIF file may be shared with other modelers to repeat a model run along with mesh and other time series data files referred to in the SIF file.

==> CASE-NAME

One word is entered to serve as the name of the model run. In this manual, “**case**” is assumed to be the case name and used throughout this manual. Users may use any other word for the case name. Once entered, the case name is used to identify most input and output files associated with the model run. For example, the script input file is named `case_SIF.dat`, the script output file is `case_SOF.dat`, the input file created by the preprocessor and used to run SRH-2D is named `case.dat`, and so forth.

==> SIMULATION-DESCRIPTION

This provides users with an opportunity to describe the simulated case. The description is limited to one line and it does not impact the model results. The ENTER key may be pressed to skip providing such a description. Note that case description can be added to the SIF file once it exists. Any lines starting with `//` are treated as comment lines and are ignored by SRH-2D.

==> SRH-MODULE-SELECTION

Users are prompted to select the module/solver to be used. Two options are available:

- **FLOW** is for flow-only modeling,
- **MOBILE** activates both the flow solver and sediment transport mobile-bed module.

==> MONITOR-POINT-INFORMATION

Enter the number of monitor points within the model domain. At each monitor point, a time series data file of main output variables will be written as an output text file that can be used with other software such as Microsoft Word. This output file is named as the name of the case and point ID, for example: `case_PTi.dat`, where *i* the monitor point ID. This output file can be processed using software such as Excel so that the time variation of a main variable at the monitor point can be viewed.

The output variable list and the associated units are included in the headers of the file. Only the first monitor point, PT1, is displayed in the monitoring window.

==> COORDINATES-OF-ALL-MONITORING-POINTS

Enter the X and Y coordinates of all monitoring points. A total of 2*N real values are needed (N is the total number of monitoring points). The units of (X,Y) should be the same as those used in the 2D mesh. If an (X,Y) point is outside the model domain, the preprocessor will issue a warning at the end of the preprocessor and the point is excluded from the output. The mesh generation program, such as SMS, may be used to determine the coordinates of the monitoring points.

==> UNSTEADY-MODELING-TIME-PARAMETERS

Three time parameters are entered for each model run:

TSTART DT T_SIMU

where:

TSTART: a real value for the simulation starting time; it is always in **Hours** (0.0 is typically used unless there is a good reason to use other values).

DT: a real value for the time step of the simulation; the unit is always in **Seconds**.

T_SIMU: a real value for the total simulation time to be performed; the unit is always in **Hours**.

Both *DT* and *T_SIMU* may also be dynamically changed before and during SRH-2D model run using the *_DIP.dat* file, where DIP stands for dynamic input—a special file for providing dynamic input. See APPENDIX C of the flow modeling 2008 User Manual for more information on the *_DIP* file.

==> GENERAL-SEDIMENT-PARAMETERS

Users enter two general sediment parameters: the specific gravity of the sediments and the total number of the sediment size classes to be used for the modeling.

The specific gravity is generally 2.65, but different values may be entered. At present, all sediment size classes are assumed to have the same specific gravity.

Some of the notes are listed below in choosing the number of size classes:

- If the number of size classes is one, only one uniform size is simulated. A size that represents the medium sediment (d_{50}) is usually selected.

- The size range covered should include all possible sizes in the simulated system.
- It is not recommended to use more than seven (7) size classes, as the computing time will be increased significantly.
- If there are cohesive sediments present in the system, they should be lumped together and represented by size class number one (1). The size range of the cohesive class is not used by SRH unless users did not provide the fall velocity, or the user-supplied fall velocity is smaller than those based on the Stokes law equation.

Note that the properties of the cohesive sediment size can vary spatially and vertically although only one size is used to represent the cohesive sediment. This will be discussed later.

==> SEDIMENT-DIAMETER-&-BULK-DENSITY

The lower and upper diameter boundaries of each sediment size class are entered sequentially in units of millimeters (mm). The listing begins with the finest size fraction and progresses to coarser fractions. The cohesive sediment should be listed as the first class if it exists.

To determine the porosity of the size class on the bed, users may specify the dry bulk density and its associated units for each class. If not provided, a porosity of 0.4 for non-cohesive sediments and porosity of 0.81 for the cohesive sediments are used. For the cohesive sediment class, the porosity specified is for sediments in suspension in the water column. The porosity of the cohesive sediments in the bed layer is entered later in another manner.

==> SEDIMENT-TRANSPORT-CAPACITY-EQUATION-for-Non-Cohesive-Sediment

Choose a sediment transport capacity equation for all non-cohesive sediment classes. This equation determines the sediment erosion rate. Theoretical equations of the capacity equations are discussed in Section 4.4.8 of this manual. The erosion-deposition rate of the cohesive sediment is computed in another way and the erosion-deposition rate parameters will be entered into the model later.

Available sediment transport capacity equations and their recommended use are:

- **EH** → The Engelund-Hansen (1972) (EH) equation is applicable to total load transport in sandy-bed rivers. It is the recommended equation for sandy rivers.
- **MPM** → The Meyer-Peter-Muller (MPM) equation as modified by Wong and Parker (2006) is used. It is applicable to bedload dominated, gravel-bed rivers, and is the recommended equation to use for gravel rivers. One additional parameter may be entered: the hiding factor, which can range from 0.0 (no hiding factor) to 0.9 (highest hiding factor). This way, MPM may also be applicable to mixed sand-gravel rivers.

- **PARKER** → The equation developed by Parker (1990) for bedload transport in mixed sand- and gravel-bed rivers. It is the recommended equation to use for mixed sand-gravel rivers. Two additional parameters may be entered with this equation: THETA and HF. THETA is the reference Shields parameter for the mean bed surface particle size and HF is the exponent representing the hiding effect. See Section 4.4.8 for more details. The default values are THETA=0.04 and HF=0.65, respectively.
- **WILCOCK** → The equation reported by Wilcock and Crowe (2003). It is applicable to bedload transport in mixed sand and gravel rivers, similar to the Parker (1990). Three additional parameters may be entered: T1, T2, D_{sand}. T1 and T2 are used to compute the reference Shields parameter THETA used in the Parker (1990) equation: $THETA = T1 + (T2 - T1) * \text{Exp}(-20F_{\text{sand}})$, where F_{sand} is the fraction of sediments on the bed surface finer than the diameter specified by D_{sand} in mm. The default values of the three are T1 = 0.021, T2 = 0.036, and D_{sand} = 1.0.
- **WU** → The equation according to Wu et al. (2000a). It is applicable to bedload transport in sand, gravel or mixed sand and gravel rivers. An additional parameter may be entered with the WU option: the critical shields number which may range from 0.01 to 0.07. The default value is 0.03. The WU equation is also recommended for purely sand, purely gravel or mixed sand-gravel rivers.
- **YANG73** → This is the capacity equation based on Yang (1973). It is primarily for the total transport in a sand or gravel river.
- **YANG79** → This is based on the work of Yang (1979). It is applicable to the total transport in a sand or gravel system.
- **MIXED** → This is the option that may specify two sediment transport equations: one for the finer portion of the sediment size spectrum and the other for the coarser part of the spectrum. This option has not been extensively tested nor has it been verified.

==> WATER-TEMPERATURE

Water temperature is used to compute the water molecular viscosity, which impacts the fall velocity computation. The default value is 25 degrees Celsius (°C).

==> Start Time for the Sediment Module

The default simulation start time for the sediment module is the same as the flow module (TSTART). Proper initial flow conditions should be used using the restart (RST) option and results from a Flow-Only run. Occasionally, however, the start time of the sediment module can be delayed using the variable TS_SED. If TS_SED is larger than TSTART, SRH-2D will carry out a Flow-Only simulation in the time period between TSTART and TS_SED. Sediment transport kicks in after TS_SED. The purpose is to compute a proper initial flow field prior to initiating sediment transport.

==> ADAPTATION-COEFFICIENTS-FOR-SUSPENDED-LOAD

The two adaptation coefficients, A_DEP (deposition) and A_ERO (erosion), are used to determine the rate at which suspended sediment concentrations reach the equilibrium concentration determined by the sediment capacity equations entered above.

Due to the variable nature of the flow conditions in natural rivers, the concentration in transport may locally increase in regions of greater shear stress and decrease in regions of lesser shear stress. A new equilibrium concentration is usually not attained instantaneously. The distance traveled by a given packet of sediment in an assumed constant flow environment is defined as the adaptation length (L). L is incorporated into the sediment governing equation in the source form as:

$$S_e = \frac{(q_s^* - q_s)}{L}$$

where q_s^* is the local sediment transport capacity and q_s is the sediment transport flux advected into the local area from upstream.

SRH-2D computes L differently for the suspended load and for bedload. For suspended load, L is computed as:

$$L = \zeta U h / \omega_s$$

where U is the local depth-averaged water flow velocity, h is the local flow depth, ω_s is the particle fall velocity, and ζ is a user-specified parameter. A_DEP is the ζ value if there is a net deposition, while A_ERO is the value used for net erosion.

Default values for the two adaptation coefficients are 0.25 and 1.0 for deposition and erosion, respectively. The default values are recommended as we do not have enough cases which show that using values other than the default values are advantageous.

==> ADAPTATION-LENGTH-FOR-BEDLOAD-TRANSPORT

Bedload transport adaptation length concepts are similar to the above adaptation concepts. The adaptation length needs to be determined for bedload transport so that the instantaneous flux is not the same as the capacity flux. Two parameters may be entered:

- **Mod_adap_Lng = 0** → A constant adaptation length is used. We found this option works the best for gravel rivers and Length can be selected to be one to five times the river channel width.
- **Mod_adap_Lng = 1** → The adaptation length is computed automatically using the bedload saltation length computed by the Philips-Sutherland Formula: $\text{Length} = 4000(S h - Sh_c) * d_{50}$, where S is channel energy slope, h is local flow depth, h_c is the critical flow depth for particle entrainment, and d_{50} is the median sediment grain size on the bed. We found that this formulation works for most sand-bed rivers.

==> ACTIVE-LAYER-THICKNESS-SPECIFICATION

A small portion of the top bed surface is used to facilitate the sediment exchange between the sediments on the bed and those in transport. This top layer is called the active layer. The active layer thickness needs to be specified. Two parameters may be entered: Mod_AL and T_PARA.

- **Mod_AL = 1** → A constant thickness is specified and T_PARA = the thickness in meters;
- **Mod_AL = 2** → The active layer thickness is computed as $\text{Thickness} = T_PARA * d_{90}$ where T_para is the user input here and d_{90} is the sediment diameter on bed at which 90% of sediments are finer.

Our experience showed that Mod_AL = 2 is a good option for many applications. It is recommended that T_PARA be between 1 to 3 for gravel rivers and 5 to 14 for sand rivers. For rivers with silt and clay, option 1 for constant thickness is recommended.

In general, the active layer thickness has a negligible effect in cases of deposition; it is positively correlated to the eroded depth in cases of erosion.

==> COHESIVE-SEDIMENT-MODELING

Enter 0 or press ENTER key if there is no cohesive sediment class present in the system. Or enter an integer larger than 0 to specify n_Cohesive, the number of cohesive sediment types. Each cohesive type can have different properties (e.g., fall velocity, erosion, and deposition rates) and be assigned to different bed layers in different mesh zones. This will be discussed more later.

==> COHESIVE-SEDIMENT-GENERAL-PROPERTIES

Enter the dry bulk density of the cohesive type.

==> COHESIVE-SEDIMENT-FALL-VELOCITY

The fall velocity of each cohesive sediment type must be specified as a function of the sediment concentration in the water column. The three options are:

- **Option -1** → The fall velocity versus concentration data is taken from those typical for kaolinite clay mineral. The four data points of the [C(g/L); FV(mm/s)] are as follows: (0.2; 0.012), (6; 0.15), (20; 0.15), (100; 0.012)
- **Option 0** → The fall velocity data is the same as those from the Severn River in Great Britain. The four data points of the [C(g/L); FV(mm/s)] are as follows: (0.09; 0.025), (2; 2), (9; 2.2) (90; 0.028).

- **Option Filename** → Users may supply a text file containing Conc(g/L) versus Fall_vel(mm/s). The file format is:

```
// Any rows starting with // are treated as comment lines and ignored
// Two values on each row provides: conc(g/L) fall_vel(mm/s)
// Below is the data used for our Rio Grande modeling:
// CONC(kg/m3) Fall_Velocity(mm/s)
0.0 0.0
0.2 0.0012
6.0 0.015
20.0 0.015
100.0 0.0012
```

==> EROSION-RATE-OF-COHESIVE-SEDIMENT

Erosion of cohesive sediment is different from non-cohesive sediments and does not use sediment transport capacity. The shear stress-based approach is used to compute the erosion rate of the cohesive sediment, and the theory is discussed in Section 4.6. Inputs are needed for each cohesive sediment type. Two input options are available:

- **Option 1** → Enter 0 for the four-parameter option. With this option, the four parameters are entered and they are: Tau_es, Tau_em, S_s, and S_m [UNIT]
 - Tau_es = critical shear stress for surface erosion
 - Tau_em = critical shear stress for mass erosion
 - S_s = surface erosion slope constant
 - S_m = mass erosion slope constant

The UNIT is optional and SI or EN; For SI, shear stresses are in Pa (N/m²) and slope constants are in mm/s; for EN, shear stresses are in pounds per square foot (lb/ft²) and slope constant in lb/ft²/hour. By default, SI is used.

The erosion rate is computed by:

$$\text{Rate} = S_s + S_m \cdot (\text{Tau} / \text{Tau}_{em} - 1) \text{ if } \text{Tau} > \text{Tau}_{em};$$

$$\text{Rate} = S_s \cdot [(\text{Tau} - \text{Tau}_{es}) / (\text{Tau}_{em} - \text{Tau}_{es})] \text{ if } \text{Tau}_{es} < \text{Tau} < \text{Tau}_{em}$$

where Tau is the hydraulic shear stress on the bed.

For example, the following inputs are used for the Rio Grande modeling: 0.125 2.84 0.25 1.07 EN

- **Option 2** → Enter the name of a file containing a list of Shear Stress (Pa) versus Erosion_Rate (kilograms per square meter per hour [kg/m²/hr]). The data file uses the following format:

```
// Any rows starting with // are treated as comment lines and ignored
// Two values on each row provides: Shear_Stress(Pa) Erosion_Rate(kg/m^2/hr)
SS1 ER1
SS2 ER2
...
```


Note the specific units required for the file.

==> **THREE-PARAMETERS-FOR-COHESIVE-SEDIMENT-DEPOSITION-RATE**

Deposition of cohesive sediment suspended in the water column is also different from non-cohesive sediments, and its properties need to be specified for each cohesive sediment type. Similar to the erosion approach, the shear stress-based approach is used

At present the three-parameter approach is adopted. Users need to provide Tau_df Tau_dp and Conc_eq as described below.

- Tau_df = critical shear stress for full deposition (Pa or lb/ft²)
- Tau_dp = critical shear stress for partial deposition (Pa or lb/ft²)
- Conc_eq = equilibrium concentration in kilograms per cubic meter (kg/m³)

The equilibrium concentration is used to control when deposition occurs: if the suspended concentration is smaller than Conc_eq or the bed shear stress is larger than Tau_dp, deposition stops. With the above inputs, the deposition rate is computed as:

$$\text{Rate} = \text{Fall_velocity} * (1.0 - \text{Tau} / \text{Tau_ref})$$

Where:

$$\text{Tau_ref} = \text{Tau_df} * \text{Tau_dp} / [r * \text{Tau_df} + (1-r) * \text{Tau_dp}], \text{ and}$$

$$R = \text{MAX}[0, 1 - \text{Conc_eq} / \text{Conc}]$$

Conc is the suspended cohesive sediment concentration

As an example, the following inputs are used for the Rio Grande modeling: 0.005 0.021 3.0 EN

==> **SPATIAL-VARIATION-METHOD-OF-SUBSURFACE-PROPERTIES**

The subsurface sediment properties, such as the layering, layer thickness, and layer gradation, may vary in space. At present, three options are available to enter how the subsurface sediments are distributed in space:

- **UNIFORM** → There is no spatial variability of the properties and one set of properties is used in the entire model domain.
- **ZONAL** → The model domain is divided into an arbitrary number of zones and each zone are assigned different properties. Zonal IDs may be assigned using a 2DM mesh file such that the material identification numbers (ID) correspond to the zonal IDs. Create this 2DM file by:
 - a) Opening the 2DM file with SMS
 - b) Selecting each mesh zone and assign a material ID to it
 - c) Saving the 2DM file

Note that the material IDs in the original 2DM mesh file is used to define the zonal Manning's roughness coefficients.

- **POINT** → A separate data file is used to define the bed layer properties at survey points. Nearest-point interpolation is used to distribute the properties to the mesh cells.

2.2. Bed Layer Properties

In the following, the bed layer properties are entered and described.

==> **NUMBER-OF-SUBSURFACE-LAYERS-in-Zone-i**

This is to specify the number of subsurface layers (NLayer) to be simulated. Note that this property is not important for deposition but important for erosion. As different sediments may be deposited on the otherwise uniform layer, a minimum of two layers is recommended—even if they have the same properties. Assigning NLayer = 0 specifies that the bed is non-erodible but that deposition is allowed, and assigning NLayer = -1 specifies that no changes in bed elevations are allowed.

==> **BED-LAYER-PROPERTIES-FOR-ZONEi-and-Layerj**

Enter the following parameters: THICKNESS UNIT [COHESIVE_TYPE], where

- THICKNESS = Bed layer thickness
- UNIT = EN or SI; Thickness is in feet with EN and in meter with SI.
- [COHESIVE_TYPE] = This is needed if the bed layer is composed of one of the cohesive sediment types. It specifies which cohesive sediment type whose properties were defined earlier is present in the bed layer.

==> **BED-SEDIMENT-COMPOSITION**

The bed layer gradation or composition may be entered here. The options of entry are listed below:

- **FRACTION** v₁ v₂ ... v_{sed_nclass}
 - The volume fraction (v_i) of each sediment size class is given
 - v_i is the volume fraction of i_{th} sediment size class
 - The sum of all v_i may be 1.0 or 100.0
- **CUMULATIVE** d₁ P₁ d₂ P₂ ... d_n P_n
 - The cumulative distribution, diameter versus percentage, is given. SRH-2D will automatically compute the v_i over the size classes based on the cumulative distribution provided.
 - d_i is the sediment diameter in mm
 - P_i is the percentage of sediments smaller than d_i so P_n=100 is anticipated
 - up to 19 data points of (d_i P_i) is allowed

- GRADATION CurveFileName
 - With this option, a cumulative distribution is stored in a separate file.

==> FLOW-ROUGHNESS

For flow simulation, users specify the total Manning's roughness coefficient only. With the mobile-bed modeling turned on, SRH-2D asks for more input. Three entries are required:

- **SPATIAL** specifies the spatial distribution of the bare-bed Manning's roughness coefficient and will be either CONST or VARY. Entering CONST means the bare-bed Manning's roughness coefficient is a constant over the entire model domain; VARY means different bare-bed Manning's roughness coefficient are used in different bed zones. The material ID in the mesh is used for the spatial distribution.
- **VEGE** specifies whether an extra roughness due to vegetation should be added to the bare-bed roughness to compute the flow. Vegetation roughness is not used to compute the sediment transport. One of two options can be entered: NONE or YES.
- **GRAIN** provides the method used to compute the grain shear stress from the bare-bed roughness provided. The grain stress is used to carry out the sediment transport modeling. Two options may be used: PERCENTAGE or D90. With the PERCENTAGE option, grain stress is a constant percentage of the bare-bed stress. This option is more appropriate for sandy rivers and suspended sediment transport. The second option, D90, computes the grain Manning's roughness coefficient from the 90th percentile sediment size according to the theory described later in this manual. The D90 approach is more appropriate for bedload transport.

==> Boundary Conditions of the Sediment Rate

A sediment rate or flux at the model inlet is a necessary boundary conditions for mobile-bed modeling. Two options are available to specify the boundary conditions:

- **Capacity.** To compute the sediment rates at the inlets using the capacity equation , simply enter the text "CAPACITY". The CAPACITY approach is the easiest way to carry out a mobile-bed simulation.
- **Time series.** Users can also specify a time series of volumetric sediment fluxes in units of volume per unit time for each sediment size class. Often, the fractional sediment transport rates are computed using the rating curves established in previous studies or developed from measured data; or they may be obtained from other model runs, e.g., a 1D model or a larger domain model.

Chapter 3. Tutorial Cases

This chapter provides tutorial cases to train users on how to use SRH-2D with examples. The solution process for other modeling problems is similar. All tutorial cases come with the SRH-2D distribution package. Users are encouraged to run these tutorial cases to get hands-on experience. The documentation below was originally based on SRH-2D version 3.2.4 and updated with version 3.3.0. While modifications are possible for future versions, these are usually minor.

3.1. Non-Cohesive Sediment Degradation Modeling

This tutorial case simulates the degradation process in a straight channel with a non-cohesive sediment bed. The case corresponds to the flume experiment of Ashida and Michiue (1971) and details are presented both in Section 7.2. *Degradation in a Straight Channel* and Appendix A.

3.1.1. Model Domain, Mesh, and Model Inputs

The model domain is a rectangle 20 m long and 0.8 m wide. The bed is flat initially with a slope of 1%. The 2D mesh was generated with SMS, consisting of 41 by 5 quadrilateral cells (for a total of 205 cells). The SRHGEOM format of the 2D mesh was created with SMS and is supplied to users for the tutorial training.

Boundary conditions include the upstream boundary on the left with a constant flow rate of 0.0314 cubic meters per second (m^3/s) and clear water inflow. The downstream boundary on the right maintains a constant water elevation (stage) at 0.06 m (the bed elevation at the exit is 0.0). The two side boundaries (bottom and top) are treated as SYMMETRY.

The bare-bed Manning's roughness coefficient is 0.025 and the vegetation roughness is zero. The grain stress is based on the D90 approach as described in Section 4.2 of this Manual. The d_{90} multiplier is 3.0. The sediment capacity equation uses the Parker equation.

3.1.2. Running SRH-2D Preprocessor

As explained in Chapter 2, run the SRH-2D pre-processor in the Partial-Interface mode and select the Interactive input method for the first time so that a Script Output File (SOF) may be generated. Once the Q-and-A interactive preprocessing is complete, the SOF file should be renamed as the SIF file; this way, future model runs may be carried out by simply text-editing the SIF file.

Two BATCH files, *srh2D_Pre.bat* and *srh2D.bat*, are included in the distributed SRH-2D package. Once the package has been copied to a local drive, say D:\, users should edit the text of the batch files so that the first line of each file points to the SRH executable locations:

- start D:\Version_330\SRH-2D_Package\Exec_bin\srh2d_pre.exe
- start D:\Version_330\SRH-2D_Package\Exec_bin\srh2d.exe

The steps of running the pre-processor are:

1) Start Pre-Processing

Click *srh2D_Pre.bat* file, an interactive screen will appear (Figure 1):

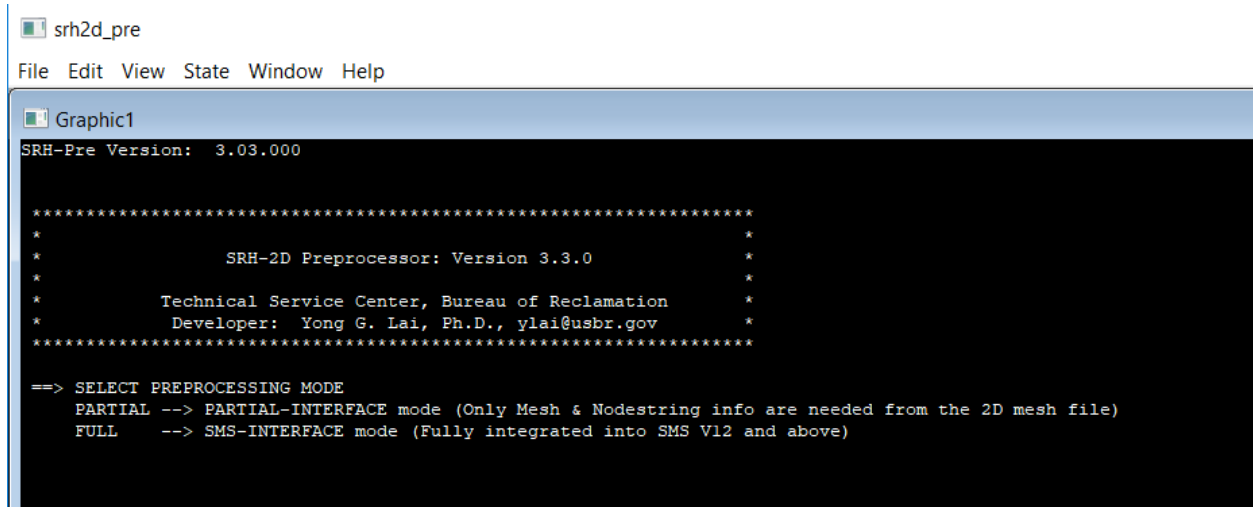


Figure 1. Interactive screen for *srh2D_Pre.bat*.

The preprocessor is a Q-and-A session, and users need to provide answers for each question. For our training, only Partial-Interface mode is used so users should enter PARTIAL. The Partial-Interface mode provides assistance on how to input the answer to each question. If more information on sediment modeling is needed, consult this manual for more details. The SRH User's Manual should be consulted for flow-only modeling questions.

For our tutorial case, enter number 1 at the prompt of "SELECT INPUT METHOD" for the interactive processing. This input method is required if this is the first time this model run is created and there is no SIF file yet.

(2) Case Name

Enter case for the "CASE NAME" question; this way, all input and output files will be named case_XXX.dat.

(3) Simulation Description

Any sentence may be entered to describe the case. This entry is not used though by the model and is for documentation purpose only.

(4) Solver Selection

Enter MOBILE, so that the mobile-bed sediment transport module is activated.

(5) Monitor Point Information

Enter number 3 to indicate that three monitor points will be entered. Then sequentially enter the (x y) coordinates of the three points: 13. 0.4, 10. 0.4, and 7. 0.4 for this tutorial case. Note that the unit of the (x y) should be the same as the units of the 2D mesh. There are experimental data of scour depth at the three points.

(6) Unsteady Modeling Time Parameters

Three parameters are entered: 0.0, 1.0, and 15.1. This means that the simulation starts from time 0.0 hour; 1.0 is the time step of the modeling (both flow and sediment) in seconds; and 15.1 is the total simulation time in hours.

(7) Turbulence Model Selection

Enter: PARA followed by a constant 0.7.

The entries select the parabolic turbulence model with the model constant of 0.7.

(8) Mesh Unit

Enter: meter for the tutorial case as the 2D mesh prepared in SMS is in meters.

(9) Import Mesh File

For the tutorial case, the 2D mesh has already been provided with the file name mesh.SRHGEOM. The entry is the mesh name and type as follows: mesh.srhgeom SRHGEOM. Note that the accompanying material ID file, mesh.SRHMAT is needed in addition to the mesh file.

(10) Sediment General Properties

Enter the following two parameters: 2.65 and 12, where 2.65 is the sediment specific gravity and 12 is the total number of size classes used for the simulation. Next, enter the lower and upper bounds of the sediment size classes in millimeters:

0.2 0.3
0.3 0.4
0.4 0.6
0.6 0.8
0.8 1.0
1.0 1.5
1.5 2.0
2.0 3.0
3.0 4.0
4.0 6.0

6.0 8.0
8.0 10.0

(11) Sediment Transport Capacity Equation for Non-Cohesive Sediment

Enter PARKER to choose the Parker transport capacity equation for the non-cohesive sediment classes.

Next, enter 0.04 and 0.65 to set the reference Shields number and the hiding coefficient, respectively.

(12) Water Temperature

The average water temperature is 29.0 °C for the case, and it impacts the fall velocity computation only.

(13) Start Time of the Sediment Module

Enter 0.1 for the START-TIME-SED entry. This means that flow-only simulation is carried out from time 0 to 0.1 hour. This provides time for the flow to establish an almost steady state field before sediment modeling starts. The mobile-bed simulation starts at time 0.1 hour and continues until the end of the run. An alternative method for establishing the flow conditions is to carry out a flow-only run first and then use those results as the initial condition for the mobile-bed run.

(14) Adaptation Coefficients

First enter the non-equilibrium suspended load adaptation coefficients: A_DEP,A_ERO): 0.25 1.0.

Next enter a constant bedload adaptation coefficient method with the length of 1.e- (for this tutorial, enter 0 1.e-6).

(15) Active Layer Thickness

The two parameters entered, 2 and 5.0, are to set the active layer thickness to $5d_{90}$

(16) Cohesive Sediment

Enter 0 to indicate that no cohesive sediment is present.

(17) Initial Flow Condition

For mobile-bed modeling, a time-accurate unsteady simulation is always performed. Normally, a flow-only simulation is carried out first and then the results are used as the initial condition of the mobile-bed modeling. In this example, however, the initial flow is stationary (i.e., zero velocity) but with a constant water depth. So the ZONAL option is entered so that the entire domain has an initial water depth of 0.06 m.

Next, specify the number of zones after choosing the ZONAL approach. For the example case, enter 1 as the entire domain has the same water depth initially.

Finally, enter 0 0 -0.06 SI to specify that the velocity components are 0 and the water depth is 0.06 m (all with SI units).

(18) Soil-Type/Bed-Property Spatial Distribution

Enter UNIFORM as the spatial distribution option to specify the bed sediment properties. UNIFORM means the entire model domain will have the same subsurface properties, which will be specified next.

(19) Number of Subsurface Layers

Enter 1 for the number of bed layers.

(20) Bed Layer Properties

First, enter 10 SI to specify a bed layer thickness of 10 meters. Next, enter the bed layer gradation as

```
FRACTION
.0745
.1235
.1594
.0440
.0360
.0679
.0400
.0918
.1017
.1812
.0599
.0201
```

In the above bed layer gradation, the volume fractions of all size classes are entered (for a total of 12 gradations).

(21) Flow Roughness/Resistance Input

Enter CONST NONE D90 to specify that a constant Manning's roughness coefficient for the bare bed spans the entire model domain, that no vegetation roughness is present, and that the grain shear stress for sediment modeling is based on the D90 approach.

Next, enter 0.025 3.0 to specify a bare-bed Manning's coefficient of 0.025 and that the multiplier to the d_{90} for the grain stress formula is 3.

Finally, to specify that no special modeling options are used with the tutorial case, simply press the ENTER key.

(22) Boundary Condition Inputs

There are four boundaries (nodestrings) specified in the 2D mesh. The first two are the top and bottom side boundaries, the third is the inlet on the left and the fourth is the exit on the right.

So, the first two entries are

```
SYMM  
SYMM
```

The third entry is: INLET-Q, followed by: 0.0314 0 0 0 0 0 0 0 0 0 0 0 SI

This specifies that the left boundary is an inlet with a constant flow discharge of 0.0314 m³/s and clear water sediment inputs (the 12 zeros are entered for the volume sediment rates of 12 size classes).

The fourth and final entry is: EXIT-H, followed by: 0.06 SI

This entries specifies that the fourth boundary on the right is an exit with a fixed water elevation of 0.06 m.

Note that the next three inputs are simply the ENTER key to skip the inputs for: (a) extra vertical wall toughness height entry; (b) pressurized zone entry; and (c) instream flow obstruction entry.

(23) Results Output Format

For the tutorial case, enter: TEC SI to specify that the TECPLOT format and the SI unit are selected for the output of the model results. Users can easily change the output format once the SIF file is created.

(24) Output Maximum Value File

An option is offered to output a file, _MAX.dat, that contains the maximum values of the following variables: WSE WD VELOCITY FROUD SHEAR_STRESS, along with the times at which the maximum values occurred for each variable. For the tutorial case, it is not used so simply press the ENTER key.

Meaning of the variables are: WSE = water surface elevation; WD = water depth; VELOCITY = velocity magnitude; FROUD = Froude number; and SHEAR_STRESS = bed shear stress.

(25) Output Interval

Enter "-1" to specify that no intermediate outputs will be generated and only final results are output.

3.1.3. Pre-Processing Summary

The above completes the interactive pre-processing process. Once completed, a Script Output File (SOF) is created with a name case_SOF.dat for the tutorial case. The SOF file should be renamed as SIF immediately (e.g., case_SIF.dat) so that the SIF file may be used for future modeling needs (e.g., repeat and parametric runs or error corrections).

The SOF file contains all user entries during the interactive processing. Once renamed to SIF, case_SIF.dat may be used to re-run the pre-processor by selecting 2 in the SELECT-INPUT-METHOD prompt. The SRH-2D simulation may be repeated exactly as it was done before using the SIF file.

The content of the SOF file of the tutorial case is listed below as a reference:

```
// Simulation Description:
Ashida-Michiue Case: Degradation Study
// Solver Selection (FLOW MOBILE)
MOBILE
// Monitor-Point-Info: NPOINT + Coordinates: x1 y1 x2 y2 ...
3
13. 0.4 10. 0.4 7. 0.4
// Tstart Time_Step and Total_Simulation_Time: TSTART DT T_SIMU [FLAG]
0.0 1.0 15.1
// Turbulence-Model and the constant
PARA
0.7
// Mesh-Unit (FOOT METER INCH MM MILE KM GSCALE) + the mesh file name
METER
mesh.srhgeom SRHGEOM
// General Sediment Parameters: spec_grav sed_nclass
2.65 12
// Diam_Lower(mm) Diam_Upper(mm) [Den_Bulk] [SI/EN] for each size class
0.2 0.3
0.3 0.4
0.4 0.6
0.6 0.8
0.8 1.0
1.0 1.5
1.5 2.0
2.0 3.0
3.0 4.0
4.0 6.0
6.0 8.0
8.0 10.0
// Sediment Capacity Eqn (EH MPM PARK WILC WU YANG73 YANG79)
PARKER
```

```

0.04 0.65
// Water Temperature (Celsius):
29
// Start Time in hours for the Sediment Solver
0.1
// Adaptation Coefs for Suspended Load: A_DEP A_ERO (0.25 1.0 are defaults)
0.25 1
// Bedload Adaptation Length: MOD_ADAP_LNG LENGTH(meter)
0 1.e-6
// Active Layer Thickness: MOD_ALayer NALT (1=const;2=Nalt*d90)
2 5.0
// MOD_COHESIVE (0=non-cohesive >0 --> number of cohesive classes)
0
// Initial Flow Condition Method (DRY RST AUTO ZONAL Vary_WSE/Vary_WD)
ZONAL
// Constant Setup for Initial Condition: n_zone [2DM_filename]
1
// Constant-Value Initial Condition for Mesh Zone: U V WSE [TK] [ED] [T]
0 0 -0.06 SI
// Soil Type Spatial Distribution Method (UNI ZON POINT)
UNIFORM
// Number of Bed Layers
1
// Thickness Unit(SI/EN) Cohesive_TYPE for each layer within a zone
10 SI
// FRACTION V1 V2 ... Vsed_nclass for each bed layer and bed zone
FRACTION .0745 .1235 .1594 .0440 .0360 .0679 .0400 .0918 .1017 .1812 .0599 .0201
// Manning: SPATIAL VEG GRAIN (CONST NONE PERCENTAGE)
CONST NONE D90
// Manning-n Multiplier_to_d90
0.025 3.0
// Any-Special-Treatments? (0 or empty = NO; 1=YES)

// Boundary Type (INLET-Q EXIT-H etc)
SYMM
SYMM
INLET-Q
0.0314 0 0 0 0 0 0 0 0 0 0 0 0 SI
EXIT-H
0.06 SI
// Wall-Roughness-Height-Specification (empty-line=DONE)

// Pressurized Zone exists? (empty-line or 0 == NO)

// Any In-Stream Flow Obstructions? (empty-line or 0 = NO)

```

```
// Results-Output-Format-and-Unit(SRHC/TEC/SRHN/XMDF/XMDFC/PARA;SI/EN) +
Optional STL FACE
TEC SI
// Output File _MAX.dat is requested? (empty means NO)

// Intermediate Result Output Control: INTERVAL(hour)
-1
```

3.2. Cohesive Sediment Modeling of Rio Grande

This tutorial case simulates erosion and deposition processes of combined cohesive and non-cohesive sediments. The example is taken from the application cases discussed in Section 8.4. 8.4. Channel Morphology Prediction Upstream of the Elephant Butte Reservoir. The primary purpose is to provide an example of simulating both cohesive and non-cohesive sediments; users may use this to model their own cases with some modifications to the input SIF file.

Briefly, the tutorial case performs a morphologic analysis of a 18-mile Rio Grande reach upstream of the Elephant Butte reservoir. The subsurface bed layers of the reach consist of two sediment layers. The top layer has a thickness of 6 ft consisting of primarily non-cohesive materials (10% silt/clay and 90% sand); while the bottom layer is comprised of 19 ft of primarily cohesive materials (80% clay + 20% sand).

3.2.1. Model Domain, Mesh and Other Conditions

The model domain of the case covered a Rio Grande, New Mexico, reach about 18 miles upstream of the Elephant Butte Reservoir (from river mile [RM] 42 to RM 60) (Figure 64 in Section 8.4). The 2D mesh was generated with SMS and consists of mixed quadrilaterals and triangles and a total of 14,628 mesh cells as shown in the same figure. The mesh, named mesh1999_no_tempchannel2.2DM, is supplied for the tutorial.

The upstream boundary at RM 60 is close to the U.S. Geological Survey (USGS) gage #8358300 at San Marcial. The daily discharge records for that gage were downloaded from the automated USGS database for January 1, 2000 to July 31, 2010. Only discharges above 500 cubic feet per second (cfs) were retained for the morphological modeling, since low flows do not mobilize sediments. The input hydrograph is saved in a file named, q_sanmarcial_500cfs.dat, and is plotted in Figure 2. The sediment load at the upstream boundary was computed using the rating curves developed by Collins (2006) but modified using new field data collected by Tetra Tech (2008). The fractional sediment rates are stored in a data file named: qs_option6.dat.

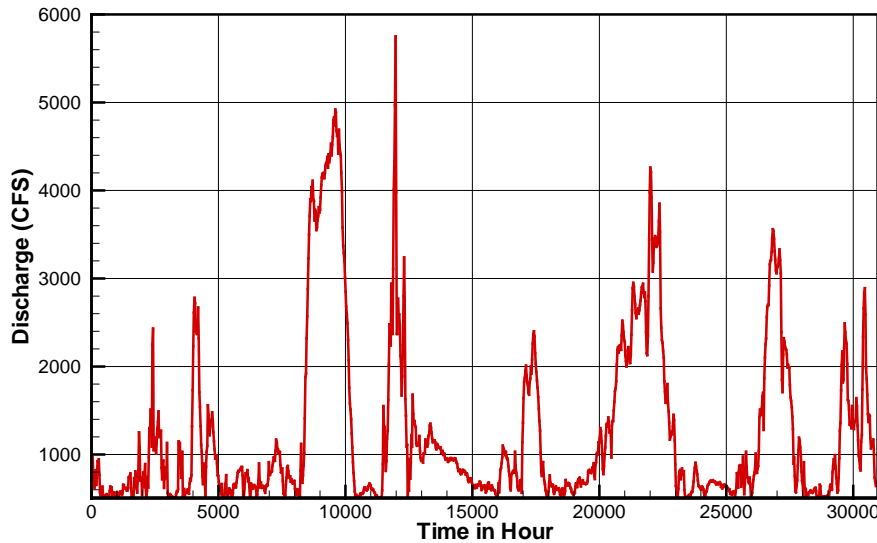


Figure 2. Flow discharge time series data above 500 cfs at the San Marcial gage of the Rio Grande. The time is from January 1, 2000 to July 31, 2010.

Flow roughness was calibrated using the measured water surface elevations. The entire reach was assigned a constant Manning's roughness coefficient of 0.017.

The subsurface layering and its properties are based on 20-foot deep holes drilled during July 23 to 30, August 31 to September 4, 2001, and on January 17, 2003. The data from most drill holes showed alternating layers of fine sand and silt-clay. On average, the bed can be described as consisting of two layers: a top sandy layer and a bottom silt-clay layer. The top layer has a thickness of six feet and the bed gradation listed in **Table 1**. The bottom layer has a thickness of ten feet and a silt-clay content of 80%.

Table 1. Rio Grande Bed Gradation

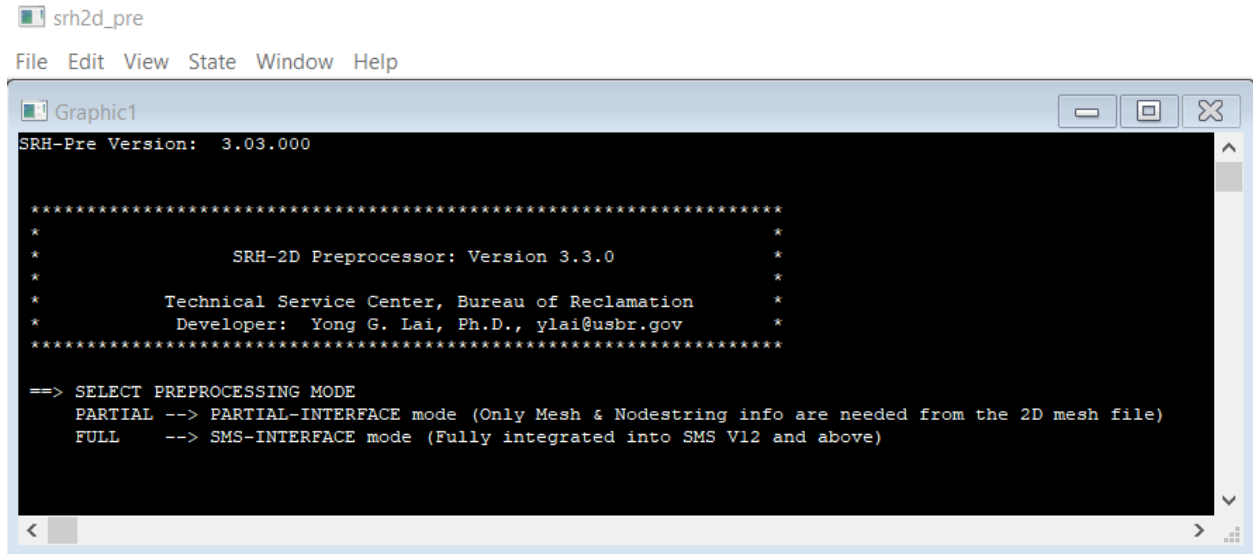
Cohesive content	d(mm)	Up to 0.625	0.125	0.25	0.5	1	2
10%	% pass by weight	10	13.5	33.3	98.5	99.6	100

3.2.2. Running the SRH-2D Preprocessor

The steps of running the pre-processor for the tutorial case are:

(1) Start the Pre-Processor

Start the pre-processing by clicking the srh2D_Pre.bat file. An interactive panel (Figure 3) will show up:



```

srh2d_pre
File Edit View State Window Help
Graphic1
SRH-Pre Version: 3.03.000

*****
*                               *
*           SRH-2D Preprocessor: Version 3.3.0           *
*                               *
*   Technical Service Center, Bureau of Reclamation      *
*   Developer: Yong G. Lai, Ph.D., ylai@usbr.gov         *
*                               *
*****

==> SELECT PREPROCESSING MODE
PARTIAL --> PARTIAL-INTERFACE mode (Only Mesh & Nodestring info are needed from the 2D mesh file)
FULL    --> SMS-INTERFACE mode (Fully integrated into SMS V12 and above)

```

Figure 3. Screenshot of the interactive panel for the preprocessing mode.

The pro-processor is a Q_and_A session. For each question, users provide the answer. For the tutorial, only the Partial Interface mode is used as it is simple to use and provides assistance on how select the inputs.

Once PARTIAL is entered, the INPUT METHOD should be selected. Select number 1 and press the Enter key. This input method is required if no SIF file exists.

(2) Case Name

Enter CASE for the CASE-NAME when prompted. All input and output files will be named after case.

(3) Simulation Description

A sentence may be entered to describe the case. This entry is not used by the model and is for documentation purpose only.

(4) Solver Selection

Enter MOBILE to activate the mobile-bed sediment transport module.

(5) Monitor Point Information

First, enter number 2 so that two monitor points are to be entered. Next, sequentially enter the (x y) coordinates of the two points: 1393300 940794.5 and 1358678.8 857885.5. Note that the units of coordinates are the same as the units of the 2D mesh. The first point is near the upstream

boundary, about 1,590 feet downstream of RM 60. The second point is near the exit boundary about 300 feet upstream of RM 42.

(6) Unsteady Modeling Time Parameters

Enter the three time parameters for the present case: 0.0, 5.0, and 1000.0. The entry specifies that the simulation starts from time 0.0, which corresponds to the start time of the hydrograph used for the simulation. The second number, 5.0, is the modeling time step, and 1000 is the duration of the input hydrograph in hours. Although the simulation spans 30,000 hours (a 10-year period) in real world time, the tutorial case simulates only 1,000 hours because the periods of low flows have been removed.

(7) Turbulence Model

Enter: PARA followed by a constant 0.7.

These inputs select the parabolic turbulence model with the model constant of 0.7.

(8) 2D Mesh Inputs

A 2D mesh for the tutorial case caked mesh1999.2DM is provided. Enter FOOT for the mesh unit and then the mesh file name and format: mesh1999.2DM SMS

(9) Sediment General Properties

Enter 2.65 8, where 2.65 is the sediment specific gravity and 8 is the total number of size classes used for the simulation. Next, enter:

```
0.0025 0.0625 500.0 SI
0.0625 0.125
0.125 0.177
0.177 0.25
0.25 0.354
0.354 0.5
0.5 1.0
1.0 16.0
```

The first two values in these eight lines represent the lower and upper bounds of the sediment diameter in millimeters for each sediment size class. The first line is the cohesive sediment class and requires two more entries: 500.0 and SI. The value of 500 is the dry bulk density of the cohesive sediment in the water column. Its unit is determined by the fourth entry, where SI indicates units of kilograms per cubic meter (kg/m^3). This corresponds to a porosity of the suspended cohesive sediment of 0.811.

(10) Sediment Capacity Equation for Non-Cohesive Sediments

For this tutorial case, the Engelund-Hansen capacity equation (EH) is used for the non-cohesive sediments. EH is the recommended choice for sandy rivers.

(11) Water Temperature

The average water temperature is chosen to be 25.0 °C for the case.

(12) Start Time of the Sediment Module

Press ENTER key to specify that the start time of the mobile bed module is the same as the flow solver (i.e., TSTART).

(13) Adaptation Coefficients

The recommended default values of the non-equilibrium suspended load adaptation coefficients are used (A_DEP,A_ERO): 0.25 1.0 The Sutherland saltation equation is selected to compute the bedload adaptation length by entering 1 0.0, where 1 selects the Sutherland equation, and 0.0 is a dummy value that SRH-2D does not use.

(14) Active Layer Thickness

Enter 1 0.01, where 1 means the active layer thickness is a constant and assigns a thickness of 0.01 meters.

(15) Cohesive Sediment

Enter 1 to specify that one type of cohesive sediment is present in the simulated system. Note that multiple types may be specified, and each type can be assigned to different mesh zones and in different bed layers.

(16) Cohesive Sediment General Property

Enter 58 EN to specify the dry bulk density of the cohesive sediment and the unit of the entry.

(17) Cohesive Sediment Fall Velocity

The fall velocity of the cohesive sediment is a function of the cohesive sediment concentration in the water column. For this tutorial, a file named fall_velo1.dat is used to provide the data of fall-velocity versus concentration as follows:

```
// CONC(kg/m3) Fall_Velocity(mm/s)
0.0 0.0
0.2 0.0012
6.0 0.015
20.0 0.015
100.0 0.0012
```

(18) Cohesive Sediment Erosion Rate Data

First, enter 0 to specify that the 4-parameter-method is adopted.

Next, the four erosion rate parameters, SS_es, SSs_em, Slope_s and Slope_m, are entered along with the unit. The entry for the case is: 0.125 2.84 0.25 1.07 EN

The entry specifies that SS_es = 0.125 lb/ft², SS_em = 2.84 lb/ft², Slope_s = 0.15 pounds per square feet per hour (lb/ft²/hr), and Slope_m = 1.07 lb/ft²/hr.

(19) Cohesive Sediment Deposition Rate Data

Three deposition parameters needed are: SS_df, SS_dp and Conc_eq along with the unit.

The entry for the tutorial case is: 0.005 0.021 3.0 EN

That is, Ss_df = 0.005 lb/ft², SS_dp = 0.021 lb/ft², and Conc_eq = 3.0 g/L.

Note that Conc_eq is always in the unit of grams per liter (g/L); the conversion from parts per million (ppm) to g/L may be done with: 1 g/L = 2,650 ppm.

(20) Initial Flow Condition

For mobile-bed modeling, the unsteady simulation is always performed. Therefore, a flow-only simulation is usually carried out first to establish the flow conditions at time TSTART. The constant-discharge flow results are stored in Flow/case_RST1.dat for the tutorial case. Therefore, the two initial condition entries are:

```
RST
Flow/case_RST1.dat
```

SRH-2D offers a convenient way to obtain the flow-only simulation so that the Flow/case_RST1.dat may be available for mobile-bed modeling. It is described in the Section 3.2.3 *Pre-Processing Summary*.

(21) Bed Property Spatial Distribution Option

Enter the option of UNIFORM so that the entire model domain will have the same bed subsurface properties, specified in the next step.

(22) Number of Bed Layers

Enter 2 for the number of bed layers.

(23) Bed Layer Properties

Enter 6.0 EN 1 to specify the properties of the top bed layer. It sets the top layer thickness to 6 ft and indicates that the cohesive class type 1 is present. The bed layer gradation is entered as:

```
CUMULATIVE 0.0625 10.0 .125 13.5 .25 33.3 .5 98.5 1. 99.6 2.0 100.0.
```

The cumulative distribution is at diameters (mm) and percentages 0.0625 at 10%, 0.125 at 13.5%, 0.25 at 33.3%, 0.5 at 98.5%, 1.0 at 99.6%, and 2.0 at 100%. Percentage refers to the cumulative distribution function of sediment volume with sediment diameter.

Thus, 0.0625 10.0 means 10% of the sediment volume is less than diameter 0.0625 mm. At diameter 2.0mm, 100% is less than 2 mm.

Next, enter the properties for the second bed layer. Similar to the top first bed layer, the second bottom layer uses the two entries below:

```
19.0 EN 1
CUMULATIVE 0.0625 80.0 .125 90.0 .25 99.0 .5 100.0
```

(24) Flow Roughness/Resistance Input

First, enter CONST NONE PERCENTAGE

The entries specify that a constant Manning's roughness coefficient for the bare bed will be specified over the model domain, no vegetation roughness is present, and the PERCENTAGE approach is used to compute the grain shear stress.

Next enter 0.027 100, where 0.017 is the bare-bed Manning's roughness coefficient and 100 specifies the bare-bed stress is used as the grain shear stress.

Finally, press ENTER to choose that no special modeling options will be used. .

(25) Inlet Boundary Condition

There is only one inlet for this tutorial case, so enter:

```
INLET-Q
q_500cfs.dat qs_option6.dat EN
```

INLET-Q specifies that a given discharge is provided along with the fractional sediment supply rates for the mobile-bed modeling. The file q_500cfs.dat contains the input hydrograph, while file qs_option6.dat contains a time series of fractional sediment rates. The entry of "EN" specifies that the discharge and sediment rate files are given with units of hours for time and cfs for water and sediment discharge rates.

The beginning portion of the q_500cfs.dat is shown in Figure 4:

```
//
// Daily flow at San Marcial USGS Gage from Oct 11 2000 to July 2010
// but Q less than 500 cfs is removed
// time(hour)   Q_daily(cfs)       year(not used)
//
0.00000000E+00  5.92000000E+02  2.000775956E+03
2.40000000E+01  6.54000000E+02  2.000786885E+03
4.80000000E+01  9.65000000E+02  2.000816940E+03
7.20000000E+01  7.64000000E+02  2.000819672E+03
9.60000000E+01  6.60000000E+02  2.000822404E+03
1.20000000E+02  6.24000000E+02  2.000825137E+03
1.44000000E+02  7.48000000E+02  2.000827869E+03
1.68000000E+02  8.21000000E+02  2.000830601E+03
1.92000000E+02  6.55000000E+02  2.000833333E+03
2.16000000E+02  7.72000000E+02  2.000836066E+03
2.40000000E+02  9.24000000E+02  2.000838798E+03
2.64000000E+02  9.12000000E+02  2.000841530E+03
2.88000000E+02  9.46000000E+02  2.000844262E+03
3.12000000E+02  7.70000000E+02  2.000846995E+03
3.36000000E+02  5.69000000E+02  2.000849727E+03
3.60000000E+02  5.40000000E+02  2.000857923E+03
3.84000000E+02  5.72000000E+02  2.000860656E+03
4.08000000E+02  5.77000000E+02  2.000863388E+03
4.32000000E+02  6.34000000E+02  2.000901639E+03
4.56000000E+02  5.25000000E+02  2.000909836E+03
4.80000000E+02  5.28000000E+02  2.000912568E+03
5.04000000E+02  5.12000000E+02  2.000915301E+03
```

Figure 4. The beginning portion of the q_500cfs.dat.

Note that the third column of the file is the time of the discharge and not used by SRH-2D.

The beginning portion of the qs_option6.dat file is shown in Figure 5:

```
TIME_SERIES
DIFFERENT_SIZE_CLASSES
6
0.0625 0.125 0.25 0.5 1.0 16.0
// t(hour) Qs1(cfs) Qs2(cfs) ... Rating_C: A=0.0582 N=1.5075
// Rating Curve: San_Marcial_RC/3.5 & June 12 2008 Gradation (24.7 11.7 38.6 24.9 0.1 0.0)
0.00000000E+00  3.03933983E-02  1.43968729E-02  4.74973754E-02  3.06394986E-02  1.23050195E-04  0.00000000E+00
2.40000000E+01  3.53173203E-02  1.67292570E-02  5.51922495E-02  3.56032905E-02  1.42985102E-04  0.00000000E+00
4.80000000E+01  6.34861824E-02  3.00724022E-02  9.92132244E-02  6.40002406E-02  2.57029079E-04  0.00000000E+00
7.20000000E+01  4.46444550E-02  2.11473734E-02  6.97682577E-02  4.50059486E-02  1.80746782E-04  0.00000000E+00
9.60000000E+01  3.58069039E-02  1.69611650E-02  5.59573478E-02  3.60968383E-02  1.44967222E-04  0.00000000E+00
1.20000000E+02  3.29037242E-02  1.55859746E-02  5.14203950E-02  3.31701512E-02  1.33213458E-04  0.00000000E+00
1.44000000E+02  4.32425152E-02  2.04832967E-02  6.75773719E-02  4.35926570E-02  1.75070912E-04  0.00000000E+00
1.68000000E+02  4.97595675E-02  2.35703215E-02  7.77619153E-02  5.01624790E-02  2.01455739E-04  0.00000000E+00
1.92000000E+02  3.53987599E-02  1.67678336E-02  5.53195195E-02  3.56853895E-02  1.43314817E-04  0.00000000E+00
2.16000000E+02  4.53510523E-02  2.14820774E-02  7.08724946E-02  4.57182672E-02  1.83607499E-04  0.00000000E+00
2.40000000E+02  5.94640910E-02  2.81672010E-02  9.29276888E-02  5.99455816E-02  2.40745308E-04  0.00000000E+00
2.64000000E+02  5.83037524E-02  2.76175669E-02  9.11143661E-02  5.87758476E-02  2.36047581E-04  0.00000000E+00
2.88000000E+02  6.16112721E-02  2.91842868E-02  9.62832026E-02  6.21101488E-02  2.49438349E-04  0.00000000E+00
3.12000000E+02  4.51740529E-02  2.13982356E-02  7.05958883E-02  4.55398347E-02  1.82890902E-04  0.00000000E+00
3.36000000E+02  2.86309679E-02  1.35620374E-02  4.47431320E-02  2.88627976E-02  1.15914850E-04  0.00000000E+00
3.60000000E+02  2.64598806E-02  1.25336277E-02  4.13502588E-02  2.66741307E-02  1.07125023E-04  0.00000000E+00
3.84000000E+02  2.88588354E-02  1.36699747E-02  4.50992327E-02  2.90925102E-02  1.16837390E-04  0.00000000E+00
4.08000000E+02  2.92399635E-02  1.38505090E-02  4.56948418E-02  2.94767243E-02  1.18380419E-04  0.00000000E+00
4.32000000E+02  3.37018580E-02  1.59640380E-02  5.26676809E-02  3.39747475E-02  1.36444769E-04  0.00000000E+00
4.56000000E+02  2.53597190E-02  1.20124985E-02  3.96309779E-02  2.55650609E-02  1.02670927E-04  0.00000000E+00
4.80000000E+02  2.55784914E-02  1.21161275E-02  3.99728651E-02  2.57856047E-02  1.03556645E-04  0.00000000E+00
5.04000000E+02  2.44190494E-02  1.15669182E-02  3.81609437E-02  2.46167745E-02  9.88625483E-05  0.00000000E+00
5.28000000E+02  2.40604523E-02  1.13970563E-02  3.76005448E-02  2.42552737E-02  9.74107379E-05  0.00000000E+00
```

Figure 5. The beginning portion of the qs_option6.dat file

Normally, sediment transport rates should be provided for each of the 8 sediment size classes, as specified earlier. In the above example, however, a special feature of the entry is used: the fractional sediment rates at the inlet are given in 6 size classes rather than 8. This difference is flagged by the entry "DIFFERENT_SIZE_CLASSES," And the 6 classes are entered as:

```
0.0625
0.125
0.25
0.5
1.0
16.0
```

(26) Exit Boundary Condition

There is only one exit at the downstream of the model domain. Since no data is available at the location and the exit is in a relatively straight and constant cross-section channel, the normal depth boundary condition is used. So only two entries are needed:

```
EXIT-ND
9
5.0e-4
```

EXIT-ND specifies that the normal depth boundary condition is applied so the water surface elevation at the exit is computed from the total discharge at a cross-section upstream and the equilibrium channel slope at the exit.

The entry "9" specifies that the discharge used to compute the water elevation at the exit is based on the total discharge computed at monitor line number 9 (to be entered next). The entry "5.0e-4" is the anticipated slope at the exit.

(27) Monitor Lines

A total of 9 monitor lines are created for the tutorial cases so 9 entries of "MONITOR" are needed for the case. Note that monitor line 9 is used by the normal depth boundary condition at the exit.

Three entries of the ENTER key are used next for the tutorial case to skip over the following three options: (a) Extra Roughness at Walls; (b) Pressure Zone Setup; and (c) Instream Flow Obstructions.

(28) Results Output Format

For the tutorial case, the following entry is used: TEC EN

It specifies that TECPLOT format and English unit are selected for the output of the model results. Users can easily change the output format once the SIF file is created.

(29) Output Maximum Value File

An option is offered to output a file, _MAX.dat, that contains the maximum values of the following variables: WSE WD VELOCITY FROUD STRESS_STRESS, along with the times at which the maximum values occurred for each variable. This option is not used for this tutorial case, so simply press the ENTER key.

(30) Output Interval

The entry for the tutorial case is “-1”, which specifies that no intermediate outputs will be generated and that the output only provides final results.

3.2.3. Pre-Processing Summary

The above completes the interactive pre-processing stage. Once completed, the Script Output File (SOF) is created with the name case_SOF.dat. The SOF file should be renamed as SIF immediately (e.g., case_SIF.dat) so that the SIF file can be used for future modeling needs (e.g., repeat and parametric runs or error corrections).

The SOF file contains all user entries during the interactive process. Once renamed to case_SIF.dat, it may be used to re-run the pre-processor by selecting 2 in the SELECT-INPUT-METHOD prompt. The SRH-2D simulation may be repeated exactly as it was done before with the SIF file. Also, users may modify the SIF directly.

The SOF file of the tutorial case is listed below as a reference:

```
// Simulation Description:  
Sediment Modeling with Temp channel of Rio Grande  
// Module/Solver Selected  
MOBILE  
// Monitor-Point-Info: NPOINT + (x y) coordinates  
2  
1393300 940794.5 1358678.8 857885.5  
// Time_Step and Total_Simulation_Time: TSTART DT T_SIMU [FLAG]  
0.0 5.0 1000.0  
// Turbulence-Model-Selection(PARA or KE) + Model Constant (A_Turb)  
PARA  
0.7  
// Mesh-Unit + // Mesh FILE_NAME and FORMAT(SMS...)  
FOOT
```

```

mesh1999.2DM SMS
// General Sediment Parameters: spec_grav & total number of size classes (#1 is cohesive
material)
2.65 8
// Diam_Lower(mm) Diam_Upper(mm) [Den_Bulk] [SI/EN] for each size class
0.0025 0.0625 500.0 SI
0.0625 0.125
0.125 0.177
0.177 0.25
0.25 0.354
0.354 0.5
0.5 1.0
1.0 16.0
// Sediment Capacity Equation for non-cohesive sediment
EH
// Water Temperature (Celsius):
25.0
// Start time of Sediment module

// Non-Equilibrium Coef for Suspended Load: A_DEP A_ERO
0.25 1.0
// Bedload Adaptation Length: mod_adap_lng Length (0=const;1=Sutherland; 2/3=van
Rijn)
1 0.0
// Active Layer Thickness: MOD_ALayer NALT
1 0.01
// MOD_COHESIVE
1
// Cohesive class general properties: Dry Bulk Density and UNIT
58 EN
// Cohesive Sediment Fall Velocity Method
fall_velo1.dat
// Cohesive Sediment Erosion Rate data: 0 means the 4-parameter-method; or a filename
0
// Cohesive Sediment Erosion rate parameters: ss_es ss_em slope_s slope_m
0.125 2.84 0.25 1.07 EN
// Cohesive Deposition Parameters (lb/ft2 lb/ft2 kg/m3): ss_df ss_dp conc_eq
0.005 0.021 3.0 EN
// Initial Condition Method (DRY RST AUTO ZONAL)
RST
// Restart File Name for initial condition setup
Flow/case_RST1.dat
// Bed Property Spatial Distribution Method (UNI ZON POINT)
UNIFORM
// Number of Bed Layers
2

```

```

// Top Layer Properties: Thickness(ft or m) Unit(EN or SI) Type_ID
6.0 EN 1
// Top Layer gradation: CUMULATIVE data (di Pi); 10% silt/clay
CUMULATIVE 0.0625 10.0 .125 13.5 .25 33.3 .5 98.5 1. 99.6 2.0 100.0
// Bottom Layer properties + gradation
19 EN 1
CUMULATIVE 0.0625 80.0 .125 90.0 .25 99.0 .5 100.0
// Flow roughness entry
CONST NONE PERCENTAGE
// Constant Manning Coefficient + percentage of bare-bed stress for grain stress
0.017 100
// Any-Special-Treatments? (0 or empty = NO; 1=YES)

// Boundary Type (INLET-Q EXIT-H etc) + Q Qs UNIT
INLET-Q
q_500cfs.dat qs_option6.dat EN
// Boundary Type (INLET-Q EXIT-H etc): Normal-Depth BC is used
EXIT-ND
// Monitor-ID that is where Q is computed + Bed Slope intended at the exit
9 5.0e-4
// first 8 Monitor lines
MONITOR
MONITOR
MONITOR
MONITOR
MONITOR
MONITOR
MONITOR
MONITOR
// Monitor line #9 --> on RM 42.5, used for exit_normal Q computation
MONITOR
// Wall-Roughness-Height-Specification (empty-line=DONE)

// Pressurized Zone exists? (empty-line or 0 == NO)

// Any In-Stream Flow Obstructions? (empty-line or 0 = NO)

// Results-Output-Format-and-Unit
TEC EN
// _MAX.dat file output?

// Intermediate Result Output Control: METHOD INTERVAL
-1

```


3.2.4. Flow-Only Simulation Option

SRH-2D offers a convenient way to obtain a constant-discharge flow-only simulation so that an initial condition file, e.g. Flow/case_RST1.dat for the tutorial case, may be available for mobile-bed modeling.

To make the flow-only run after the SIF file has been created in the MOBILE setup:

- Create a local directory as “Flow” and copy relevant files from the mobile directory to Flow directory (case_SIF.dat and fall_velo1.dat for the tutorial case)
- Open case_SIF.dat file created above
- Go to the 2D mesh entry line, and change the mesh file input to: ..\mesh1999.2DM SMS for the case so that the 2D mesh file does not need to be copied into the Flow directory
- Go to “// Initial Condition Method” line; change “RST” to “DRY” and then comment out the RST file input “Flow/case_RST1.dat”
- Go to “// Boundary Type” and “INLET-Q” lines; replace the entry “q_sanmarcial_500cfs.dat qs_option6.dat EN” with the values “592.0 1 0 0 0 0 0 0 0 EN”. This is to specify that the inlet has a constant discharge of 592 cfs, corresponding to the discharge at time 0 in the q_500cfs.dat.
- Save the case_SIF.dat file
- Open case_DIP.dat file or create one if it does not exist
- Add line “USER(9)=1” to the DIP file and save it
- Click SRH2D_Pre.bat to run the pre-processor
- Click SRH2D.bat to run the flow-only simulation
- Once steady state results are reached, the case_RST1.dat should have been created which may be used as the initial condition for the MOBILE run

The case_DIP.dat file used to make the flow-only simulation is shown below:

```
$DATAC
irest = 0
dtnew = 5.0
niter = 1
total_simulation_time = 200.0
user(9) = 1
$ENDC
```

3.2.5. Mobile-Bed Simulation

The mobile-bed run now can be carried out by simply clicking the SRH2D.bat. The pop-up screen looks like Figure 6:

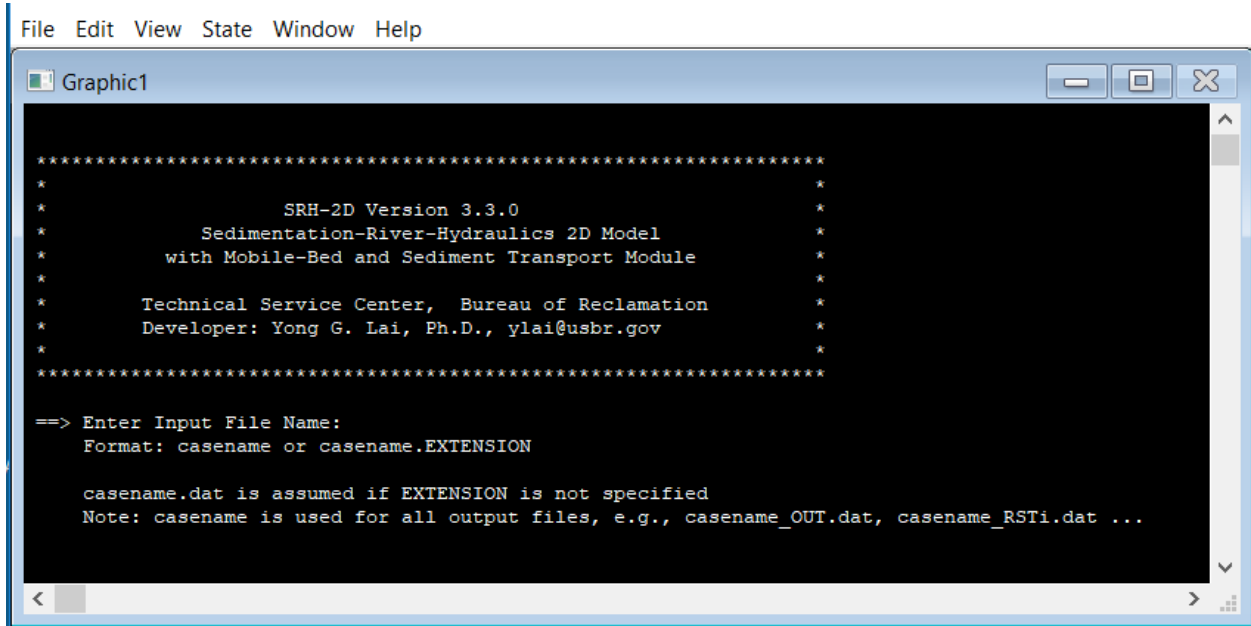


Figure 6. Screenshot of pop-up screen to run the mobile-bed simulation

By entering the case name “case” for the case, SRH-2D starts to simulate with the following windows. A window will pop up that displays the bed elevation changes with time at the first two monitor points (Figure 7). The red line on the left y axis is the first monitor point elevation, and the blue one on the right axis is for the second monitor point if it is specified by the user.

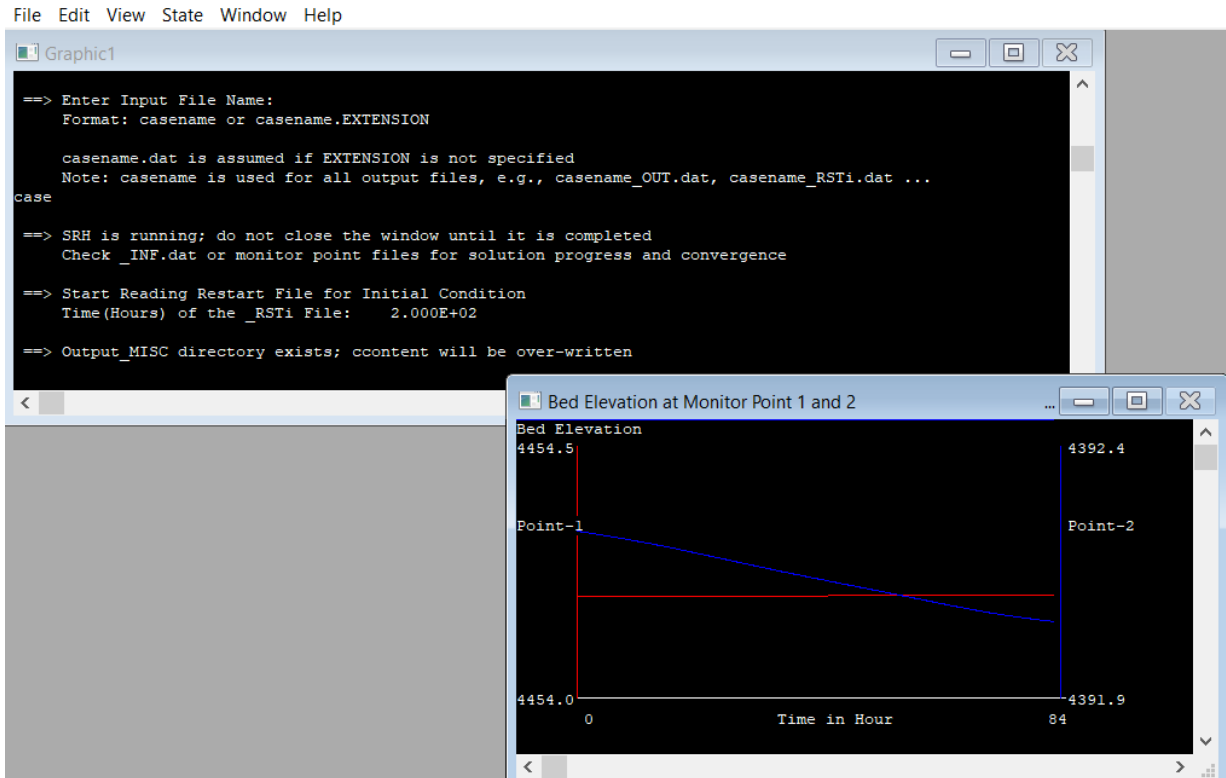


Figure 7. Screenshot of bed elevation changes with time at the first two monitor points.

The case_DIP.dat used to run the mobile-bed for the tutorial case is:

```

$DATAC
irest = 0
dtnew = 5.0
Total_simulation_time=1000
time_interval =50.0
itime_freq = 100
$ENDC

```

The DIP specifies that the time step of the simulation is 5 seconds and the total modeling time is 1,000 hours. DIP file further specifies that the intermediate results will be output every 50 hours, so users should expect a total of 20 outputs; e.g., 20 RSTi files and 20 TECi files for the tutorial case. The time stamp of each output file is stored in the file case_TSO.dat and it is shown below for the tutorial case:

```
*****
* Time Series Output Correspondence between index i and Actual time *
* _RSTi.dat _SRHi.dat etc: i refers to time as shown below *
*****
i_Index ITIME TIME(hour) = 1 36000 50.00
i_Index ITIME TIME(hour) = 2 72000 100.00
i_Index ITIME TIME(hour) = 3 108000 150.00
i_Index ITIME TIME(hour) = 4 144000 200.00
i_Index ITIME TIME(hour) = 5 180000 250.00
i_Index ITIME TIME(hour) = 6 216000 300.00
i_Index ITIME TIME(hour) = 7 252000 350.00
i_Index ITIME TIME(hour) = 8 288000 400.00
i_Index ITIME TIME(hour) = 9 324000 450.00
i_Index ITIME TIME(hour) = 10 360000 500.00
i_Index ITIME TIME(hour) = 11 396000 550.00
i_Index ITIME TIME(hour) = 12 432000 600.00
i_Index ITIME TIME(hour) = 13 468000 650.00
i_Index ITIME TIME(hour) = 14 504000 700.00
i_Index ITIME TIME(hour) = 15 540000 750.00
i_Index ITIME TIME(hour) = 16 576000 800.00
i_Index ITIME TIME(hour) = 17 612000 850.00
i_Index ITIME TIME(hour) = 18 648000 900.00
i_Index ITIME TIME(hour) = 19 684000 950.00
i_Index ITIME TIME(hour) = 20 720000 1000.00
```

This example shows that i_Index 10 is at Time(hour) = 500, so users know the output file case_TEC10.dat represents conditions at time = 500 hours.

3.2.6. Results

The model results after 1,000 hours may be graphically inspected and processed in many ways. For example, the net erosion and deposition depths are plotted as Figure 8 as a reference.

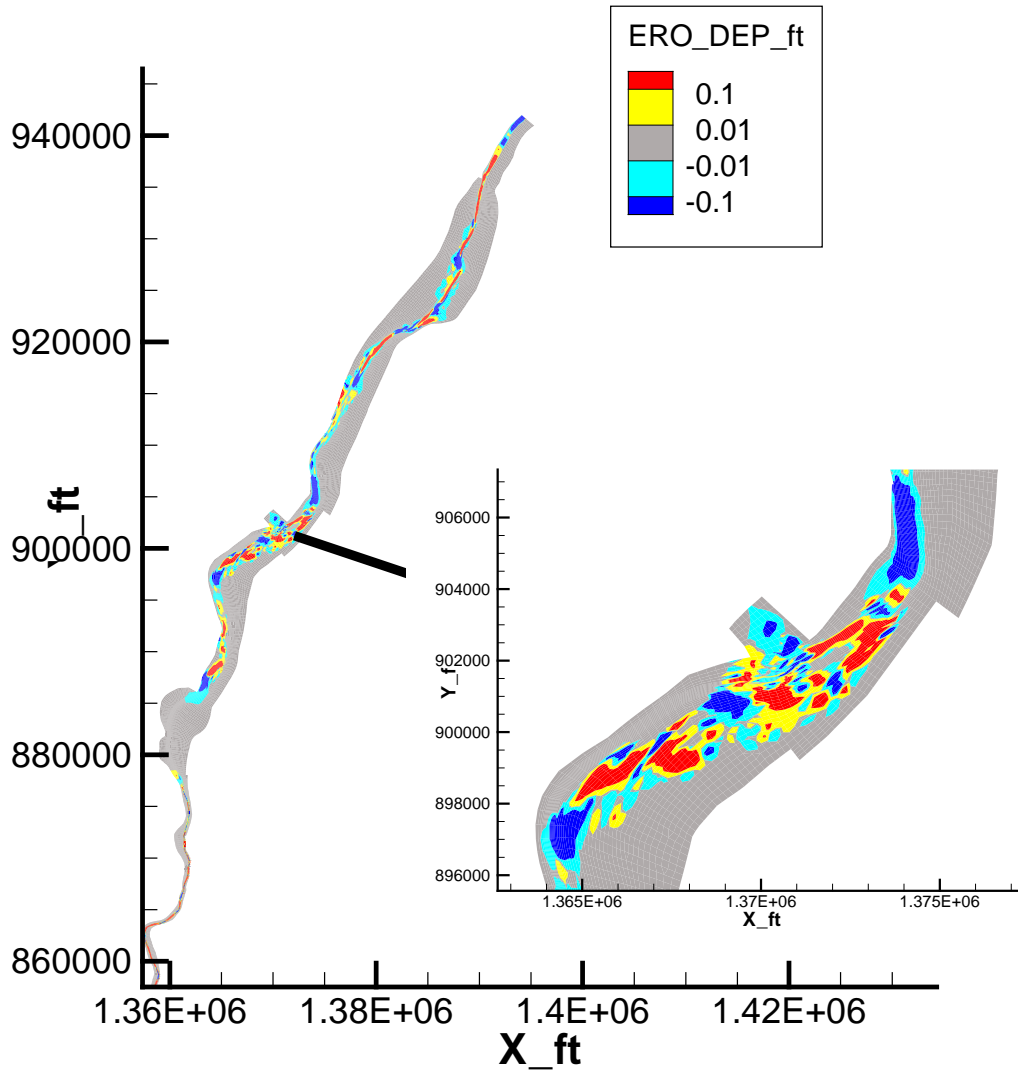


Figure 8. Sample plot of the net erosion and deposition depths.

Chapter 4. Mathematical Equations

An alluvial river is a complex dynamic system governed by a set of mathematical equations describing various interacting physical processes. In this chapter, all relevant governing equations adopted by SRH-2D are presented and discussed.

In general, the mathematical equations for alluvial rivers may be divided into four categories corresponding to four interrelated physical processes:

- **Hydraulic flow.** Flow hydrodynamics described in detail in the User's Manual of SRH-2D version 2 (Lai, 2008).
- **Sediment transport** described in this chapter (see also Lai 2020)
- **Bed dynamics** described in this chapter (see also Lai 2020)
- **Bank erosion.** The bank erosion module is still under research and development and has not been released in the current version. The bank erosion modeling was described by Lai (2014 and 2017) and Lai et al. (2015) if readers are interested.

4.1. Flow Equations

4.1.1. Flow Solver

The flow solver is based on the verified model of Lai (2008) and Lai (2010). Details may be found from these references; only the governing equations are presented herein. The 2D depth-averaged flow equations are:

$$\begin{aligned} \frac{\partial h}{\partial t} + \frac{\partial(hU)}{\partial x} + \frac{\partial(hV)}{\partial y} &= 0 \\ \frac{\partial hU}{\partial t} + \frac{\partial hUU}{\partial x} + \frac{\partial hVU}{\partial y} &= -gh \frac{\partial z}{\partial x} + \frac{\partial(hT_{xx})}{\partial x} + \frac{\partial(hT_{xy})}{\partial y} - \frac{\tau_{bx}}{\rho} \\ \frac{\partial hV}{\partial t} + \frac{\partial hUV}{\partial x} + \frac{\partial hVV}{\partial y} &= -gh \frac{\partial z}{\partial y} + \frac{\partial(hT_{xy})}{\partial x} + \frac{\partial(hT_{yy})}{\partial y} - \frac{\tau_{by}}{\rho} \end{aligned}$$

Where: x and y are horizontal Cartesian coordinates, t is time, h is water depth, U and V are depth-averaged velocity components in x and y directions, respectively, g is gravitational acceleration, T_{xx} , T_{xy} and T_{yy} are depth-averaged stresses due to turbulence and dispersion, $z = z_b + h$ is water surface elevation, z_b is bed elevation, ρ is water density, and τ_{bx} and τ_{by} are the total bed shear stresses.

4.1.2. Bed Stresses

The total bed stresses are computed by the Manning's equation:

$$(\tau_{bx}, \tau_{by}) = \rho U_*^2 \frac{(U, V)}{\sqrt{U^2 + V^2}} = \rho C_f \sqrt{U^2 + V^2} (U, V)$$

where $C_f = gn_t^2/h^{1/3}$, n_t the total Manning's roughness coefficient, and U_* is bed frictional velocity.

Effective stresses are computed by:

$$T_{xx} = 2(\nu + \nu_t) \frac{\partial U}{\partial x}$$

$$T_{yy} = 2(\nu + \nu_t) \frac{\partial V}{\partial y}$$

$$T_{xy} = (\nu + \nu_t) \left(\frac{\partial U}{\partial y} + \frac{\partial V}{\partial x} \right)$$

where ν is kinematic viscosity of water, and ν_t is eddy viscosity of turbulence.

4.1.3. Turbulence Model

The turbulence eddy viscosity needs a turbulence model. Two models are adopted (Rodi 1993): the depth-averaged parabolic model and the two-equation k- ϵ model. With the parabolic model, the eddy viscosity is calculated by $\nu_t = C_t U_* h$. The model constant C_t may range from 0.3 to 1.0; but the default value of $C_t = 0.7$ is recommended. The k-model computes the eddy viscosity by $\nu_t = C_\mu k^2/\epsilon$ and the two additional partial difference equations for k and ϵ are solved. The two turbulence equations are not presented in this manual. See Lai (2008) or Lai (2010) for further details.

4.2. Shear Stress Partition

The total Manning's roughness coefficient, (i.e., the total shear stress), is sufficient for flow-only simulation and is usually calibrated using available water surface elevation data.

For sediment transport modeling, however, the total shear stress should be split into at least two portions: grain shear stress and form drag. The grain shear stress is primarily responsible for sediment entrainment and movement while form drag is the rest of the flow resistance.

In SRH-2D sediment modeling, the total shear stress is split into the bare-bed term (τ_{bare}) and vegetation term (τ_V) as follows:

$$\tau_b = \tau_{bare} + \tau_V$$

And the bare-bed term consists of two contributions (grain and form roughness):

$$\tau_{bare} = \tau_g + \tau_f$$

Where τ_g is grain and τ_f is form roughness. Each term is determined using the Manning's equation as:

$$\tau_i = \frac{\rho g n_i^2}{h^{1/3}} V_t^2$$

where the Manning's roughness coefficient, n_i , is used to represent each shear stress term (grain, form, non-vegetation, or vegetation). This means the total Manning's roughness coefficient is computed by:

$$n_t = \sqrt{n_{bare}^2 + n_v^2} = \sqrt{n_g^2 + n_f^2 + n_v^2}$$

In SRH-2D, users may specify the bare-bed and vegetation Manning's roughness coefficients separately—so that the vegetation stress does not contribute to the sediment transport. Further, two options are used to obtain the grain stress from the bare-bed stress. The first option is for users to provide the ripple factor r_f so that $\tau_g = r_f \tau_{bare}$. This is a recommended option for the sandy rivers. According to Defina (2003), $r_f = 0.74$ was used for beds with ripples and small dunes. In general, the ripple factor may range from 0.5 (strong bedform) to 1.0 (plane bed). The side wall correction may also be included in the ripple factor which tends to decrease the grain stress.

In the second approach, the Manning's roughness coefficient attributed to the bed material grains is computed from the effective roughness height with the following formula (García, 2008):

$$n_g = \frac{k_e^{1/6}}{8.1\sqrt{g}}$$

The effective roughness height (k_e) is a representation of sediment grain sizes and several relations have been proposed for alluvial rivers which ranged from $0.95D_{50}$ to $3D_{90}$. López and Barragán (2008) found that $2.4D_{90}$, $2.8D_{84}$, and $6.1D_{50}$ all gave equivalent predictions of Manning's roughness coefficient for riverbeds with gravel size or larger sediment with a non-sinusuous alignment and a flow path free of vegetation or obstacles. In SRH-2D, $k_e = r_g D_{90}$ is adopted with the constant r_g a user input (1.5 to 4.0 is recommended). The second approach is generally more applicable to gravel or mixed sand-gravel rivers. Note that Wu and Wang (1999) proposed a similar approach which adopted the following equation: $n_g = \frac{d_{50}^{1/6}}{20}$, which is equivalent to the Garcia approach above by adopting $k_e = 4.164d_{50}$.

In modeling applications, users need only to enter two Manning's roughness coefficients: bare-bed coefficient ($n_{bare} = \sqrt{n_g^2 + n_f^2}$) and vegetation coefficient (n_v). Normally, the total

roughness should still be calibrated with the measured water surface elevation data; but the grain roughness is computed by SRH-2D using the above approaches.

Note that the above grain stress is relevant to only those sediment capacity equations that use the bed shear stress. Some equations are not impacted such as van Rijn, Ackers and White, and Laursen.

4.3. Representation of Vertical Layers

Sediment transport and bed morphological changes in a river depend on many variables such as flow hydraulics, bed gradation, bank properties, and upstream sediment supply. The bed gradation changes from its initial state as sediment particles are eroded from or deposited on the bed. In turn, changes in river morphology also alter flow hydraulics and sediment transport rates.

In general, the water column and channel bed may be divided into four separate vertical layers as shown in Figure 9 for numerical modeling purposes:

- **Suspended.** The suspended layer is in the water column where sediment particles are in suspension and transported as suspended load. Wash load is a special class of the suspended load that moves with the water and has negligible fall velocity (i.e., it does not interact with sediments on the bed and so is excluded from the bed materials).
- **Bed load.** The bed load layer is the water column near the riverbed where sediment particles roll, slide, or saltate. Sediments in the bed load layer are transported as bed load.
- **Active.** The active layer is a thin layer at the top of the riverbed where sediment exchange occurs between the sediments in the water column and those in the subsurface layer. The active layer is used primarily for numerical modeling purpose.
- **Subsurface.** The subsurface layer represents the bed materials underneath the active layer. Often one or a number of sub-layers may be used for representation of vertical stratigraphy. Note that the vertical sediment distribution is important if erosion is of interest. Physical processes within each layer are different and may be modeled separately. In particular, sediment exchanges between layers occur and have to be modeled.

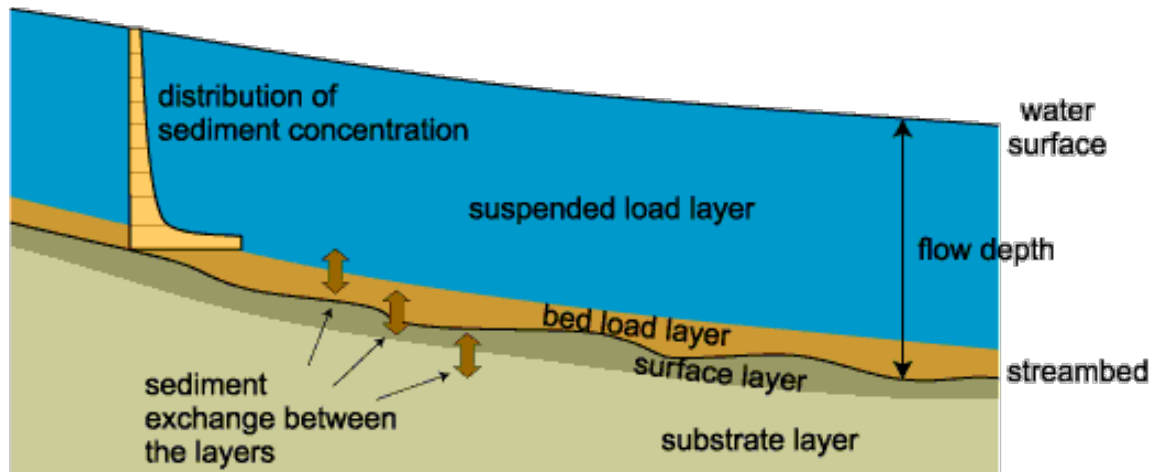


Figure 9. Schematic illustrating four vertical layers.

4.4. Sediment Transport Equations

4.4.1. Introduction

Sediment transport in a water column includes both suspended load and bed load. Two approaches are widely used. The two-load approach treats the suspended load and the bed load separately, while the total load approach simulates the suspended and bed load together.

- Two-load.** The two-load approach adopts two sets of governing equations and has the capability of incorporating more physical processes into modeling; it, however, suffers from modeling complexities. For example, it is still uncertain how to separate the two transport modes—additional information is required concerning the sediment exchange between the two loads. Laboratory-based empirical formulae have been developed for the inter-mode exchange, but their accuracy is questionable for natural rivers. In the field, load may change its transport mode frequently in response to local flow changes. This imposes further challenges to numerical modeling.
- Total load.** The total load approach adopts a simpler strategy by modeling the combined transport of the two loads. This approach eliminates the need for the inter-mode exchange modeling and is simpler in model interpretation and sediment accounting. The method offers also savings in computing time by reducing the number of sediment transport equations. In our view, the total load approach is consistent with the spirit of modeling with the depth-averaged equations. For limited applications where separate treatment of suspended load and bed load is needed, three-dimensional modeling may have to be used.

SRH-2D adopts the variable-load approach, a variant of the total load approach, as described by Greimann et al. (2008). Our new variable-load formulation overcomes several weaknesses of the existing approaches and has these features:

- **Variable-load sediment transport equation.** One variable-load sediment transport equation is adopted for all modes of sediment transport. A transport mode parameter is introduced to model suspended load, bed load, or mixed load. The mixed load refers to those sediment classes a portion of which are transported as suspended load and the rest of which are the bed load. Combined with the non-uniform representation of sediments, all transport modes are modeled simultaneously.
- **Sediment movement velocity.** The sediment movement velocity may be explicitly tracked and is continuous in transition from suspended load, to mixed load, and to bed load. This option is particularly useful to simulate the movement of bed load sediments after their release from a source in unsteady modeling.
- **Lateral sediment movement.** The lateral sediment movement caused by secondary flows and gravity force is incorporated in the variable-load transport equation. This option is needed for flows with meander bends.

4.4.2. Variable-Load Equation

The derivation of the variable-load sediment transport equation was reported by Greimann et al. (2008). The final equation is presented below.

The entire range of possible sediments in the simulated river system are divided into an arbitrary number of sediment size classes, say N_{sed} size classes. Each size class k in the water column is governed by the following non-equilibrium mass conservation equation:

$$\frac{\partial hC_k}{\partial t} + \frac{\partial \cos(\alpha_k)\beta_k V_t hC_k}{\partial x} + \frac{\partial \sin(\alpha_k)\beta_k V_t hC_k}{\partial y} = \frac{\partial}{\partial x} \left(hf_k D_x \frac{\partial C_k}{\partial x} \right) + \frac{\partial}{\partial y} \left(hf_k D_y \frac{\partial C_k}{\partial y} \right) + S_{ek}$$

In the above, subscript k denotes that the variable is for sediment size class k , C_k is the depth-averaged sediment concentration by volume, $\beta_k = V_{sed,k}/V_t$ is the sediment-to-flow velocity ratio, $V_t = \sqrt{U^2 + V^2}$ is the depth-averaged flow velocity, α_k is the angle of the sediment transport direction relative to x -axis, f_k is the transport mode parameter representing the suspended load fraction, D_x and D_y are the sediment mixing coefficients in the x - and y -directions, respectively, and S_{ek} is the sediment exchange rate between sediments in the water column and those in the active layer or on the bed. The above equation was derived from the mass conservation law by Greimann et al. (2008) and took the non-equilibrium nature of a sediment load into account.

Auxiliary relations are needed for five variables in the above equation; they are the transport mode parameter f_k , sediment transport direction α_k , velocity ratio β_k , exchange term $S_{e,k}$, and mixing coefficients D_x and D_y .

4.4.3. Sediment Transport Mode Parameter

The sediment transport mode parameter f_k is introduced to represent the percentage of sediments transported as the suspended load. A similar parameter was introduced by Holly and Rahuel (1990) as the “allocation coefficient.” An empirical equation developed by Greimann et al. (2008) is used as follows:

$$f_k = \text{Min}(1.0, 2.5e^{-Z_k})$$

In the above, $Z_k = \omega_{sed,k} / (\kappa U_*)$ is the suspension parameter, $\omega_{sed,k}$ is the particle fall velocity and κ is von Karmán constant (0.41). If bed load is dominant, $f_k = 0$ is used; $f_k = 1$ is used for suspended load.

4.4.4. Currents and Gravity Force

The sediment movement direction is assumed to be coincident with the depth-averaged velocity direction for the suspended load, but it may deviate from the flow velocity for the bed load if there are secondary currents. Several approaches may be used to include the effect of secondary flows and gravity force effect. The approach of Struiksmá and Crosato (1989) is adopted by SRH-2D. In this approach, the actual sediment transport angle is computed as:

$$\tan(\alpha_k) = \frac{\sin(\delta_k) - \frac{(1-f_k)C_{g1}}{0.85\sqrt{\theta_k}} \frac{\partial Z_b}{\partial y}}{\cos(\delta_k) - \frac{(1-f_k)C_{g1}}{0.85\sqrt{\theta_k}} \frac{\partial Z_b}{\partial x}}$$

In the above, $\theta_k = \tau_b / [\rho g(s-1)d_k]$ is the Shields parameter (τ_b is the bed shear stress, $s = \frac{\rho_s}{\rho} - 1$, ρ_s is the sediment density, d_k is the sediment diameter for size class k), C_{g1} is the particle shape factor, and δ_k is the angle of the bed shear stress. The study of Talmon et al. (1995) suggested that C_{g1} ranged from 0.5 to 1.0, with 0.5 for laboratory cases and 1.0 for field cases. A default value of 0.75 is used by SRH-2D. The bed shear stress angle includes the flow direction and secondary flow effect and is computed by:

The bed shear stress angle reflects the effect of the secondary current (or spiral motion) and the sediment size, and is computed as:

$$\delta_k = \tan^{-1}\left(\frac{V}{U}\right) - (1-f_k)\tan^{-1}\left[\frac{2C_{spi}}{\kappa^2}\left(1 - \frac{n\sqrt{g}}{\kappa h^{1/6}}\right)\frac{h}{R_c}\right]$$

In the above, the second term on the right-hand side is the deviation of the bed shear stress from the depth averaged flow direction due to secondary currents and induced by the flow curvature. In the equation, R_c is the local radius of curvature of flow streamlines, and C_{spi} is a model coefficient (1.0).

4.4.5. Sediment Movement Velocity

The ratio of sediment-to-flow velocity, β_k , was assumed to be 1.0 by most previous studies, which is adequate for many applications. For some applications, such as the unsteady movement of a specified sediment load from a reservoir outlet or a plug, the ratio is not 1.0, and an empirical relation should be developed. In SRH-2D, the modified equation of Greimann et al. (2008) is used as:

$$\beta_k = \text{Max}(\beta_{k,sus}, \beta_{k,bed})$$

$$\beta_{k,bed} = \frac{U_*}{V_t} \frac{1.1\Phi_k^{0.17}[1-\exp(-5\Phi_k)]}{\sqrt{\theta_r}}; \quad \Phi_k = \frac{\theta_k}{\theta_r} < 20$$

$$\beta_{k,sus} = 1 + \frac{U_*}{2\kappa V_t} [1 - \exp(2.7Z_k)]; \quad Z_k < 1.0$$

where θ_r is the reference Shields parameter with a default value of 0.045. In field applications, the critical Shields parameter in the above equations may be viewed as a calibration parameter.

4.4.6. Sediment Exchange Between Water Column and Bed

The sediment exchange term has traditionally been modeled separately for the suspended load and bed load as:

$$S_{e,k} = \begin{cases} \zeta \omega_{s,k} (C_{s,k}^* - C_{s,k}) & \text{for suspended load} \\ \frac{1}{L_{b,k}} (q_{t,k}^* - q_{b,k}) & \text{for bed load} \end{cases}$$

where ζ is a parameter for the rate of suspended load exchange, $C_{s,k}^*$ is the suspended load sediment transport capacity, $q_{t,k}^*$ is the equilibrium capacity for the bed load transport rate (volume sediment rate per unit width), and $L_{b,k}$ is the bed load adaptation length (Holly and Rahuel, 1990).

SRH-2D uses a single sediment rate equation which is related to the sediment transport capacity:

$$S_{e,k} = \frac{1}{L_{t,k}} (q_{t,k}^* - \beta_k V_t h C_k)$$

$$L_{t,k} = (1 - f_k) L_{b,k} + f_k \zeta V_t h / \omega_{s,k}$$

The non-equilibrium adaptation length characterizes the distance for sediments to adjust from a non-equilibrium state to an equilibrium state, and is related to the scales of sediment transport, bedform and geometry. It is also a function of the sediment size such that an increase in size leads to a decrease in the adaptation length. Note that the selection of proper $L_{b,k}$ is relevant only for problems where non-equilibrium sediment transport is important. This is usually the case for local scours due to in-stream structures and channel contraction, channel incision

downstream of a dam, bed discontinuity, or rapid unsteady transport. Very small values for $L_{b,k}$ (e.g., 1.e-6) may be used to simulate the case of equilibrium transport. For non-equilibrium transport, however, several methods may be used. For example, Thuc (1991) applied the sand ripple length, Rahuel et al. (1989) used the numerical mesh size, while Wu (2004) recommended the dominant length of bedforms such as sand dunes and alternate bars. Gaeuman et al. (2014) reviewed these methods.

In SRH-2D, several options are provided:

1. A constant $L_{b,k}$ may be specified.
2. Saltation Length Formula (Philips and Sutherland, 1989):

$$L_{b,k} = C_{sl}(\theta_k - \theta_c)d_k \text{ for } \theta_k > \theta_c = 0.045$$

In the above, C_{sl} is a model constant with a default value of 4,000 used by SRH-2D. The saltation length may be used if the bed form is predominately ripple such as those occur often in the flumes.

3. Dune Length Formula (van Rijn, 1984c):

$$L_b = 7.3h$$

The dune length formula may be used if dune is the dominant bed form.

Determining the suspended sediment coefficient, ζ , relies on empirical data. Studies by Han (1980) and Han and He (1990) suggested that a constant ζ ranging from 0.25 to 1.0 may be used, and its value depended on whether the bed had net deposition or erosion. In SRH-2D, ζ equals 1.0 for net erosion and 0.25 for net deposition. Another option was recommended by Armanini and Di Silvio (1988) who suggested that ζ was not a constant. The relationship proposed by Armanini and dSilvio (1988) is:

$$\zeta = \eta + (1 - \eta)\exp\left(-1.5\eta^{-1/6} \varpi_{s,k}/U_*\right)$$

where η is the relative roughness height computed as: $\eta = 33\exp(-1 - \kappa V_t/U_*)$.

4.4.7. Sediment Mixing and Dispersion

The mixing coefficients, D_x and D_y , include both horizontal sediment mixing due to turbulence and dispersion due to depth averaging. Currently, SRH-2D sets these mixing coefficients to zero as their importance has not been demonstrated based on our experience. There is also a lack of study on the subject. The mixing terms can be turned on if necessary, and users who have such needs may contact the model developer on how to include them.

4.4.8. Equilibrium Sediment Transport Equations

The total load transport capacity (q_t^*) may be obtained with many existing sediment capacity equations. Several equations have been selected by SRH-2D due to their consistently good predictions with many cases tested at Reclamation. They include the Engelund and Hansen (1972) equation for sandy rivers, Meyer-Peter and Muller equation (1948) for gravel rivers, and Parker (1990) and Wilcock and Crowe (2003) equations for mixed sand-gravel rivers. Some of the equations are discussed below.

The Engelund-Hansen sediment transport equation is a popular choice for sandy rivers due to its simplicity and relatively good performance. The total load is related to the bed shear stress and total velocity as:

$$\frac{q_{t,k}^*}{\sqrt{sgd_k^3}} = 0.05p_{ak} \frac{V_t^2}{gd_k\sqrt{s(s-1)}} \left[\frac{\tau_b}{(s-1)\rho gd_k} \right]^{1.5}$$

where p_{ak} is the volume fraction of sediment size class k in the active layer, V_t is flow velocity, $s = \rho_s / \rho$, and g is gravitational acceleration.

The Meyer-Peter-Muller transport equation is widely used for gravel-bed channels. In SRH-2D, the modified equation proposed by Wong and Parker (2006) is used. This modification has been needed for many studies that Reclamation has conducted using SRH-2D. The equation may be written as:

$$\frac{q_{t,k}^*}{\sqrt{sgd_k^3}} = 4.93p_{ak} \left[\frac{\tau_b}{(s-1)\rho gd_k} - 0.047 \right]^{1.6}$$

In the above, $s = \rho_s / \rho$, p_{ak} is the volumetric fraction of sediment size class k in the active layer.

The Parker (1990) sediment transport equation was originally developed for gravel bed load transport but was later found to be applicable to sand and gravel mixture (Andrews, 2000). Wilcock and Crowe (2003) used basically a similar form but with modified coefficients. Both Parker and Wilcock-Crowe equations may be expressed as:

$$\frac{q_{t,k}^* g^{(s-1)}}{(\tau_b/\rho)^{1.5}} = p_{ak} G(\Phi_k)$$

$$\Phi_k = \frac{\theta_k}{\theta_r} \left(\frac{d_k}{d_{50}} \right)^\alpha$$

In the above, $q_{t,k}^*$ is the volumetric sediment transport rate per unit width ($C_k^* = q_{t,k}^* / q$ is the total load capacity/equilibrium concentration and q is the flow discharge per unit width), p_{ak} is the volumetric fraction of the k th sediment size class in the bed, α is the exposure factor, τ_b is bed shear stress, $\theta_k = \tau_b / [\rho g (s-1) d_k]$ is Shield's parameter of sediment size class k , θ_r is the

reference Shield's parameter, d_k is diameter of sediment size class k, and d_{50} is the median diameter of the sediment mixture in bed. The function in the transport equation was fit to field data by Parker (1990) and is expressed as:

$$G(\Phi) = \begin{cases} 11.933 (1 - 0.853/\Phi)^{4.5}, & \Phi > 1.59 \\ 0.00218 \exp[14.2(\Phi - 1) - 9.28(\Phi - 1)^2], & 1.0 \leq \Phi \leq 1.59 \\ 0.00218\Phi^{14.2}, & \Phi < 1.0 \end{cases}$$

Two parameters must be defined by a user to apply the Parker equation: θ_r and α . The parameter θ_r is a reference value above which sediment is mobilized and α is the exposure (or hiding) factor to account for the reduction in critical shear stress for larger particles and increase in critical shear stress for smaller particles. Ideally, the two parameters are calibrated to the river reach to be simulated. Without site specific data, a number of previous studies, along with our own experience with SRH-2D, may provide guidance (Komar, 1989; Buffington and Montgomery, 1997; Andrews, 2000; and Wilcock and Crowe, 2003). In general, θ_r varying from 0.03 to 0.08 and α from 0.2 to 0.9 are recommended.

Wilcock and Crowe (2003), however, used a different G function:

$$G = \begin{cases} 14.0(1 - 0.894/\sqrt{\phi})^{4.5}, & \phi \geq 1.35 \\ 0.002\phi^{7.5}, & \phi < 1.35 \end{cases}$$

Different θ_r and α were used, and they are computed by:

$$\theta_r = 0.021 + 0.015 \exp(-20 p_{sand})$$

$$\alpha = 1.0 - \frac{0.67}{1 + \exp(1.5 - d_k / d_{50})}$$

In the above, p_{sand} is the fraction of sand in the active layer.

The fall velocity for the non-cohesive sediment is calculated using the recommendation by the U.S. Interagency Committee on Water Resources Subcommittee on Sedimentation (1957).

Many other popular sediment capacity equations have also been incorporated into SRH-2D such as Wu (2004), Yang (1973) and Yang (1979). They are described in Appendix A.

4.5. Bed Dynamics

Bed dynamics concerns the ways that sediments in a riverbed interact with flow and sediment transport in the water column. On one hand, sediment movement in an alluvial river modifies the bed topography and the sediment contents in the bed. The flow and sediments in the water column, on the other hand, are altered due to bedform change. Therefore, modeling of the riverbed dynamics is important and an integral part of alluvial river modeling.

As described previously, sediments in the bed are divided into the active layer and one or more subsurface layers. The volume or mass fractions within each layer are tracked during the sediment transport modeling. It may be shown that the two fractions are equivalent if the specific gravity is the same for all sediment size classes which is assumed by SRH-2D.

The top elevation of a mobile-bed surface layer changes due to net erosion and deposition. Elevation changes are contributed by all sediment size classes and computed by the net sediment exchanges between those in the water column and those in the active layer. The change in Z_b due to sediment size class k obeys the following equation:

$$\eta_{ak} \left(\frac{\partial Z_b}{\partial t} \right)_k = -\dot{V}_k = -\frac{q_{t,k}^* - \beta_k V_t h C_k}{L_{t,k}}$$

where $\eta_{ak} = 1 - \sigma_{ak}$ is the porosity parameter of the active layer, σ_{ak} is the porosity for the k -th size class in the active layer, and \dot{V}_k is the net volumetric rate of erosion per unit area (or net rate of eroded depth) for size class k . The above equation provides the net erosion and deposition of the sediments which would alter the sediment contents in the active layer.

In SRH-2D, the active layer is the top bed surface layer participating in the sediment exchange between the water column and the bed while subsurface layers provide sediments to or receive sediments from the active layer. The volume fraction and the porosity of both the active layer and subsurface layers are the two primitive variables, and governing equations for the two are needed for each bed layer.

The volume fraction changes in the active layer are given as:

$$\begin{aligned} \frac{\partial m_a p_{ak}}{\partial t} &= -\dot{V}_k + p_{2k} \sum_i \dot{V}_i && \text{if net erosion } (\sum_i \dot{V}_i \geq 0) \\ \frac{\partial m_a p_{ak}}{\partial t} &= -\dot{V}_k + p_{ak} \sum_i \dot{V}_i && \text{if net deposition } (\sum_i \dot{V}_i < 0) \end{aligned}$$

In the above, m_a is the total sediment volume in the active layer, p_{ak} is the volume fraction of k -th class in the active layer, p_{2k} is the volume fraction of k -th class in the first subsurface layer (beneath the active layer). The total volume per unit area in the active layer (m_a) is computed at the beginning of the computation and kept constant throughout the simulation. This is in contrast to previous studies in which the mass was kept constant. The active layer volume is a user input via the active layer thickness (δ_a). In general, the active thickness δ_a is a function of flow and sediment conditions as well as the bedform evolution. In SRH-2D, δ_a is a user supplied

parameter. By default, δ_a is set as takes the value of $N_a d_{90}$ with N_a ranging from 1.0 for large boulders to more than 14.0 for fine sediments. Other selection methods may also be used. For example, Wu (2004) set δ_a as half the dune height.

The porosity of the active layer is governed by the volume conservation equation—a kinematic constraint—and is expressed as:

$$\frac{\partial \delta_{ak}}{\partial t} = -\frac{\dot{V}_k}{\tilde{\eta}_k} + p_{2k} \frac{\sum_i \dot{V}_i}{\eta_{2k}} \text{ if } \sum_i \dot{V}_i \geq 0$$

$$\frac{\partial \delta_{ak}}{\partial t} = -\frac{\dot{V}_k}{\tilde{\eta}_k} + p_{ak} \frac{\sum_i \dot{V}_i}{\eta_{ak}} \text{ if } \sum_i \dot{V}_i < 0$$

In the above, δ_{ak} is the size k volumetric fraction per unit area of the active layer thickness including voids; relation between δ_{ak} and η_{ak} are: $\delta_{ak} \eta_{ak} = p_{ak} m_a$.

In the above, $\tilde{\eta}_k$ is computed by:

$$\tilde{\eta}_k = \eta_{ak} \text{ if } \dot{V}_i \geq 0$$

$$\tilde{\eta}_k = \eta_{sk} \text{ if } \dot{V}_i < 0$$

and η_{sk} is the porosity parameter for the suspended sediments in the water column.

The above equations may be more conveniently written as:

$$\frac{\partial \delta_{ak}}{\partial t} = -\frac{\dot{V}_k}{m_a p_{ak}} \delta_{ak} + p_{2k} \frac{\sum_i \dot{V}_i}{\eta_{2k}} \quad \text{if } \sum_i \dot{V}_i \geq 0 \text{ and } \dot{V}_k \geq 0$$

$$\frac{\partial \delta_{ak}}{\partial t} = -\frac{\dot{V}_k}{\eta_{sk}} + p_{2k} \frac{\sum_i \dot{V}_i}{\eta_{2k}} \quad \text{if } \sum_i \dot{V}_i \geq 0 \text{ and } \dot{V}_k < 0$$

$$\frac{\partial \delta_{ak}}{\partial t} = \frac{p_{ak} \sum_i \dot{V}_i - \dot{V}_k}{m_a p_{ak}} \delta_{ak} \quad \text{if } \sum_i \dot{V}_i < 0 \text{ and } \dot{V}_k \geq 0$$

$$\frac{\partial \delta_{ak}}{\partial t} = -\frac{\dot{V}_k}{\eta_{sk}} + \frac{\sum_i \dot{V}_i}{m_a} \delta_{ak} \quad \text{if } \sum_i \dot{V}_i < 0 \text{ and } \dot{V}_k < 0$$

The volume fraction (p_{Lk}), the porosity parameter (η_{Lk}), and the thickness (t_L) of subsurface layer L (1 to the total number of subsurface layers) are continuously updated during a simulation.

In SRH-2D, the first subsurface layer immediately underneath the active layer exchanges sediments with the active layer so that the total volume of the active layer is maintained. As a result, the thickness of the immediate subsurface layer may increase or decrease. The remaining subsurface layers are unaltered until the upper subsurface layer is depleted completely. After this

complete depletion, the lower subsurface layer plays the role of the upper layer—unless all specified subsurface layers are eroded. For the first subsurface layer, termed “layer 2,” the volume fraction (p_{2k}), the porosity parameter (η_{2k}), and its thickness need to be re-computed. For net erosion, p_{2k} and η_{2k} do not change but the thickness change is governed by:

$$\frac{dt_{2k}}{dt} = -\left(\sum_i \dot{V}_i\right) \left(\sum_i \frac{p_{2i}}{\eta_{2i}}\right)$$

where subscript i runs through all sediment size classes. For net deposition, the thickness change is governed by:

$$\frac{dt_{2k}}{dt} = -\left(\sum_i \dot{V}_i\right) \left(\sum_i \frac{p_{ai}}{\eta_{ai}}\right)$$

and p_{2k} and η_{2k} are updated by fully mixing the new depositions from the active layer with the sediments in layer 2.

4.6. Cohesive Sediment Equations

Cohesive sediments are lumped together as one unit and modeled as a single size class in SRH-2D. The cohesive sediment may be mixed together with other non-cohesive sediment size classes. No interaction between cohesive and non-cohesive sediments is allowed. A cut-off diameter, in the silt or clay range, is used to distinguish the cohesive sediment from the non-cohesive sediments. The same sediment transport equation governs the cohesive sediment transport, but $f_c = 1.0$ and $\beta_c = 1.0$ are used (subscript c is used in place of k for the cohesive sediment). In addition, the sediment exchange term changed to:

$$S_{e,c} = V_e p_c - V_d C_c$$

where p_c is the volume fraction of the cohesive sediment in the active layer and V_e and V_d are the cohesive sediment erosion and deposition rates, respectively.

The erosion rate may be determined by considering two erosion modes: the surface and mass erosions. Surface erosion occurs when the bed shear stress is just above a critical value. But at higher bed shear stress levels, mass erosion where a layer of bed material is lifted and eroded will happen as the bed stress exceeds the bulk shear strength of the material on the bed. The erosion rate incorporating both modes may be written as:

$$V_e = 0 \quad \text{if} \quad \tau_b \leq \tau_{es} \quad \text{(a)}$$

$$V_e = S_s \left(\frac{\tau_b - \tau_{es}}{\tau_{em} - \tau_{es}} \right) \quad \text{if} \quad \tau_{es} < \tau_b \leq \tau_{em} \quad \text{(b)}$$

$$V_e = S_s + S_m \left(\frac{\tau_b - \tau_{em}}{\tau_{em}} \right) \quad \text{if} \quad \tau_b > \tau_{em} \quad \text{(c)}$$

where τ_{es} the critical bed shear stress above which surface erosion starts, τ_{em} is the critical bed stress above which mass surface erosion begins, S_s is the surface erosion constant, and S_m is the mass erosion constant. Equation (b) is based on Partheniades (1965). The above erosion model needs four parameters, $\tau_{es}, \tau_{em}, S_s, S_m$, which users may specify for a specific project site. For example, in the study of the erosion upstream of the San Acacia Dam on the Rio Grande River (Lai and Bauer 2007), the laboratory measured data used were: $\tau_{es} = 0.125 \text{ lb/ft}^2$,

$$\tau_{em} = 2.84 \text{ lb/ft}^2, S_s = 0.25 \text{ lb/hr} \cdot \text{ft}^2, \text{ and } S_m = 1.07 \text{ lb/hr} \cdot \text{ft}^2.$$

Deposition rates also depend on a number of processes. Deposition occurs when the bed shear stress is less than a critical value. Only the near-bed aggregates with a sufficient shear strength to withstand the disruptive flow will adhere to and remain on the bed. Based on the cohesive sediment depositional behavior study by Mehta and Partheniades (1973) in a laboratory setting, deposition is controlled by: shear stress on the bed, turbulence near the bed, settling velocity, sediment type, flow depth, suspended concentration, and ionic constitution.

Two deposition processes may be modeled: full and partial. The deposition rate is computed as follows:

$$V_d = \left(1 - \frac{\tau_b}{\tau_{ref}}\right) \omega_c \quad \text{if} \quad \tau_b \leq \tau_{df} \quad \text{(a)}$$

$$V_d = \left(1 - \frac{\tau_b}{\tau_{dp}}\right) \omega_c \left(1 - \frac{C_{eq}}{C_c}\right) \quad \text{if} \quad \tau_{df} < \tau_b < \tau_{dp} \text{ and } C_c > C_{eq} \quad \text{(b)}$$

$$V_d = 0 \quad \text{if} \quad \tau_b \geq \tau_{dp} \text{ or } C_c \leq C_{eq} \quad \text{(c)}$$

In the above equations, τ_{df} is the critical bed shear stress below which full deposition dominates, τ_{dp} is the critical stress above which no deposition happens ($\tau_{dp} \geq \tau_{df}$), C_{eq} is the equilibrium cohesive sediment concentration representing the relatively weak flocks that are broken apart before reaching the bed or eroded immediately after deposition, and

$$\tau_{ref} = \frac{\tau_{df} \tau_{dp}}{\chi \tau_{df} + (1 - \chi) \tau_{dp}} \text{ and } \chi = 1 - \frac{C_{eq}}{C_c}. \text{ Full deposition allows the concentration to reduce to}$$

zero and is appropriate for floodplains and low shear areas; while partial deposition is for concentration to reduce to an equilibrium value (C_{eq}) and is appropriate for main channels. Note that if $\tau_{df} = \tau_{dp}$, only equation (a) will be used and C_{eq} will be ignored as partial deposition is not modeled.

If $C_{eq} = 0$ is specified, equations (a) and (b) collapse into one calculation, and separation of full and partial is meaningless—only τ_{dp} is used under the scenario where $\tau_{df} = \tau_{dp}$ and τ_{df} is ignored. Equation (a) is based on Krone (1962) and equation (b) is based on van Rijn (1993).

Three parameters are needed in the deposition model: τ_{df} , τ_{dp} , and C_{eq} . Many experiments were performed to determine τ_{df} . There is quite a scatter and the value of τ_{df} may range from 0.06 and 1.1 N/m^2 , depending upon the sediment type and concentration. At present, the behavior of τ_{df} , τ_{dp} , and C_{eq} are not well understood. Thus, they should be either determined through laboratory or field measurements, or they should be determined through calibration. Krone (1962) conducted a series of flume experiments. For the San Francisco Bay sediment, he found that $\tau_{df} = 0.06 N/m^2$ when $C_c < 0.3 kg/m^3$, and $\tau_{df} = 0.078 N/m^2$ when $0.3 < C_c < 10 kg/m^3$. Mehta and Partheniades (1973) found that $\tau_{df} = 0.15 N/m^2$ for kaolinite in distilled water. In the study of the erosion upstream of the San Acacia Dam on the Rio Grande River (Lai and Bauer 2007), the laboratory measured data were used as follows: $\tau_{df} = 0.005 lb/ft^2$, $\tau_{dp} = 0.021 lb/ft^2$, and $C_{eq} = 1.0 kg/m^3$.

The cohesive sediment settling velocity (ω_c) is needed, and its determination is very difficult. Cohesive sediments tend to aggregate to form large, low-density units—and tremendously impact the settling velocity. The aggregation process is strongly dependent on the sediment type, the type and concentration of ions in the water, and flow conditions (Mehta et al., 1989). Cohesive sediments are composed primarily of clay-sized materials, which have strong inter-particle forces because of their surface ionic charges. As particle size decreases, the inter-particle forces dominate the gravitational force, and the settling velocity is no longer a function of only particle size. McAnally and Mehta (2001) provided a new formulation of the collision efficiency and collision diameter function through a dimensional analysis of the significant parameters in collision, aggregation, and disaggregation. In engineering models, aggregation is often indirectly considered by the change in settling velocity.

A number of methods may be used to decide the fall velocity using SRH-2D. In one way, the settling velocity may be a user input and a data series in the form of $\omega_c = f(C_c)$ may be the input (mm/s versus g/L).

The second way is to provide four pairs of data for the two parameters (conc, fv) and linear interpolation is used between the two.

In another way, the fall velocity is calculated as follows:

$$\begin{aligned} \omega_c &= \frac{1000(\gamma - 1)gd_c^2}{18\nu} && \text{for unhindered settling } C_c < C_{fv1} \\ \omega_c &= \alpha_{fv} C_c^{\beta_{fv}} && \text{for flocculation } (C_{fv1} < C_c < C_{fv2}) \\ \omega_c &= \alpha_{fv} C_{fv2}^{\beta_{fv}} [1 - \kappa_{fv} (C_c - C_{fv2})]^{\gamma_{fv}} && \text{for hindered settling } (C_c \geq C_{fv2}) \end{aligned}$$

In the above, ω_c is in millimeters per second (mm/s), C_c is in the unit of kg/m^3 , and the water viscosity may be calculated as:

$$\nu = \frac{1.792 \times 10^{-6}}{1.0 + 0.0337T + 0.000221T^2}$$

where T is the water temperature in Celsius. Six parameters are needed:

$C_{fv1}, C_{fv2}, \alpha_{fv}, \beta_{fv}, \kappa_{fv}, \eta_{fv}$. To calculate these parameters, various equations could be used.

Based on the SRH-1D manual, $C_{fv1} \approx 0.1$ and $C_{fv2} \approx 10$ may be used. Krone (1962), Cole and Mile (1983), and SRH-1D recommended $\alpha_{fv} = 0.6$, $\beta_{fv} = 1.0$, $\kappa_{fv} = 0.01 m^3 / kg$, $\eta_{fv} = 5.0$.

Chapter 5. Initial and Boundary Conditions

SRH-2D needs proper initial and boundary conditions for simulation. This chapter discusses the type of initial and boundary conditions relevant to mobile-bed module.

5.1. Initial Conditions

Sediment transport mobile-bed modeling is always performed using the unsteady, time-accurate mode—so an initial condition is needed. It is recommended that constant-discharge flow-only modeling be carried out first with discharge and other relevant boundary conditions that correspond to the flow conditions at the initial time (TSTART) of the sediment modeling. Once the flow results are obtained, they are used as the initial condition through the RST option offered by SRH-2D. The initial sediment concentrations are assumed to be zero at the start of the mobile-bed simulation. It is found that the impact to the final results are negligible.

5.2. Inlet Boundary

An inlet boundary is defined as a boundary segment on the solution domain where flow is expected to move into the domain. Multiple inlets may be specified for a solution domain. Users specify the flow discharge at an inlet. For mobile-bed simulation, sediment rates (or fluxes) for each size classes are specified as the boundary conditions. These specified fractional sediment rates serve as the sediment supply from the upstream. The inlet sediment supply rates may be in the form of constant values or time-series sedi-graphs. They may be based on the measured sediment rate data or computed using the developed sediment rating curve relations obtained through other means.

For some project applications, the fractional sediment rates at an inlet may not be available. SRH-2D offers a CAPACITY option so that the fractional sediment rates are computed using the sediment capacity equation. Using the CAPACITY option offers the benefit of simple boundary condition specification without resorting to expensive sediment data collection. When the CAPACITY option is selected, the actual fractional sediment rates used at the inlet are provided as output so that sensitivity studies can be carried out by using a smaller or a larger sediment supplies at the inlet. Users may multiply the CAPACITY computed rates by a scaling factor and use the results as the new boundary conditions.

5.3. Exit Boundary

An exit boundary is defined as a boundary segment on the solution domain where flow is expected to move out of the domain. Multiple exits may be specified for a problem.

At an exit, SRH-2D requires no additional boundary conditions related to the sediment transport.

Chapter 6. Numerical Methods

This chapter provides the numerical methods and algorithms used to solve the mobile-bed equations. Numerical methods used for the flow solver has been discussed in Chapter 8 of the Users' Manual of SRH-2D flow model (Lai, 2008).

6.1. Sediment Transport Equation Discretization

The sediment transport governing equations are discretized using the finite-volume method with SRH-2D, following the work of Lai (1997 and 2000) and Lai et al. (2003). The solution domain is covered with an unstructured mesh with each mesh cell in the shape of a polygon. Commonly used polygons are triangles and quadrilaterals. All dependent variables are stored at the centroid of a polygon.

The sediment transport equation may be generally expressed as:

$$\frac{\partial h\Phi}{\partial t} + \nabla \cdot (h\vec{V}\Phi) = \nabla \cdot (\Gamma\nabla\Phi) + S_{\Phi}^*$$

Here Φ denotes a sediment dependent variable (concentration), Γ is the diffusivity, and S_{Φ}^* is the source/sink term. Integration over an arbitrarily shaped polygon P shown in Figure 10 leads to:

$$\frac{(h_P^{n+1}\Phi_P^{n+1} - h_P^n\Phi_P^n)A}{\Delta t} + \sum_{all-sides} (h_C V_C |\vec{s}|)^{n+1} \Phi_C^{n+1} = \sum_{all-sides} (\Gamma_C^{n+1} \nabla\Phi^{n+1} \cdot \vec{n} |\vec{s}|) + S_{\Phi}$$

In the above, Δt is time step, A is polygon area, $V_C = \vec{V}_C \cdot \vec{n}$ is the velocity component normal to the polygon side (e.g., P_1P_2 in Figure 10) and evaluated at the side center C , \vec{n} is polygon side unit normal vector, \vec{s} is the polygon side distance vector (e.g., from P_1 to P_2 in Figure 10), and $S_{\Phi} = S_{\Phi}^*A$.

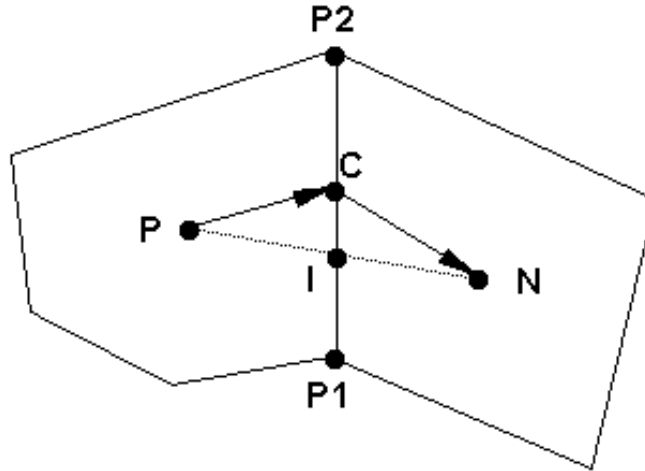


Figure 10. Schematic illustrating a polygon P along with one of its neighboring polygons N.

Subscript C indicates a value evaluated at the center of a polygon side and superscript, n or $n+1$, denotes the time level. In the remaining discussion, superscript $n+1$ will be dropped for ease of notation. Note that the first-order Euler implicit time discretization is adopted. The main task of the discretization is to obtain appropriate expressions for the convective and diffusive fluxes at each polygon side.

Discretization of the diffusion term, the first term on the right-hand side of the above equation, needs further attention. The final expression for $\nabla\Phi \cdot \vec{n}$ can be written as:

$$\nabla\Phi \cdot \vec{n}|\vec{s}| = D_n(\Phi_N - \Phi_P) + D_c(\Phi_{P2} - \Phi_{P1})$$

$$D_n = \frac{|\vec{s}|}{(\vec{r}_1 + \vec{r}_2) \cdot \vec{n}}; D_c = -\frac{(\vec{r}_1 + \vec{r}_2) \cdot \vec{s} / |\vec{s}|}{(\vec{r}_1 + \vec{r}_2) \cdot \vec{n}}$$

In the above, \vec{r}_1 is the distance vector from P to C and \vec{r}_2 is from C to N. The normal and cross diffusion coefficients, D_n and D_c , at each polygon side involve only geometric variables; they are calculated only once in the beginning of the computation.

Calculating a variable, say Y , at the center C of a polygon side is an interpolation operation used frequently for variables. A second-order accurate expression is derived below. As shown in Figure 10, a point I is defined as the intercept point between line PN and line P₁P₂. A second-order interpolation for point I may be derived to be:

$$Y_I = \frac{\delta_1 Y_N + \delta_2 Y_P}{\delta_1 + \delta_2}$$

with $\delta_1 = \vec{r}_1 \cdot \vec{n}$ and $\delta_2 = \vec{r}_2 \cdot \vec{n}$. Y_I may be used to approximate the value at the side center C. This treatment, however, does not guarantee second-order accuracy unless \vec{r}_1 and \vec{r}_2 are parallel. A truly second-order expression is derived as:

$$Y_C = Y_I - C_{side}(Y_{P2} - Y_{P1})$$

$$C_{side} = \frac{(\delta_1 \vec{r}_2 - \delta_2 \vec{r}_1) \cdot \vec{s}}{(\delta_1 + \delta_2) |\vec{s}|^2}$$

The extra term in the above is similar in form to the cross-diffusion term.

Φ_c in the above convective term adopts the second-order scheme with a damping term. It is derived by blending the first-order upwind scheme with the second-order central difference scheme and may be expressed as:

$$\Phi_C = \Phi_C^{CN} + d(\Phi_C^{UP} - \Phi_C^{CN})$$

$$\Phi_C^{UP} = \frac{1}{2}(\Phi_P + \Phi_N) + \frac{1}{2} \text{sign}(V_C)(\Phi_P - \Phi_N)$$

In the above, Φ_C^{CN} is the second-order interpolation scheme, and d defines the amount of damping used. In most applications, $d = 0.2 \sim 0.3$ may be used.

With expressions for the diffusion and convection terms done, the final discretized governing equation at the cell P may be organized as the following linear equation:

$$A_P \Phi_P = \sum_{nb} A_{nb} \Phi_{nb} + S_{diff} + S_{conv} + S_\Phi$$

where “nb” refers to all neighboring polygons surrounding polygon P . The coefficients in this equation are:

$$A_{nb} = \Gamma_C D_n + \text{Max}(0, -h_C V_C |\vec{s}|)$$

$$A_P = \frac{h_P^2 A}{\Delta t} + \sum_{nb} A_{nb}$$

$$S_{diff} = \frac{h_P^2 A}{\Delta t} + \sum_{all-sides} \Gamma_C D_c (\Phi_{P2} - \Phi_{P1})$$

$$S_{conv} = \sum_{all-sides} (h_C V_C |\vec{s}|) \left\{ (1-d) \left[\frac{\delta_1}{\delta_1 + \delta_2} - \frac{1 - \text{sign}(V_C)}{2} \right] (\Phi_N - \Phi_P) \right\} \\ - \sum_{all-sides} (h_C V_C |\vec{s}|) [(1-d) C_{side} (\Phi_{P2} - \Phi_{P1})]$$

6.2. Bed Dynamics

The right-hand side of the bed dynamics equation is known and p_{ak} can be solved. The equation, however, is implicit and may be solved analytically as follows:

$$p_{ak} = \frac{\dot{V}_k}{\sum_i \dot{V}_i} + \left(p_{ak}^o - \frac{\dot{V}_k}{\sum_i \dot{V}_i} \right) \exp \left(\frac{\sum_i \dot{V}_i}{m_a} \Delta t \right)$$

But preferred approach is to use the implicit discretization, to be consistent with volume

conservation equation as follows (the following may be derived if $-\frac{\sum \dot{V}_i}{m_a} \Delta t$ is assumed to be small through Taylor expansion):

$$P_{ak} = P_{ak}^o \frac{1 - \Delta t \frac{\dot{V}_k}{m_a P_{ak}^o}}{\sum \dot{V}_i \frac{1 - \Delta t \frac{\dot{V}_i}{m_a}}{m_a}}$$

A better and more consistent way of solving the equations is to substitute the two equations into the above and then use the implicit finite difference. Analytical solution of them may lead to numerical trouble.

The solution to the above equation is:

$$\frac{\delta_{ak}}{m_a P_{ak}} = \frac{\delta_{ak}^o + \frac{P_{k2} \sum \dot{V}_i}{\eta_{2k}}}{m_a P_{ak}^o + P_{k2} \sum \dot{V}_i} = \frac{\delta_{ak}^o}{m_a P_{ak}^o} \frac{1 + \Delta t \frac{P_{2k} \sum \dot{V}_i}{m_a P_{ak}^o} \eta_{ak}^o}{1 + \Delta t \frac{P_{2k} \sum \dot{V}_i}{m_a P_{ak}^o}}$$

or

$$\eta_{ak} = \eta_{ak}^o \frac{1 + \Delta t \frac{P_{2k} \sum \dot{V}_i}{m_a P_{ak}^o}}{1 + \Delta t \frac{P_{2k} \sum \dot{V}_i}{m_a P_{ak}^o} \eta_{ak}^o}$$

The above equation has the benefit that porosity is constant if $\eta_{2k} = \eta_{ak}^o$ which is true for non-cohesive sediment. If $P_{ak}^o \rightarrow 0$, $\eta_{ak} = \eta_{2k}$.

Solution of the equation lead to:

$$\eta_{ak} = \eta_{ak}^o \frac{P_{ak}}{P_{ak}^o + (P_{ak} - P_{ak}^o) \frac{\eta_{ak}^o}{\eta_{2k}} + \frac{\dot{V}_k \Delta t}{m_a} \left(\frac{\eta_{ak}^o}{\eta_{2k}} - \frac{\eta_{ak}^o}{\eta_{sk}} \right)}$$

In the above, η_{ak} does not change for non-cohesive sediment; last term in denominator is positive. Or another solution is:

$$\eta_{ak} = \eta_{ak}^o \frac{1}{\frac{p_{ak}^o}{p_{ak}} + \Delta t \frac{p_{2k} \sum_i \dot{V}_i}{m_a p_{ak}} \frac{\eta_{ak}^o}{\eta_{2k}} - \Delta t \frac{\dot{V}_k}{m_a p_{ak}} \frac{\eta_{ak}^o}{\eta_{sk}}}$$

Note $p_{ak} > p_{ak}^o$ should hold for this case as k-th class is gaining mass both from flow and sub-surface layer.

Another solution is:

$$\eta_{ak} = \eta_{ak}^o \frac{1 - \frac{\dot{V}_k \Delta t}{m_a p_{ak}^o}}{1 - \frac{\dot{V}_k \Delta t}{m_a p_{ak}^o} \frac{\eta_{ak}^o}{\eta_{sk}}}$$

The above guarantees that porosity does not change if volume fraction of sediment does not change.

6.3. Time Integration

Sediment equations such as the bed elevation equation and the bed dynamics equations may be discretized similarly. In terms of time integration, the fraction step method of Yanenko (1971) is used:

$$\frac{(hC)^{int} - (hC)^n}{\Delta t} + \frac{\partial \cos(\alpha) V_t (hC)^{int}}{\partial x} + \frac{\partial \sin(\alpha) V_t (hC)^{int}}{\partial y} = 0 \quad (a)$$

$$\frac{(hC)^{n+1} - (hC)^{int}}{\Delta t} = \frac{q_t^* - V_t (hC)^{n+1}}{L_b} \quad (b)$$

The advection equation (a) is solved implicitly to obtain an intermediate solution $(hC)^{int}$ with known values at time level n ; the initial value problem of (b) is solved analytically to obtain the new solution $(hC)^{n+1}$ at time level $(n+1)$. The solutions of the bed elevation equation and bed dynamics equations are relatively straightforward, and details are not presented.

Chapter 7. Model Verification

This chapter provides a number of verification cases conducted with SRH-2D mobile-bed modeling capability. Most cases have measured data for comparison so that the model may be tested and verified to lend credence to its validity. In the process, model applicability range and parameter selection guidelines may be established. Selected field cases of the SRH-2D mobile-bed model are presented in the Chapter 8.

7.1. Aggradation in a Straight Channel

Aggradation in alluvial channels may occur due to a variety of reasons. One such case is an oversupply of incoming sediment above the transport capacity. This may happen in the field (e.g., after heavy precipitation in a large tributary area). In this test, Soni's (1981) flume experiment is selected to test the aggradation modeling of SRH-2D.

The test case represents one dimensional, unsteady sediment transport with uniform sediment gradation. Bedload transport was the only mode of transport observed in the flume experiment; so the bedload mode is used for the simulation. The flume case consisted of a flat plate bed with 30 meters (m) long, 0.2 m wide, with a slope of 0.00427. The bed was covered with uniform sand with a medium sieve diameter (d_{50}) of 0.32 mm, 0.15 m deep, and specific gravity of 2.65. The case had a constant flow discharge of 0.0355 m³/s, average velocity of 0.493 m/s, and average water depth of 0.072 m. An equilibrium flow was established first before excessive sediment is released to the channel from the upstream. Soni (1981) found that a Manning's roughness coefficient of 0.02294 would establish an equilibrium flow with the above slope and velocity with the model. A sudden increase in sediment supply was applied at the upstream entrance at time zero, initiating the aggradation process simulated with SRH-2D. The rate of excess sediment supply was $0.9 q_{seq}$ where q_{seq} is the equilibrium sediment transport rate determined by the adopted capacity transport equation.

A 31-by-6 uniform Cartesian mesh covering the 30m-by-0.2m flume was used. The time step was 1.0 second. Further refinement of the mesh or reductions in the time step did not change the results by more than one percent. The simulation was first run for a duration of 100 minutes with an upstream sediment supply of q_{seq} to establish an equilibrium flow. Aggradation simulation with a sediment supply of $1.9 q_{seq}$ at the upstream boundary was then initiated. The Engelund-Hansen (1972) sediment transport equation was used for the simulation since it works relatively well for sand bed streams.

A comparison of simulated and measured bed elevation changes is shown in Figure 11a. Overall agreement is fair; discrepancies exist near the upstream section and at a late stage (90 minutes). No attempt has been made to adjust various model parameters for a better agreement between the model results and the measured ones since the measured data had a high reported uncertainty. For example, Soni (1981) reported that up to 15% uncertainty existed in the rate of sediment addition at upstream. Using a higher sediment addition would increase the aggradation and yields

better agreement. For example, if 15% more sediment is added at the upstream, a much better agreement is obtained (Figure 11b).

SRH-2D modeling showed that the model results were most sensitive to the choice of the sediment transport equation for capacity. It is recommended that users be familiar with the suitability and applicability range of each sediment transport equation. A specific sediment capacity equation should be chosen first, based either on experience or through calibration study if measured data are available.

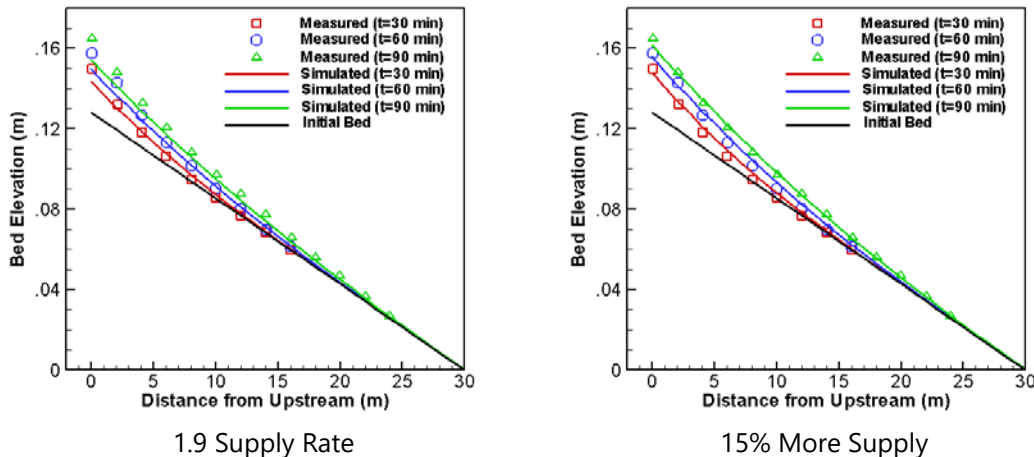


Figure 11. Comparison of bed elevation changes between model prediction and flume data for the aggradation case of Soni (1981).

Results of all other transport equations are shown from Figure A-1 to Figure A-10 in Appendix A.6.1. *Aggradation in a Straight Channel*. Note that only some equations were presumed to be developed for sand transport. At least for this case, we found that the Engelund-Hansen equation performs the best in comparison with the flume data.

7.2. Degradation in a Straight Channel

Channel degradation and armoring occur in many situations (e.g., downstream of a dam); they represent an important class of alluvial processes. In this section, the flume experiment of Ashida and Michiue (1971) is chosen to test the SRH-2D version capability.

This case represents one dimensional, unsteady sediment transport, with non-uniform sediment gradation and bed degradation. Only bedload transport was observed and used for the simulation. The flume used in the experiment was rectangular; it had width of 0.8 meters, length of 20 meters, and bed slope of 0.01. The flume bed was filled with non-uniform sediments, a mixture of sand and fine gravel, with size from 0.2 to 10.0 mm. The sediment mixture had a medium size of 1.5 mm and a standard deviation of 3.47 mm (see Figure 12 for the initial bed gradation). The simulated case has a constant clear water flow of $0.0314 \text{ m}^3/\text{s}$, an average velocity of 0.654 m/s, and the water depth of 6.0 mm at the downstream boundary.

A 42-by-6 Cartesian mesh was used for the simulation, covering the 20m-by-0.8m solution domain; and the time step was 1.0 second. Further refinement of the mesh or reduction of the time step did not change the solution by more than one percent. Twelve sediment size classes were used to represent the mixture. The range of each size and the corresponding initial (original) fractional content (gradation) on the bed are listed in Table 2 (see Figure 12 for the initial gradation). The Manning's roughness coefficient was 0.025, based on the modeling to achieve flow equilibrium. For mixed sand-gravel bed, Reclamation recommends the Parker (1990) sediment capacity equation in which the default model constants, $\theta_c=0.04$ and $\alpha=0.65$, are used. At time zero, clear water flows into the channel, and the channel degradation process was initiated.

Table 2. Sediment Size Classes and the Initial Fractional Content (Gradation) on Bed

Diameter range (mm)	0.2-0.3	0.3-0.4	0.4-0.6	0.6-0.8	0.8-1.0	1.0-1.5	1.5-2.0	2.0-3.0	3.0-4.0	4.0-6.0	6.0-8.0	8.0-10.
Content (%)	7.45	12.4	15.9	4.4	3.6	6.79	4.0	9.18	10.2	18.1	6.0	2.0

The experimental data showed that degradation was initiated quickly and the scour depth increased fast for the first 100 minutes. Afterwards, degradation slowed and an armor layer was formed. The predicted armored bed gradation 10 meters upstream from the downstream boundary is shown in Figure 12. A comparison with the measured armored gradation is relatively good, indicating the ability of the model to predict the armoring process.

Furthermore, the degradation process is compared in Figure 13 at three locations. It is seen that the prediction of the scour process is less satisfactory. In view of the better prediction reported by Wu (2004) in his calculations for this case, an effort was made to find out the cause. Based on the discussion of Wu (2004) and a personal communication with Dr. Wu, the cause is attributed to the bedform changes in the simulated case. Wu (2004) reports that the surface of the flume changed from a flat bed to a fully-developed dune bed for the flume case. As a result, Wu (2004) implemented a time-dependent variation of the bed grain shear stress. The same functional form of grain shear stress change used by Wu (2004) is therefore adopted and implemented into SRH-2D. The model was run again with only this change. The new predicted scour results are shown in Figure 13, designated as 'Predicted: Wu Grain Stress' in dashed lines. It is seen that the procedure used by Wu (2004) does improve the agreement between the prediction and the measured data for the first 100 minutes of degradation process. Since the procedure for modifying grain stresses used in this simulation is not general, it is not implemented as a feature in the SRH-2D model. We prefer to take the results in solid lines as the model prediction. The study, however, points to potential uncertainty in the model prediction. If the stream bed form is changing during the unsteady simulation period, the numerical model with a constant form-correction factor as implemented in SRH-2D may not predict the scour timing accurately.

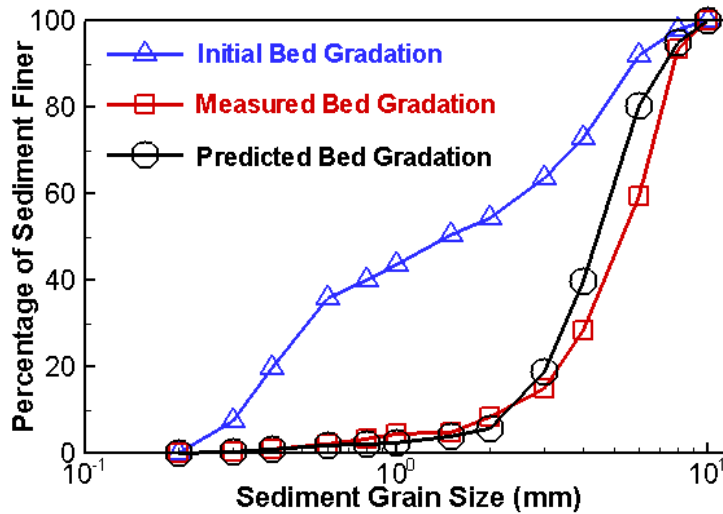


Figure 12. Comparison of predicted and measured armored bed gradation 10 meter upstream from the exit for the Ashida-Michiue (1971) case.

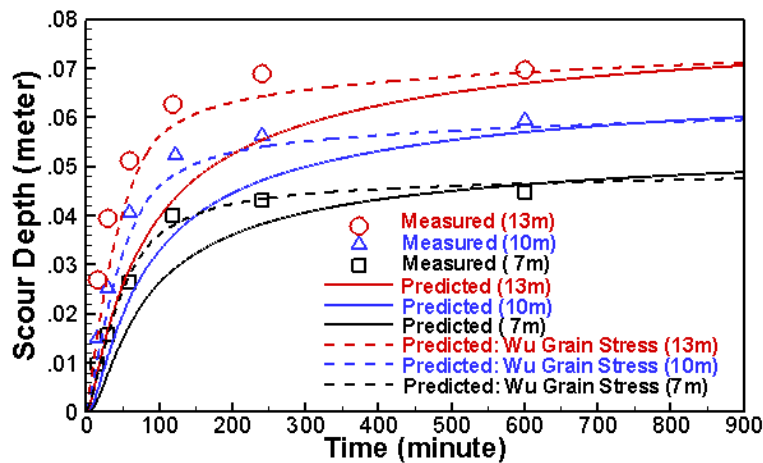


Figure 13. Comparison of predicted and measured scour depth variation with time at three locations: 13m (red), 10m (blue), and 7m (black) from the downstream boundary for the Ashida-Michiue (1971) case; “Wu Grain Stress” refers to results obtained with the modified grain shear stress calculation.

A discussion of a mixed sand-gravel bed is in Appendix A.6.2. and results of all other transport equations are shown from Figure A-1 to Figure A-21.

7.3. Contraction Scour Simulation

7.3.1. Introduction

Scour can be classified into two general forms (Briaud et al., 2004). General scour is bed elevation change due to variation in flow discharge, sediment input, and bed slope. Local scour is the scour due to local changes such as flow area and obstacles. Local scour includes contraction scour due to reduction in flow area, pier scour around the foundation of a pier, and abutment scour around an abutment at the junction between a bridge and embankment. Other scour mechanism exists (e.g., from flow meander and other in-stream structures).

Often, contraction scour, and local scour in general, are better predicted with multi-dimensional models. The benefit of such models is that it is not limited to a particular class of problems and may take complex flow features into account. Empirical and analytical methods, on the other hand, are mostly limited to certain configurations. Therefore, this study concerns with the multi-dimensional modeling of contraction scour which is often encountered in rivers due to natural channel contraction and manmade features such as revetments, embankments, dikes, etc.

However, it was reported that the 2D depth-averaged model was not adequate for modeling contraction scour (e.g., Weise [2002] and Marek and Dittrich [2004]). These studies showed that their 2D model obtained unsatisfactory results for the morphological processes in the contraction channel. Marek and Dittrich (2004) attributed the poor results to two potential problems of the 2D model: inability to account for the three-dimensional (3D) effect and deficiency in the turbulence model. Their findings led to an effort to use 3D models to study the contraction scour.

SRH-2D modeling aims to investigate the matter further to see if other factors may play roles in the poor performance of 2D models. In the process, improved prediction may be found using 2D models. The motivation of the study stems from the fact that a 3D model is still too complex, and many engineering applications have to rely on 2D models. In the end, it can be concluded that the SRH-2D is adequate for predicting the contraction scour, and results comparable with the 3D model may be obtained.

7.3.2. Flume Case Description

A series of experiments were conducted to study the contraction erosion process on a non-cohesive uniform bed in the laboratory of the Federal Waterways Engineering and Research Institute Karlsruhe (BAW). Details may be found in the thesis by Weise (2002). The flume had a test section 16.5 m long and a contraction and expansion part with a width change between 1.0 m and 0.5 m (Figure 14). The channel had a rectangular cross section with vertical side walls. The channel straight wall was made of smooth glass while the curved one was rough concrete. The initial bed was flat and covered with a 20 centimeter (cm) layer of fine gravels with a mean diameter of $d_m=5.5$ mm and the standard deviation of $\sigma = 1.47$ mm. Stream flows at different rates were passed through the flume to study the scour process. No sediment was supplied at the flume inlet, as it was estimated that no sediment would be mobilized at the inlet with the discharges studied. Water depths for the different flows were recorded at the flume. The discharge, water depth, and durations of three of the flume runs are listed in Table 3. After the flume was run for the indicated duration for each case, the erosion and deposition characteristics of the bed were observed and compared with numerical model results.

Table 3. Flume Geometry and Experiment Conditions

Flume Cases	Discharge (l/s)	Water Depth at exit (m)	Duration (minutes)
1	80	0.268	150
2	130	0.300	150
3	150	0.312	125

7.3.3. Numerical Model Details

The simulation domain and the mesh used for the simulation are shown in Figure 14 and Figure 15. The numerical model used a relatively fine mesh of 200 by 24 cells with the spacing between adjacent mesh points ranging from 0.042 m in the contraction and expansion sections to a maximum of 0.18 m at the beginning of the inlet section. The lateral distribution of mesh points was uniform. A much finer mesh of 400 by 48 cells was also created to study model sensitivity to mesh resolution; but the 200 by 24 mesh was shown to be adequate. Therefore, all results are based on the 200 by 24 mesh unless otherwise stated.

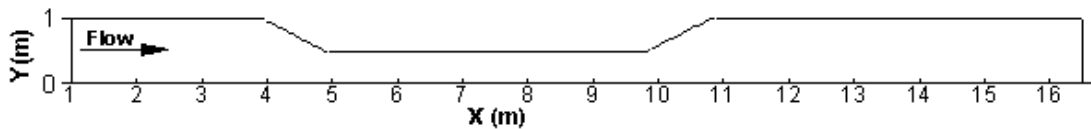


Figure 14. Simulated Contraction-Expansion Case geometry.

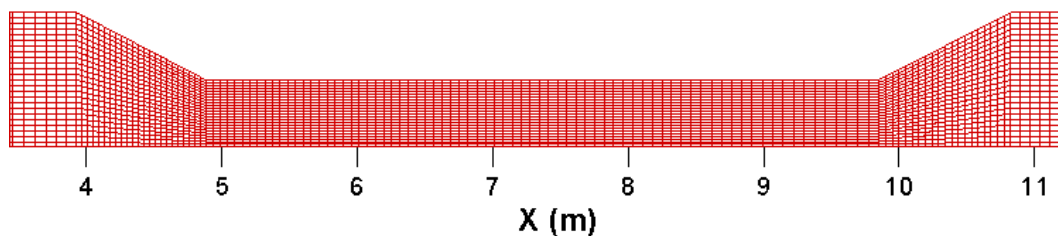


Figure 15. A portion of the 200 by 24 mesh used for modeling.

For each simulation, a fixed-bed flow-only simulation was carried out first. The flow hydraulics thus obtained were then used as the initial condition for the mobile bed simulation. A time step of 1.0 second was used for the unsteady sediment transport modeling for all cases. The boundary conditions were applied:

At the inlet ($x = 1.0$ m), the flow discharge as shown in Table 3 was imposed and the zero sediment input condition was applied. At the exit ($x = 16.5$ m), the water depth in Table 3 was specified.

The boundary conditions at the two side walls need some discussion. In the current SRH-2D modeling, the standard wall function approach used in the 3D models, e.g., Wu et al. (2000), was extended to the 2D model. In the wall function treatment, the first mesh point near a wall was placed outside the viscous sublayer and above the roughness height. The resultant wall shear stress, $\bar{\tau}_w$, was calculated using the depth-averaged velocity, \bar{V}_p , at the first mesh point, P :

$$\bar{\tau}_w = -\frac{\rho\kappa C_\mu^{1/4} K_p^{1/2} \bar{V}_p}{\ln(Ey_p^+)}; \quad y_p^+ = \frac{u_\tau y_p}{\nu}$$

where y_p is the normal distance to a wall for the first mesh point, ρ is the water density, $\kappa = 0.41$, $C_\mu = 0.09$, K_p is the turbulence kinetic energy at point P , $u_\tau = \sqrt{|\bar{\tau}_w|/\rho}$ is the friction velocity, ν is the water kinematic viscosity, and E is the roughness parameter. The Cebeci and Bradshaw (1977) formula is used to compute E :

$$E = \exp\{\kappa(5.2 - \Delta)\}$$

$$\Delta = \begin{cases} 0, & k_s^+ < 2.25 \\ \left[\ln(k_s^+)/\kappa - 3.3 \right] \sin\{0.4258[\ln(k_s^+ - 0.811)]\}, & 2.25 \leq k_s^+ < 90 \\ \ln(k_s^+)/\kappa - 3.3, & k_s^+ \geq 90 \end{cases}$$

where $k_s^+ = u_\tau k_s / \nu$, and k_s may be interpreted as the roughness height. At present, the roughness height k_s is unknown for the 2D depth-averaged application. A value of zero should be used for a smooth wall, while $3d_{90}$ is recommended following van Rijn (1984c). In this study, however, it is a calibration parameter to be determined as one of the boundaries is a rough concrete wall.

7.3.4. Calibration Simulation

The bed roughness and the side wall roughness height need to be determined first through a calibration process using the flume data. As will be shown later, the roughness is an important element in ensuring that the sediment transport model can predict the erosion process, at least for the flume case simulated. Therefore, bed roughness and the side wall roughness height need to be considered carefully. In this study, the Wu and Wang's formula (1999) is used to compute the Manning's roughness coefficient for movable beds:

$$n = \frac{d_{50}^{1/6}}{A}$$

For a stationary flat loose bed, $A = 20$ is usually recommended (Wu and Wang, 1999), and this equation is regarded as the grain roughness. For the movable bed with sand waves, form roughness should be added to the grain roughness according to one of the formulae based on Wu and Wang (1999):

$$\log\left(\frac{A}{g^{1/2} F_r^{1/3}}\right) = 0.911 - 0.273 \log T - 0.051 (\log T)^2 + 0.135 (\log T)^3$$

$$T = \left(\frac{n'}{n}\right)^{3/2} \frac{\tau_b}{\tau_{c50}}$$

where g is the gravitational acceleration, F_r is the Froude number, $n' = \frac{d_{50}^{1/6}}{20}$ is the Manning's roughness coefficient due to grain roughness, n is the total Manning's roughness coefficient, τ_b is the total bed shear stress, and τ_{c50} is the critical stress computed with the Shields curve as proposed by Chien and Wan (1983).

The case with the discharge of 80.0 liters per second (l/s) is selected for calibration. Once calibrated, the same Manning's roughness coefficient for the bed, along with the curved wall roughness height, are fixed for other flow discharges.

Under the flow of 80.0 l/s, no sediment transport was observed and the bed was flat. Therefore, the Manning's roughness coefficient on the bed is expected to be close to the grain shear stress. Based on the estimate, the Manning's roughness coefficient of 0.0215 is chosen while the roughness height on the curved wall is calibrated to be $k_s = 9.0\text{mm}$. A comparison of the simulated and measured water surface elevation at the 80.0 l/s discharge shows that the agreement between the predicted and measured water elevations is favorable (Figure 16). There is a drop in water surface elevation in the contracted section, as has been found also by other researchers (e.g., Briaud et al., 2004).

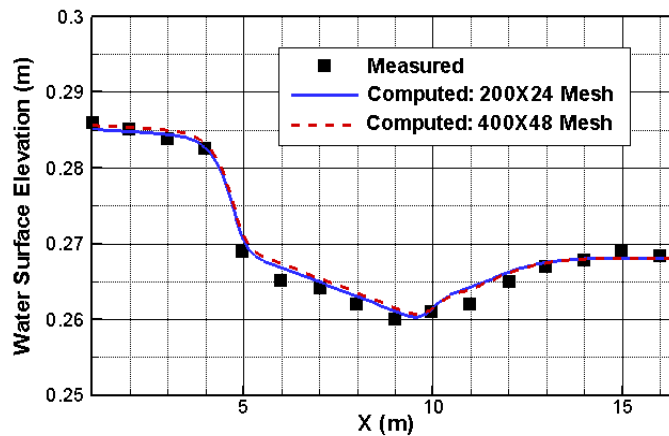


Figure 16. Comparison of computed and measured water surface elevation for the case of 80.0 l/s (KE model $n=0.0215$ $k=9\text{mm}$).

7.3.5. Erosion and Deposition Simulation Results

The flume experiments showed that scour was initiated at the beginning of the contraction and developed downstream at the flow discharge of 130 l/s. The eroded sediment from the scour hole moves downstream and formed a large dune at the expansion section. At a flow discharge of 150 l/s, a similar erosion and deposition pattern was observed—but with more intensity. In this section, the results obtained by using the k-e turbulence model, the Meyer-Peter-Muller transport equation, and the Philip-Sutherland adaptation length are presented with the flow of 150 l/s. The predicted bed elevation change and the water surface elevation compared with the measured data shows good agreement (Figure 17 and Figure 18).

The erosion and deposition pattern is also compared with the measured data in Figure 19. It is seen that the model predicted the depth and size of the contraction scour well; and the location of the maximum deposition is slightly upstream. The present results represent a marked improvement compared with the 2D model results of Marek and Dittrich (2004), which are not shown here. We argue that the improvement of the present 2D model is mainly due to using different process models and parameters. The most important models and parameters are the sediment transport equation, the non-equilibrium adaptation length, and flow roughness. The least important include the turbulence model and effect of secondary flow.

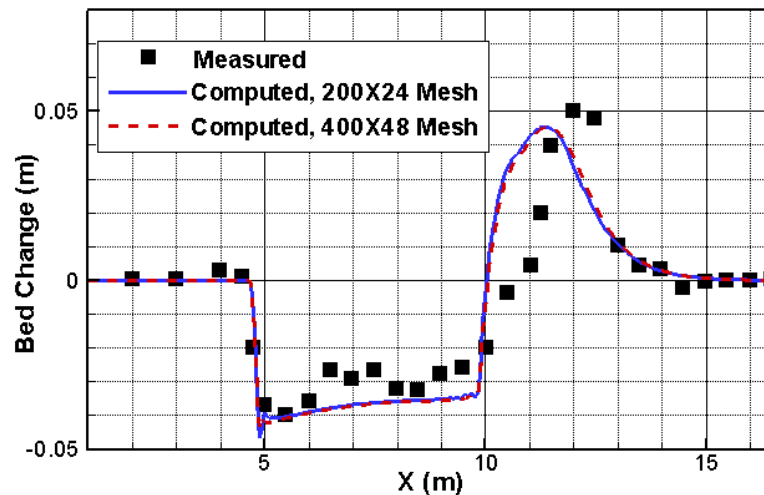


Figure 17. Comparison of predicted and measured average bed elevation change for the case of 150.0 l/s.

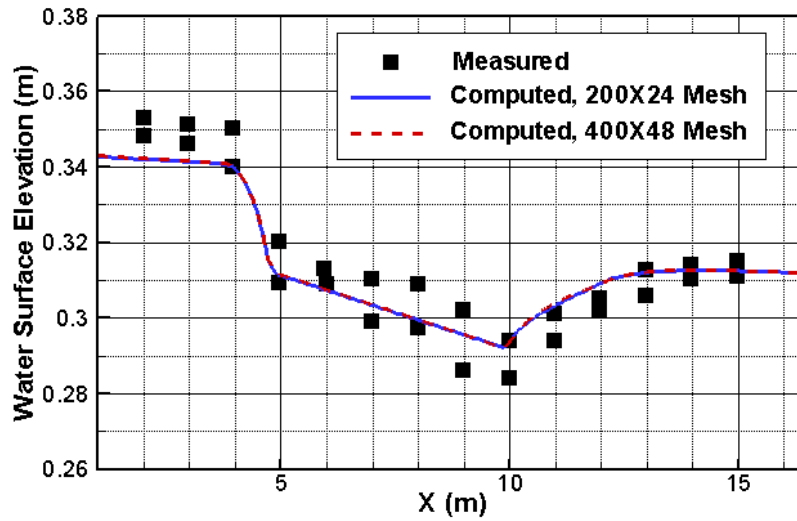


Figure 18. Comparison of computed and measured average water surface elevation for the case of 150.0 l/s.

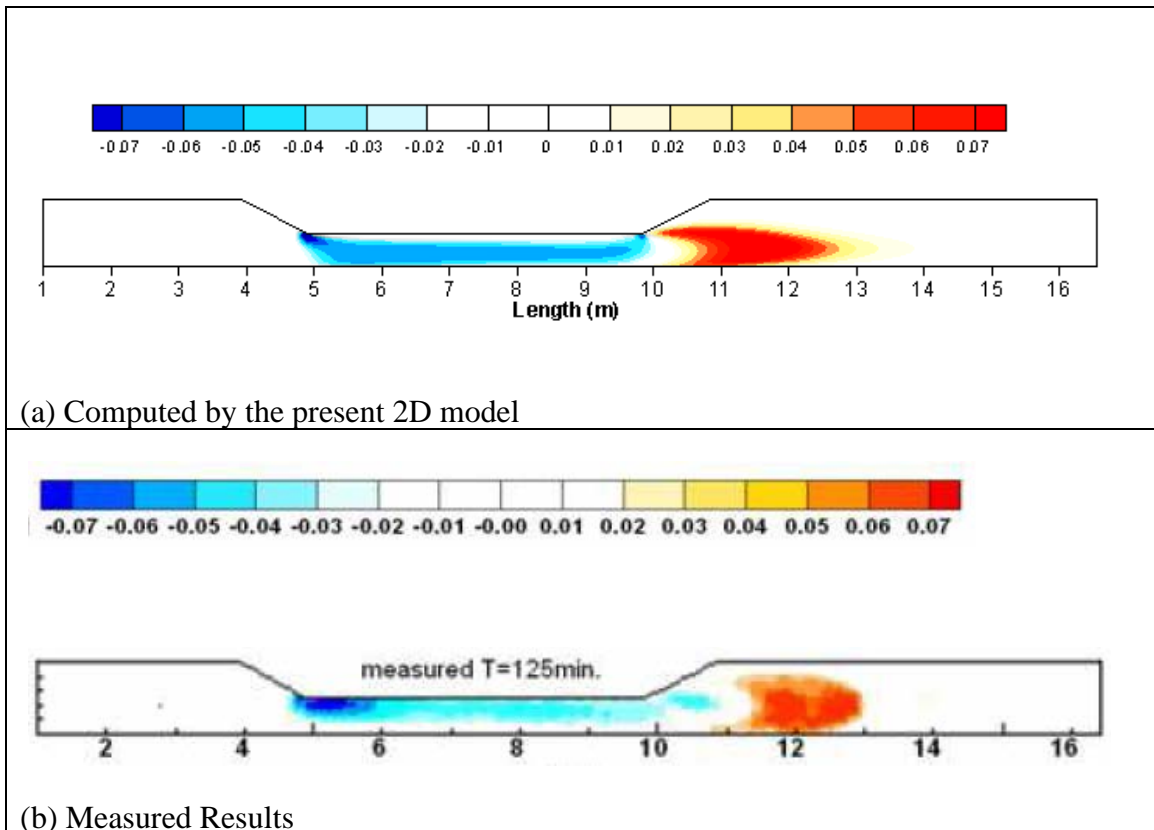


Figure 19. Computed and measured bed change (m) for the flow of 150 l/s at time 125 minutes.

7.3.6. Concluding Remarks

A 2D depth-averaged numerical model was developed to simulate contraction scour to evaluate whether a 2D model is adequate for that application. As a 3D model is still too complex for routine applications, so many engineering applications have to rely on 2D models. Therefore, this study investigated what factors play important roles in determining the performance of 2D models. .

This study uses different models and parameters than previous studies and shows that a 2D model can be adequate for predicting the contraction scour. The sediment transport equation, the non-equilibrium adaptation length, and flow roughness are important for modeling the contraction scour correctly; while the turbulence model and effect of secondary flow are less critical.

7.4. Alternate Bar Formation Downstream of a Dike

7.4.1. Introduction

Straight rivers are rare in nature, and meandering rivers with alternate bars are commonplace. Alternate bars are large bedforms with height and length comparable to the depth and width of a river. Alternate bar and pool development in a river, therefore, has always intrigued scientists and engineers as they were regarded as the beginning of meandering process (Lewin, 1976). Numerous attempts have been made to explain the initiation and development of alternate bars.

In early years, it was recognized that a flat cohesionless bed in a straight channel, under certain conditions, would become unstable in a turbulent stream. The perturbed configuration was in the form of an alternating sequence of bars and pools that migrate downstream (Callander, 1968). This finding prompted an extensive investigation into the instability process and subsequently led to the development of the linear 'bar' theory (Seminara and Tubino, 1989). The sinuous migrating thalweg produced was interpreted as incipient meandering at the time. In the early eighties, the 'bend' theory was developed by Ikeda et al. (1981) who showed that meander formation was in fact associated with a planimetric instability due to secondary flows induced by channel sinuosity. Later, a unified view of the bar and bend theories was put forth by Blondeaux and Seminara (1985). Results indicated that the forcing effect of curvature might provide the initiation mechanism for spatially periodic, steady, and non-migrating perturbations. Their theoretical framework led to a consistent picture of the initial process of meander formation in alluvial channels (Seminara and Tubino, 1989). That is, for an initially straight channel with cohesionless and uniform sediment, instability in the form of migrating alternate bars (or 'free' bars) would occur when the channel width-to-depth ratio exceeds a critical value. As channel widening proceeds and the thalweg becomes sinuous, a second instability, a planimetric one, would occur once the width ratio exceeds a second threshold. The planimetric instability leads to the development of non-migrating steady alternate bars (or 'forced' bars) that are often observed in meandering rivers. As the amplitude of a meander increases, free bars tend to decrease their amplitude and disappear completely, leaving only the forced bars.

The critical condition for free bar initiation and growth may be predicted with linear theories, along with bar wavelength and celerity (e.g., Parker, 1976). But the linear theory is less satisfactory once the condition is far above critical, and non-linear effects have to be incorporated (Blondeaux and Seminara, 1985). Attempts have been made to adopt weakly non-linear theories such as that of Colombini et al. (1987), but limited improvements have been achieved.

For fully non-linear free and forced bar development, more comprehensive numerical models have been developed (e.g., Struiksmma, 1985; Nelson and Smith, 1989; Mosselman, 1998; and Defina, 2003). Nelson and Smith (1989) developed a finite difference model based on the hydrodynamic and sediment transport equations. The model was applied to study the alternate bar evolution for an initially flat bed and the model captured the bar generation with predicted characteristics qualitatively in agreement with observations. Colombini and Tubino (1991) used a spectral method to solve the hydrodynamic and sediment equations to study the non-linear competition among modes. They predicted the importance of non-linear interactions in the bar development process. Defina (2003) developed a finite element model for the morphodynamic evolution of a cohesionless bed. Defina (2003) simulated the formation and evolution of free bars and results compared favorably with the experimental data.

Most of the existing studies have concentrated on the initiation process of free bars or the development of forced bars due to the presence of meander bends. Bed evolution in a constant-curvature bend has received considerably more attentions. However, forced stationary bars may also be formed by other mechanisms such as channel width change and at confluences. For example, near the end of 19th century, many gravel bed rivers in Central Europe were straightened and substantially narrowed for land reclamation, flood control, and navigational purposes. Several of these rivers now display the well-known features of alternate bars (Jaeggi, 1984).

To develop this module, forced bar formation due to the presence of in-stream structures is investigated. The scenario selected may find many practical applications in natural streams, as the process is relevant to river works for restoration, habitat, and channel infrastructure protection and maintenance. For example, hydraulic structures such as jetties, bendways, and diversion dams are often used in streams for various purposes. Despite many benefits, these structures produce unforeseen geomorphic impacts as they act as 'disturbances' to the stream. Even worse, the geomorphic impacts are often not carefully investigated, leading to undesirable consequences.

Also, many of the previous non-linear numerical models are based on the body-fitted orthogonal curvilinear coordinate system. These models are applicable to channels with simple geometry such as straight channels and constant-curvature bends but are problematic for natural channels. Generalization and improvement are needed to simulate practical problems. This study developed an unsteady two-dimensional (2D) depth-averaged mobile-bed model can handle complex geometry.

7.4.2. Numerical Modeling and Comparison

The mobile-bed model SRH-2D is used to investigate the alternate bar formation process observed in a laboratory setting for test and verification. The flume experiment was carried out at the Delft Hydraulics Laboratory by Struiksma and Crosato (1989). When a dike was inserted into a straight channel, forced alternate bars were formed downstream.

Struiksma and Crosato's (1989) flume experiment started with a straight channel 0.6 m wide with a 0.3% slope under a well-defined constant flow. At the upstream boundary, a plate (dike) was inserted to restrict the inflow section. The channel bed was flat and was covered with almost uniform fine sediments with a median diameter (d_{50}) of 0.216 mm. Once an equilibrium development was established, bed topography was measured. The experimental conditions are shown in Table 4.

For the modeling, the solution domain, the dike geometry, and the mesh are shown in Figure 20. The mesh consists of 236-by-24 cells and it is sufficiently fine that a further refinement in mesh would not change the results noticeably, as discussed later in this section. An unsteady simulation is carried out with a time step of 5.0 seconds and continued until an equilibrium bed topography developed. At the upstream boundary ($x = -15.0$ meters), a constant discharge of $0.00685 \text{ m}^3/\text{s}$ was imposed and the sediment supply rate was set to be the sediment capacity as an equilibrium solution was sought. At the downstream boundary ($x = 25$ meters), a water depth of 0.044 meter was specified.

Model results clearly show the development of forced alternate bars caused by the inserted dike. The predicted equilibrium bed topography, in the form of net erosion and deposition, is displayed in Figure 21; and a comparison of the equilibrium bed profile between prediction and measured data is shown in Figure 22 along a line 0.1 meter from the bottom boundary. A series of alternating bars were developed downstream of the dike. The bar and pool depths (amplitude) are, on average, about 25% of the average water depth and the amplitude is mildly damped downstream. The average bar wavelength is approximately eleven (11) times the channel width—much larger than typical downstream migrating free bars. Comparison between the prediction and measured data for bed topography in Figure 22 is found to be good. The amplitude of the alternate bars is predicted satisfactorily while the wavelength is slightly over-predicted. The results demonstrate that the fully non-linear model such as SRH-2D is capable of predicting the alternate bar development as a response to disturbances introduced into a stream.

Table 4. Flume Geometry and Experimental Conditions

Flume Width (m)	Discharge (m^3/s)	Water Depth (m)	Velocity (m/s)	Surface Slope	Froude Number	Manning's Roughness Coefficient
0.60	0.00685	0.044	0.26	0.3%	0.39	0.0263

The bed is covered with fine and almost uniform sediments with a median diameter (d_{50}) of 0.216 mm. The measured bed topography data were obtained after the establishment of equilibrium conditions.

A 236-by-24 mesh is developed for our simulation. The simulation domain, the plate inserted, and the mesh are shown in Figure 20. The simulation time step is 5.0 seconds. The mesh and the time step are sufficient to get an accurate simulation and further refinement does not lead to appreciable change of the results. In this study, the Parker (1990) sediment capacity equation is finally chosen with the default model constants of $\theta_c=0.045$ and $\alpha=0.65$. At the inlet ($X=-15.0$ m), discharge of $0.00685 \text{ m}^3/\text{s}$ and equilibrium sediment transport were specified; and at the exit ($X=25$ m), the water depth of 0.044 m was specified. Note that only bedload transport mode was used for the simulation.

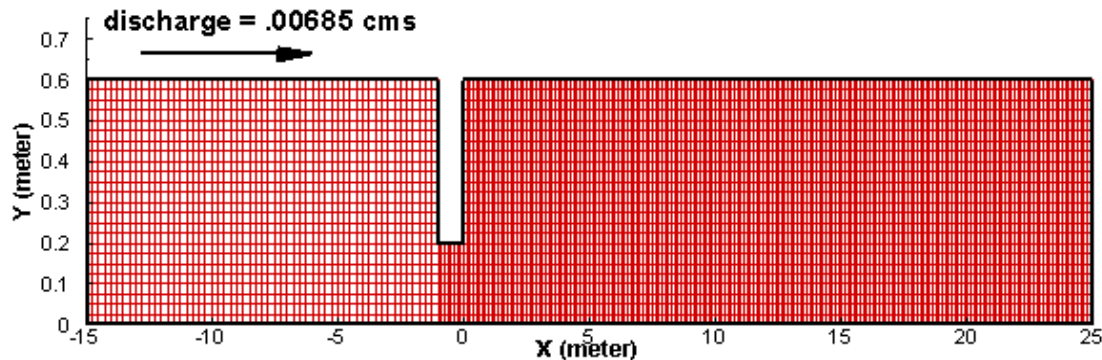


Figure 20. Channel geometry and simulation mesh for the Struikma and Crosato (1989) case.

Unsteady simulation was continued until steady state bed topography was developed. Figure 21 shows the predicted equilibrium bed topography in the form of net deposition and scour depth, and Figure 22 shows the comparison of equilibrium bed profile between measurement and simulation along a line 0.1 m from the bottom boundary. It is seen that a series of steady state alternating bars were developed downstream of the obstacle (or disturbance). The bar and pool depths are about 25% of the average water depth on average, and the amplitude is mildly damped downstream. The average wavelength of the bars is approximately 11 times the channel width—much larger than typical downstream migrating alternate bars. Comparison between the measured and calculated bed topography in Figure 22 is quite good. The amplitude of the alternate bars is predicted satisfactorily, and the wavelength is slightly over-predicted.

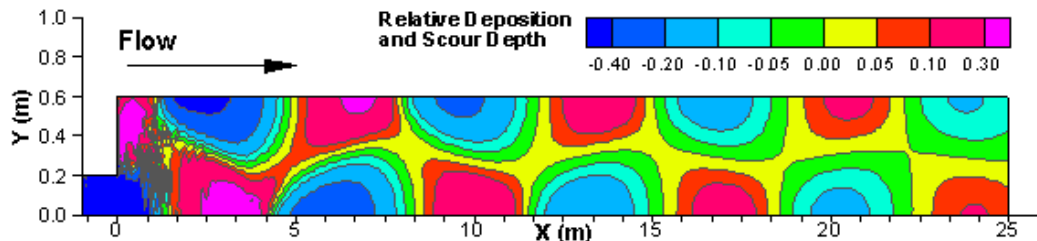


Figure 21. Equilibrium bed deposition and scour depth; depth is normalized by average water depth of 0.044 m.

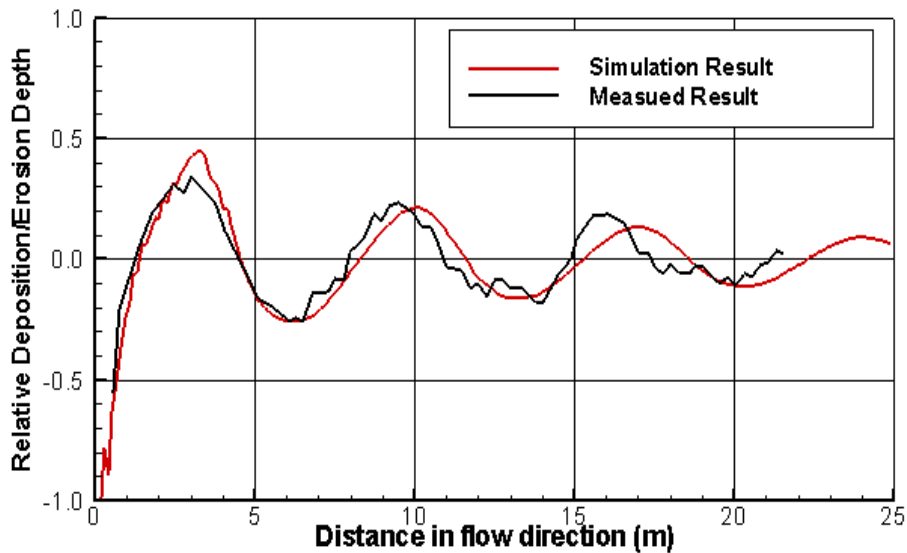


Figure 22. Comparison of measured and simulated equilibrium deposition/scour depth along the $Y=0.1$ m line; depth is normalized by average water depth of 0.044 m (Parker 1990 model).

7.4.3. Sensitivity Study

A number of physical models and corresponding model parameters are used in the SRH-2D mobile-bed mode, and their relative importance and model sensitivity are of interest to anyone who intend to apply the model. In addition, the numerical solution itself is also subject to numerical errors. Therefore, we carried out and reported a sensitivity study to help identify important parameters in applying the model for morphological modeling. These important parameters may need to be calibrated if possible for a specific application while others are less important and need not be changed from case to case.

Selected model parameters for the sensitivity study include mesh size, gravity coefficient (C_{g1}), secondary flow coefficient (C_{spr}), non-equilibrium adaptation length ($L_{b,k}$), the turbulence model, sediment supply at the upstream boundary, sediment capacity, and the roughness coefficient. Some parameters are found to be important while others are not. Those identified as important, at least for the case studied, are presented and discussed next in this section.

Mesh size is important as it is related to the amount of numerical discretization error. These errors should be minimized through a mesh refinement study before examining other model parameters. Three (3) meshes are used for the mesh refinement study: coarse mesh (80-by-12 cells), medium mesh (236-by-24 cells), and fine mesh (396-by-24 cells). A profile of the equilibrium bed along the line of $y=0.1$ meters is compared in Figure 23 between model results and measured data. The medium mesh is adequate, but the coarse mesh leads to an over-prediction of the bar wavelength and a faster decay of the bar height. In all subsequent modeling, the medium mesh is used. In modeling for field cases, two to three different sized meshes are recommended to identifying an appropriate mesh.

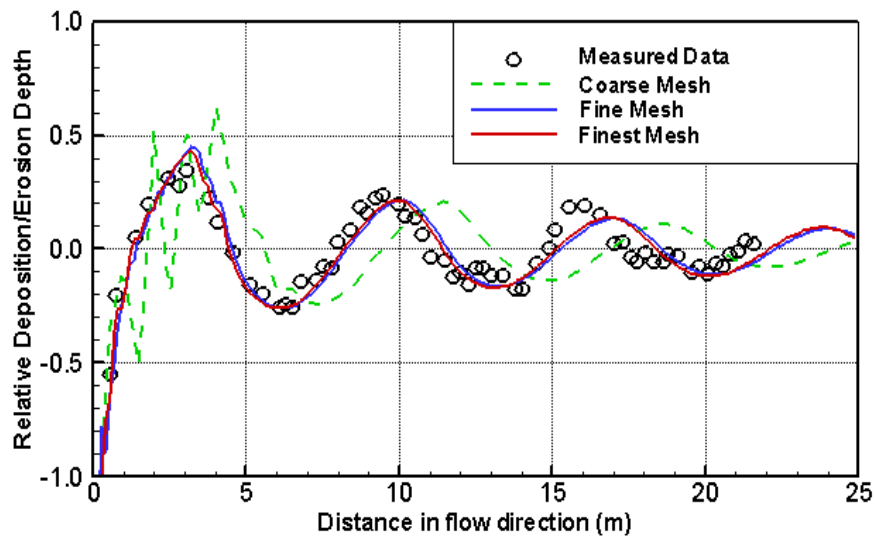


Figure 23. Comparison of predicted erosion and deposition depth along a straight line of $y = 0.1$ m with three meshes; depth is normalized with the average water depth of 0.044 m.

This study found that the gravity effect model coefficient (C_{g1}) is the most important parameter. The recommended range for C_{g1} is from 0.5 to 1.0 (Talmon et al., 1995). Three values: 0.6, 0.75 and 1.0, were tested and the results are compared in Figure 24. Model results are sensitive to changes in C_{g1} . Smaller values lead to increases in both bar height and wavelength, as a smaller gravity effect is implied on the lateral sediment movement. Secondary flow promotes lateral sediment transport, leading to higher bars, but gravity acts to counterbalance the secondary flow effect. To gain a better understanding of the effect on model results, the secondary flow coefficient (C_{spr}) is also varied with three values: 0.6, 1.0, 1.5 and results are shown in Figure 25. It is seen that the results are less sensitive to C_{spr} , and the default value of $C_{spr} = 1$ should not be altered. However, the gravity coefficient (C_{g1}) may be an important parameter that may need to be calibrated if bar height and wavelength are to be predicted.

Sensitivity to the turbulence model is also investigated in the current study. In addition to the parabolic model with $C_t = 0.7$, two more models are applied: the parabolic model with $C_t = 0.07$ and the $k-\varepsilon$ model. Figure 26 compares model results and shows that sensitivity to the turbulence model is less significant.

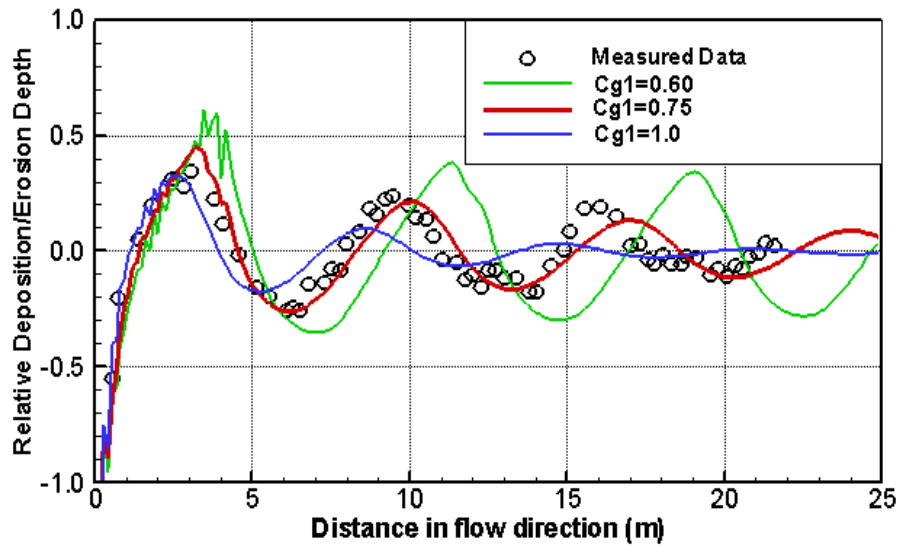


Figure 24. Comparison of predicted erosion and deposition depth along a straight line of $y = 0.1$ m with three gravity coefficient (C_{g1}) values; depth is normalized with the average water depth of 0.044 m.

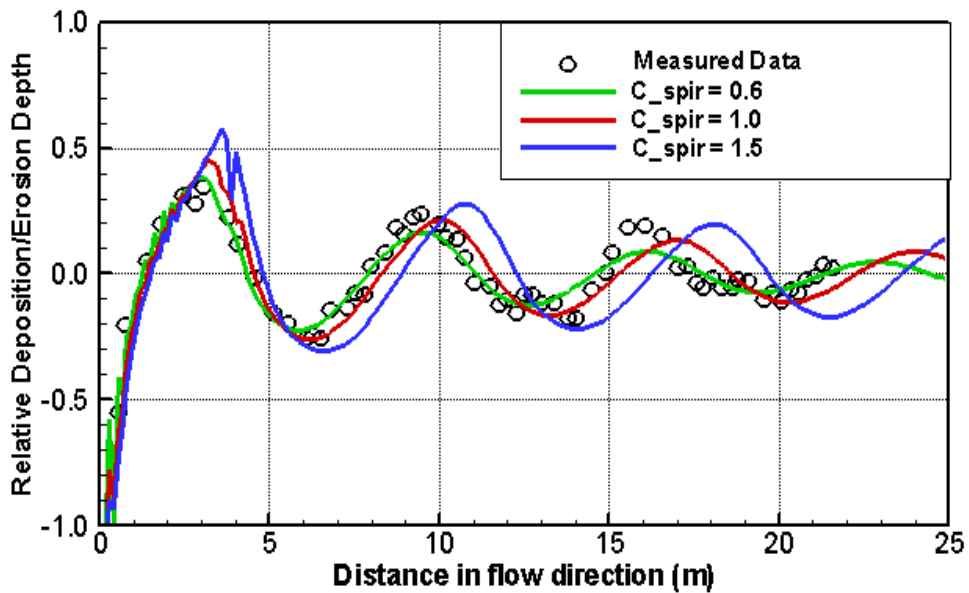


Figure 25. Comparison of predicted erosion and deposition depth along a straight line of $y = 0.1$ m with three secondary flow coefficient (C_{spr}) values; depth is normalized with the average water depth of 0.044 m.

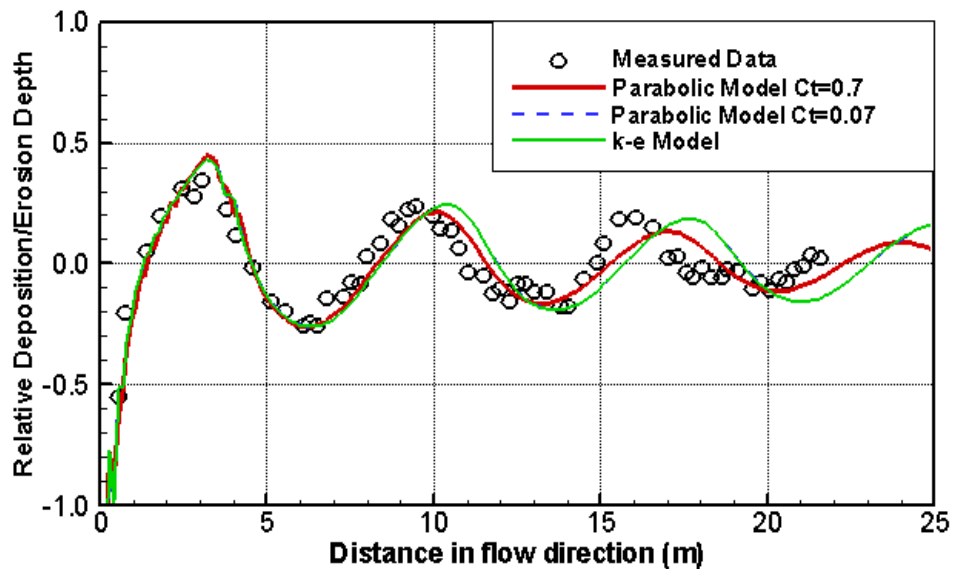


Figure 26. Comparison of predicted erosion and deposition depth along a straight line of $y = 0.1$ m with three turbulence models; depth is normalized with the average water depth of 0.044 m.

7.5. Pool and Bar Formation in Channel Bends

7.5.1. Introduction

It is well known that erosion and deposition in alluvial rivers are often associated with channel meandering. The channel bed near the outer bank is subject to erosion while the inner side is subject to deposition. The knowledge of erosion and deposition at a meandering bend, such as the location and the maximum depth of a scour, the time to reach the equilibrium, and the deposition depth and sediment sorting on a point bar, is of both scientific interest and practical importance.

Bank failure is mostly preceded by erosion at the toe and is often encountered upstream of diversion dams and other structures. Bank failures in these areas endanger the dam and nearby infrastructures and need to be prevented. A numerical model to predict the location, size, and depth of potential erosion at the site is critical to design protection measures. For example, the right bank (looking downstream) upstream of the San Acacia Diversion Dam, located at RM 116.3 on the Middle Rio Grande river, failed during the spring runoff in 2005 (Lai and Bauer, 2007). A long-term solution was sought to ensure the safety of the dam and the Drain Unit 7 Canal.

River restoration projects often need data about the deposition depth and pattern, as well as sediment sorting, as deposition on point bars is directly linked to riparian habitat along a river along a river so that appropriate river management plans may be drafted. For example, the cottonwood recruitment, establishment, and survival along the Sacramento River have been subject of an extensive study recently (Greimann et al., 2007). Information of sediment

deposition on point bars is one of the critical components which may be obtained using numerical models.

In this study, a two-dimensional depth averaged model was developed to predict the erosion and deposition for meandering channels. This model deviates from previous models as a more general numerical method is developed for natural rivers with complex geometry.

7.5.2. A Bend with Uniform Bed

The first bend simulated is case T2 which was conducted using the Delft Hydraulics Laboratory (DHL) curved flume. The experiment used a 140° bend with a straight section attached to the up- and down-stream of the bend (Struiksmma, 1983). The bed sediment was filled with almost uniform sand with a median diameter (d_{50}) of 0.45 mm and a standard deviation of 1.19 mm. During the experiment, the bank was fixed. Some of the experimental parameters for the case is shown in Table 5. The case serves as a test and verification for modeling flows in a bend with the secondary flow and gravity effects in action.

Table 5. Flume Geometry and Experimental Conditions Used for in Struiksmma, 1983

Flume Width (m)	Discharge (m ³ /s)	Water Depth (m)	Velocity (m/s)	Surface Slope	Froude Number	Manning's Roughness Coefficient
1.5	0.062	0.10	0.41	0.203%	0.41	0.023

The planform of the bend (Figure 27) has a radius of curvature of 12 m and a bend length of 29.32 m. Note that the bend does not fit the features of freely meandering streams. According to Leopold et al. (1964), the meander length is about 10 times the width. The flume had a flat lateral bed initially and equilibrium bed topography was obtained after long enough time duration. The bed elevation was averaged over more than 20 independent soundings to smooth out the noise of bedforms. A 120-by-8 mesh was used to cover the solution domain: 30 cells each were placed in the up- and downstream straight channels and 60 cells for the bend (Figure 27). Unsteady simulation started with a flat bed and a time step of 10 seconds. At the inlet ($x=0$), flow discharge of 0.062 m³/s and equilibrium sediment transport rate were applied; at the exit the water surface elevation of 0.1m was used. The Engelund-Hansen model was used for the sediment capacity calculation, and the bedload mode was selected for simulation. The equilibrium bedform was obtained after a sufficient computing time (about 10 hours) and the computed bed elevation and water surface elevations are shown in Figure 28 and Figure 30. In addition, comparison of computed and measured water depths along two profiles (0.375 m from the inner and outer banks) is shown in Figure 29. A bar is formed at the inner bank while a pool occurs at the outer bank. Comparison between the computation and measurements is satisfactory.

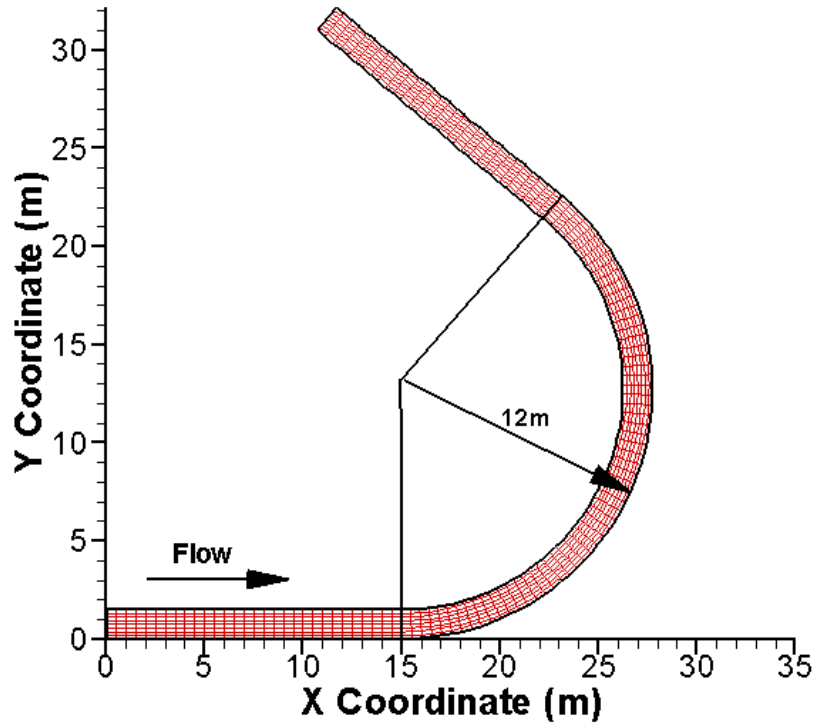


Figure 27. Bend geometry and mesh used for the Struiksma (1983) case T2.

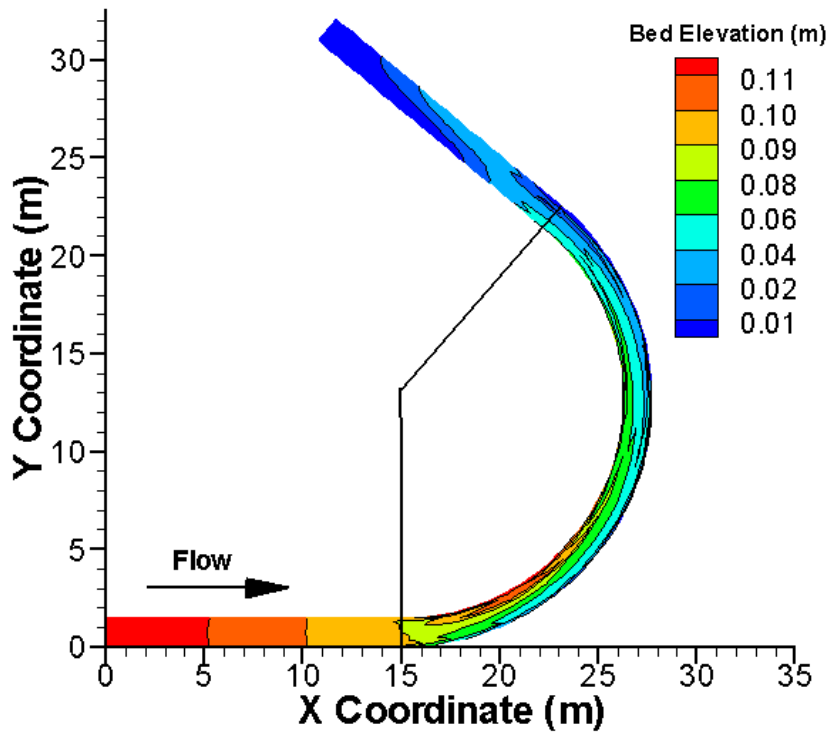


Figure 28. Computed equilibrium bed elevation for the Struiksma (1983) case T2.

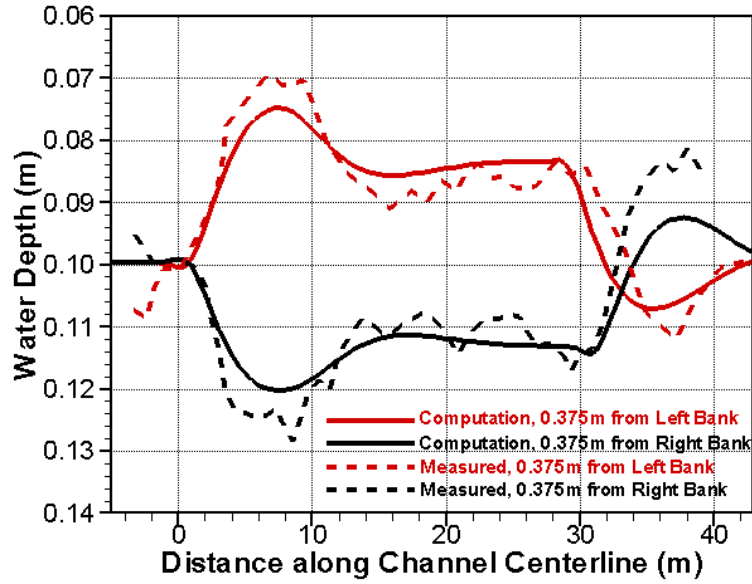


Figure 29. Computed equilibrium water depth for the Struiksma (1983) case T2.

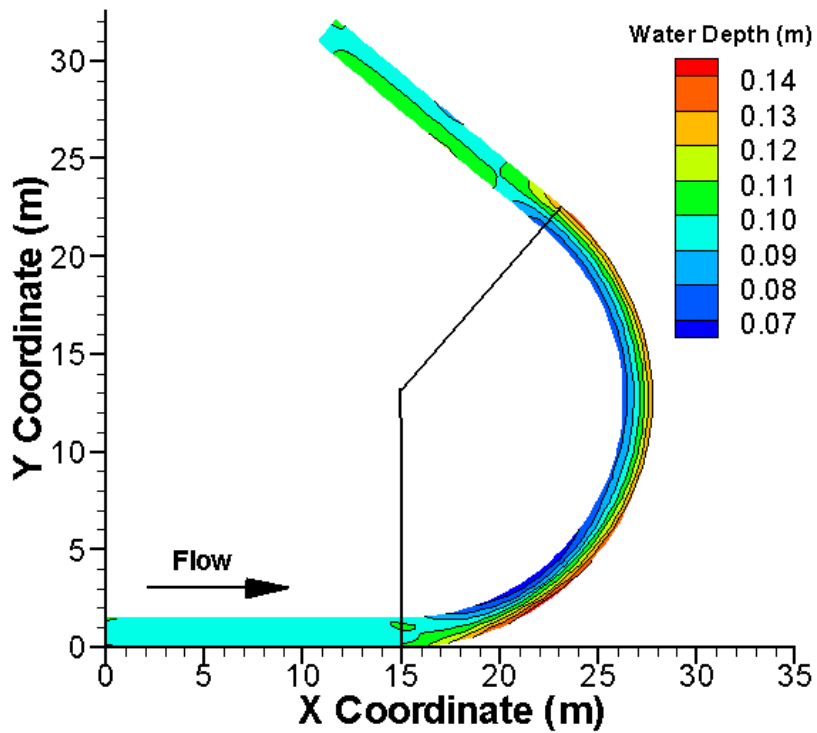


Figure 30. Comparison of computed and calculated water depths along lines 0.375 m from inner and outer banks for the Struiksma (1983) case T2.

7.5.3. A Bend with Non-Uniform Bed

The second bend simulated is case T4 as reported by reported by Struiksma (1985). The bend is 41.5 m long, makes a 108.1° turn, and has a non-uniform bed sediment distribution ($\sigma_g = 2.3$ mm). The geometry of the flume test section as well as of the numerical model solution domain is shown in Figure 31. The flume experiment was carried out at DHL with Waal Bend flume. Note that the same bend is attached to the primary test bend both upstream and downstream. The radius of the bend from the bend centerline is 22 m. The initial bed had a slope of 0.128% longitudinally and was flat laterally. The bed was covered with non-uniform sediments having $d_{50} = 0.6$ mm and $\sigma_g = 2.3$ mm. Some characteristic parameters of the case are listed in Table 6.

Table 6. Flume Geometry and Experimental Conditions for Case T4 of Struiksma (1985)

Flume Width(m)	Discharge (m ³ /s)	Water Depth (m)	Velocity (m/s)	Surface Slope	Froude Number	d_{50} (mm)	Manning's Roughness Coefficient
2.3	0.121	0.12	0.44	0.128%	0.41	0.60	0.02

The numerical simulation used a mesh of 114-by-16 cells: 30 cells were placed in the upstream 90° bend and 30 cells in the downstream 90° bend and 54 cells for the test section of the 108.1° bend. Further mesh refinement would not change the final results by more than 2%. The sediment mixture is divided into four size classes: 15.9% of fine sand (0.125 to 0.26 mm), 34.1% medium sand (0.26 to 0.6 mm), 34.1% coarse sand (0.6 to 1.38 mm), and 15.9% of very coarse sand (1.38 to 2.0 mm). The unsteady simulation was carried out with a time step of 10 seconds. The bed was initially flat laterally and filled with the sediment mixture uniformly in space. At the upstream boundary ($x=0$), a flow discharge of 0.121 m³/s was imposed, and the sediment supply was calculated using the equilibrium sediment transport rate. At the exit, the water surface elevation of 0.12 m was imposed. The Wilcox-Crowe (2003) sediment transport equation was used as the hiding effect is incorporated in this sediment transport equation.

The equilibrium bedform was obtained after a sufficient computing time (about 10 hours) and the computed bed elevation is shown in Figure 32. In addition, a comparison of the computed and measured water depth and d_{50} are shown in Figure 33 and Figure 34 along two profiles (0.11B from the inner and outer banks; B=2.3 m is the channel width). The model can predict the sediment sorting. Overall agreement between the model and measured data is good.

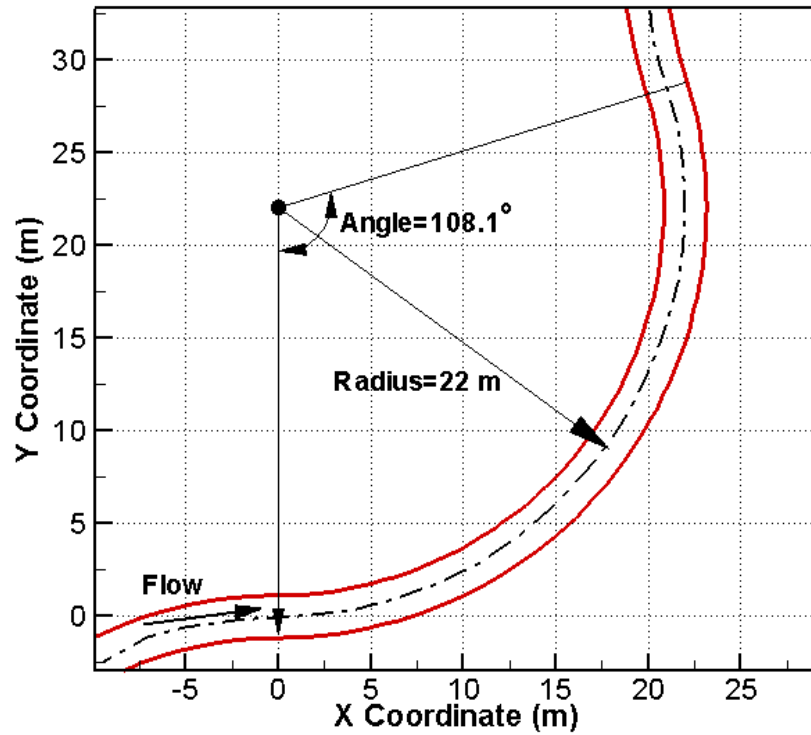


Figure 31. Bend geometry used for the Struiksmma (1985) case T4.

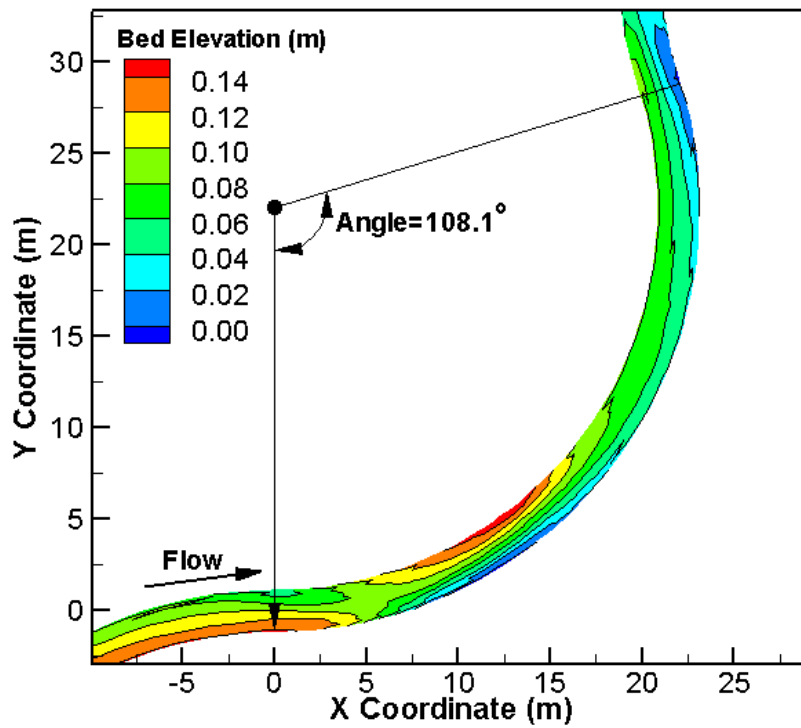


Figure 32. Computed equilibrium bed elevation for the Struiksmma (1985) case T4.

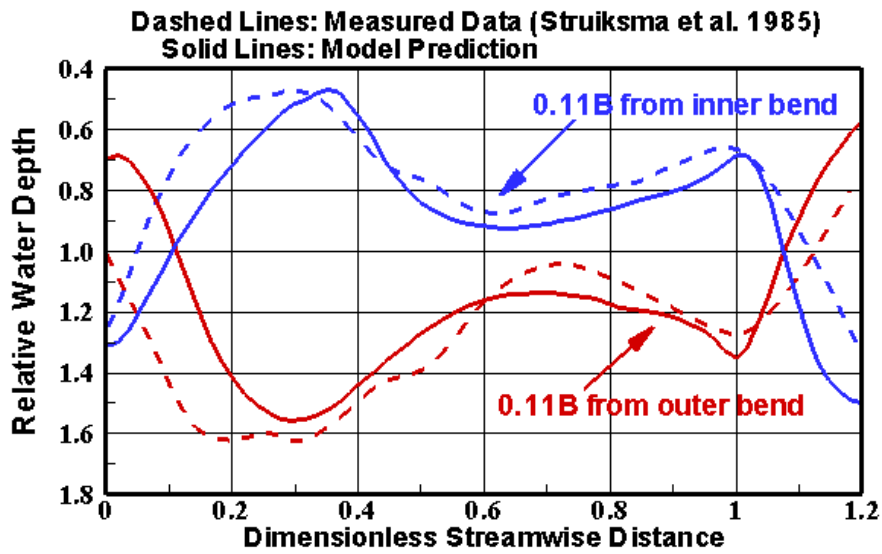


Figure 33. Comparison of computed and measured water depth along lines 0.11B from inner and outer banks for the Struiksma (1985) case T4.

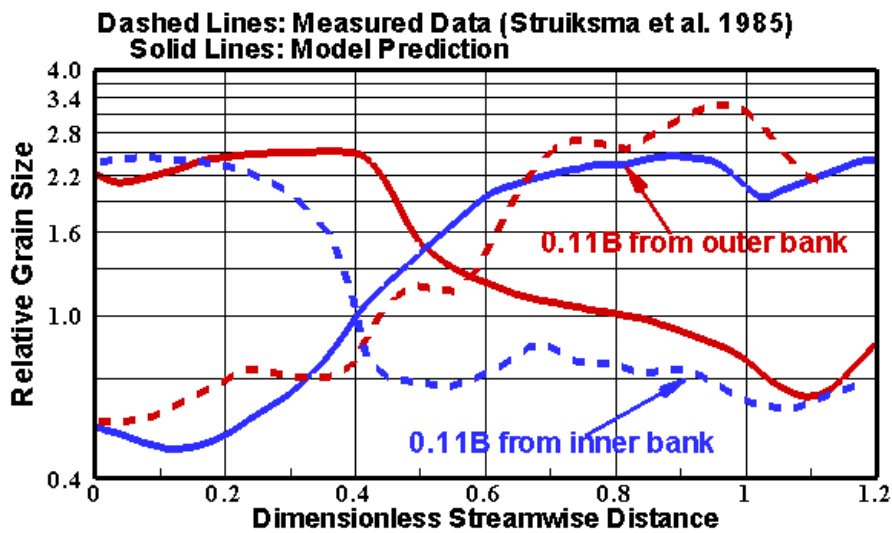


Figure 34. Comparison of computed and measured grain size d_{50} along lines 0.11B from inner and outer banks for the Struiksma (1985) case T4.

Chapter 8. Model Applications

SRH-2D has been applied to an extensive number of engineering projects to answer a wide range of study questions. This chapter presents examples of these projects so readers can see how 2D sediment models such as SRH-2D could be used for practical applications.

8.1. Scour Analysis along an Outer Bank of a Section of the Rio Grande

8.1.1. Background

The right (north) bank of the Rio Grande, approximately 500 feet upstream of the San Acacia Diversion Dam and situated on a spoil levee protecting an irrigation facility, has experienced persistent bank erosion due to toe erosion. The erosion has been extensive enough in the recent past to warrant immediate maintenance repairs (e.g., in spring 2005). The bankline section that is actively eroding is approximately at RM 116.3 and is labelled as the Drain Unit 7 priority site in Figure 35.

As part of the design process, a one-dimensional (1D) hydraulic model, SRH-1D, was developed first to reflect the existing conditions and provide the variables necessary to proceed with a bankline protection design. As part of this process, a suite of empirical scour equations were evaluated to provide an estimate of the scour depth. The wide range of values estimated with these equations resulted in the implementation of the SRH-2D model to predict the location and depth of scour under a number of scenarios, further refining the process by which a design scour depth was determined.

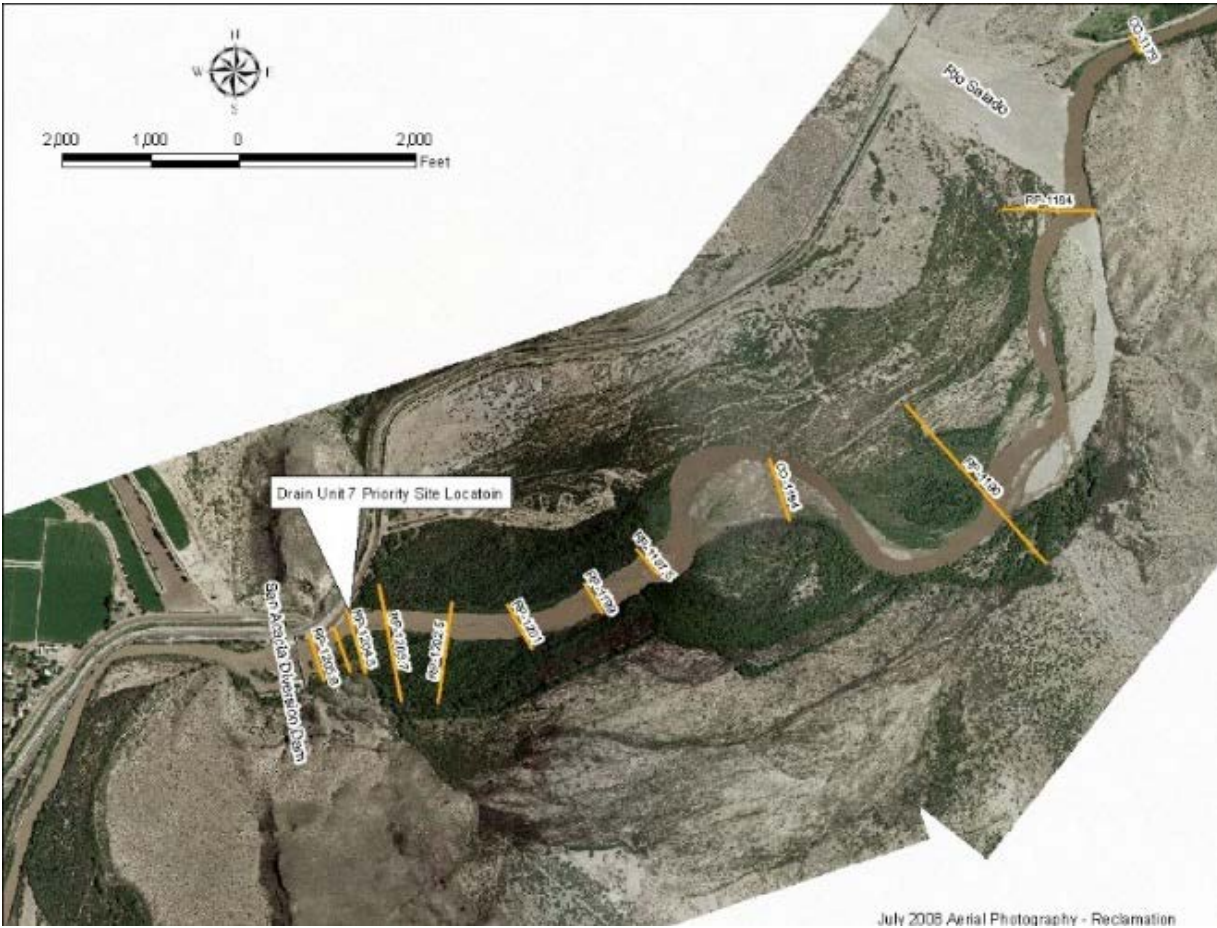


Figure 35. An aerial photo showing the bank erosion site.

8.1.2. Empirical Analysis

Scour results, based on empirical equations, were estimated at the design flow (16,450 cfs - 10 year return flow at San Acacia [Bullard and Lane, 1993]) using methods described in Pemberton and Lara (1984), Derrick and Freeman (2004), and Vanoni (2006). Two average bed size materials were used for these calculations (d_{50}): 0.40 mm and 2.7 mm. The sand-sized materials (0.40 mm) were sampled on top of the riverbed at the site in 2007, while the fine gravel materials (2.7 mm) were sampled upstream in 2000 (just downstream of the Rio Salado confluence). The fine gravel sediments were assumed to represent the armoring strata at the scour location, while the sand sized particles were assumed to represent the surface strata. A summary of the computed scour results are listed in Table 7. While the wide range of predicted values is to be expected given the different underlying assumptions and predictions of the empirical equations, it was desirable to further refine the scour depth predictions. The SRH-2D model was developed and used in order to gain a better understanding of the sediment processes at this project site and provide a more reliable estimate of the scour depth.

Table 7. Scour Depth Based on Various Empirical Methods

	Method	Depth (ft) $d_{50}=0.4$ mm	Depth (ft) $d_{50}=2.7$ mm
General Scour for Moderate Bend (Pemberton and Lara, 1984)	Neill	6.0	6.0
	Lacey	5.8	4.2
	Blench	10.5	9.5
	Competent velocity	16.0	8.3
Bend Scour (Derrick and Freeman, 2004)	Thorne	11.0	11.0
	Maynard	9.1	9.1
	Zeller	3.5	3.5
	Apmann	5.1	5.1
Constriction Scour (Vanoni, 2006)	Straub	3.3	3.3
	Komura	3.5	3.5
	Griffith	3.5	3.5

8.1.3. Numerical Model Description

A large solution domain is used (Figure 36a) to predict the scour (Lai and Bauer, 2007). The upstream boundary is about 1.8 miles from the San Acacia Diversion Dam and the downstream boundary is approximately 1,120 feet downstream of the dam. The model's lateral dimension was created to be wide enough to contain the 25-year flood. The mesh used consists of both quadrilaterals and triangles with a total of 12,595 cells and 11,640 points (see Figure 36a). Elevation data for this model was compiled from a number of sources. River bathymetric data for the Rio Grande was collected in 2007 by Reclamation using an Acoustic Doppler Current Profiler, ADCP (Bauer, 2007). Floodplain topography was based on USGS Digital Elevation Models (DEM), light ranging and detection (LiDAR) data from 1999, photogrammetrically derived cross section data obtained in 2002, and topographical surveys conducted in 2003. A compilation of this data, shown in Figure 36b, was used to create the surface from which the mesh point elevation was interpolated.

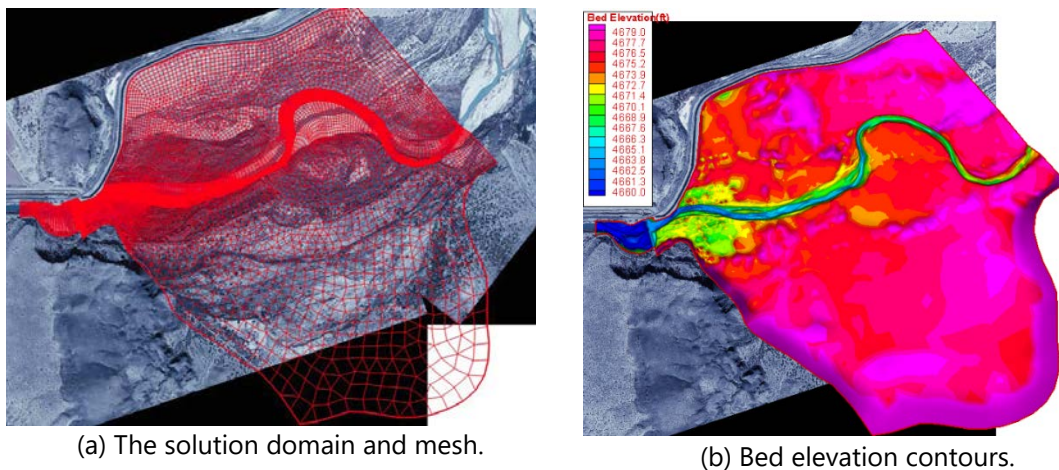


Figure 36. The solution domain, mesh, and topography for the simulation.

Manning's roughness coefficient (n) for bed roughness (flow modeling) and the gradation for representing the surface and subsurface bed sediments (scour and mobile-bed analysis) are needed for the entire solution domain. In this study, the solution domain was divided into twelve bed-type zones; in each zone, Manning's roughness coefficient (n) and bed gradation were assigned (Lai and Bauer, 2007). Manning's roughness coefficients were based on a previous modeling study for this project site using a 1D, Hydrologic Engineering Center's River Analysis System (HEC-RAS) model that used a main channel value of 0.026 and an overbank value ranging from 0.04 to 0.06. The bed gradation data was obtained from bed samples collected at the site in 2007 during this study.

The scour area was represented by a single bed-type zone. Two bed gradations were used in this zone: the cohesive-bed and the non-cohesive-bed. With the cohesive-bed, two bed layers were used: the surface layer and the subsurface layer. The surface layer had a one foot depth and was composed of sands and gravels with a gradation consistent with field measurements in the project area (see Table 8 –cohesive bed top sediment). The subsurface layer consisted of cohesive materials with erodibility properties as described above. It was assumed with the cohesive-bed condition that this subsurface layer had an infinite thickness. It is possible, based on observations elsewhere on the Rio Grande, that multiple, alternating layers of cohesive and non-cohesive sediments exist, but the assumption of an infinitely thick cohesive bed provides a lower end estimate of the scour depth, as cohesive sediment is very resistance to bed erosion. This provides a means of bracketing the possible scour that may occur at the project site.

The non-cohesive bed represents the other extreme of the bed materials and was intended to provide a high-end estimate of the scour depth, giving the other bracket for possible scour at the project site. For the non-cohesive condition, the bed was assumed to have an infinite thickness and consist of sand sized particles with a $d_{50}=0.4$ mm (see non-cohesive in Table 8).

Table 8. Measured Bed Gradations at Two Locations Used for Modeling

Bed Condition	64 mm	32 mm	16 mm	8 mm	4 mm	2 mm	1 mm	0.5 mm	0.25 mm	.125 mm	.063 mm	.004 mm
Cohesive-bed top sediment	100	96.0	85.2	66.0	51.2	42.9	38.5	30.1	12.3	3.30	1.10	0
Non-cohesive	100	98	92.4	82.6	74.9	70.3	67.3	59.6	24.	6.85	1.65	0

Eight size classes (see Table 9) were used to represent the non-uniformity of the sediments at the project site. Size class 1 represents cohesive sediment while size class 8 represents non-erodible bedrock. Since the existing bank is lined with riprap, the bankline at this location was modeled as non-erodible.

Table 9. Sediment Diameter Bounds of Each Size Class for Modeling

Size Class No.	1	2	3	4	5	6	7	8
Lower d(mm)	<.0625	.0625	0.25	1.0	2.0	8.0	32.0	rock
Upper d(mm)		0.25	1.0	2.0	8.0	32.0	125.0	

8.1.4. Boundary Conditions and Other Parameters

Boundary conditions at both the upstream and downstream model boundaries are needed.

- For the **upstream**, both the discharge and sediment supply rate were specified. The discharge (16,400 cfs) was based on the 10-year return flow at San Acacia (Bullard and Lane, 1993). The sediment supply rate was assumed to equal the transport capacity for the non-cohesive sediments and the equilibrium concentration ($C_{eq} = 1.0 \frac{g}{l}$) for the cohesive sediments. Since the upstream boundary is significantly upstream of the project site location, this transport capacity assumption was considered adequate.
- For the **downstream**, the water surface elevation from a previous HEC-RAS modeling for this project site was applied. Since flow is supercritical across the exit of the San Acacia Diversion Dam, the downstream boundary condition is less critical.

Other modeling parameters include the bulk dry density for the non-cohesive sediment (99.26 pounds per cubic foot [lb/ft^3]), the bulk dry density for the suspended cohesive sediment ($30.0 lb/ft^3$), and the bulk dry density for the bed cohesive sediment ($58.0 lb/ft^3$). These parameters were based on previous modeling efforts, SRH-1D, on the Rio Grande at other locales.

8.1.5. Results and Discussion

The unsteady, mobile-bed simulations were run for 40 days. The predicted scour at day 40 for both the cohesive and the non-cohesive bed conditions are shown in Figure 37. Observations of the maps in this figure reveal that the maximum scour is near cross section line RP-1205, being upstream of the line for the non-cohesive bed and downstream of the line for the cohesive bed. With the cohesive-bed, the scour depth is about 6.6 feet and the maximum scour is located about 76 feet downstream of the RP-1205 line (channel cross line used specifically for Rio Grande). With the non-cohesive-bed, the maximum scour depth predicted is 19.2 feet and is located about 43 feet upstream of the RP-1205 line. Field measurements made at the site showed that the deepest scour is upstream of the RP-1205 line. It seems likely, therefore, that the actual bed condition is probably closer to the non-cohesive bed condition, though the two bed scour estimates provide a probable bracket for the design scour.

The time evolution of the scouring process can be viewed by plotting the bed elevation along two lines: one on the RP-1205 line, shown in Figure 37 and another along the toe of the right bank. Figure 38 and Figure 39 show the bed elevation changes with time along the two lines for the two scenarios. As mentioned previously, the equilibrium maximum scour depth is not attained for the cohesive bed, as the scour process is slow and a much longer time than 40 days is required. Continued bed scour is expected for the cohesive bed condition until the bed shear stress is below the critical erosion stress. For the cohesive bed condition, the surface erosion critical stress is $0.125 lb/ft^2$ (or $4.0 \text{ pound mass}[lbm]/ft/s^2$) and the mass erosion critical stress is $2.84 lb/ft^2$ (or $91.3 lbm/ft/s^2$). The bed shear stress predicted at day 40 for the cohesive bed is still above $100 lbm/ft/s^2$ (Lai and Bauer, 2007), which is significantly higher than the surface erosion critical stress and slightly higher than the mass erosion critical stress. In contrast, the scouring

process for the non-cohesive-bed is much faster. For example, the scour reached a depth of 10 feet between RP-1205 and RP-1204.5 after 6 hours. As the depth of scour increases the scour process slows down significantly and reaches equilibrium after a few days. The graphs in Figure 38 and Figure 39 show that the difference in scour between 10 and 40 days is small.

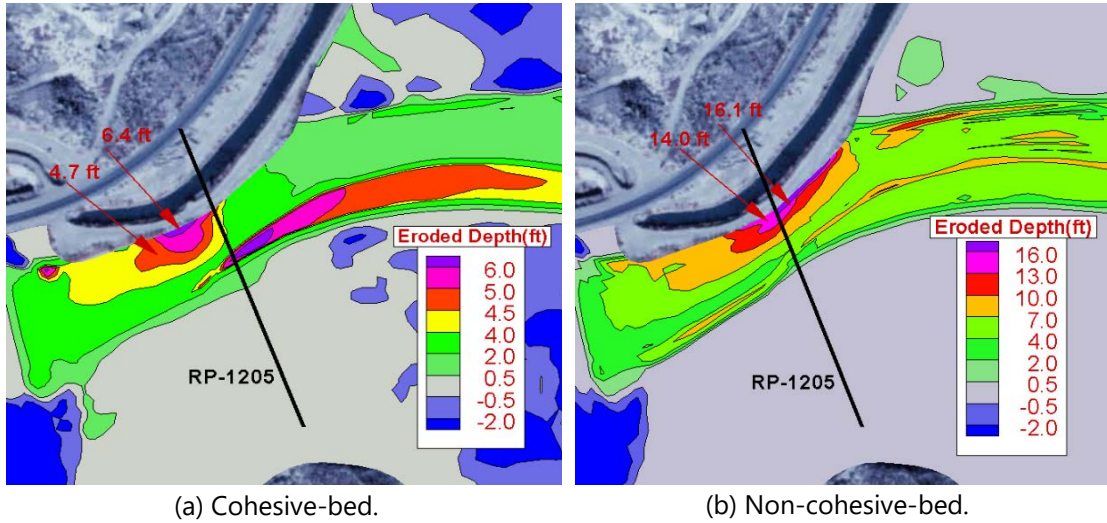


Figure 37. Predicted scour depth after 40 days (positive for net erosion and negative for deposition).

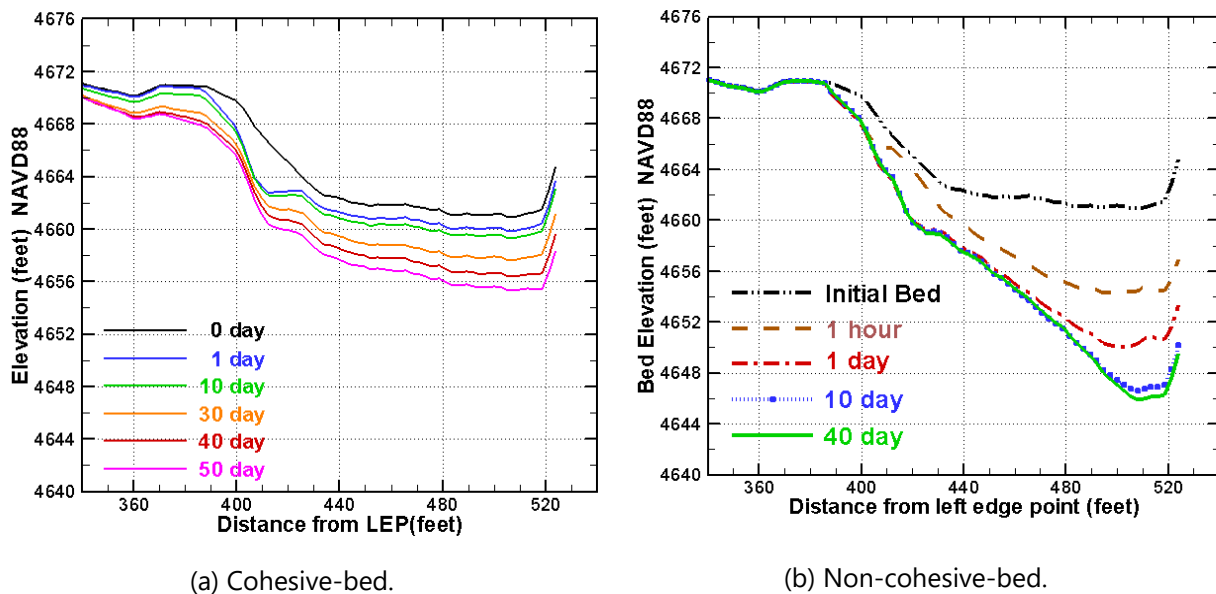
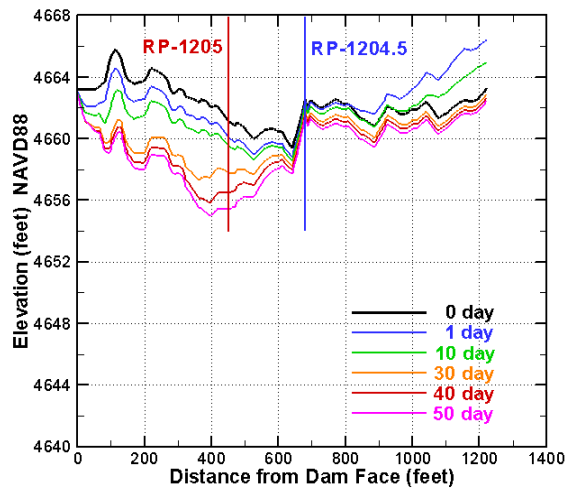
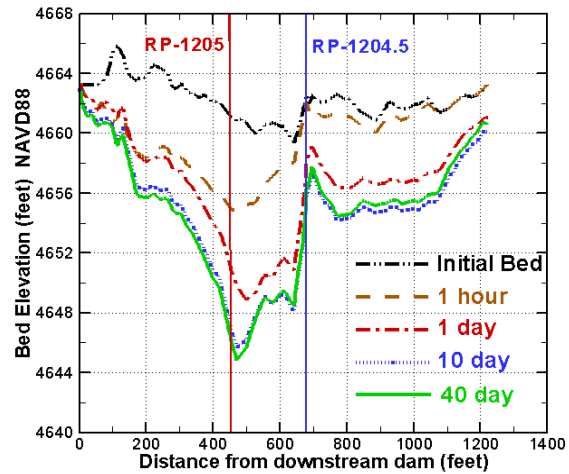


Figure 38. Predicted bed elevation change along the RP-1205 line.



(a) Cohesive-bed.



(b) Non-cohesive-bed.

Figure 39. Predicted bed elevation change along the toe of the right bank.

8.1.6. Concluding Remarks

A 2D, depth-averaged, mobile-bed, numerical model was developed to simulate the scouring process at an outer bend upstream of the San Acacia Diversion Dam on the Rio Grande. The purpose was to gain a better understanding of the scouring process and obtain a more reliable estimate of the scour at the project site. The predicted scour from the 2D model range from a value of 6.6 feet in the cohesive sediment to 19.2 feet in the non-cohesive sediment after a 40-day simulated run. Empirical equations were also used to estimate the scour at this site and provide scour component estimates ranging from 3.1 to 16.0 feet, implying a total scour estimate within the range predicted by the 2D modeling effort.

The benefit of the 2D modeling effort was that the results are based on field site conditions, as opposed to trying to match the site conditions upon which the empirical equations are based. The ability of the 2D model to predict the actual location of the maximum scour also helped, when compared to field data measurements of the actual maximum scour depth, to flush out which bed scenario was more pertinent to the project site, thereby further helping to choose a design scour depth. This study shows that, while there is still a level of uncertainty with predicting scour depth, 2D mobile-bed models have been advanced in recent years to such a point that they may be used to predict the scouring process and help delineate the design scour with reasonable confidence.

8.2. Trinity River Gravel Injection Study

8.2.1. Purpose of the Simulation

The Trinity River Restoration Program constructed the Lowden Ranch Channel Rehabilitation Project the Trinity River in northern California in the fall of 2010. Prior to construction, the reach was characterized by a nearly straight channel with planar bed topography (Figure 40). Restoration objectives for the reach were to increase aquatic habitat quality and hydraulic diversity by adding planform curvature and increasing local bed relief. These objectives were achieved in part by constructing a large meander bend near the upstream end of the site, constructing channel anabranches around two islands near the downstream end of the site, and by floodplain lowering and slight channel widening in the center of the site. A primary intent of the channel widening in the center of the site was to encourage gravel deposition to accelerate the growth of an incipient mid-channel bar that gradually forming there. To that end, the project was designed with the intent to inject coarse sediment just upstream from the widened section during the 2011 spring high-flow release from Lewiston Dam. It was expected that the injected sediment would route downstream and deposit as a new bar along the left bank immediately downstream from the injection point and on the incipient medial bar located near the middle of the site.

Planning the high-flow injection required answers to several key questions, including how much coarse sediment to inject, where to inject it, how much bar growth might be achieved, and where maximum deposition would occur. Of particular interest was whether an upstream gravel injection might cause excessive deposition in one or more of the channel anabranches surrounding the constructed islands. Morphodynamic modeling with SRH-2D was chosen as a primary tool to assist in answering these questions.

8.2.2. The Solution Domain

The area of interest for this modeling effort encompasses the bend in the upper right corner of Figure 41, and extends downstream about 2,000 feet past the pair of islands at lower left. In order to dissipate errors associated with inaccurate boundary conditions and numerical boundary effects, the full computational mesh that defines the model domain extends well outside this area of interest (Figure 42). The upstream and downstream boundaries of the computational mesh are about 1,500 feet upstream and 2,000 feet downstream from the area shown in Figure 41.

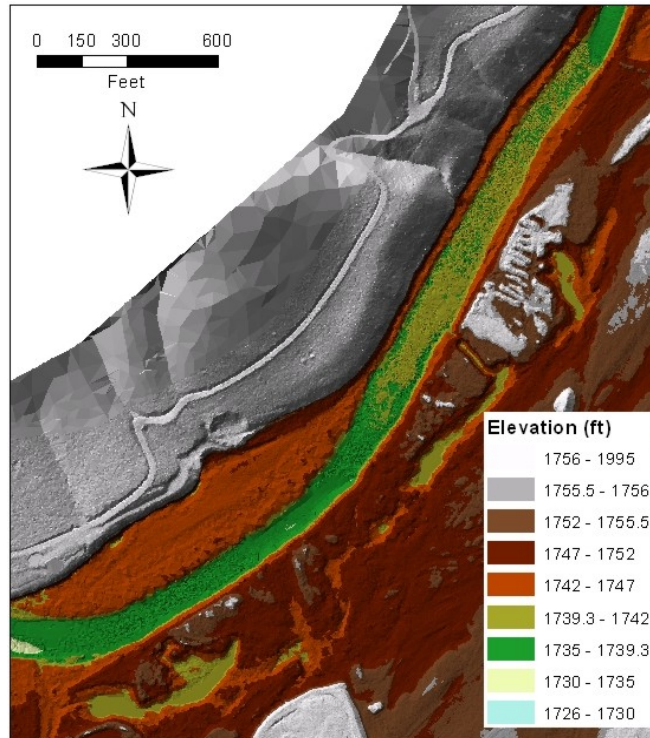


Figure 40. Pre-construction topography at the Lowden Ranch rehabilitation site.

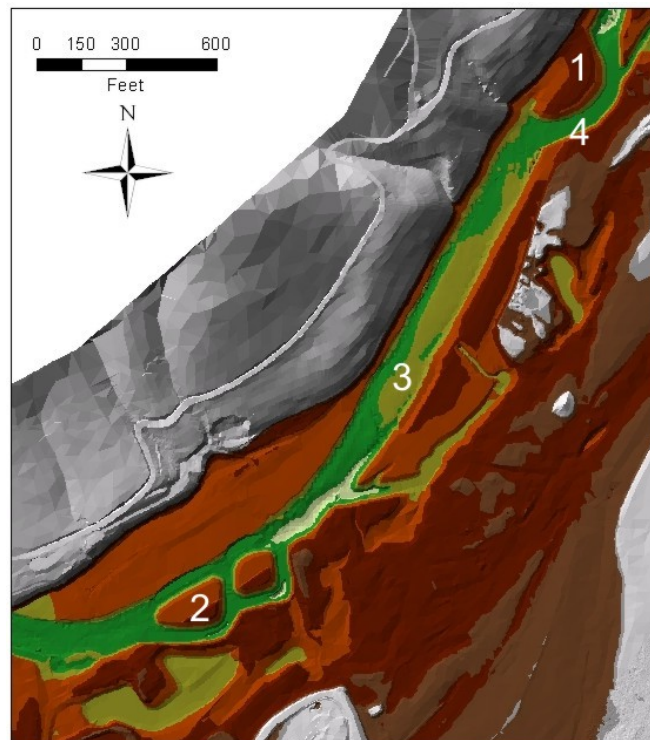


Figure 41. Design topography at the Lowden Ranch rehabilitation site. Areas discussed in the text are 1) constructed meander, 2) constructed islands and split-flow channels, 3) incipient medial bar, 4) high-flow coarse sediment injection point.

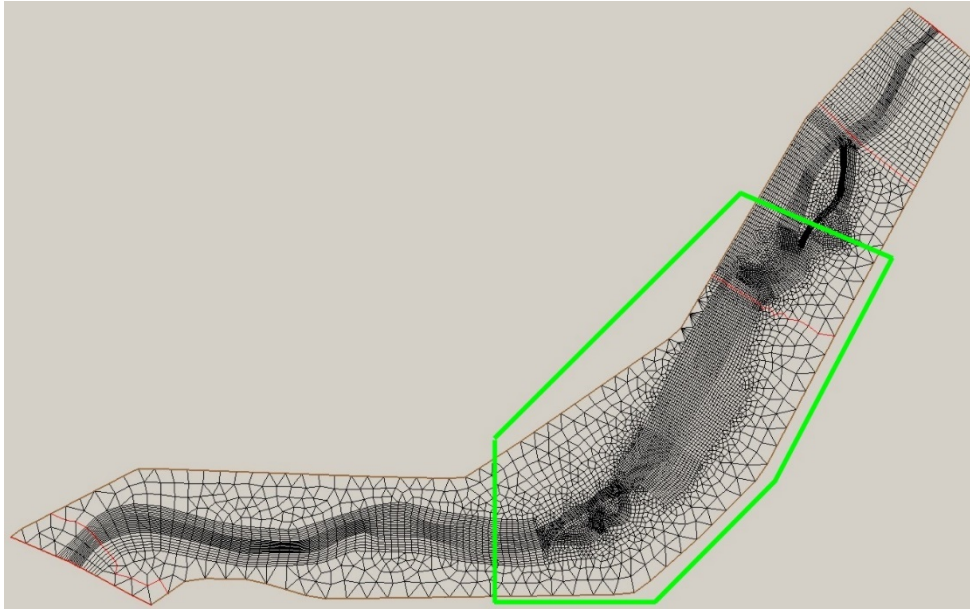


Figure 42. The computational mesh for modeling the Lowden Ranch rehabilitation site. The green polygon denotes the area of interest and approximate extents of Figure 40 and Figure 41.

For mobile-bed simulations, it is useful to include two or three interior boundaries in addition to the upstream, downstream, and wall boundaries required for hydraulic simulations (Figure 42). These interior boundaries serve as transects where sediment fluxes can be monitored. When a mobile-bed run is performed, SRH-2D creates n monitoring files denoted “casename_LNi.dat,” where casename is the user-specified case name for the simulation, i is a number from 1 to n , and n is the number of monitoring transects defined for the run. It is particularly useful to define a monitoring transect near the upstream boundary of the model domain, as that transect can be used to identify errors in the input sediment fluxes.

8.2.3. Initial Calibration and Parameter Selection

This section briefly summarizes the reasoning behind the selection of hydraulic roughness parameters and sediment transport options for modeling the coarse sediment augmentation at the Lowden Ranch Rehabilitation site. A detailed description of the inputs and model setup for the coarse sediment augmentation simulations themselves are given in subsequent sections.

Initial calibration and parameter selection for modeling the Lowden Ranch coarse sediment injection was accomplished through preliminary model runs using pre-construction topography. Runs with the hydraulic module only showed that pre-project water surface elevations at a near bankfull discharge of 7,000 cfs could be adequately approximated using Manning’s roughness coefficient values of 0.035 for the main channel bed and 0.06 for vegetated areas along the channel margin.

The Trinity River is a coarse-bedded river with a substrate composed of gravel, cobble, and coarse sand. The sediment transport equations available in SRH-2D most suited to this type of river environment include the equations proposed by Parker (1990), Wilcock and Crowe (2003), and the modification to the Wilcock and Crowe equations (Gaeuman et al., 2009). These three

transport models were tested using various optional parameters by comparing test results with known geomorphic trends at the site prior to site construction. Bed elevation monitoring in 2009 and 2010 in the center of the Lowden site showed that most of that area underwent slight degradation during the 2010 spring flow release, whereas the downstream center portion of the incipient median bar in the area aggraded slightly (Figure 43). After trial model runs with different sediment transport equations, the Trinity modification to the Wilcock and Crowe (2003) equations was determined to approximate this spatial pattern of erosion and deposition as well or better than the alternative formulations. Additional survey data and observation from 2009 and 2010 indicated that the depth of a pool at the downstream end of the site remained nearly constant over the 2010 release. However, all transport relations tended to incorrectly predict aggradation of the pool at the downstream end of the site for all transport equations tested. Additional testing showed that specifying larger values of the dimensionless reference shear stress for the mean bed surface grain size (τ^*_{m}) and of the bedload adaptation length (L) reduced the rate and magnitude of pool filling. The Trinity transport equation was therefore parameterized with $T1 = 0.032$, $T2 = 0.05$, and $D_{\text{sand}} = 4$ mm so that the computed values of τ^*_{m} would be larger than those produced by the default parameters by about 0.014. In addition, a value for L of 80 m, or about 2 to 2.5 channel widths, was selected.

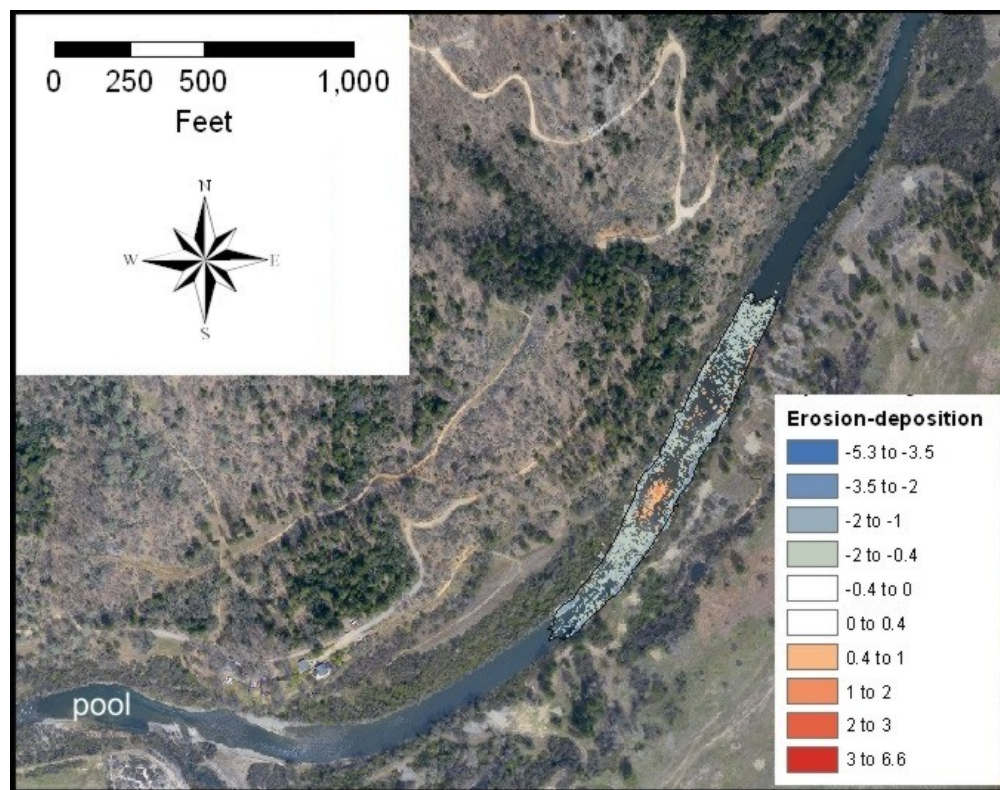


Figure 43. Air photo of the Lowden Ranch site prior to construction with changes in bed elevation between 2009 and 2010 topographic surveys indicated. The pool discussed in the text is labeled.

8.2.4. Initial Conditions

Required initial conditions for a SRH-2D Mobile Bed model run include a mesh that defines stream topography and hydraulic roughness throughout the modeling domain, a restart file specifying initial hydraulic conditions, and information describing the initial composition of the substrate.

8.2.4.1. Initial Topography and Hydraulic Roughness

A primary model mesh defining the topographic surface within the modeling domain is required for any SRH-2D run. Individual mesh elements within the primary mesh are also coded with material type IDs used to assign values of Manning's roughness coefficient, n , to areas of the mesh. The primary mesh for modeling the Trinity River gravel injection is "Lowden_design.2dm."

8.2.4.2. Initial Hydraulic Conditions

Modeling of the Trinity River gravel injection requires using an unsteady flow hydrograph. As for any unsteady SRH-2D run, including flow-only runs, the required initial condition is a restart file generated by a steady flow simulation using the same mesh. The restart file used to define initial hydraulic conditions for modeling the Trinity River gravel injection is "Steady3000_RST.dat." This restart file was generated by modeling flow only at a steady discharge of 3,000 cfs.

8.2.4.3. Initial Substrate Particle Size Distribution

Defining the initial substrate conditions for modeling the Trinity River gravel injection was accomplished in four steps. First, the primary topographic mesh was copied and the material type IDs were adjusted to define two zones with different substrate characteristics. This modified mesh is "Lowden_design_substrate.2dm" (Figure 44). Next, the number and thicknesses of substrate layers in each zone and an initial particle size composition of those layers was defined by user input to the SRH-2D pre-processor.

The third step was to conduct a preliminary "zeroing" Mobile Bed run using the substrate conditions specified in the previous two steps to evolve an active layer with a spatially-distributed particle size distribution. This preliminary run was shortened to model only the rising limb of the hydrograph used for the final model run.

Finally, the active layer particle size distribution developed with the zeroing run was substituted back into the original site topography, replacing the active layer size distribution that was initially specified with pre-processor input alone. This substitution was accomplished by invoking a special pre-processor option to identify the restart file "gradation_RST.dat" (Figure 45) as the source of the initial composition of the active sediment layer, as described in the next section. Using the evolved active layer as the initial bed surface condition yields more accurate predictions of subsequent sediment transport and bed evolution.

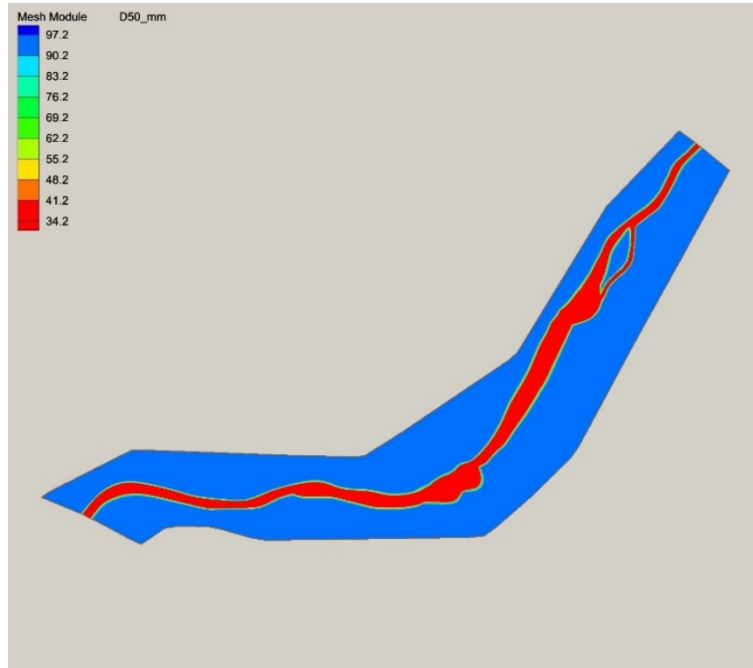


Figure 44. Median active layer particles sizes in two mesh zones, as defined by a version of the computational mesh with modified material types and input to the SRH-2D pre-processor.

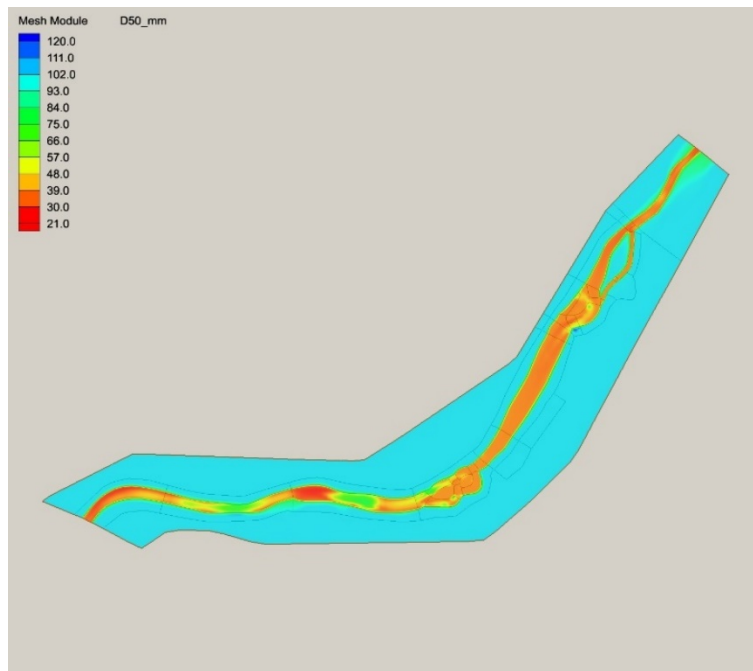


Figure 45. Median active layer particles sizes stored in a restart file following a preliminary "zeroing" model run. This evolved bed surface is the initial condition for subsequent runs.

8.2.5. Water and Sediment Boundary Conditions

The following data input files were prepared prior to running the SRH-2D pre-processor.

8.2.5.1. Inlet Discharge

For this simulation, a flow hydrograph lasting 600 hours was specified at the upstream boundary of the model domain by the text file "inlet_q_D.dat":

```
//t, Q (english)
0,3000
24,4000
48,6000
72,7000
96,8500
120,10000
144,11000
240,9000
264,8000
288,7000
312,6000
336,5690
360,5322
384,4977
408,4655
432,4354
456,4072
480,3809
504,3562
528,3500
```

The file format consists of any number of comment lines beginning with // followed by a sequence of lines containing time and discharge. Time is given in hours and, in this case, discharge is given in English units of cfs. Time and discharge pairs in this file are comma delimited, but may also be space or tab delimited.

Flows in the modeled reach of the Trinity River are almost entirely regulated by Lewiston Dam, about 8 river miles upstream. Although environmental high-flow releases from Lewiston Dam are implemented every spring, the precise release schedule for the 2011 release had not yet been determined at the time of this modeling. Consequently, the actual hydrograph released from Lewiston Dam differed slightly from the modeled hydrograph (Figure 46).

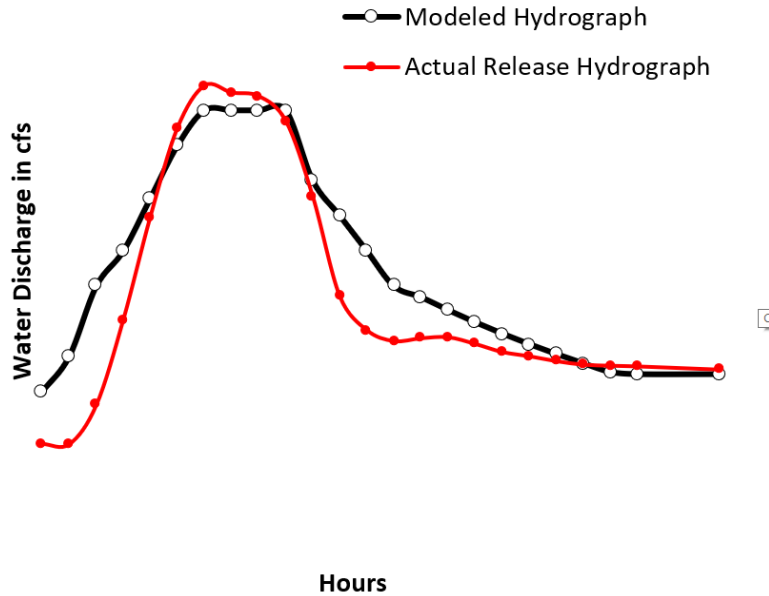


Figure 46. Modeled hydrograph compared with the actual 2011 spring release from Lewiston Dam.

8.2.5.2. Inlet Sediment Discharge

All of the transport equations applicable to coarse-bedded streams that are available in SRH-2D compute bedload transport only. For this reason, the sediment size classes and input fluxes specified for these model runs exclude particle fractions smaller than 0.25 mm. These finer fractions travel almost entirely in suspension and are found in the bed of the Trinity River in trace amounts only.

For sediment fractions larger than 0.5 mm, sedigraphs specifying the input bedload sediment discharge at the upstream boundary of the model domain were computed using fractional sediment rating curves based on bedload transport samples collected in the model reach during the 2006 high-flow release from Lewiston Dam (Figure 47). Data from 2006 was selected for this purpose because 2006 was only year in which the maximum daily mean discharge released from Lewiston Dam approached the magnitude planned for the 2011 release (10,100 cfs versus 11,000 cfs).

No bedload sample data is available for the 0.25-0.5 mm fraction because these particles can pass through the 0.5 mm mesh bag used on the bedload sampler. However, bedload transport rates computed with the Wilcock-Crowe or Trinity formulae are sensitive to the presence or absence of this fraction in the bed and bedload through its effect on the mean particle size on the bed surface. Bedload fluxes of the medium sand fractions (0.25-0.5 mm) at the upstream boundary of the model domain were therefore estimated as 25% of the coarse sand bedload (0.5-2 mm) inputs. This approximation is based on the assumptions that the total medium sand load is equal to or larger than the total coarse sand load, but that a smaller proportion of the medium sand travels as bedload and interacts with the bed.

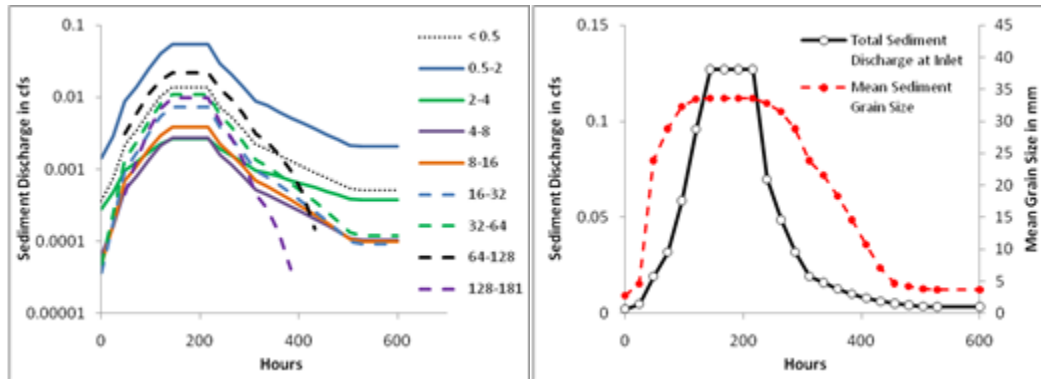


Figure 47. Left: Sedigraphs of fractional bed material input fluxes at the upstream boundary of the model domain with size fractions are given in mm. Right: Sedigraph of the total bed material input flux at the upstream boundary of the model domain and the mean grain size of the mixture.

Fractional sediment fluxes at the upstream boundary were specified by the text file “inlet_qs_D.dat”:

```
// t(h), Qs (9 fractions starting with 0.25-0.5)
0, .00036,.00140,.00030,6.44E-5,4.75E-5,3.67E-5,4.76E-5,0,0
24,.00072,.00290,.00048,.00016,.00017,.00018,.00024,0,0
48,.00222,.00890,.00097,.00050,.0007,.00095,.00135,.00311,.00046
72,.00348,.01393,.00126,.00080,.0011,.00166,.00239,.00592,.00133
96,.00621,.02484,.00173,.00136,.0019,.00321,.00470,.01114,.00356
120,.0101,.04055,.00226,.00212,.00299,.0054,.00806,.01739,.00693
144,.0135,.05415,.00264,.00273,.00385,.0073,.01096,.02205,.00982
240,.0074,.02950,.00190,.00159,.00224,.0039,.00570,.01312,.00455
264,.0052,.02071,.00157,.00116,.00161,.0026,.00382,.00928,.00269
288,.0035,.01393,.00126,.00080,.00110,.0017,.00239,.00592,.00133
312,.0022,.00888,.00097,.00052,.00069,.0010,.00135,.00311,.00046
336,.0019,.00762,.00089,.00045,.00058,.0008,.00110,.00238,.00028
360,.0016,.00630,.00079,.00037,.00047,.0006,.00084,.00159,.00013
384,.0013,.00522,.00070,.00030,.00037,.0005,.00064,.00096,4.50e-5
408,.0011,.00435,.00063,.00025,.00030,.0003,.00048,.00048,3.95e-6
432,.0009,.00363,.00056,.00020,.00023,.0003,.00036,.00015,0
456,.0008,.00304,.00049,.00017,.00018,.0002,.00026,0,0
480,.0006,.00256,.00044,.00014,.00014,.0001,.00019,0,0
504,.0005,.00216,.00039,.00011,.00012,9.96E-5,.00013,0,0
528,.0005,.00207,.00038,.00011,9.82E-5,9.07E-5,.00012,0,0
```

The file format consists of any number of comment lines beginning with // followed by a sequence of lines containing time in hours and volumetric sediment discharge for each sediment size fraction defined for the model run. In this case, discharge is given in English unit of cfs. Fields on each line are comma delimited in this file, but may also be space or tab delimited.

Note that if an input file specifying fractional sediment input rates is used, the data must be supplied using the same size classes used to define the substrate in the model domain. A simpler alternative for specifying sediment fluxes at the upstream boundary is to use the transport capacity computed by the sediment transport equations chosen for the simulation, as explained in a later section.

8.2.5.3. Outlet Stage

For this model run, the downstream boundary condition is specified by the input file “exit_stage_D.dat” which lists time and water surface elevation pairs:

```
// t, stage (english)
0, 1733.8
24, 1734.5
48, 1735.4
72, 1735.8
96, 1736.2
120, 1736.6
240, 1736.4
264, 1736.1
288, 1735.8
312, 1735.4
336, 1735.3
360, 1735.1
384, 1735.0
408, 1734.8
432, 1734.7
456, 1734.5
480, 1734.4
504, 1734.2
528, 1734.2
```

The file format consists of any number of comment lines beginning with // followed by a sequence of lines containing time in hours and a corresponding water surface elevation at the downstream boundary in feet. Time, elevation pairs on each line are comma delimited in this file, but may also be space or tab delimited. Elevations given in this file were derived from a discharge-stage rating curve fit to water surface elevations output from a one-dimensional hydraulic simulation using HEC-RAS.

8.2.5.4. Sediment Injection Mesh Zones

The location at which coarse sediment is injected within a modeled reach is specified using a sediment drop zone mesh created for that purpose. The drop zone mesh must be identical in node and element structure to the main numerical mesh, differing only in the material types assigned to the elements (Figure 48). To simulate the Lowden Ranch injection, a small region of channel near the injection point was coded with material type 2 and the remainder of the mesh was coded with material type 1. User input to the SRH-2D pre-processor can then be used to define material type 2 as the zone that coarse sediment will be added to the channel during the model run.

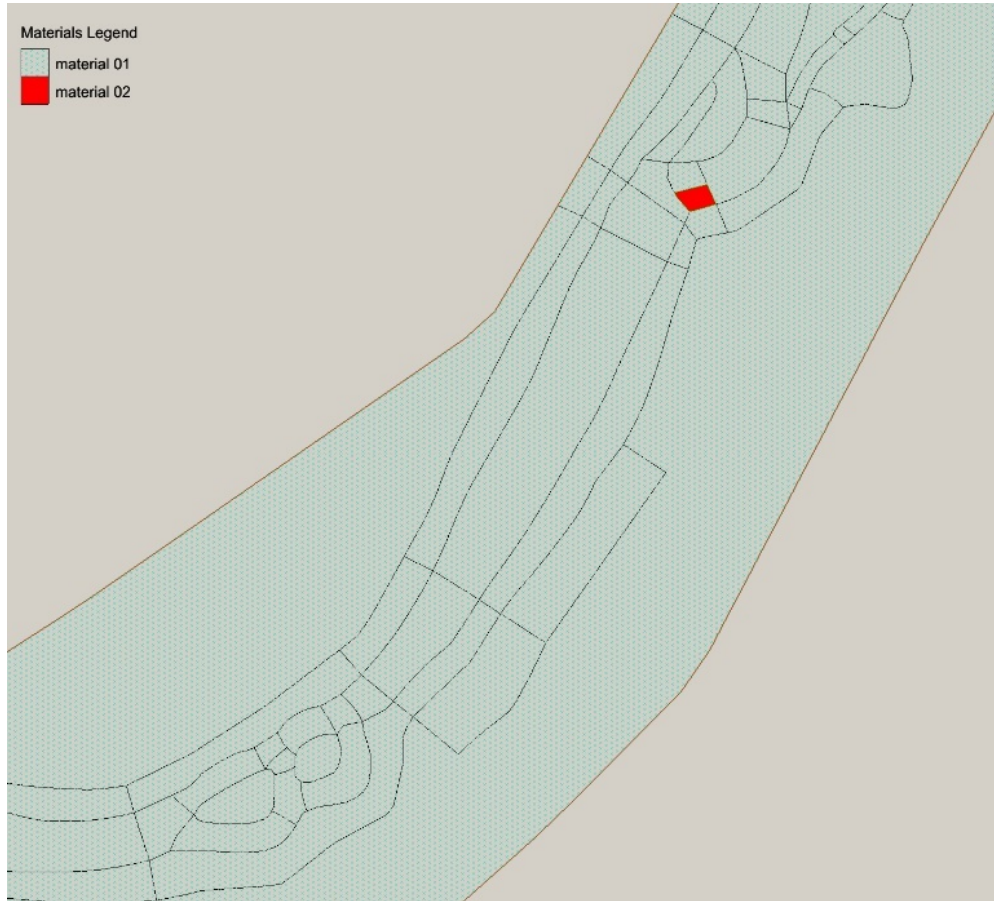


Figure 48. Polygons used to create the computational mesh with the location of the material type designating the sediment drop zone shown in red.

8.2.5.5. Sediment Injection Input File

The rate and timing of coarse sediment additions and the size distribution of the injection material are specified in a separate text file. Two such files specifying 2 alternative total injection volumes (2,000 cubic yards [yd³] and 3,000 yd³ in bulk volume) were prepared for the simulations described here. The file “augment_D_2000.dat” provides an example of the format:

```
//9 fractions starting with 0.25-0.5
//cumulative distribution from augmentation_specs.xls
0
0.5 2 4 8 16 32 64 128 181
0 2 3 5 22 48 75 100 100
//time, rate (english)
CFS
127.9, 0
128,0.347
137.9, 0.347
138.1,0
151.9, 0
152,0.347
161.9, 0.347
```

```
162,0  
175.9, 0  
176,0.347  
185.9, 0.347  
186,0
```

Lines are in this order:

- The format begins with any number of comment lines beginning with //.
- The next line indicates that 9 size classes will be used to specify the particle size distribution.
- The next line lists the upper size limit for the 8 classes from smallest to largest
- The line after that gives a cumulative percentage of particles smaller than the corresponding class size limit.
- This file then includes another comment line to document the fact that the remaining lines will give time and injection rate in cfs, followed by lines containing one time-rate pair each.

Note that because the injection grading is given as a cumulative distribution, the size classes used in the file are not required to match those used to define the modeled substrate. A second file called “augment_D_3000.dat” was prepared to simulate adding the larger total volume of sediment. That file is identical to “augment_D_2000.dat” except that injection rates during the three injection periods are 0.521 cfs.

The Lowden Ranch coarse sediment injection was to be implemented during the early part of the release peak to maximize sediment entrainment and the duration during which the sediment could be redistributed downstream. Thus, the first two time-rate pairs indicate that the injection rate ramps up from zero to 0.347 cfs at about 128 hours. Cross-referencing to the inlet flow hydrograph shows that this occurs after water discharge has reached 10,000 cfs and immediately before the peak of the release. It was assumed that sediment would be actively injected for 10 hours per day and stop overnight, and that injection of the full 2,000 yd³ would be accomplished over a 3-day period (Figure 49).

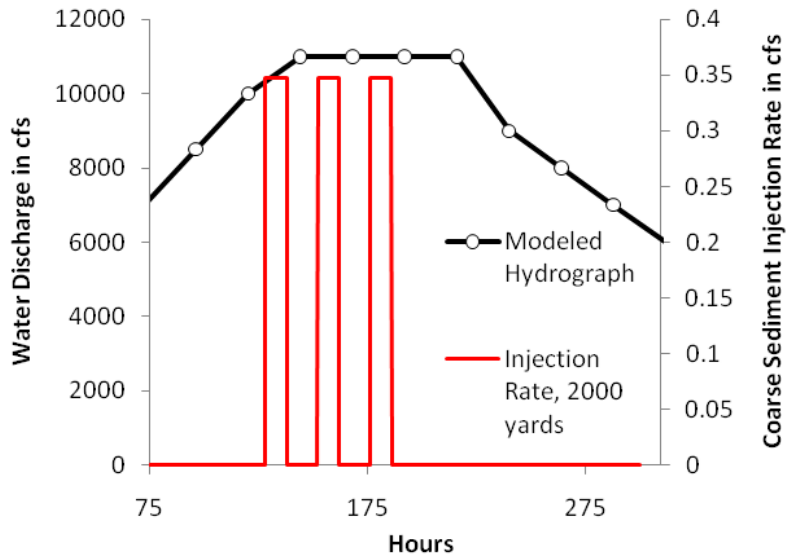


Figure 49. Modeled coarse sediment injection rate and timing for total injection of 2,000 yd³. The injection schedule for 3,000 yd³ is identical, except that injection rates during the three injection periods are 0.521 cfs.

8.2.6. Pre-Processor Interactive Input

The SRH-2D pre-processor presents the user with a series of prompts for user input. Input choices used for the Lowden Ranch gravel augmentation simulation are given below. Much of the entry for a MOBILE simulation is the same as for a flow only simulation. Inputs that are identical to those used in a flow only simulation are in smaller font below. The first prompt is:

```
==> SELECT PREPROCESSING MODE (enter 1 or 2):
1 --> FULL-INTERFACE (All inputs are set up in SMS)
2 --> PART-INTERFACE (Only mesh&nodestring are set up)
```

Enter: 2

This selects part-interface.

```
==> SELECT INPUT METHOD WITH SRHPRE (1 or 2):
1 --> Interactive ( _SOF.dat will be generated)
2 --> Use a Script Input File ( _SIF.dat file is needed and used)
3 --> Mesh Generation Only (2D unstructured or 2D/3D Structured)
```

Enter: 1

This selects interactive mode.

```
==> CASE NAME
```

Enter: LR

The case name is the filename prefix that will be given to all output files created by SRH-2D.

```
==> SIMULATION DESCRIPTION:
```

Enter: Optional text describing the simulation.

==> SOLVER-SELECTION

Enter one of the following options:

FLOW --> FLOW simulation only

MORPH --> FLOW + MORPHological Analysis

MOBILE --> MOBILE-Bed Sediment Transport added to FLOW

Enter: mobile

This invokes the sediment transport and bed evolution module.

==> RESULT-OUTPUT-FORMAT-AND-UNIT:

Enter two parameters: FORMAT UNIT

Enter: XMDF EN

XMDF is a special SMS output format that allows for easy display in SMS. EN specifies that the output will be in English units.

==> MONITOR-POINT-INFORMATION:

Enter one integer: NPOINT

Enter: 1

NPOINT is the number of monitoring points defined in the model domain.

==> COORDINATES-OF-ALL-MONITOR-POINTS:

Enter: X1 Y1 X2 Y2 ...

Enter: 6325340 2138870

X, Y coordinate pairs are entered for all NPOINT monitoring points.

==> TIME_STEP-and-TOTAL_SIMULATION_TIME-for-FLOW:

Enter 3 parameters: TSTART DT T_SIMU

Enter: 0 2 600

This entry specifies that the simulation begins at time 0 and ends at time 600 hours. Numerical solutions are computed using time steps of 2 seconds.

==> FULLY-UNSTEADY-SEDIMENT-MODELING?

Enter CARRIAGE-RETURN if Fully Unsteady Modeling Mode

or Enter: TIME_INTERVAL DT_SED

Press Enter.

Select a fully-unsteady sediment modeling mode. A quasi-unsteady option is available for experimental purposes only.

==> TURBULENCE-MODEL-SELECTION

Enter: para

This chooses a parabolic turbulence model with default parameters.

==> GENERAL-SEDIMENT-PARAMETERS

Enter: SPEC_GRAV SED_NCLASS

Enter: 2.65 9

This entry sets the sediment-specific gravity used for transport calculations to the standard value for silicate minerals of 2.65 and specifies that 9 size classes that will be used to describe the grain size distribution of the substrate and sediment fluxes at the upstream boundary of the model domain.

```
==> SEDIMENT-DIAMETER-AND-BULK-DENSITY-FOR-SIZE# 1
      Enter: D_Low D_Up [DEN_Bulk] [UNIT]
```

Enter: 0.25 0.5

Enter: 0.5 2

Enter: 2 4

Enter: 4 8

Enter: 8 16

Enter: 16 32

Enter: 32 64

Enter: 64 128

Enter: 128 181

The first number in each line is the lower size limit for a size class in mm, and the second number is the upper limit of the size class. Size classes are entered in order from finest to coarsest. On each line, the size class limits can be followed by a bulk density and a specification for whether density is given in English units (lb/ft³) or SI units (kg/m³). Note that if bulk density and its units had not been included in the input, then a default value that implies a sediment porosity of 0.4 would have been used.

```
==> WATER-TEMPERATURE
```

Enter: 15

A temperature is entered in °C. Note that if no value had been entered, then a default value of 25 would be used.

```
==> SEDIMENT-TRANSPORT-CAPACITY-EQUATION-for-Non-Cohesive-Sediment:
      Enter: MOD_SED_CAP
```

Enter: Trinity

This entry selects the Trinity modification to the Wilcock and Crowe (2003) bedload transport equations.

```
==> TRINITY-EQUATION-COEFFICIENTS:
      Press ENTER key if default is used
      or Enter 3 Parameters: T1 T2 D_sand
```

Enter: 0.032 0.05 4

The user is prompted to enter values for three parameters: T1, T2, and D_sand. These parameters are used to compute the dimensionless reference shear stress for the mean bed surface particle size (τ^*_{m}) according to:

$$\tau^*_{rm} = T1 + (T2 - T1) \text{Exp}(-20 F_s)$$

where F_s is the fraction of particles on the bed surface finer than the diameter specified by D_{sand} in mm. Note that if no user-specified values had been entered for these parameters, default values of $T1 = 0.021$, $T2 = 0.036$, and $D_{\text{sand}} = 1.0$ would be used.

```
==> START-TIME-FOR-SEDIMENT-SOLVER
      Press ENTER key if it is the same as flow solver
      or Enter: TIME_START_SED
```

Press Enter.

Pressing Enter indicates that the sediment solver will use the same start time as the flow solver. This option is available for experimental purposes only. Note that this option to specify a different start time for the sediment solver was not used in this case.

```
==> OLD-BANK-EROSION-MODELING
      Press ENTER key if no bank erosion model is used
      or Select the following Bank Erosion Module:
      1 --> Old Crude Way using the Angle-of-Repose
```

Press Enter.

A bank erosion model is currently in development, but not yet available.

```
==> ADAPTATION-COEFFICIENT-FOR-SUSPENDED-LOAD
      Press ENTER key if default values are used (A_DEP=0.25 A_ERO=1.0)
      or Enter: A_DEP A_ERO
```

Press Enter.

Pressing Enter selects default parameters for computing the suspended load adaptation length. Suspended sediment adaptation length is not applicable to this case because suspended sediment transport is not modeled.

```
==> ADAPTATION-LENGTH-FOR-BEDLOAD-TRANSPORT
      Press ENTER key if is used (mod_adap_lng=0 lbmin=1.e-6)
      or Enter 2 Parameters: MOD_ADAP_LNG LENGTH
```

Enter: 0 80

Entering zero as the first parameter in this entry indicates that a constant length will be used for the bedload adaptation length, and 80 specifies a constant length of 80 m.

```
==> ACTIVE-LAYER-THICKNESS-INFO
      Enter: MOD_AL T_PARA
```

Enter: 1 0.15

Entering 1 as the first parameter in this entry indicates that a constant thickness for the active layer will be given in m, and 0.15 is the constant thickness value. Alternatively, entering an initial 2 would indicate that the thickness of the active layer will be specified as a multiple of the 90th-percentile bed surface particle size (D_{90}). For example, entering "2 3" would specify that the active layer thickness will be calculated as 3 times the D_{90} .

SRH-2D User's Manual: Sediment Transport and Mobile-Bed Modeling

```
==> COHESIVE-SEDIMENT-MODELING?  
    Press ENTER key if non-cohesive sediment  
    or Enter: integer 1 if the sediment is cohesive
```

Press Enter.

Pressing Enter indicates that the modeled sediment is non-cohesive. Entering 1 instead would invoke prompts for additional input related to modeling cohesive sediment. Cohesive sediment is not modeled in this example case.

```
==> INITIAL-CONDITION-SETUP-METHOD
```

Enter: RST

Entering RST indicates that a restart file will be used to define the initial hydraulic conditions for the MOBILE simulation. Sediment transport modeling is almost always performed using unsteady flow hydrographs. As with any unsteady flow simulation, the initial condition is the output from a previous steady flow-only simulation.

```
==> INITIAL-CONDITION: RESTART-FILE-NAME  
    Enter the FILENAME that contains the SRH-2D RST file
```

Enter: Steady3000_RST.dat

This entry is the filename of the restart file used to define initial hydraulic conditions at the beginning of the MOBILE run.

```
==> MESH-UNIT  
    Enter one of the following for the unit of the input mesh:  
    FOOT METER INCH MM MILE KM
```

Enter: foot

This specifies that the mesh used for the run is in units of feet.

```
==> IMPORT-MESH-FILE  
    Enter: FILE_NAME FORMAT
```

Enter: Lowden_design.2dm SMS

This entry identifies the input mesh filename as Lowden_design.2dm and specifies that it is in the SMS 2dm format.

```
==> SPATIAL-DISTRIBUTION-OF-BED-SEDIMENT-PROPERTY:
```

Enter: ZONAL

This indicates that the spatial distribution of bed sediment properties will be specified according to zones of different material types in the input mesh or a copy of the input mesh that differs only in the material types assigned.

```
==> 2DM-FILE-NAME-USED-TO-DEFINE-ZONES  
    Enter: FILENAME
```


Enter: Lowden_design_substrate.2dm

This entry is the name of a copy of the input mesh in which the material types have been modified slightly to define 2 zones with different substrate properties.

```
==> NUMBER-OF-BED-PROPERTY-ZONES
      Enter an integer: N_ZONE
```

Enter: 2

Two zones with different substrate characteristics will be defined.

```
==> NUMBER-OF-BED-LAYERS-below-Bed-Surface-for-zone: 1
      Enter: NLAY
```

Enter: 2

The substrate zone corresponding to material type 1 will have 2 layers below the active layer.

```
==> BED-LAYER-PROPERTIES-FOR-ZONE# 1 (LAYER# 1)
      Enter: THICKNESS UNIT [DEN_CLAY]
```

Enter: 0.15 SI

This entry is the thickness of the uppermost substrate layer in zone 1, followed by an indication that the thickness is specified in SI units of m. In this case, the top substrate layer has been set equal to the thickness of the active layer to simulate a surface armor layer.

```
==> BED-SEDIMENT-COMPOSITION
      Enter one of the following options:
      FRACTION v_1 v_2 ... v_sed_nclass
      CUMULATIVE d1 P1 d2 P2 ... dn Pn
```

Enter: Cumulative 0.5 0 2 2 4 5 8 8 16 27 32 48 64 68 128 94 181 100

The keyword “cumulative” indicates that the particle size distribution of bed layer 1 of zone 1 will be given in cumulative percentages. The numeric values are pairs of upper class size limits followed by the percent of the distribution that is finer than that limit. For example, the initial “0.5 0” indicates that 0% of the substrate is finer than 0.5 mm, and the next pair indicates that 2% of the substrate is finer than 2 mm. This layer is a relatively coarse surface layer in the active channel.

```
==> BED-LAYER-PROPERTIES-FOR-ZONE# 1 (LAYER# 2)
      Enter: THICKNESS UNIT [DEN_CLAY]
```

Enter: 10 SI

This entry is the thickness of the lower substrate layer in zone 1, followed by an indication that the thickness is specified in SI units of m. The lower substrate layer has been set to a thickness of 10 m.

```
==> BED-SEDIMENT-COMPOSITION
      Enter one of the following options:
      FRACTION v_1 v_2 ... v_sed_nclass
      CUMULATIVE d1 P1 d2 P2 ... dn Pn
```

Enter: Cumulative 0.5 0 2 10 4 20 8 22 16 30 32 55 64 72 128 96 181 100

The keyword “cumulative” followed by paired numeric values indicating the upper class size limits and the percent of the distribution that is finer than that limit is entered for substrate layer 2 in zone 1. This subsurface layer contains more fines than the surface of the active channel.

```
==> NUMBER-OF-BED-LAYERS-below-Bed-Surface-for-zone: 2
      Enter: NLAY
```

Enter: 2

The substrate zone corresponding to material type 2 will also have 2 layers below the active layer.

```
==> BED-LAYER-PROPERTIES-FOR-ZONE# 2 (LAYER# 1)
      Enter: THICKNESS UNIT [DEN_CLAY]
```

Enter: 0.7 SI

This entry is the thickness of the uppermost substrate layer in zone 2, followed by an indication that the thickness is specified in SI units of m.

```
==> BED-SEDIMENT-COMPOSITION
      Enter one of the following options:
      FRACTION v_1 v_2 ... v_sed_nclass
      CUMULATIVE d1 P1 d2 P2 ... dn Pn
```

Enter: Cumulative 0.5 15 2 25 4 30 8 31 16 32 32 33 64 35 128 60 181 100

The keyword “cumulative” followed by paired numeric values indicating the upper class size limits and the percent of the distribution that is finer than that limit is entered for substrate layer 1 in zone 2. This layer represents a layer of fines deposited along channel banks and on floodplains.

```
==> BED-LAYER-PROPERTIES-FOR-ZONE# 1 (LAYER# 2)
      Enter: THICKNESS UNIT [DEN_CLAY]
```

Enter: 10 SI

This entry is the thickness of the lower substrate layer in zone 2, followed by an indication that the thickness is specified in SI units of m. The lower substrate layer has been set to a thickness of 10 m.

```
==> BED-SEDIMENT-COMPOSITION
      Enter one of the following options:
      FRACTION v_1 v_2 ... v_sed_nclass
      CUMULATIVE d1 P1 d2 P2 ... dn Pn
```

Enter: Cumulative 0.5 0 2 10 4 20 8 22 16 30 32 55 64 72 128 96 181 100

The keyword “cumulative” followed by paired numeric values indicating the upper class size limits and the percent of the distribution that is finer than that limit is entered for substrate layer 2 in substrate zone 2. This subsurface layer is composed of the same alluvium underlying the channel bed.

```
==> SPECIAL-BED-PROPERTY-SETUP-OPTIONS
    Enter: YES if at least one option listed below is used
    or Enter: NO to skip this input option
```

Enter: YES

Entering "YES" invokes additional prompts for specifying special properties setup options. Note that entering "NO" would have skipped these options.

```
==> SPECIAL-BED-LAYER-THICKNESS-SPECIFICATION
    Enter: FILE_NAME ID_LAYER
    OR: Enter Carriage-Return to skip this input
```

Press Enter.

Pressing Enter skips an option to specify a spatially-variable bed layer thickness with a special mesh file.

```
==> SPECIAL-SURFACE-LAYER-GRADATION-SPECIFICATION
    Enter: FILE_NAME
    OR: Enter Carriage-Return to skip this input
```

Enter: gradation_RST.dat

This entry is the name of the restart file defining the initial grain size gradation of the active bed surface layer. This restart file is generated by a previous Mobile Bed run in which the initial grain size gradation of the top-most bed layer was defined using mesh zones, as described above.

```
==> MANNINGS-ROUGHNESS-COEF(n)-INPUT-METHOD
    Enter: ICHOICE
```

Enter: 2

Entering 2 indicates that different values of the Manning roughness coefficient will be used in different mesh zones. Alternatively, a constant value across all mesh elements is indicated by entering 1.

```
==> NUMBER-OF-MATERIAL-TYPES-USED-FOR-n
    Enter an integer: n_mat_type
```

Enter: 3

The primary model mesh contains 3 material type zones defining zones with different values of Manning's roughness coefficient, n.

```
==> MANNING-COEFFICIENT-FOR-MATERIAL-TYPE: 1
Enter: MANNING-COEFFICIENT, the Manning roughness coefficient
```

Enter: 0.035

Manning's roughness coefficient, n, for main channel bed.

```
==> MANNING-COEFFICIENT-FOR-MATERIAL-TYPE: 2
Enter: MANNING-COEFFICIENT, the Manning roughness coefficient
```

SRH-2D User's Manual: Sediment Transport and Mobile-Bed Modeling

Enter: 0.06

Manning's roughness coefficient, n, for areas of riparian vegetation.

```
==> MANNING-COEFFICIENT-FOR-MATERIAL-TYPE: 3
```

```
Enter: MANNING-COEFFICIENT, the Manning roughness coefficient
```

Enter: 0.045

Manning's roughness coefficient, n, for areas of upland vegetation.

```
==> SPECIAL-MODELING-OPTIONS-AVAILABLE
```

```
Enter: CARRIAGE-RET or 0 if NO such modeling
```

```
or Enter: integer 1 if there are Special Modeling Options
```

Enter: 1

Entering 1 invokes input prompts for setting up several additional options.

```
==> NUMBER-OF-MOMENTUMLESS-SOURCE/SINK
```

```
Enter CARRIAGE-RET or 0 if there is no such source/sink
```

```
or Enter: NSOURCE
```

Press Enter.

Pressing Enter skips an option to add groundwater discharge in discrete areas of the mesh.

```
==> SPECIAL-RESERVOIR-DRAWDOW-MODELING
```

```
Enter CARRIAGE-RET or 0 if such modeling is not used
```

```
or Enter: any integer >= 1
```

Press Enter.

Pressing Enter skips this option.

```
==> OVERBANK-TREATMENT?
```

```
Enter CARRIAGE-RET or negative integer if no OVERBANK cells
```

```
or Enter: MATERIAL_ID
```

Press Enter.

Pressing Enter skips this option.

```
==> NUMBER-OF-SEDIMENT-DROPPING-MESH-ZONES
```

```
Enter CARRIAGE-RET or 0 if there is no such ZONES
```

```
or Enter: N_ZONE
```

Enter: 1

Entering 1 indicates that there is 1 sediment drop zones (sediment augmentation zones) in a special mesh developed for this purpose.

```
==> FILE-NAMES-FOR-VOLUME-RATE-TIME-SERIES-DATA-for-all-zones
```

```
Enter: Fname1 Fname2 ... Fname_N_ZONE
```

Enter: augment_D_2000.dat

This is the name of the data file defining the timing and rate of sediment augmentation, as shown in Section Y.5.5. Additional filenames would be listed if augmentation occurred in more than 1 drop zone.

```
==> 2DM-FILE-NAME-USED-TO-DEFINE-SEDIMENT-DROPPING-ZONES
      Enter: FILE_NAME ID_1 ID_2 ... ID_N_ZONE
```

Enter: Lowden_augment_left.2dm 2

This entry gives the name of the SMS mesh that was created to identify the sediment drop zone, followed by the material type ID (2) used to define the drop zone.

```
*****
* Setup Boundary Conditions for each NodeString in 2DM File *
* (Remaining unspecified boundaries are set up as WALLs) *
*****
```

```
==> SPECIFY-TYPE-for-NodeString: 1
```

Enter: INLET-Q

This entry indicates that nodestring 1 in the main mesh is an inlet boundary with a specified discharge as a boundary condition.

```
==> SPECIFY-BOUNDARY-VALUES
      Enter: Q QS UNIT [V_DIS]
```

Enter: inlet_q_D.dat inlet_qs_D.dat EN

This entry indicates the names of the data files used to define the inlet water and sediment discharges, as shown in Sections Y.5.1 and Y.5.2. "EN" specifies that the input files are in English units of cfs.

```
==> SPECIFY-TYPE-for-NodeString: 2
```

Enter: EXIT-H

This entry indicates that nodestring 2 in the main mesh is an exit boundary with a specified water surface elevation.

```
==> SPECIFY-BOUNDARY-VALUES
      Enter: W UNIT
```

Enter: exit_stage_D.dat EN

This entry indicates the name of the data file used to define the exit water surface elevations, as shown in Section Y.5.3. "EN" specifies that the input file is in English units of cfs.

```
==> SPECIFY-TYPE-for-NodeString: 3
```

Enter: Monitor

This entry indicates that nodestring 3 in the main mesh is a monitoring transect.

```
==> SPECIFY-TYPE-for-NodeString: 4
```

Enter: Monitor

This entry indicates that nodestring 4 in the main mesh is a monitoring transect.

```
==> SPECIFY-TYPE-for-NodeString: 5
```

Enter: Monitor

This entry indicates that nodestring 5 in the main mesh is a monitoring transect.

```
==> EQUIVALENT-ROUGHNESS-HEIGHT-AT-WALL-BOUNDARIES
      (Only if the wall boundary is steep and very rough.)
Press ENTER key to exit the command
or Enter: ID-Boundary --> an integer for the boundary-segment-ID
```

Press Enter.

Pressing Enter skips this option.

```
==> INTERMEDIATE-RESULT-OUTPUT-CONTROL
Enter: INTERVAL
```

Enter: 1

This entry gives the interval in hours at which intermediate output results are saved to a restart file and a graphical file format.

Following this last entry, the SRH-2D pre-processor input is complete, all pre-processor input is written to the SOF file, and the pre-processor program terminates.

8.2.7. Dynamic Input

Many model parameters can be updated dynamically during program execution using the dynamic input (DIP) file. If no DIP file already exists, running the SRH-2D main processor code creates a blank text file called CASENAME_DIP.dat where "CASENAME" is the case name for the model run designated by the user during pre-processor input. The DIP files used for modeling of the Lowden Ranch gravel augmentation included the following parameters:

```
$DATAC
  irest = 0
  dtnew = 2.0
  Total_simulation_time=600
  time_interval =15.0
  niter = 3
  relax_h = 0.8
$ENDC
```

\$DATAC and \$ENDC indicate the beginning and end of data input. The remaining variables control program execution:

- **irest:** irest is a flag indicating whether a previously interrupted run is to be resumed using a hot start. When irest = 0, execution of the SRH-2D main processor is initiated using the

initial conditions specified by the information and data files input to the pre-processor. For the Lowden Ranch run:

- initial hydraulic conditions are specified by Steady3000_RST.dat
- initial topography is given by Lowden_design.2dm
- initial “zeroed” composition of the active layer of the substrate contained in gradation_RST.dat
- subsurface substrate composition and configuration is as specified in Lowden_design_substrate.2dm and by associated pre-processor input

When $irest = 1$, a restart file from an interrupted run is used to resume program execution. A restart file from an earlier run is selected and renamed “CASENAME_RST.dat.” When execution of the SRH-2D main processor is resumed, all hydraulic, topographic, and substrate conditions are restored to the model conditions that existed when the chosen RST file was output.

- **dtnew:** This parameter overrides the time step duration specified by pre-processor input. It is useful to include this parameter in the DIP file because adjusting the time step is usually the most effective way to improve model convergence if stability problems arise.
- **Total simulation time:** This parameter overrides the total simulation time specified during pre-processor input, allowing run time to be adjusted without interrupting execution.
- **Time interval:** This parameter overrides the time interval for writing intermediate model results to restart files and graphical files specified during pre-processor input. The output interval can be adjusted without interrupting execution.
- **niter:** niter determines the number of inner iterations within each time step that will be used for iterative solution. Users usually do not change this parameter.
- **relax_h:** This parameter sets the relaxation parameter to the continuity equation. Users usually do not change this parameter.

8.2.8. Model Results

SRH-2D Mobile Bed was used to model three coarse sediment injection alternatives for the Lowden Ranch run:

- Inject 2,000 yd³ of coarse sediment over three days
- Inject 3,000 yd³ of coarse sediment over three days
- Flow release with no coarse sediment augmentation

8.2.8.1. No Augmentation

A model simulation of the flow release and sediment inputs at the upstream boundary only was conducted to assess the types of geomorphic changes that could be expected without a coarse sediment augmentation. According to this model run, an average of 0.24 feet of degradation could be expected in region defined as the sediment drop zone, with maximum scour of up to 0.5 feet occurring at the toe of the left bank (Figure 50). Modeled changes in the straight reach downstream from the drop zone were very slight, even in the vicinity of the incipient medial bar where an average increase in bed elevation of 0.14 feet is predicted. Net degradation dominates farther downstream in the split-flow region surrounding the two constructed islands, particularly around the more downstream island.

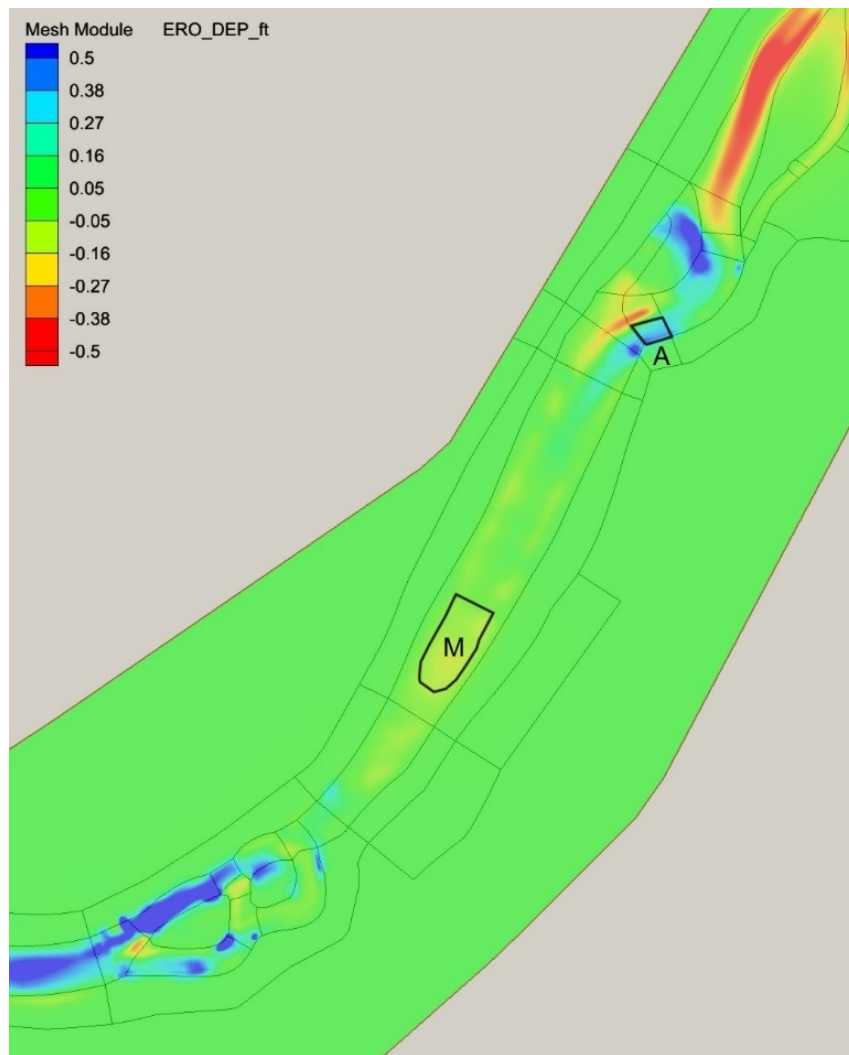


Figure 50. Modeled aggradation and degradation for the no-augmentation alternative. Aggradation is positive (blues) and degradation is negative (yellows and reds). The sediment drop zone area is indicated by the polygon labeled "A" and the location of the incipient medial bar is indicated by the polygon labeled "M."

8.2.8.2. Moderate Augmentation

SRH-2D MOBILE output indicates that a coarse sediment injection totaling 2,000 yd³ during the 2011 spring flow release would produce aggradation in the injection area and along the left bank immediately downstream, and promote a slight increase in deposition on the incipient medial bar near the downstream end of the straight section of channel (Figure 51). The model predicted that about 435 yd³, equivalent to 22% of the injection volume, would remain in the sediment drop zone, resulting in an average increase in bed elevation of about 2.5 feet. Another 580 yd³ of material (29% of the injection volume) was predicted to accumulate along the left-bank as a new lateral deposit averaging 0.35 feet thick. The total deposition over the top of the medial bar was predicted to average just 0.18 feet, accounting for a sediment volume equivalent to just 9% of the injection quantity. The area surrounding the two constructed islands farther downstream was predicted to remain largely unaffected by this gravel addition.



Figure 51. Modeled aggradation and degradation for injection of 2,000 yd³ of coarse sediment. Aggradation is positive and degradation is negative. The sediment drop zone area is labeled “A,” the location of the new lateral bar is labeled “L,” and the incipient medial bar is labeled “M.”

8.2.8.3. Maximum Augmentation

Model output suggests that a coarse sediment injection totaling 3,000 yd³ would produce considerably more aggradation in the injection area and along the left bank immediately downstream, while downstream medial bar deposition would remain relatively modest (Figure 52). This model run predicted that about 600 yd³, equivalent to 20% of the injection volume, would remain in the sediment drop zone, resulting in average aggradation of about 3.4 feet. Lateral deposition along the left-bank averaging 0.67 feet in thickness would account for another 1,110 yd³ of material (37% of the injection volume), but the average deposition on the medial bar would increase to just 0.22 feet and account for just 7% of the injection volume. Once again, this gravel injection was predicted to have little effect on geomorphic processes in reaches downstream from the medial bar.

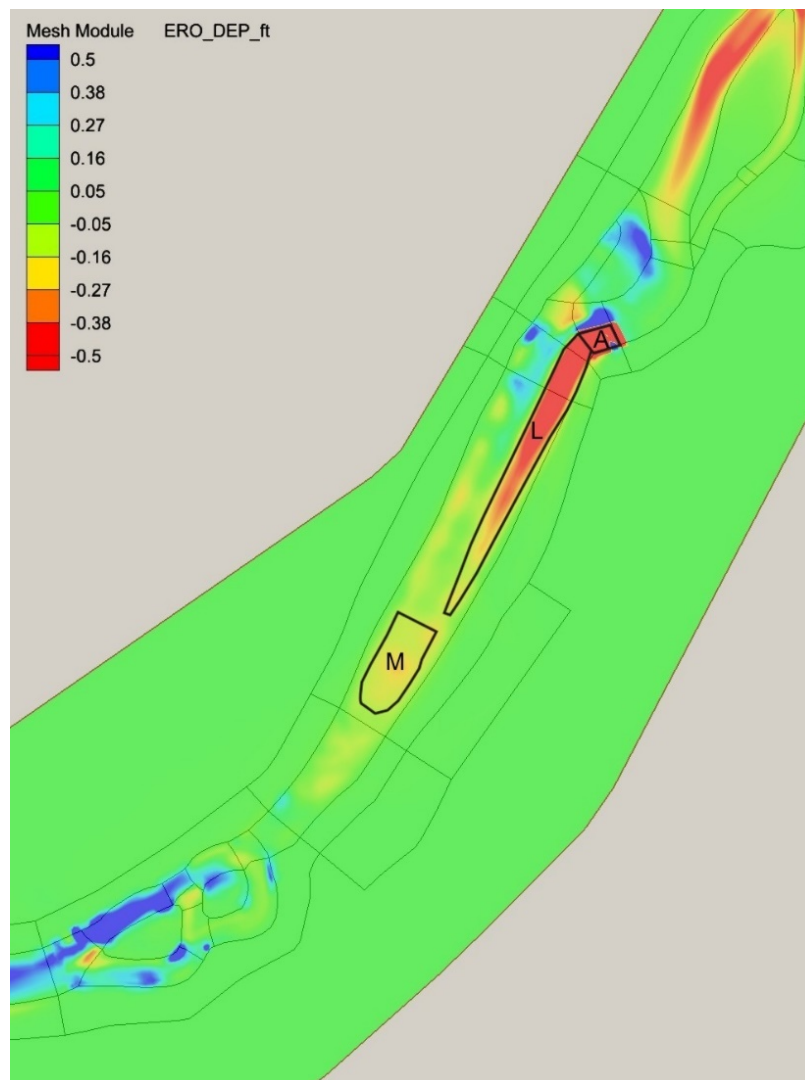


Figure 52. Modeled aggradation and degradation for injection of 3,000 yd³ of coarse sediment. Aggradation is positive and degradation is negative. The sediment drop zone area is labeled “A,” the location of the new lateral bar is labeled “L,” and the incipient medial bar is labeled “M.”

8.2.9. Recommendations for Implementation

SRH-2D MOBILE model results supported the working hypotheses that a coarse sediment injection during the 2011 spring flow release would accelerate the growth of an incipient medial bar about 1,000 feet downstream. However, the magnitudes of the predicted increases for either injection quantity were relatively small. The model results also supported an original conjecture that much of the injected material would deposit along the left bank downstream from the drop zone, although the magnitude of the lateral deposition according to the model was somewhat larger than anticipated.

The potential adverse consequences of implementing the coarse sediment injections are of special concern. These include the possibility that the injected material could aggrade the newly excavated channel branches around the constructed islands near the downstream end of the site, and the potential that excessive bed aggradation at the injection point could be a nuisance for boaters. Comparisons between both injection alternatives and the no-injection alternative suggest that the proposed coarse sediment augmentations would contribute little to deposition near the two islands. However, both runs with injected gravel indicated that substantial aggradation was possible in the injection area itself. Maximum aggradation was predicted to occur towards the middle of the river where local bed elevations increased by as much as 5 feet and 6.5 feet for the 2,000 yd³ and 3,000 yd³ injections, respectively.

As the larger injection appeared to significantly increase the risk of excessive aggradation at the injection point while apparently providing only a modest increase in the growth of the downstream medial bar, it was recommended that the volume of the 2011 coarse sediment injection at Lowden Ranch be limited to 2,000 yd³.

8.2.10. Implementation and Validation

Implementation of the 2011 high-flow coarse sediment injection at Lowden Ranch began as scheduled on May 3, 2011 when the rising limb of the release hydrograph reached 10,000 cfs. Injection activities continued on May 4 and concluded at about noon on May 5. A total of 2,050 yd³ of coarse sediment was added over that time period.

It was planned that the entire volume of coarse sediment would be dropped into the flow 30 to 50 feet from the left bank using a large conveyor belt. A conveyor was used on May 3 and through the morning of May 4, after which it was decided to begin dumping the sediment directly off the left bank using loaders. This change was motivated by considerable erosion of the left bank, which had locally retreated 20 to 30 feet. It appeared that coarse sediment from the conveyor was creating a mound in the channel that steered flow toward the bank, thereby eroding the bank, increasing channel width, and decreasing the overall transport competence of the channel. Switching the injection method to loaders permitted reconstruction of the bank toward its original position, partially restoring the flow competence needed to entrain material nearer the channel center.

Detailed monitoring data quantifying the channel changes to result from the 2011 flow release and coarse sediment injection were not yet available at the time of this writing. However, preliminary observations suggest that many of the model predictions are qualitatively correct. As

flows receded, it became clear that the stream bed in the sediment drop zone had aggraded and that a lateral bar had developed along the left bank downstream, much as the model output suggested. Deep, rapid flow through the channels surrounding the two constructed islands also showed that little or no aggradation occurred in those channels, also as predicted by the model.

The accuracy of the model predictions relative to subsequent monitoring data is discussed at length by Gaeuman (2014).

8.3. Channel Formation Due to Reservoir Drawdown

8.3.1. Background

Reservoir drawdown is often performed for reservoir management, dam maintenance/repair, and dam decommissioning, for example: for controlling aquatic plants (Cooke et al., 1993), improving water quality (U.S. Environmental Protection Agency [EPA], 1977), controlling internal phosphorus loading (Jacoby et al., 1982), and monitoring sediment erosion (Childers et al., 2000). Reservoir water level lowering may also be due to natural processes such as drought (Lai, 2011). Despite frequent occurrence of drawdown, however, drawdown impacts have not been widely studied. Some have reported the effects of dam decommissioning on channel form and sediment delivery to downstream reaches (e.g., Ligon et al., 1995; Shields et al., 2000; Doyle et al., 2002; Pizzuto, 2002; and Bountry et al., 2011). A few studied the effects that drawdown has on sediment and/or nutrient transport (e.g., Bowen, 2004 and Lai and Randle, 2007).

An important application of drawdown is often associated with dam decommissioning. In the United States, there are over 75,000 dams in the National Inventory of Dams (NID). Despite their benefits, dams have had many negative impacts on fish migration, water quality, and downstream channel processes (e.g., Baxter, 1977 and Shields et al., 2000). Consequently, dam decommissioning has become a viable option. According to Pohl (2002), over 400 dams at least 1.8 m tall or 30.5 m wide have been decommissioned from 1922 to 2002. Some mid- to large-sized dams that were or are scheduled to be decommissioned in recent years include Marmot Dam on the Sandy River, Oregon; Savage Rapids dam on the Rogue River, Oregon; dams on the Elwha River, Washington; Matilija Dam on Ventura Creek, California; and San Clemente Dam on Carmel River, California. Often, drawdown is a precursor to dam decommissioning—either as a learning/research tool or as part of the decommissioning process. For example, an experimental drawdown of Lake Mills, in northwestern Washington, was conducted in 1994 as a learning tool to determine the effects that lowering Lake Mills would have on sediment transport and water quality downstream of the reservoir (Childers et al., 2000). During drawdown rapid lateral and vertical erosion of the channel occurred in the delta of the reservoir. The maximum suspended sediment concentration reached 6,110 mg/L downstream and up to 300,000 yd³ of sediment were transported downstream during the two-week experiment (Childers et al., 2000).

In this case study, we modeled the channel processes due to drawdown of Copco 1 Reservoir on the Klamath River. This modeling effort was part of a much larger effort performed at the Reclamation's Technical Service Center to support the Secretarial Determination on Klamath Dam Removal and Basin Restoration (Reclamation, 2011). Under the Dam Removal alternative, four PacifiCorp dams (JC Boyle, Copco 1, Copco 2, and Iron Gate on the Klamath River in

Oregon and California) were under consideration for possible decommissioning. It was estimated that about 10 million cubic meters (m³) of sediment deposits were stored within the four reservoirs. A proposed dam removal alternative consisted of two stages. First, Copco 2 dam is removed as it contains negligible deposits. Second, a concurrent drawdown of the remaining three reservoirs (JC Boyle, Copco 1, and Iron Gate) would commence in late fall or early winter.

The deposits have a high water content (> 80% by volume), and the majority of the sediment particles are fine-grained (silt and clay). When the deposits are released downstream, high suspended sediment concentrations and their associated biological impacts would be the major concern, while concerns for downstream sediment deposition should be minor. This study focuses on two issues: the channel form development during drawdown and an estimate of the amount of suspended sediment that would be released downstream. The channel processes upstream helps determine the best strategies for revegetating the reservoir area and recovering a functional riparian corridor. The downstream sediment release helps determine the timing and duration of the drawdown, as well as the drawdown rate. Previous analyses of sediment impacts due to drawdown for the site have been reported by Gathard Engineering Consulting (GEC) (2006), Stillwater Sciences (2008), and Phillip Williams and Associates, Ltd (PWA) (2009), in addition to the recent study of Reclamation (2011). Stillwater Sciences analyzed the water quality impacts of dam removal (2009a) and biological effects of dam removal (2009b).

8.3.2. About the Study Site

Copco 1 Dam under study is one of the four dams on the Klamath River in southern Oregon and northern California. These dams are in the Upper Klamath Basin, downstream of Upper Klamath Lake (Figure 53), and on a 38-mile reach. The Klamath River begins at Lake Ewauna just south of Upper Klamath Lake and flows southwest into California. A profile of the Klamath River from Keno Dam to Indian Creek is given in Figure 54. The Klamath River in the four-dam area maintains a high-energy, coarse-grained channel that is frequently confined by bedrock and is comparatively steeper than the river downstream of the study area. Floodplain development is generally isolated to discreet reaches, and wider valleys that allow more alluvial channel migration processes are rare. According to PWA (2009), much of the river in the study area is geologically controlled, interspersed with comparatively-short—but important salmonid habitat—alluvial reaches.

Copco I Dam is 126 feet high and was constructed in 1918. The upstream reservoir is 4.5 miles long (RM 203.1 to 198.6), with a surface area of 1,000 acres, an average depth of 34 feet, a maximum depth of 108 feet, and a total storage capacity of 33,724 acre-feet. Water levels in Copco I Reservoir are normally maintained within 6.5 feet of full pool (i.e., elevation 2,607.5 feet).

The historical channel through Copco I Reservoir consisted of asymmetrical meanders, controlled by bedrock on the outer bends. Deep pools were probably located in these bends. In the upper portion from the high pool to about RM 200, the channel was a mostly single-thread, sinuous channel with broad asymmetrical meanders. Terraces were located along most of the reach, and were mostly 5 to 10 feet above the river channel. In addition, there were areas designated with willow and brush vegetation, which could correspond to either floodplain areas or young alluvial terraces. Downstream of RM 200 to about RM 199, the channel was more

sinuous, perhaps due to the canyon constriction that begins near the dam. In this reach, the channel contained a greater number of vegetated islands, some abandoned channel meanders, and wetland or floodplain environments. Most surfaces in the reach were less than 5 feet above the river channel, based on historical topography. A few terraces of 5-10 feet and 15-20 feet also existed in the reach, but were more limited in extent.

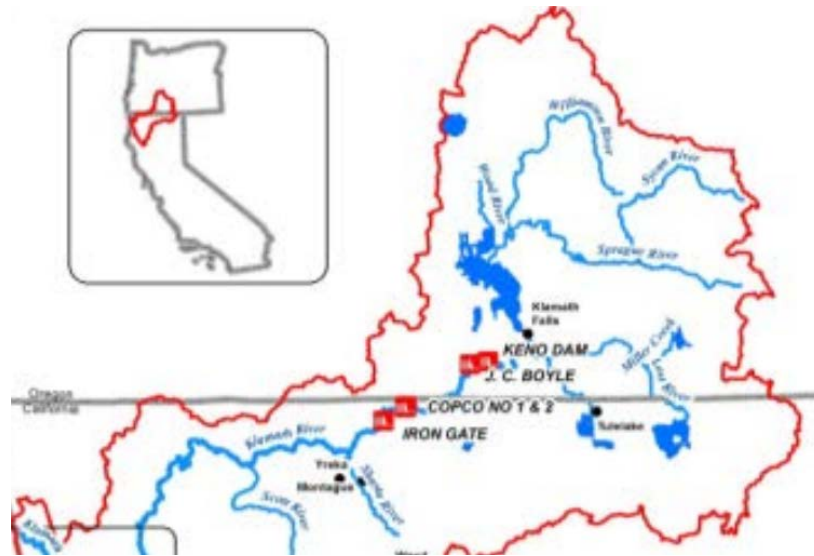


Figure 53. Overview of Klamath River from Keno and Iron Gate Dams.

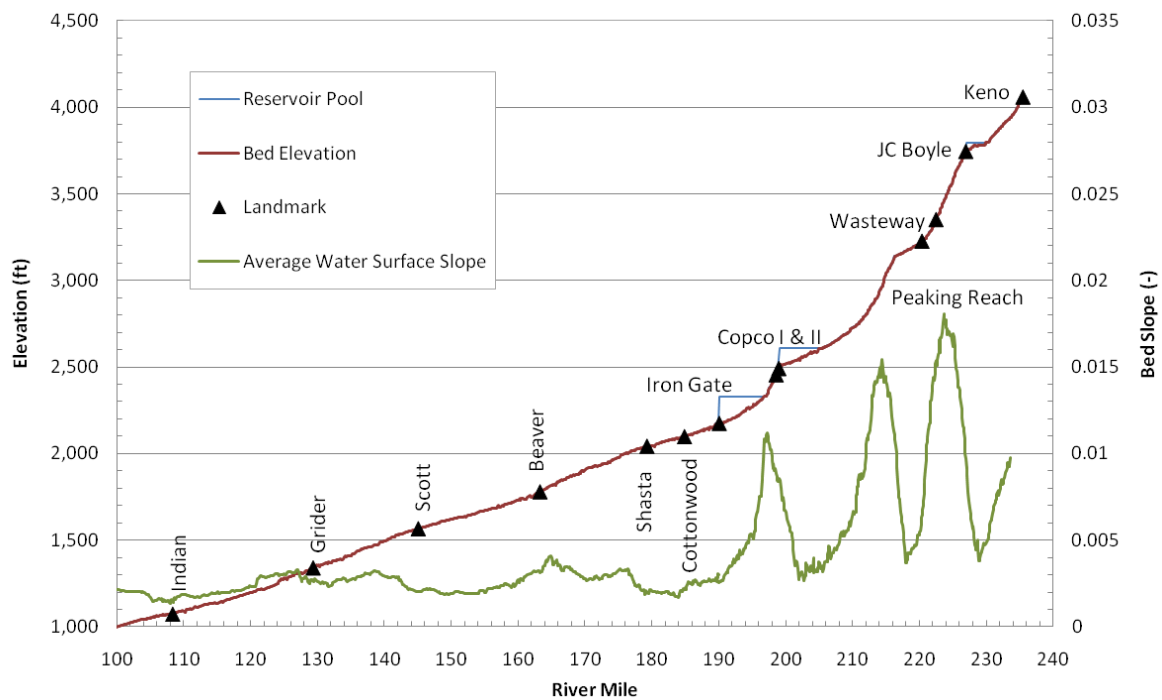


Figure 54. Bed elevation and water surface slope in reach from Keno to Happy Camp.

8.3.3. Model Details

A 2D numerical analysis begins by defining a solution domain and generating a mesh covering the domain. In this study, the solution domain includes the entire Copco 1 Reservoir and the mesh developed consists of 10,504 mixed quadrilaterals and triangles (Figure 55a). There are surveyed topographic and bathymetric data available in a digital elevation model (DEM). These DEM data were interpolated to the mesh to represent the initial bed elevation of the reservoir before drawdown (see Figure 55b for the contours of the initial bed elevation). Flow analysis requires the input of flow resistance that is calculated with the Manning's roughness coefficient equation. The Manning's roughness coefficient (n) used in this study is 0.03, uniformly distributed in space. The value is based on our 1D model analysis, as well as previous modeling experience.

The sediment transport and bed erosion modeling requires information about the subsurface sediment data. These data came from a number of sources including historical aerial photography, bathymetric and topographic survey, and geomorphic study (Reclamation, 2011). In the model, the reservoir subsurface is divided into two layers. The top layer consists of mostly reservoir deposits of silt and clay with the surveyed layer thickness as shown in Figure 56a. The bottom layer consists of mostly pre-dam river sediments. Sediment composition of the top layer was found to be different for the upstream and downstream zones (see Figure 56a) while composition of the bottom layer is assumed to be the same over the solution domain. Cumulative distributions of the bed sediment for both the top and bottom layers are shown in Figure 56b.

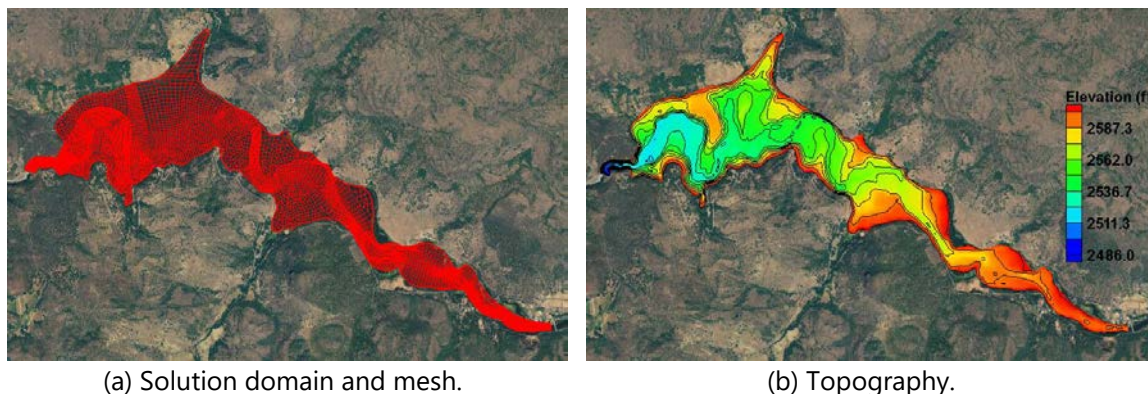
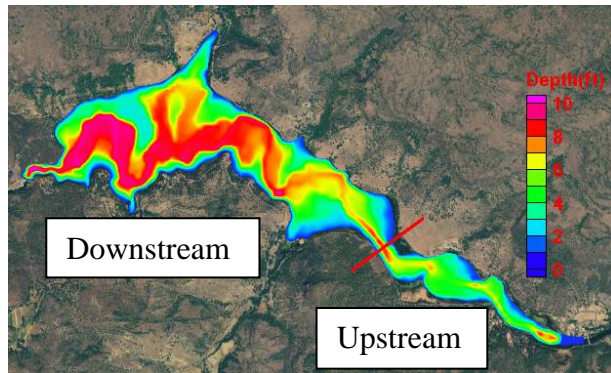
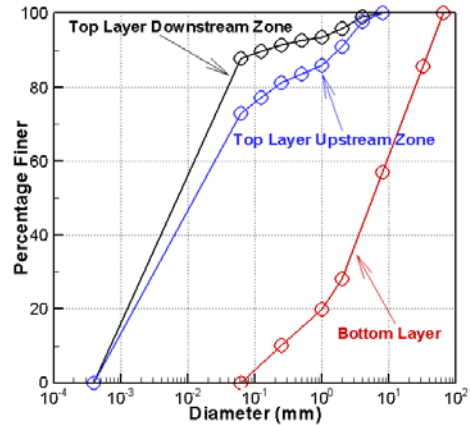


Figure 55. Model solution domain, mesh, and topography used for the numerical modeling.



(a) Top layer thickness and two zones.



(b) Cumulative distribution.

Figure 56. Subsurface sediment data in the reservoir: (a) top layer thickness and two zones of top layer sediment composition and (b) cumulative distributions of bed sediment.

8.3.4. Scenarios and Other Model Inputs

Three hydrological scenarios are simulated: a Dry-Year (2004), Average-Year (1968), and Wet-Year (1999). All simulations start on November 15 and last for six months. Flow discharges into the reservoir over the six-month period are the recorded historical data and used as the inlet boundary condition (Figure 57a). No sediment is assumed to enter reservoir as majority of inputs is wash load that simply passes through. The total sediment released downstream of Copco 1 Reservoir may be obtained by simply adding the known wash load entering Copco 1 to the predicted sediment release from Copco 1 by the present model. Initially, the reservoir is filled with water at an elevation of 2,603 feet (invert of the spillway). Drawdown is accomplished through release at an exit gate and the release rate is implemented as the exit boundary condition. The release rate is determined by the nominal drawdown rate of 3.0 feet per day (ft/day), subject to the constraint of the gate capacity characterized by the discharge capacity curve in Figure 57b.

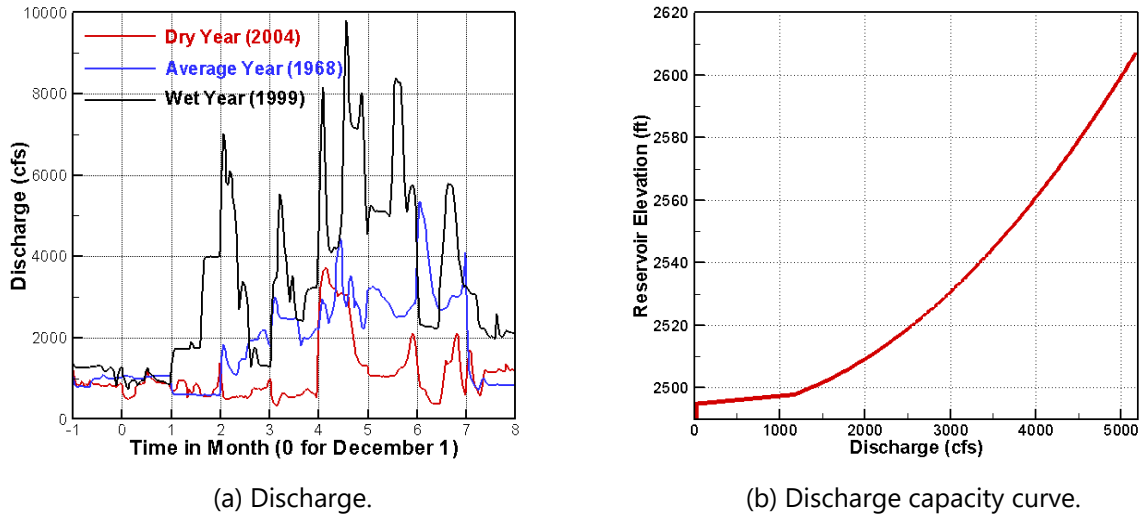


Figure 57. Flow hydrograph of three hydrological scenarios and the discharge capacity curve of exit gate at the dam face for drawdown.

Seven sediment size classes are used to represent the bed sediment, as tabulated in Table 10. Size class 1 is used to model the cohesive material in the reservoir (those smaller than 0.0625 mm in diameter) while the rest of the sediment classes represent the non-cohesive sediment.

Table 10. Size in diameter of each sediment size class

Size Class ID	1	2	3	4	5	6	7
Upper Bound of Diameter (mm)	Cohesive	0.125	0.5	2.0	8.0	32.0	128.0

For cohesive sediment, the exchange term is computed by:

$$S_k = V_e p_k - V_d C_k$$

where V_e and V_d are the rate of erosion and deposition, respectively, and p_k is the percentage of sediment size class k on the bed. Field measurement at the Copco 1 Reservoir showed that the erosion rate of the fine sediment could be computed by $V_e = k(\tau_b - \tau_{cri})$. The erodibility, $k(\text{cm}^3 / \text{N} - \text{s})$, was measured to range from 0.5 to 20.0. The minimum, medium, and maximum values are 0.5, 2.0, and 20.0, respectively. The critical shear stress, $\tau_{cri}(\text{Pa})$, ranged from 0.2 to 2.0, with the minimum, medium, and maximum values of 0.2, 0.25, and 2.0, respectively. Three erosion scenarios, each with its own set of parameters were modeled:

- Easy-Erosion ($\tau_{cri} = 0.2 \text{ Pa}$; $k = 20.0 \text{ cm}^3 / \text{N} - \text{s}$),
- Medium-Erosion ($\tau_{cri} = 0.25 \text{ Pa}$; $k = 2.0 \text{ cm}^3 / \text{N} - \text{s}$), and
- Hard-Erosion ($\tau_{cri} = 2.0 \text{ Pa}$; $k = 0.5 \text{ cm}^3 / \text{N} - \text{s}$).

8.3.5. Results and Discussion

A total of nine simulation runs were carried out, representing three hydrological scenarios (Dry-Year, Average-Year, and Wet-Year) and three reservoir bed erodibility conditions (Easy-Erosion, Medium-Erosion, and Hard-Erosion). Each model run is six months, starting on November 15 and ending on May 15 of the following year. Only model results corresponding to the Average-Year and Medium-Erosion, called baseline run, are presented in this manual, unless it is stated otherwise; more results may be found in Reclamation (2011). Comparing model results showed only small differences in most variables among three bed erodibility conditions.

The predicted reservoir water surface elevation and discharges into and out of the reservoir are displayed in Figure 58. With the 3 ft/day maximum drawdown rate and the constraint imposed by the gate capacity for drawdown, reservoir water elevations were lowered to below 2,500 feet within one month under all scenarios. However, only under the Dry-Year can the reservoir water level be maintained at such a low level. The reservoir would be filled quickly in the Wet-Year.

The predicted sediment concentration delivered downstream from Copco 1 Reservoir (Figure 59) for the three hydrological scenarios do not differ substantially between the Dry-Year and Average-Year, indicating that majority of the reservoir deposits have been mobilized. There is noticeable difference between the Wet-Year and the other two scenarios. The main reason is that reservoir water level remains low for both the Dry- and Medium-Year scenarios, leading to higher velocity and sediment carrying capacity than for the Wet-Year scenario. With the Dry- and Medium-Year simulations, the predicted high-concentration sediment pulse has an average peak of about 6,000 ppm (occasionally exceeding 7,000 ppm) and a duration of about 1.5 months. With the Wet-Year, the average peak of pulse is lowered to 4,000 ppm (occasionally exceeding 6,000 ppm). After 45 days of drawdown, sediment concentration falls to a relatively low level (about several hundreds of ppm). The model results are not sensitive to the range of erodibility parameters used for the reservoir bed sediment.

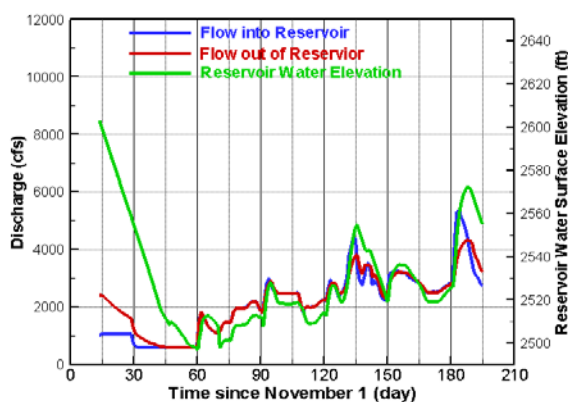


Figure 58. Simulated reservoir water surface elevation and discharges into and out of the reservoir under the Average-Year (1968) hydrology and Medium-Erosion scenario.

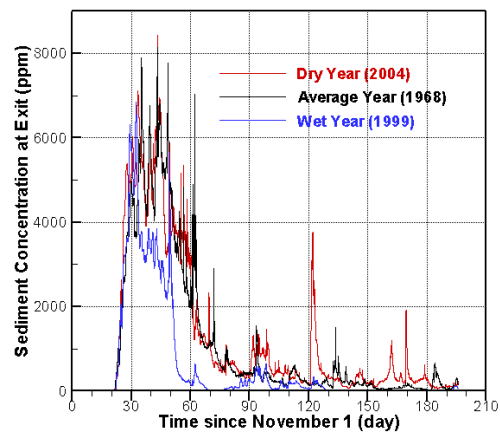


Figure 59. Predicted sediment concentration out of the drawdown gate of Copco 1 Reservoir under three hydrological scenarios.

The primary interest of this modeling is to investigate the channel form development due to drawdown. In general, channel formation due to drawdown may occur in one of two forms: retrogressive erosion and progressive erosion. The retrogressive erosion is characterized by a zone of high slope and fast erosion that is moving upstream. The point of slope change has the highest erosion rate and is called the knickpoint. Retrogressive erosion is often initiated in instances where sediment deposits are deep and located near the dam and drawdown is rapid or an initial deep slope is created. This erosion process was observed both in laboratory flumes and in the field (Morris and Fan, 1998). A recent example was reported by Major et al. (2008) when the Marmot Dam on the Sandy River in Oregon was decommissioned. The progressive erosion is characterized by the reemergence of the channel, beginning at the upstream end of the reservoir and moving and finally reaching the dam while the reservoir was emptied. Channel is often formed from upstream to downstream via fluvial processes due to increased sediment carrying capacity. Progressive erosion is often initiated when reservoirs are drawdown using some form of low-level outlet and the rate of drawdown is not very rapid.

The pre-dam geomorphology of the Copco 1 Reservoir areas was delineated, as reported by Reclamation (2011) (Figure 60). The data were based on historical aerial photography and topographic maps. The predicted bed elevation and the net depth of erosion and deposition along incised channel thalweg are compared with the initial top bed layer thickness and bed elevation in Figure 61 and Figure 62. The channel formation process due to drawdown at the Copco 1 Reservoir is examined. Snapshots of predicted channel form are shown in Figure 63 on eight different days. The model predicts the occurrence of the progressive erosion with channel cutting through the reservoir deposits from upstream to downstream. The progressive erosion was expected to occur given the assumed drawdown scenario according to the studies by GEC (2006) and PWA (2009). The reservoir pool level is approximately down to the lowest level on December 29 while May 14 is at the end of simulation.

The model predicts the formation of an incised channel caused by progressive erosion. The predicted channel thalweg agrees well with the geomorphic delineation of the pre-dam channel. Most of the reservoir deposit within the pre-dam channel is eroded after about 45 days of drawdown, particularly for the upstream half of the reservoir. The eroded sediment provides most of the suspended sediment delivered downstream. Incision into the bottom bed layer is also predicted for the upstream half of the reservoir six months after the drawdown. In the upstream area (zone 1 and 2), channel incision decreases with increased flow into the reservoir (wet year). The trend, however, is reversed in zone 4 and 5 where incision increases with increased flow.

Deposition is predicted in the area of pre-dam floodplains located in the downstream half of the reservoir. It is particularly visible in the open area near the narrow canyon. This may have implications on how revegetation and habitat restoration should be planned once the dam is decommissioned.

Finally, it is cautioned that the deposition near the drawdown gate in zone 1 may be unrealistic given that (a) only a depth-averaged model is used despite that flow is three-dimensional near the gate, and (b) "pressurized flow" is present at the gate while "open channel flow" is assumed by the model. The inaccuracy of the erosion prediction near the gate, however, is expected to have negligible effect on the predicted erosion upstream.

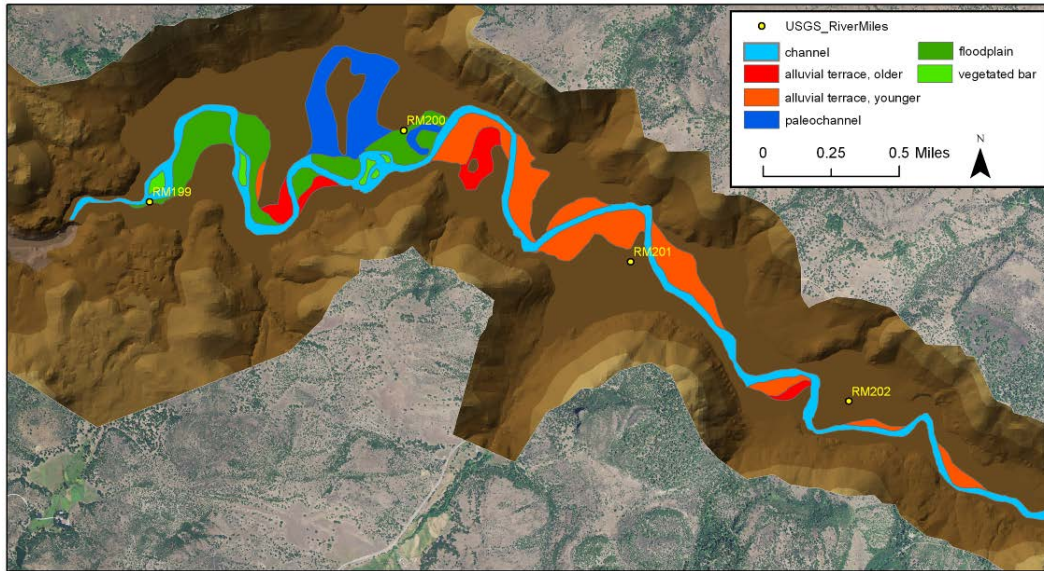


Figure 60. Geomorphic map of Copco 1 Reservoir.

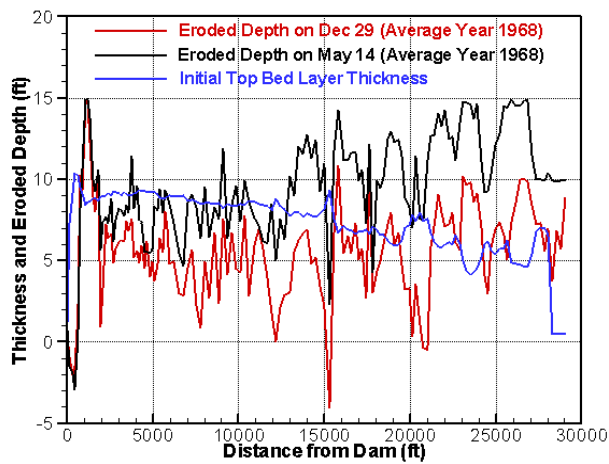


Figure 61. Predicted net depth of erosion and deposition along the thalweg of the incised channel on two dates, compared with the initial thickness of the top bed layer deposit.

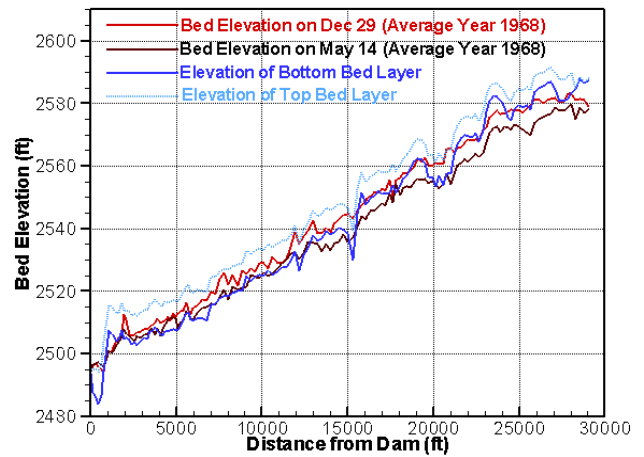


Figure 62. Predicted bed elevation along the thalweg of the incised channel on two dates, compared with the initial top and bottom bed layer elevations.

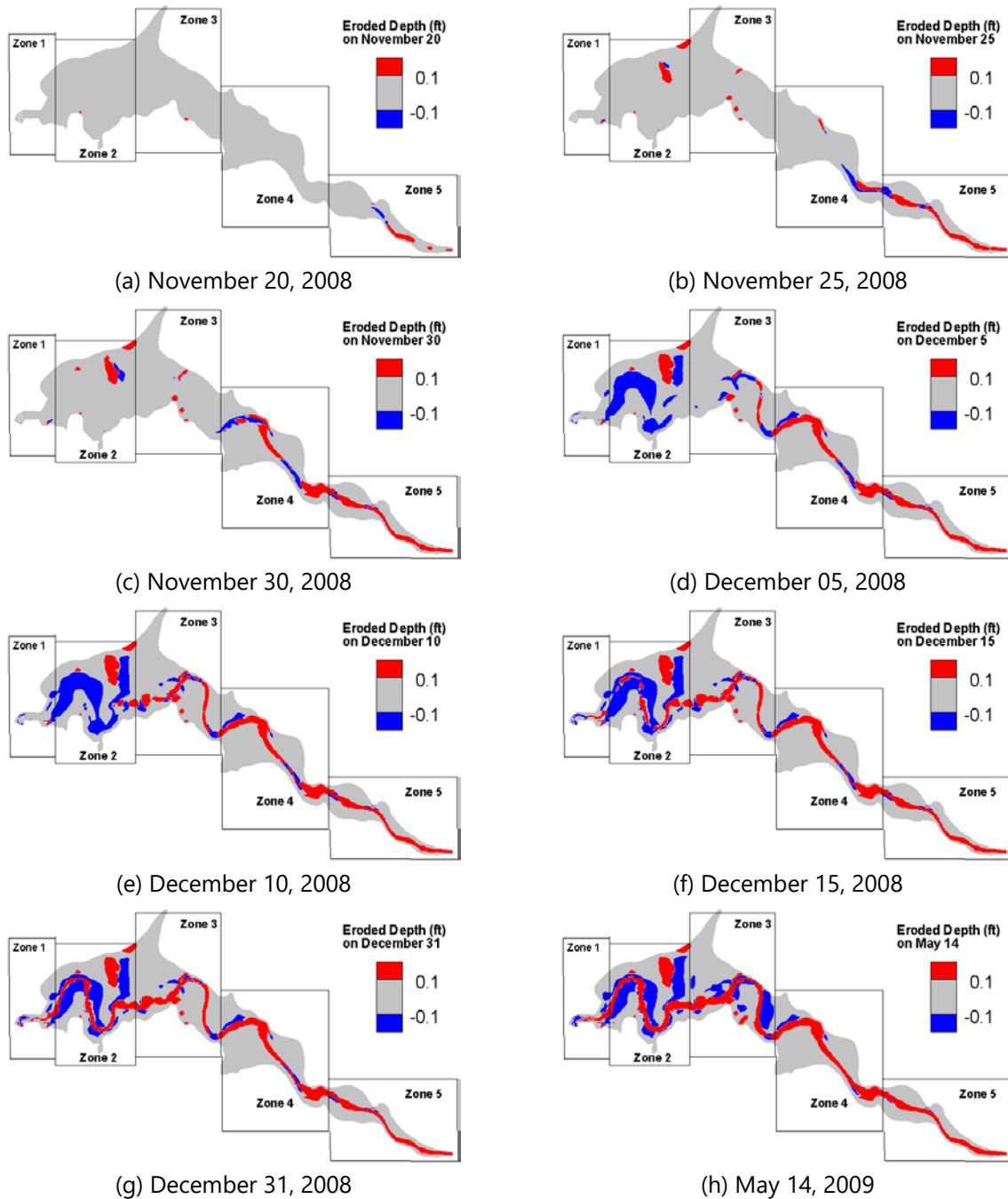


Figure 63. Predicted erosion/deposition pattern during the drawdown of Copco 1 reservoir under the Average-Year hydrology (2008) and Medium-Erosion bed sediment.

8.3.6. Remarks about the Modeling

SRH-2D is used to conduct a channel form development prediction in the Copco 1 Reservoir during a proposed drawdown. A total of nine simulation runs have been carried out, representing three hydrological scenarios (Dry-Year, Average-Year, and Wet-Year) and three reservoir bed erodibility conditions (Easy-Erosion, Medium-Erosion, and Hard-Erosion).

Progressive erosion process is predicted that is consistent with previous studies. The predicted incised channel is similar to the pre-dam channel alignment. Most of the reservoir sediment deposits within the pre-dam channel are eroded after about 45 days of drawdown, particularly for the upstream half of the reservoir. The eroded sediment provides most of the suspended sediment delivered downstream. The sediment pulse predicted has an average peak of about 6,000 ppm and a duration of about 1.5 months for hydrology up to the Medium-Year, and an average peak of 4,000 ppm and a similar duration for the Wet-Year. Model results are not sensitive to the range of erodibility parameters used for the reservoir bed sediment. Deposition is also predicted in the pre-dam floodplain area, particularly in the wide area upstream of the narrow canyon. This may have implications on how revegetation and habitat restoration should be planned once the dam is decommissioned.

8.4. Channel Morphology Prediction Upstream of the Elephant Butte Reservoir

8.4.1. Background

The drought in the 1990s resulted in a decrease of the Elephant Butte Reservoir pool elevation and inundation area. The exposed delta deposits disconnected the Rio Grande and the reservoir and led to high water losses. As a result, water deliveries under New Mexico's Rio Grande Compact were negatively impacted. In response, a temporary channel, abbreviated as Temp Channel, was constructed in 2000. The Temp Channel was also maintained through the delta area of the Elephant Butte Reservoir. After the Temp Channel construction, degradation has been observed in the Rio Grande upstream of Elephant Butte Reservoir. The degradation has propagated upstream and in recent years reached the area of the Bosque del Apache National Wildlife Refuge (approximately RM 84). The base level lowering due to the pool elevation drop of the Elephant Butte Reservoir, coupled with relatively high flows in 2005 and 2008, was considered to be the leading causes of the degradation. It is unclear, however, whether the excavation of the Temp Channel contributed to the initiation of the degradation.

Reclamation's Albuquerque Area Office (AAO), was interested in quantifying the impact of the Temp Channel on upstream channel degradation. A bigger picture question is what would occur if no Temp Channel had been excavated. Such knowledge may be obtained using numerical analyses. In this study, SRH-2D v.3 was used to predict the channel morphology with and without the Temp Channel to gain knowledge about the Temp Channel impacts. The study reach, upstream of the Elephant Butte Reservoir, is from RM 42 to 60. The objectives of the SRH-2D v.3 sediment transport modeling study were to determine the most likely channel location

through which low flows will be routed in 2010, had the Temp Channel not been excavated, and help understand the Temp Channel impacts on the river morphology within the study reach.

8.4.2. Data and Parameters

The SRH-2D v.3 simulation started from the river morphology before the excavation of the temporary channel and also before the reservoir pool lowering. The initial topography and bathymetry before 2000 was needed. A comprehensive survey of the Elephant Butte Reservoir, covering the present study area, was carried out in 1999 by Collins and Ferrari (2000). A topographic data set was constructed using a combination of the USGS quadrangle data and the underwater measured bathymetry. This 1999 data set was used as the initial bed condition for the modeling and the bed elevation contour (Figure 64a).

A 2D analysis began by defining a solution domain and then generating a mesh that covers the domain. In this study, the selected solution domain covered the river reach upstream of the Temp Channel. The modeling solution domain ranges from RM 42, near the beginning of the Narrows, to RM 60, the old Low Flow Conveyance Channel (LFCC) temporary outfall (see Figure 64b). A mesh is generated using the Surface Water Modeling System software (SMS). The mesh consists of mixed quadrilaterals and triangles, with a total of 14,628 mesh cells (Figure 64b.).

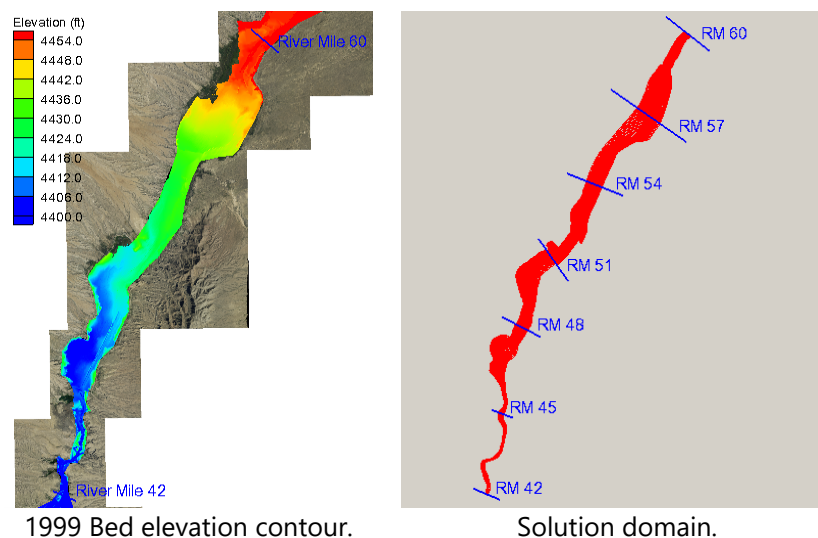


Figure 64. The bed elevation and solution domain/mesh (RM 42 to 60).

The upstream boundary at RM 60 is closer to the USGS gage #8358300 at San Marcial than other gages (e.g., San Acacia). According to a comparative study of the annual flow data between San Acacia and San Marcial by Huang (2011), the variation between the two gages is relatively small. Therefore, the hydrological data at San Marcial gage was used. The daily flow discharge was downloaded from the automated USGS database for January 1, 2000 to July 31, 2010 (Figure 65) and used as the upstream flow condition. The total sediment load at the upstream boundary was

calculated by adopting the rating curve developed by Collins (2006), but modified using the field data collected by Tetra Tech (2008). The total load rating curve was expressed as:

$$Q_s = 0.0582 Q^{1.5075}$$

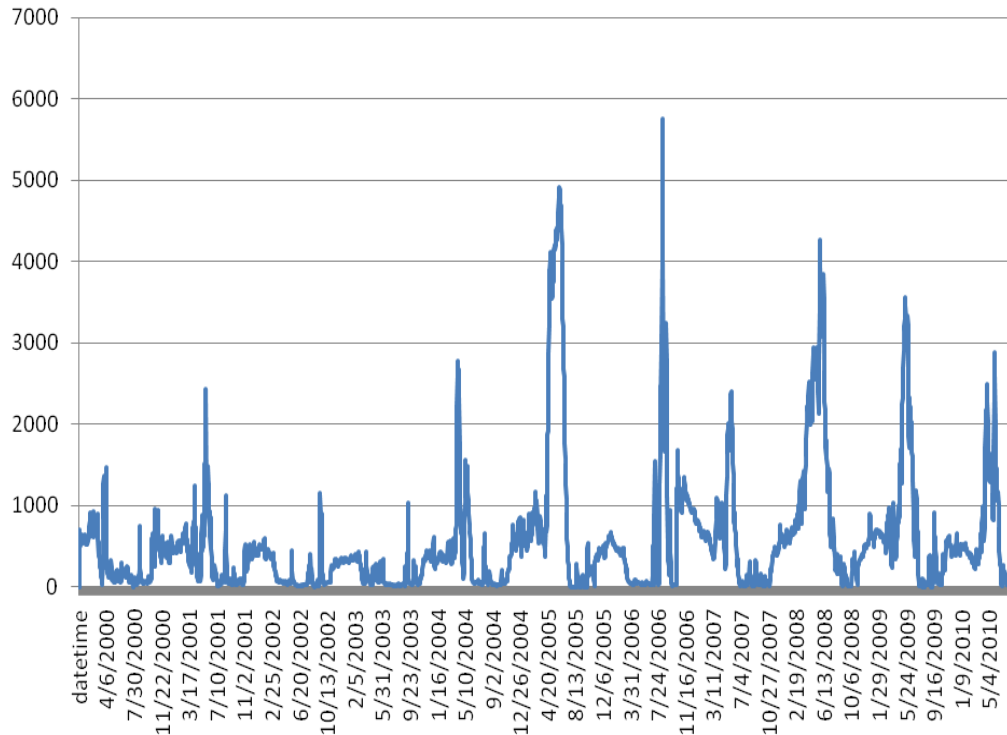


Figure 65. Daily discharge at the San Marcial gage from January 2000 to July 2010.

Flow roughness was calibrated using the measured water surface elevation data. Such a calibration has been done for the study reach using 1D models with a wide range of flow discharges (e.g., Reclamation, 2002 and Collins, 2006). Most of the previous studies resulted in a value of 0.017 for the main channel. The same value was also used in our previous SRH-2D modeling for the reach from RM 79 to 84 (Lai, 2009). Therefore, the Manning's roughness coefficient of 0.017, uniformly distributed in the entire solution domain, was used in the SRH-2D v.3 model study.

Representation of bed materials was needed, particularly in areas of degradation. A drill-hole study was carried out by Hilldale (2001) for the study reach during July 23 to July 30 and August 31 to September 4, 2001, with 20-foot deep drilling holes. Additional drilling holes were dug on Jan 17, 2003, covering EB-26 (a channel cross line used specifically for Rio Grande, AAO Office, slightly upstream of RM 59) to 2.7 miles downstream of EB-26. The study found alternating layers of fine sand and silt-clay in most sites. On average, the bed was described as consisting of two layers: the top sandy layer and the bottom silt-clay layer. The top layer is about six feet with dominant sands, while the bottom layer is about ten feet with about 80% silt-clay content.

In this study, the bed materials are represented with two bed layers using the survey data. The top layer has a thickness of six feet with the bed gradation listed in Table 11. The bottom layer has a thickness of ten feet with a silt-clay content of 80%. Surface bed materials were surveyed by Bauer (2006) between June 15 and June 20, 2006, and again between July 17 and 19, 2006. The median sediment diameter (d_{50}), excluding the scattered gravel bars, was 0.27 mm for the study area. Since the variation of the sediment gradation was relatively small, a uniform gradation was developed by averaging the surveyed gradations. The survey data were mostly concentrated in the sand bars, which generally lack silt-clay. The area was subject to reservoir deposition before 1999. Therefore, silt-clay content should be added to the above gradation data. Based on our field trip on July 26-27, 2010, it was estimated that about 5-15% of silt-clay cohesive materials were present and should be added. A modified bed sediment gradation is used (Table 11) that added 10% silt-clay.

Table 11. Bed Gradation of the Top Bed Layer

Cohesive content	d(mm)	Up to 0.625	.125	.25	.5	1	2
10%	% pass by weight	10.0	13.5	33.3	98.5	99.6	100

8.4.3. Results and Discussion

Two modeling scenarios were considered in this study: the “With-TC” scenario with the Temp Channel and the “No-TC” scenario without the Temp Channel. The No-TC scenario was based on the reservoir survey data in 1999 before the reservoir lowering and the temporary channel project. This scenario represented a prediction for the channel would evolve “naturally” if no temporary channel was dug. The With-TC scenario represented the “existing condition”. However, the model deviated from the actual existing condition. Firstly, the Temp Channel was excavated in stages from 2000 through 2005. The actual excavation process was not well documented enough for the present numerical model to replicate. In this study, the “Temp Channel” was created instantly rather than in stages. Secondly, other small projects carried out since 2000 within the study reach, e.g., berm repairs (Reclamation, 2002) might have changed the topographic features of the reach—but they were not incorporated in the numerical model. As such, the With-TC scenario should not be viewed as the actual existing condition model. Despite the above assumptions, the With-TC scenario is useful as it provides a comparison with the No-TC scenario. The difference between with- and without- the Temp Channel scenarios sheds light on the channel morphology and the impact of the Temp Channel. A detailed presentation of all model results can be found in Lai (2011). Only major findings are discussed here.

The model results show that the Temp Channel, and subsequent maintenance, achieved its primary purpose of helping to maintain the water delivery by maintaining a single channel to keep the river and the reservoir connected. The Temp Channel prevented the large evaporative loss of water as it provided a much smaller water surface area than if flows had spread out over the floodplain.

The No-TC model results showed that no competent channel would have formed had the Temp Channel not been excavated. Rather, a multi-channel form with two to three channels as

predicted at many locations in 2010. For example, Figure 66 shows a predicted channel forming from RM 57 to 54 about 10 years later than the Temp Channel. Without the Temp Channel, the developed channels are wider and shallower. At some locations, (e.g., RM 57-to-54 and RM 51-to-48), a dominant channel may still develop, although it is within a multi-channel system. Secondary channels have flowing water only with higher flows. At other locations, (e.g., between RM 48 and RM 46) flows are widespread, and no discernable channels are formed at all. More evaporative loss would be expected with such a multi-channel system. The formation of multiple channels is typical of the delta dynamics and was reported for the Elephant Butte Reservoir (Reclamation, 2002).

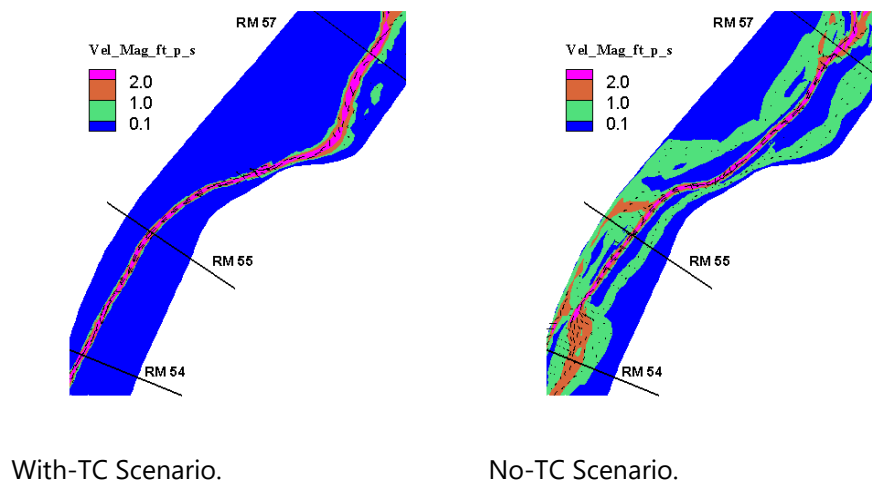
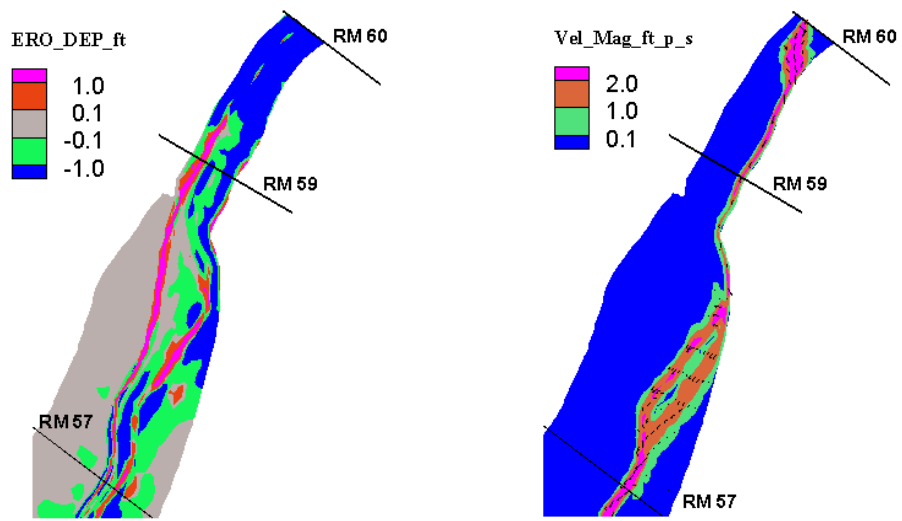


Figure 66. Predicted channel form (velocity is shown) in early 2010.

Based on the With-TC scenario, two river locations that require continued monitoring and maintenance due to high risk of aggradation were identified. Maintenance will continue to be required, even with the excavation of the temporary channel. One reach is from RM 60 to 59 (see Figure 67) where channel avulsion may occur as large aggradation is predicted. Despite high level of uncertainty of the prediction, the prediction is corroborated with field evidence. For example, it was reported that “the channel was originally constructed as designed, but persistent sediment accumulation within the channel became a maintenance problem,” during excavation of the 2000 temporary channel (AAO, 2007). Also, the temporary channel berm was breached in May 2001 and the bank had to be “reinforced” and the channel had to be “modified”. The excavation and the continued maintenance of the temporary channel is the key that prevented avulsion from occurring and allowed a single stable channel to be maintained.

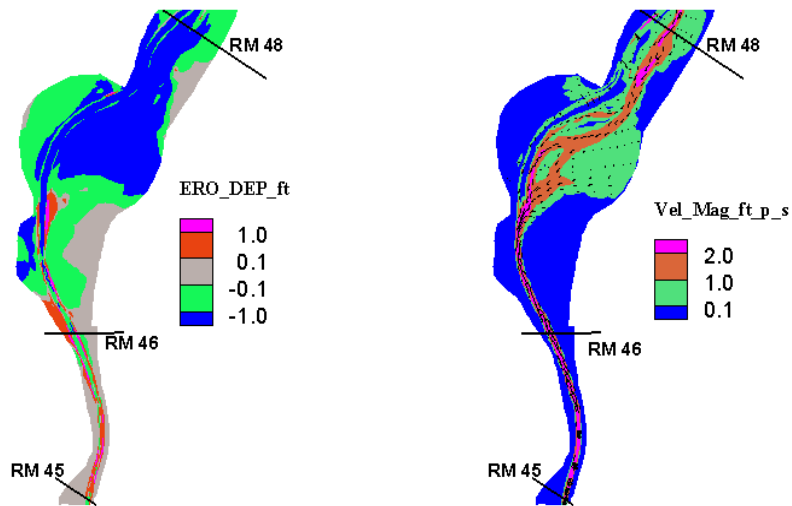
Another problem reach is between RM 50 and RM 47 where large aggradation is predicted (Figure 68). The aggradation leads to two phenomena: (a) a potential to develop a multi-channel system such as the one predicted at RM 48; and (b) a potential avulsion to the west upstream of RM 47. The model results are also partly corroborated with the field evidence. The channel in this reach did experience large aggradation in 2009, which led to the flow shifting to the west where it was still present during our July 2010 field trip.



(a) Net eroded depth.

(b) Velocity pattern.

Figure 67. Predicted results near the upstream end.



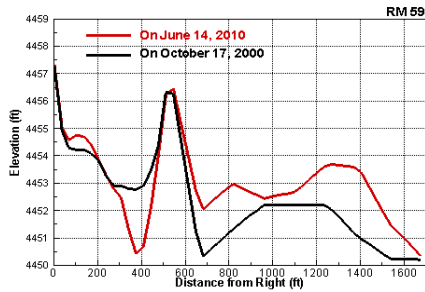
(a) Net eroded depth.

(b) Velocity pattern..

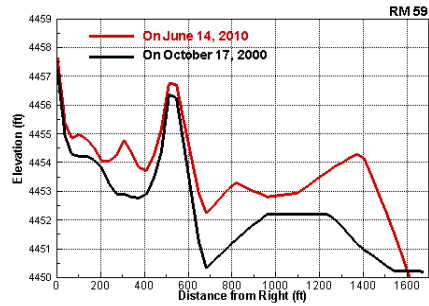
Figure 68. Predicted results between RM 48 to 45.

The model results for the rest of the temporary channel, RM 55 to RM 50 and RM 46 to RM 42 (in the Narrows), showed that they are relatively stable without significant degradation or aggradation. Maintenance needs in these areas are less likely.

Selected comparisons of the channel cross sections for the With-TC and No-TC scenarios are shown in Figure 69 through Figure 72.

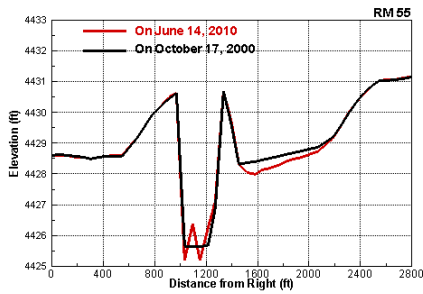


With-TC.

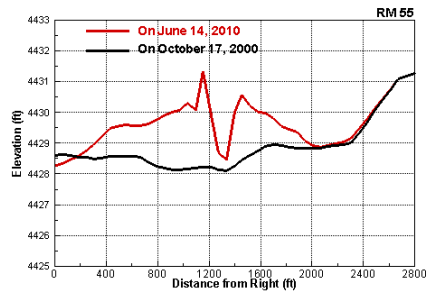


(b) No-TC.

Figure 69. Comparison of predicted channel cross section change at RM 59.

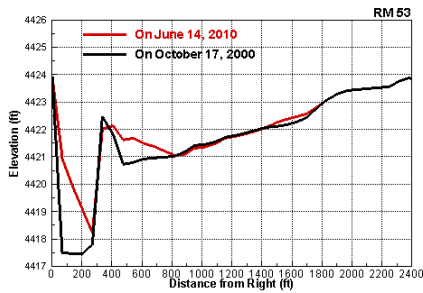


With-TC.

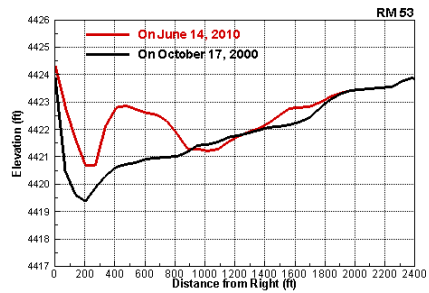


(b) No-TC.

Figure 70. Comparison of predicted channel cross section change at RM 55.



With-TC.



(b) No-TC.

Figure 71. Comparison of predicted channel cross section change at RM 53.

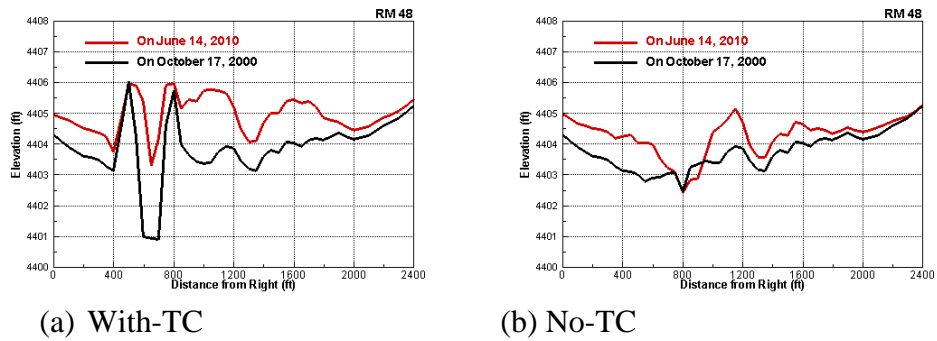


Figure 72. Comparison of predicted channel cross section change at RM 48

8.4.4. Remarks about the Modeling

SRH-2D was used to conduct a 10-year 18-mile geomorphic and sediment transport study for the reach upstream of the Elephant Butte Reservoir on the Rio Grande. Modeling study with SRH-2D v3 has the following major conclusions:

- No competent channel similar to the excavated temporary channel would form, had the temporary channel not been excavated.
- The new predicted channel morphology is mostly in the form of a multi-channel type at the end of 2009.
- The study points to the need for continued maintenance of the temporary channel at selected locations.

Appendix A. Other Sediment Equations and Their Assessment

Other sediment transport capacity equations are also incorporated in SRH-2D and some are discussed in this Appendix. An assessment of these equations is documented using sample cases and results are reported.

A.1. Wu Equation

The fractional transport rate of non-uniform bed-material load can be obtained by summing the fractional transport rates of bed-load and suspended load, as proposed by Wu et al. (2000a). The following steps are required in applying this equation:

1. Divide the non-uniform sediment mixtures into a number of fractions with different sizes and determine d_i (size diameter), ω_i (fall velocity), and p_{bi} (percentage of i class in the bed), for each fraction;
2. Calculate the hidden and exposed probabilities p_{hi} and p_{ei} ;
3. Determine the critical shear stress τ_{ci} for each size fraction;
4. Calculate the total bed shear stress τ ;
5. Determine the Manning's roughness coefficient (n) for channel bed corresponding to the grain shear stress, and then calculate the grain shear stress;
6. Calculate the fractional transport rate q_{bi} for the non-uniform bed-load with the following equation:

$$\frac{q_{bi}}{q_*} = 0.0053 \left(\frac{\tau_g}{\tau_{ci}} - 1 \right)^{2.2}$$

7. Calculate the fractional transport rate q_{si} for the non-uniform suspended load with the following equation:

$$\frac{q_{si}}{q_*} = 0.0000262 \left[\left(\frac{\tau}{\tau_{ci}} - 1 \right) \frac{V}{\omega_i} \right]^{1.74}$$

In the above equations, parameters are defined as follows:

$$\begin{aligned}
 q_* &= p_{bi} \sqrt{(\rho_s / \rho - 1) g d_i^3} & \tau_g &= \frac{d_{50}^{1/6}}{20n} \tau \\
 \tau_{ci} &= 0.03 \left(\frac{p_{hi}}{p_{ei}} \right)^{0.6} (\rho_s - \rho) g d_i & p_{hi} &= \sum_{j=1}^n \frac{p_{bj} d_j}{d_i + d_j} \\
 p_{ei} &= \sum_{j=1}^n \frac{p_{bj} d_i}{d_i + d_j} \\
 \omega_i &= \left[\left(13.95 \frac{v}{d_i} \right)^2 + 1.09 (\rho_s / \rho - 1) g d_i \right]^{0.5} - 13.95 \frac{v}{d_i}
 \end{aligned}$$

8. Sum q_{bi} and q_{si} to obtain the fractional transport rate for non-uniform bed-material load.

A.2. Bagnold Equation

The Bagnold (1980) equation was developed for bed-load transport. It may be expressed as:

$$i_b = \chi (e_b / \tan \alpha)$$

where: i_b is the rate of sediment flux by immersed weight, e_b is a bedload transport efficiency factor, $\chi = \rho g d S U = \tau U$ is stream power, ρ is fluid density, g is the acceleration of gravity, d is flow depth, S is the energy gradient of the flow, U is the mean velocity of the flow, τ is shear stress exerted by the fluid at the bed, and $\tan \alpha$ is a friction coefficient for the bed material. The final sediment transport equation may be expressed as:

$$i_b = \frac{\gamma_s}{\gamma_s - \gamma} i_{bref} \left[\frac{\omega - \omega_o}{(\omega - \omega_o)_{ref}} \right]^{3/2} \left(\frac{h}{h_{ref}} \right)^{-2/3} \left(\frac{d}{d_{ref}} \right)^{-1/2}$$

wherein i_b is specific bedload transport rate (dry weight) (kg/m-s), γ is the specific gravity of fluid (1.0), γ_s is the specific gravity of sediment (2.65), ω is specific stream power ($\omega = \tau U / g$) (kg/m-s), ω_o is critical specific stream power, h is water depth, d is characteristic particle size, usually denoted in mixtures by d_{50} (although Bagnold proposed a special procedure for bimodal sediments), and the subscript "ref" refers to some reference value obtained from a reliable data set.

Gomez and Church (1989) introduced the term $\frac{\gamma_s}{\gamma_s - \gamma}$ for the conversion of immersed

weight to dry weight, the latter being the standard for presentation of most fluvial transport formulae. The following parameters were defined by Bagnold:

$$\begin{aligned}\omega_o (kg / m - s) &= 5.75[0.04d(\rho_s - \rho)]^{3/2}(g / \rho)^{1/2} \text{Log}_{10}(12h / d) \\ i_{bref} &= 0.1kg / m - s ; \quad h_{ref} = 0.1m ; \quad d_{ref} = 0.0011m \\ (\omega - \omega_o)_{ref} &= 0.5kg / m - s\end{aligned}$$

A.3. Ackers and White Equation

Ackers and White (1973) sediment transport equation was developed for total load transport. First, a dimensionless diameter is computed as:

$$d_{gr} = d \left[\frac{g(\rho_s / \rho - 1)}{v^2} \right]^{1/3}$$

Parameters are computed as:

If $d_{gr} < 60$:

$$\begin{aligned}n &= 1.00 - 0.56\text{Log}_{10}(d_{gr}) ; \quad A = 0.14 + 0.23d_{gr}^{-0.5} \\ m &= 1.34 + \frac{9.66}{d_{gr}} \\ \text{Log}_{10}(C) &= 2.86\text{Log}_{10}(d_{gr}) - 0.98[\text{Log}_{10}(d_{gr})]^2 - 3.53\end{aligned}$$

Otherwise:

$$n=0.0; A=0.17; m=1.50; C=0.025$$

The sediment transport equation is expressed as:

$$\begin{aligned}\frac{C_s}{(d_i / h)(V / u_*)^n} &= C \left(\frac{F_{gr}}{A} - 1 \right)^m \\ F_{gr} &= u_*^n [gd_i(\rho_s / \rho - 1)]^{-1/2} \left[\frac{V}{\sqrt{32}\text{Log}_{10}(10h / d_i)} \right]^{1-n}\end{aligned}$$

Where: C_s is sediment concentration by volume; d_i is sediment diameter, h is water depth, V is depth averaged velocity, and u_* is shear velocity.

A.4. van Rijn Equation

The van Rijn (1984a and b) sediment transport equation is for bedload transport and was developed particularly for sand transport. It may be expressed as:

$$\frac{q_b}{\sqrt{g(\rho_s / \rho - 1)d_i^3}} = \frac{0.053}{D_g^{0.3}} \left[\frac{\tau_b'}{\tau_{cr}} - 1 \right]^{2.1}$$

where:

$$\tau_b' = \rho g \left[\frac{V}{18.0 \text{Log}_{10}(12h / K_s)} \right]^2$$

$$D_g = d_i \left[\frac{g(\rho_s / \rho - 1)}{v^2} \right]^{1/3}$$

$$\tau_{cr} = \theta_{cr} \rho g (\rho_s / \rho - 1) d_i$$

In general, the effective roughness height is computed as $K_s = ad_{90}$ with $a=1$ to 3 (van Rijn, 1993). In our implementation, $a=3$ is used according to the original study of van Rijn (1984a and b). D_g is computed as:

- If $D_g \leq 4$:

$$\theta_{cr} = \frac{0.24}{D_g}$$

- If $4 < D_g \leq 10$:

$$\theta_{cr} = \frac{0.14}{D_g^{0.64}}$$

- If $10 < D_g \leq 20$:

$$\theta_{cr} = \frac{0.04}{D_g^{0.10}}$$

- If $20 < D_g \leq 150$:

$$\theta_{cr} = 0.013 * D_g^{0.29}$$

- If $D_g > 150$:

$$\theta_{cr} = 0.0555917$$

A.5. Yang Transport Equations

For the sediment size fraction in the sand range, Yang (1973) equation may be used and it has the following transport equation (C_i is concentration by weight in ppm):

$$\begin{aligned} \text{Log}C_i &= 5.435 - 0.286\text{Log}\frac{\omega_i d_i}{\nu} - 0.457\text{Log}\frac{u_*}{\omega_i} \\ &+ \left(1.799 - 0.409\text{Log}\frac{\omega_i d_i}{\nu} - 0.314\text{Log}\frac{u_*}{\omega_i} \right) \text{Log}\left(\frac{V_s}{\omega_i} - \frac{V_{cr} s}{\omega_i} \right) \end{aligned}$$

where:

$$\frac{V_{cr}}{\omega_i} = \begin{cases} 131.0 & \text{for } \frac{u_* d_i}{\nu} \leq 1.2 \\ 0.66 + \frac{2.5}{\text{Log}\frac{u_* d_i}{\nu} - 0.06} & \text{for } 1.2 < \frac{u_* d_i}{\nu} < 70 \\ 2.05 & \text{for } \frac{u_* d_i}{\nu} \geq 70 \end{cases}$$

Or, another equation for sand transport based on Yang (1979) may be used and it is expressed as:

$$\begin{aligned} \text{Log}C_i &= 5.165 - 0.153\text{Log}\frac{\omega_i d_i}{\nu} - 0.297\text{Log}\frac{u_*}{\omega_i} \\ &+ \left(1.780 - 0.360\text{Log}\frac{\omega_i d_i}{\nu} - 0.480\text{Log}\frac{u_*}{\omega_i} \right) \text{Log}\left(\frac{V_s}{\omega_i} \right) \end{aligned}$$

For sediment fraction in the gravel range, Yang (1984) equation may be used and it is expressed as:

$$\begin{aligned} \text{Log}C_i &= 6.681 - 0.633\text{Log}\frac{\omega_i d_i}{\nu} - 4.816\text{Log}\frac{u_*}{\omega_i} \\ &+ \left(2.784 - 0.305\text{Log}\frac{\omega_i d_i}{\nu} - 0.282\text{Log}\frac{u_*}{\omega_i} \right) \text{Log}\left(\frac{V_s}{\omega_i} - \frac{V_{cr} s}{\omega_i} \right) \end{aligned}$$

where: $\frac{V_{cr}}{\omega_i}$ is the same as above (Yang 1973).

A.6. Comparative Study with Flume Cases

This section documents testing results of some sediment transport equations using selected flume cases.

A.6.1. Aggradation in a Straight Channel

Aggradation in alluvial channels may occur due to a variety of reasons (e.g., an oversupply of incoming sediment above the transport capacity after heavy precipitation in a large tributary area). In the following, the flume experiment of Soni (1981) is selected to test the aggradation modeling of SRH-2D.

See Section 7.2. Aggradation in a Straight Channel for a description of this case and a discussion of the comparison of simulated and measured bed elevation changes with the Engelund-Hansen equation. Our study shows that the model results are most sensitive to the choice of the sediment transport equation. It is recommended that users should be familiar with the suitability and applicability range of each sediment transport equation. A specific sediment capacity equation should be chosen first, based either on experience or through calibration study if measured data are available.

Results of all other transport equations are shown from Figure A- 73 to **Figure A- 82**. Note that only some equations were presumed to be developed for sand transport. At least for this case, we found that the Engelund-Hansen equation performs the best in comparison with the flume data.

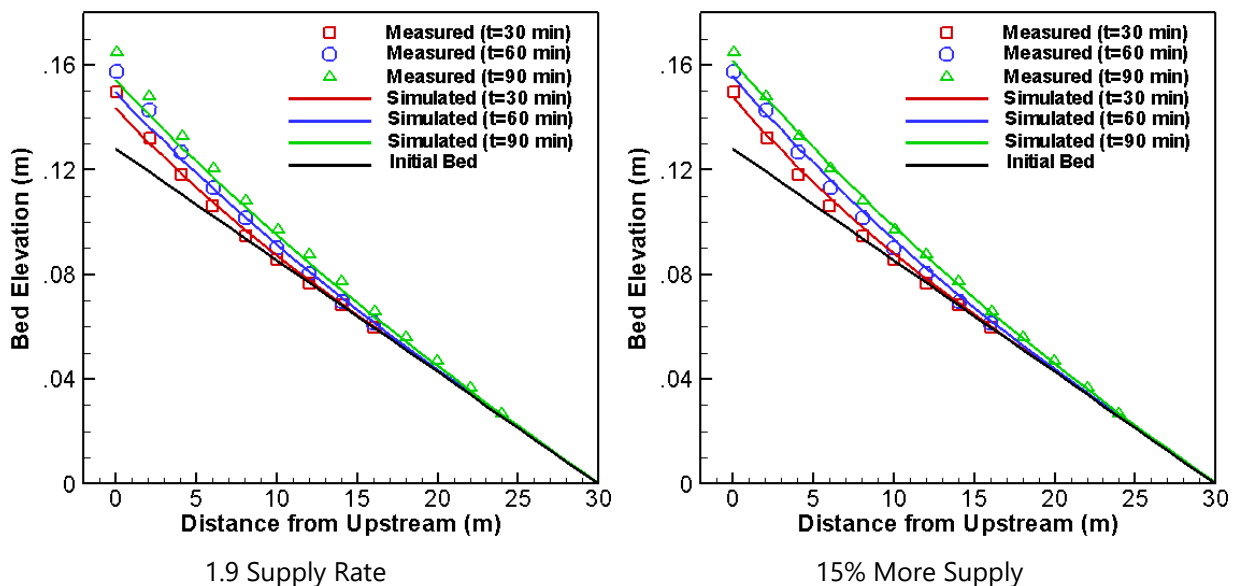


Figure A- 73. Results of Engelund-Hansen (1972) equation compared with flume data for Soni (1981) experiment.

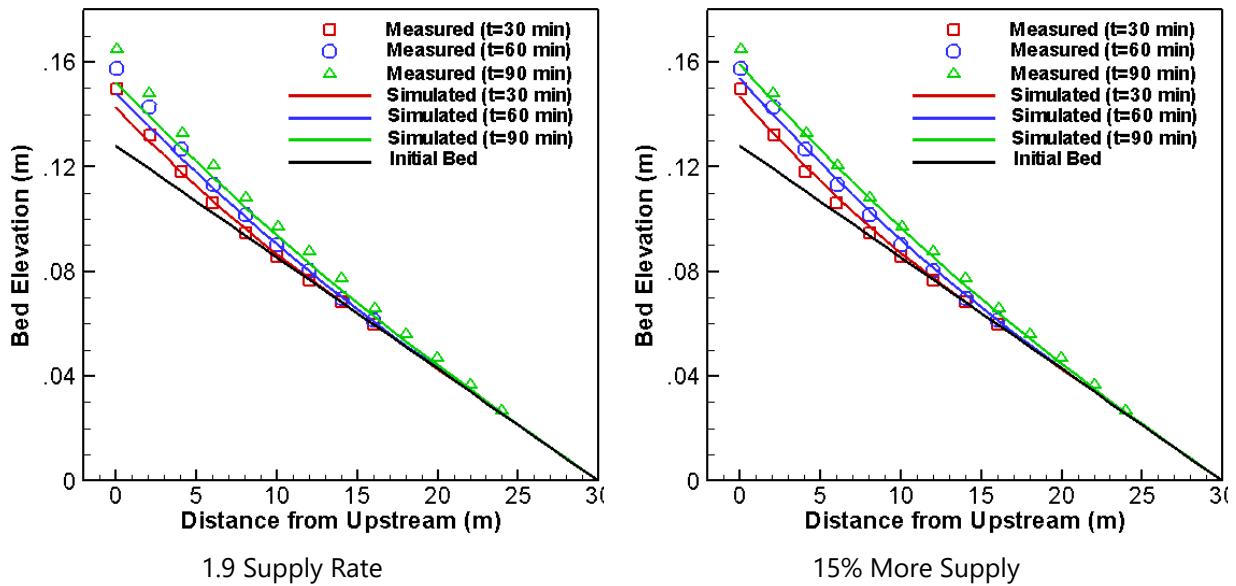


Figure A- 74. Results of Yang (1979/1984) equation compared with flume data for Soni (1981) experiment.

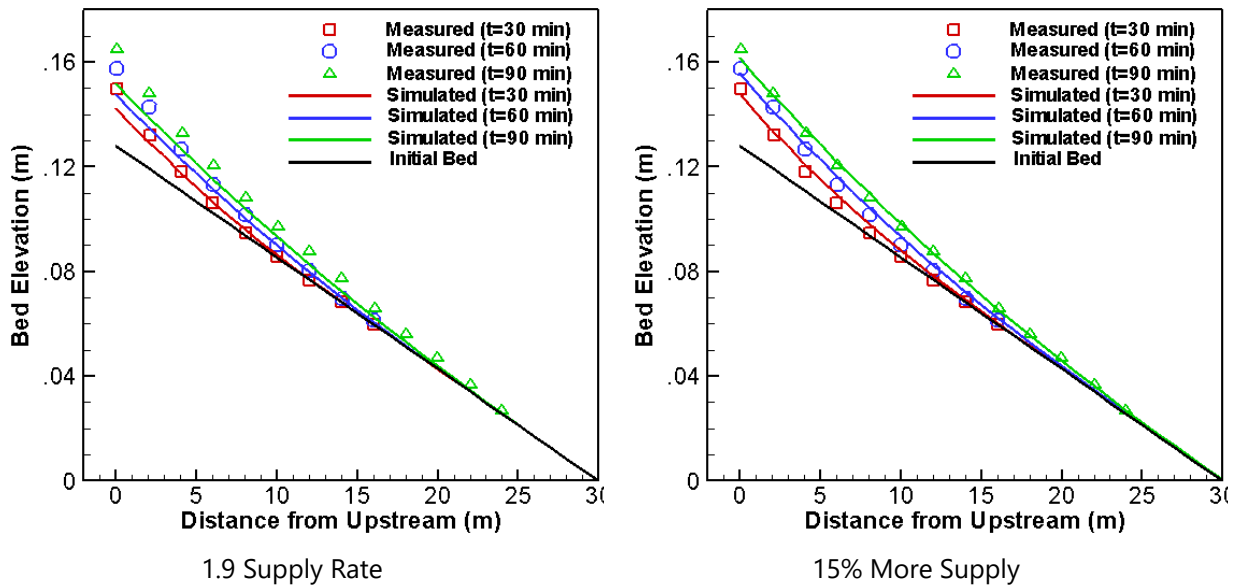


Figure A- 75. Results of Yang (1973/1984) equation compared with flume data for Soni (1981) experiment.

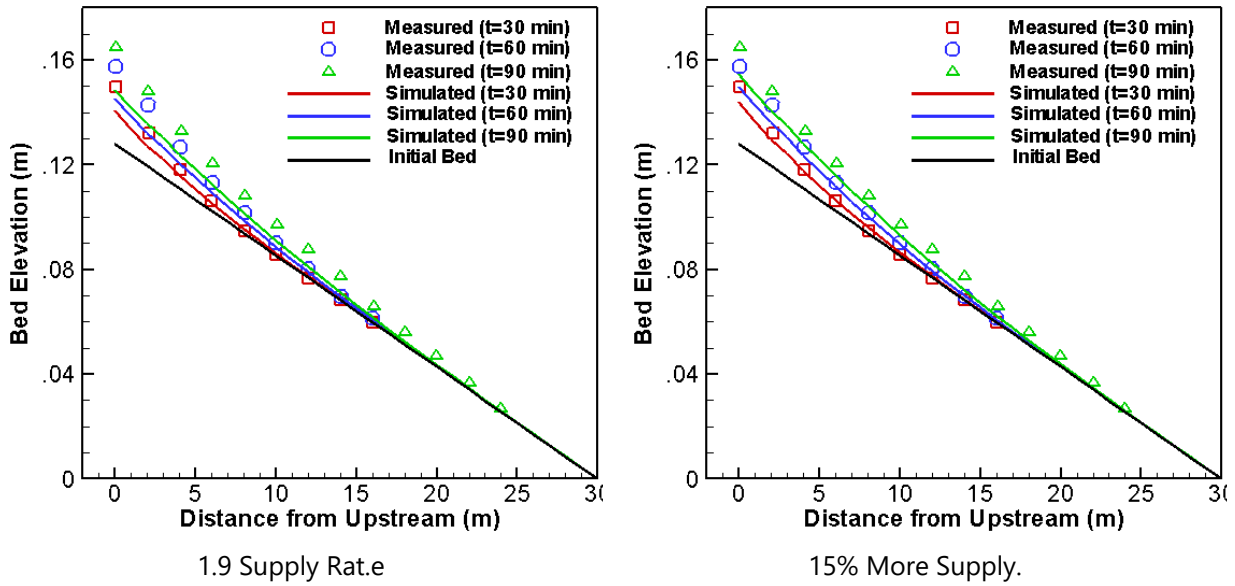


Figure A- 76. Results of Wu et al. (2000a) equation compared with flume data for Soni (1981) experiment.

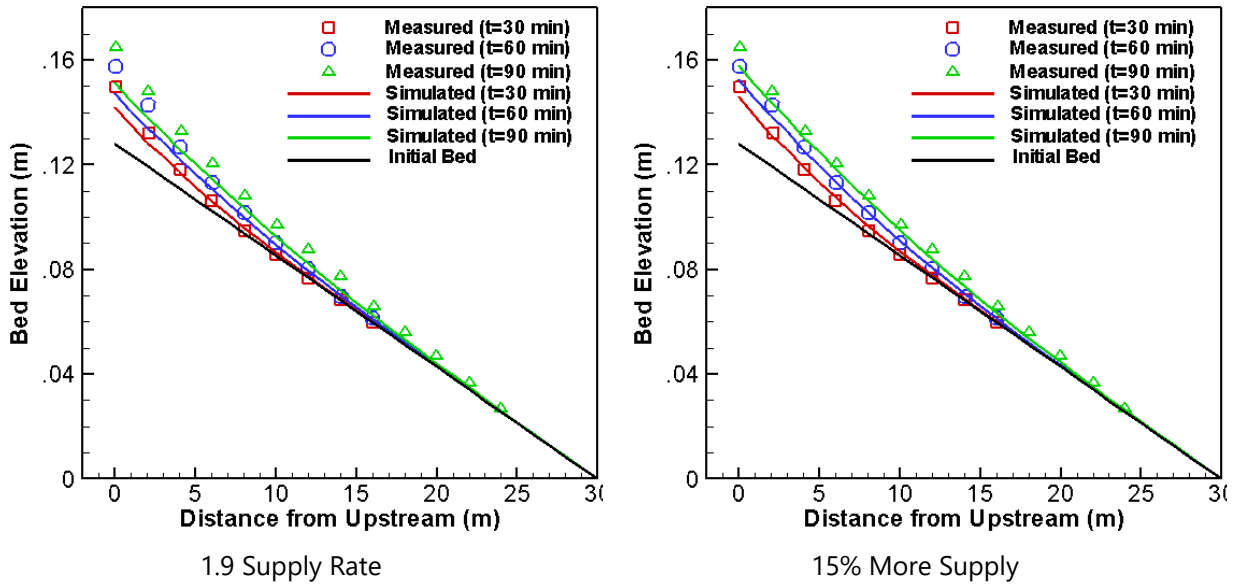


Figure A- 77. Results of Ackers-White (1973) equation compared with flume data for Soni (1981) experiment.

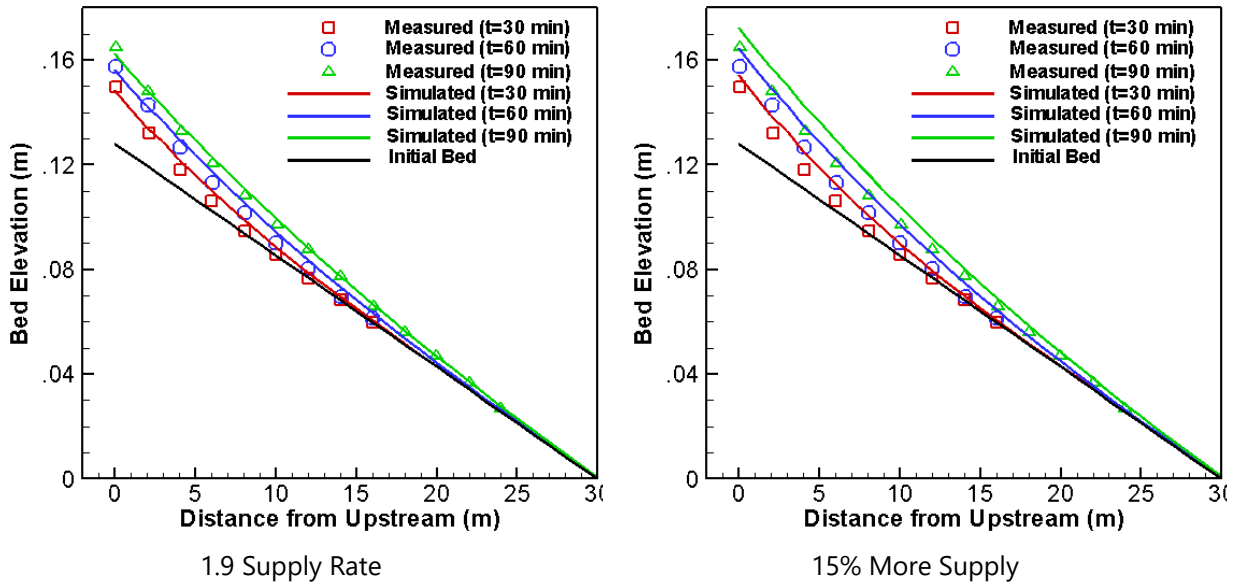


Figure A- 80. Results of Wilcock-Crowe (2003) equation compared with flume data for Soni (1981) experiment.

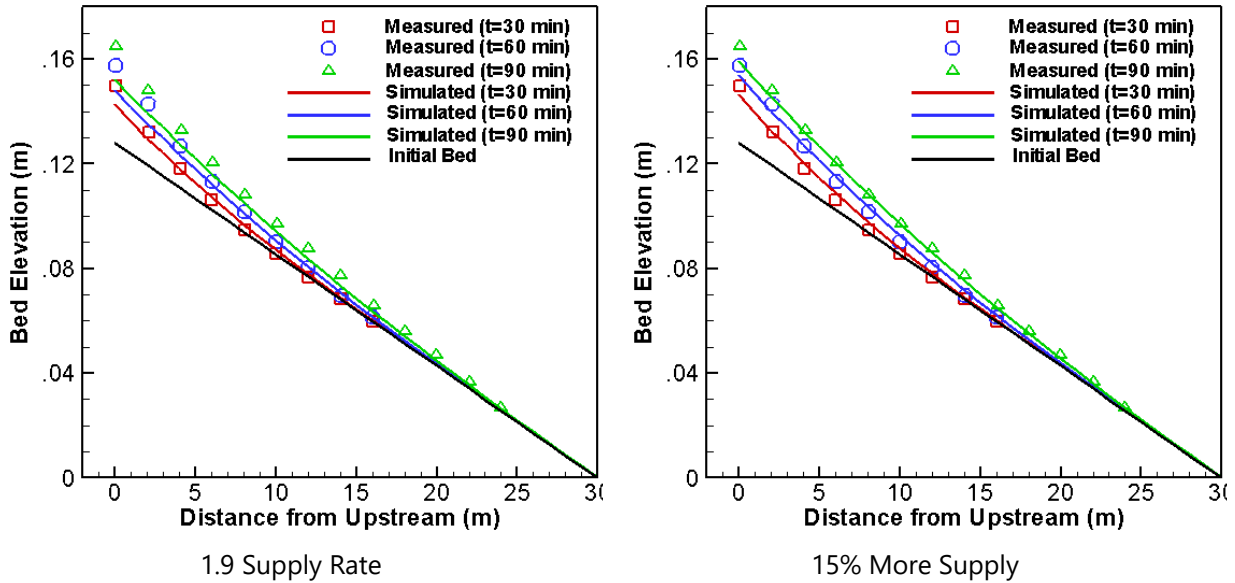


Figure A- 81. Results of Bagnold (1980) equation compared with flume data for Soni (1981) experiment.

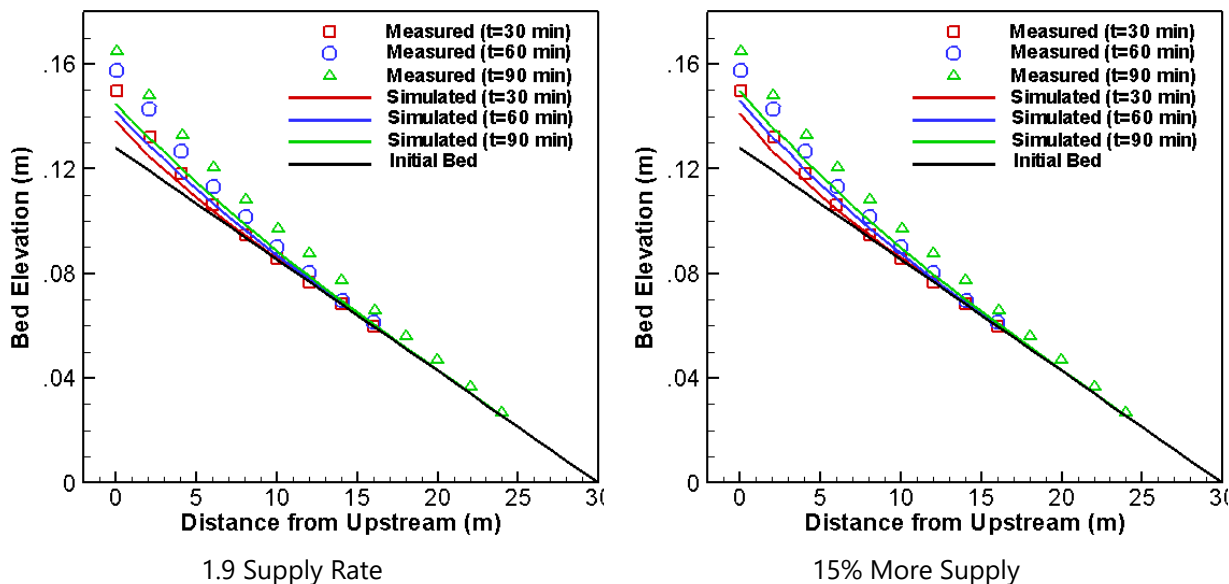


Figure A- 82. Results of van Rijn (1984a) equation compared with flume data for Soni (1981) experiment.

A.6.2. Degradation in a Straight Channel

Channel degradation and armoring occur in many situations such as downstream of a dam; they represent an important class of alluvial processes. In this section, the flume experiment of Ashida and Michiue (1971) is chosen to test the SRH-2D sediment capability. For a description of the Ashida and Michiue (1971) flume and the SRH 2D Mobile Bed verification study, see Section 7.2. Degradation in a Straight Channel in the main report. All the input parameters are discussed there.

For a mixed sand-gravel bed, Parker (1990) equation is usually recommended with a default model parameters of $\theta_c = 0.04$ and $\alpha = 0.65$. This equation is used first as a benchmark model.

The experimental data showed that degradation was initiated quickly and the scour depth increased fast for the first 100 minutes. Afterwards, degradation was slowed down and an armoring layer was formed. A comparison of the model results of Parker (1990) equation with flume data is shown in Figure A-11. The predicted gradation of the armored bed 10 meters from the downstream boundary is shown in Figure A-12. It is seen that the prediction of the degradation process is less satisfactory, while gradation of the armored bed is relatively good. In view of a better degradation prediction reported by Wu (2004), an effort is initiated to find out the cause. According to the discussion in Wu (2004) and a personal communication with Dr. Wu, the cause was attributed to the bedform change of the simulated case. It was reported that the bedform was changing from a flat bed to a fully developed bed for the flume case (Wu 2004). As a result, a time-dependent variation of the bed grain shear stress was implemented in the simulation of Wu (2004). In order to see the impact of a changing grain shear stress, the same functional form of grain shear stress change as that used by Wu (2004) is implemented into

SRH-2D. The same model is then executed again. The predicted degradation results with this change are shown in in Figure A-11. designated as ‘Predicted: Wu Grain Stress’ in dashed lines. It is seen that the procedure used by Wu (2004) improves the agreement between model predicted results and measured data for the first 100 minutes of degradation process. Since the grain shear stress changing procedure used is not general, it is not implemented as a feature in SRH-2D. We prefer to take the results in solid lines as the model prediction. The study, however, points to potential uncertainty in model results when bedform change occurs. With changing bed form, the numerical model with a constant form-correction factor may not predict the degradation timing accurately. Results of all other transport equations are shown from

Figure A- 83 to

Figure A- 93. Most equations cannot predict the degradation process well—except van Rijn equation, which provided the best agreement with the measured data without any special treatment of the changing bedform.

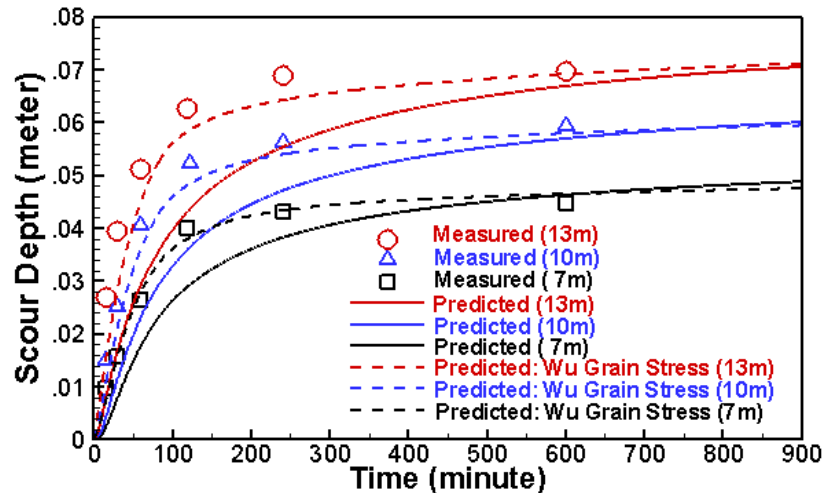


Figure A- 83. Predicted degradation process with Parker (1990) equation and a comparison with the measured data at three locations: 13 m (red), 10 m (blue), and 7 m (black) from the downstream boundary; “Wu Grain Stress” refers to results obtained with the modified grain shear stress calculation.

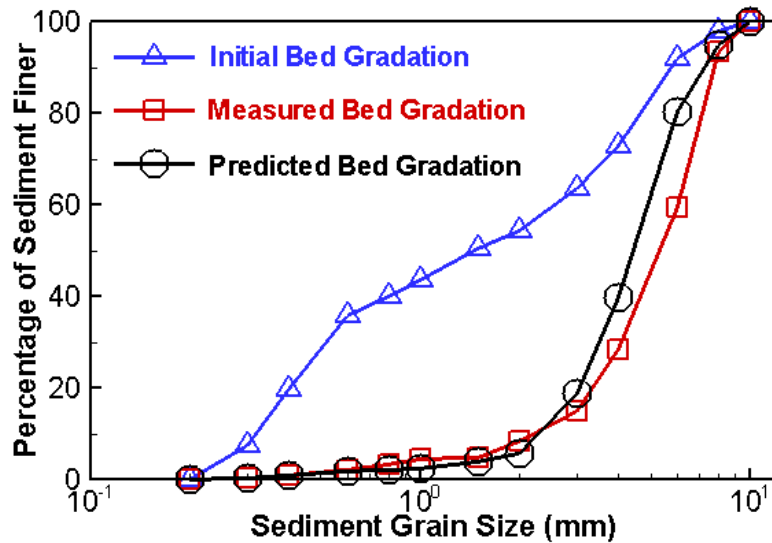


Figure A- 84. Comparison of predicted and measured armored bed gradation 10 m upstream from the exit with the Parker (1990) equation.

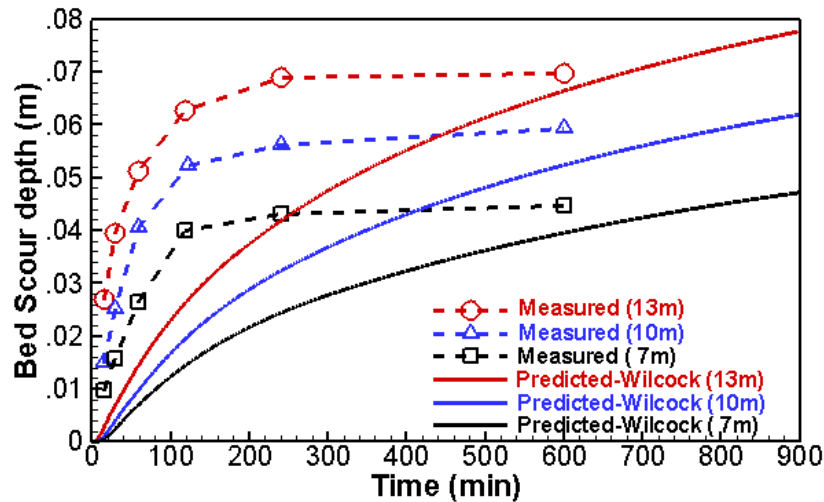


Figure A- 85. Predicted degradation process with Wilcock-Crowe (2003) equation and a comparison with the measured data at three locations: 13 m (red), 10 m (blue), and 7 m (black) from the downstream boundary.

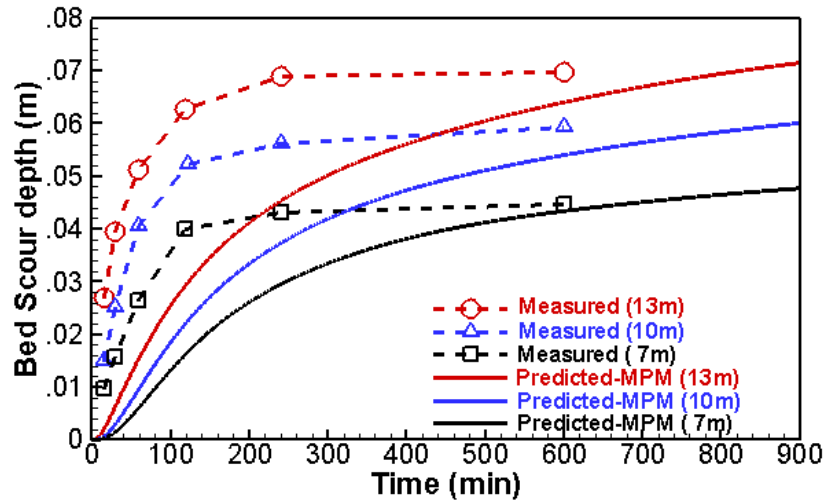


Figure A- 86. Predicted degradation process with Meyer-Peter-Muller (1948) equation and a comparison with the measured data at three locations: 13 m (red), 10 m (blue), and 7 m (black) from the downstream boundary.

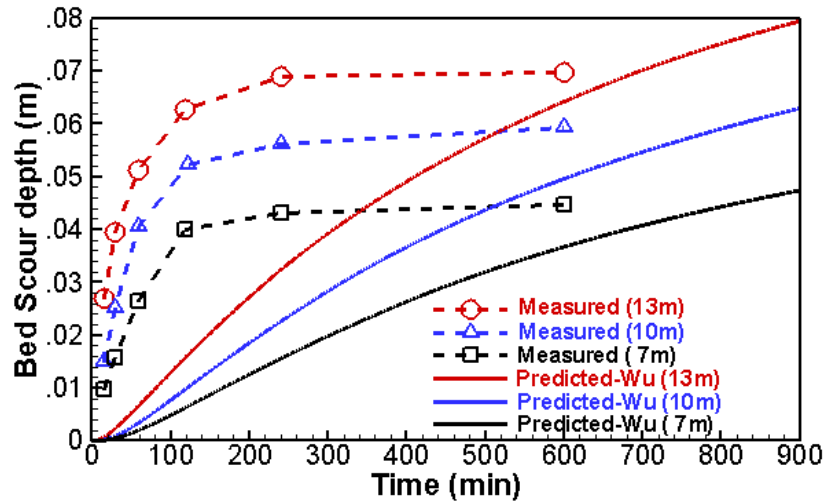


Figure A- 87. Predicted degradation process with Wu et al. (2000a) equation and a comparison with the measured data at three locations: 13 m (red), 10 m (blue), and 7 m (black) from the downstream boundary.

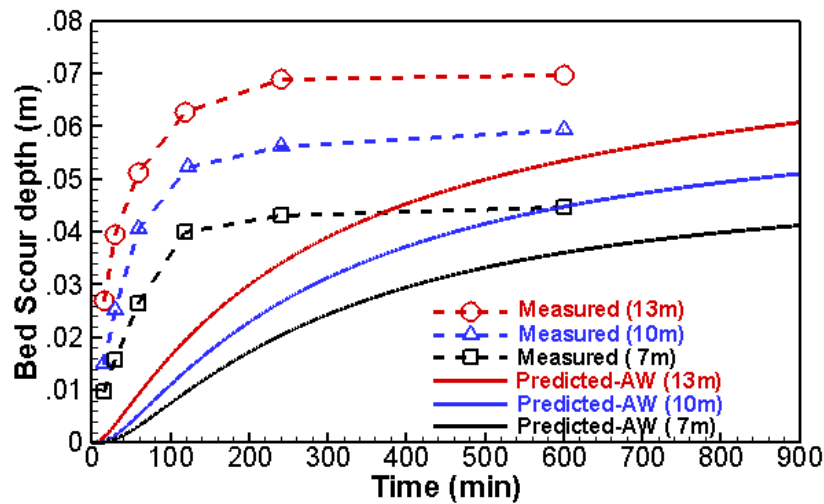


Figure A- 88. Predicted degradation process with Ackers-White (1973) equation and a comparison with the measured data at three locations: 13 m (red), 10 m (blue), and 7 m (black) from the downstream boundary.

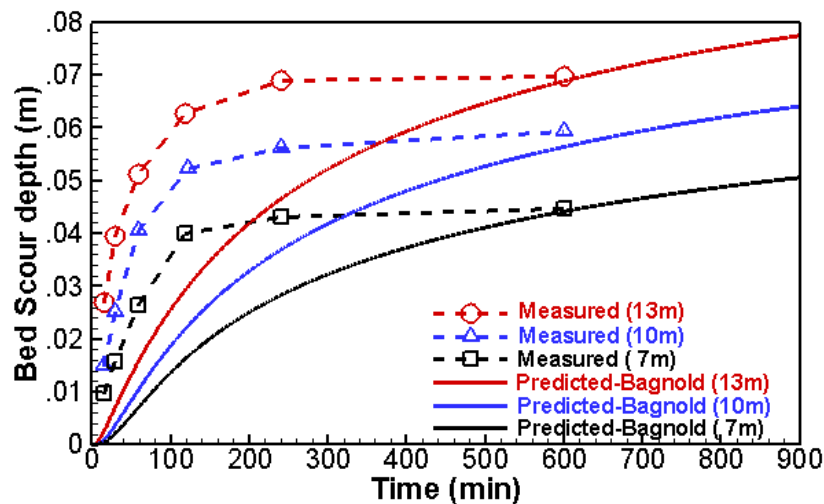


Figure A- 89. Predicted degradation process with Bagnold (1980) equation and a comparison with the measured data at three locations: 13m (red), 10m (blue), and 7m (black) from the downstream boundary.

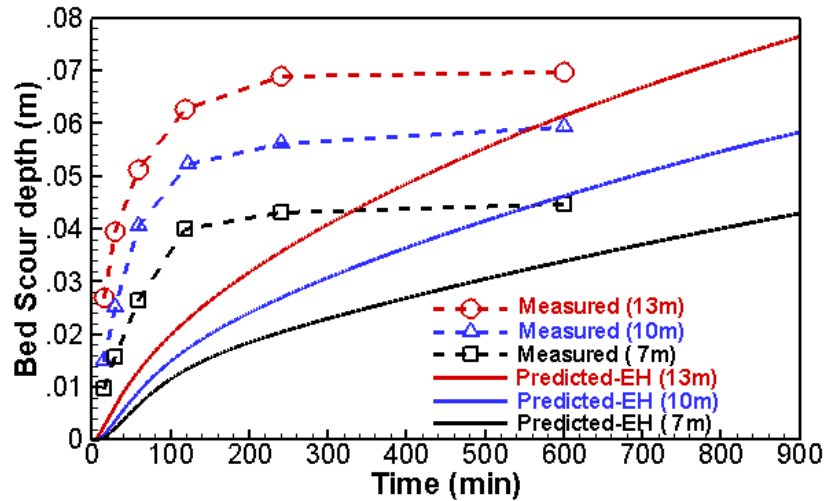


Figure A- 90. Predicted degradation process with Englund-Hansen (1973) equation and a comparison with the measured data at three locations: 13 m (red), 10 m (blue), and 7 m (black) from the downstream boundary.

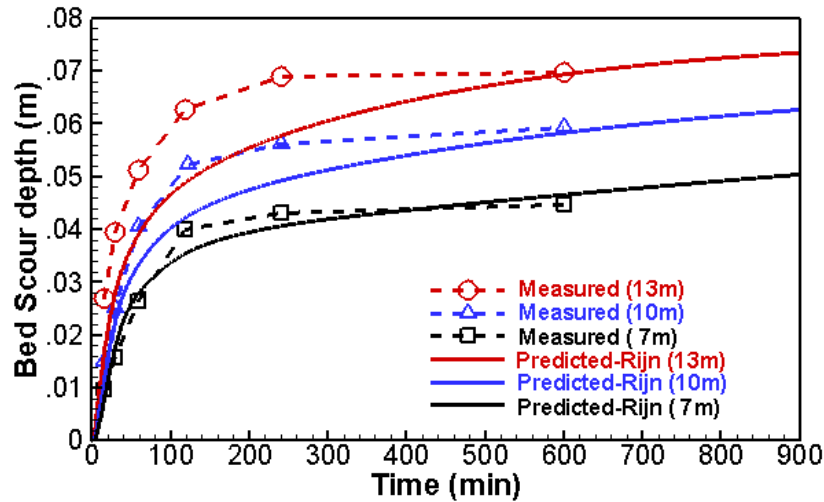


Figure A- 91. Predicted degradation process with van Rijn (1984a) equation and a comparison with the measured data at three locations: 13 m (red), 10 m (blue), and 7 m (black) from the downstream boundary.

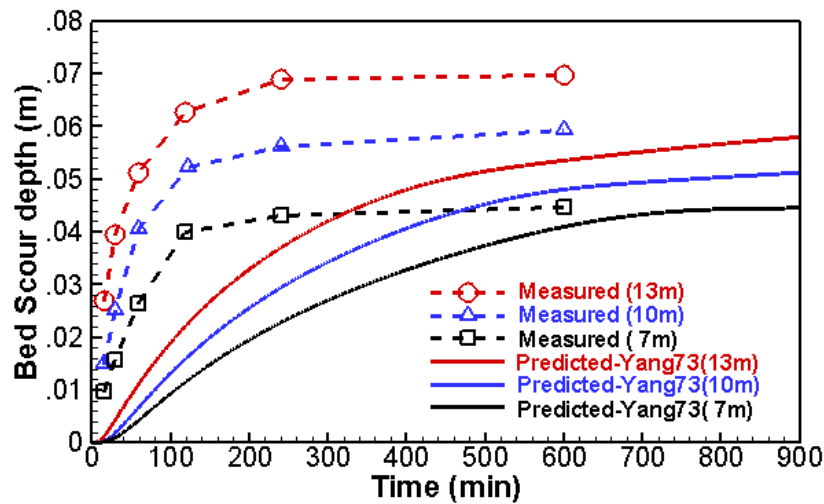


Figure A- 92. Predicted degradation process with Yang (1973/1984) equation and a comparison with the measured data at three locations: 13 m (red), 10 m (blue), and 7 m (black) from the downstream boundary.

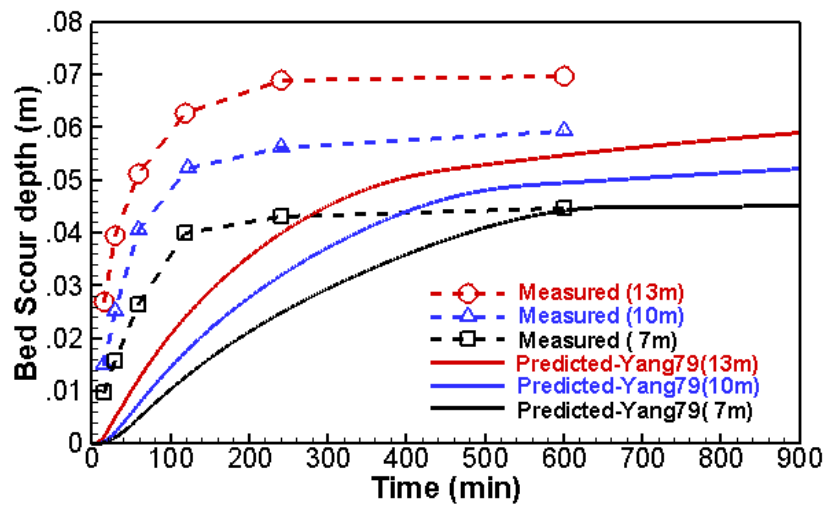


Figure A- 93. Predicted degradation process with Yang (1979/1984) equation and a comparison with the measured data at three locations: 13 m (red), 10 m (blue), and 7 m (black) from the downstream boundary.

A.7 Comparative Study with a Chosui River Reach

Sediment transport equation is one of the most important model parameters in many applications. In this section, selected sediment transport equations in SRH-2D are applied to the Chosui River reach along with bank erosion modeling to identify appropriate equations for the reach and shed light on the appropriate equations to use for typical rivers in Taiwan.

The study reach is the one from ZiQiang Bridge to XiBin Bridge. The solution domain, mesh, initial topography, and all input parameters are the same as the baseline calibration model with bank erosion. Details have been described in Chapter 8. The only change made for the current modeling study is to change the sediment transport capacity equation. The baseline model used the Engelund-Hansen (1972) equation; additional equations that are used for modeling include: Wu et al. (2000), Yang (1973), Yang (1979), Ackers-White (1973), van Rijn (1984a and b), and Bagnold (1980). All the selected equations are applicable to sandy rivers.

The predicted bed elevation changes from July 2004 to August 2007 with the above eight transport equations are plotted and compared in Figure A- 94 through **Figure A- 100**. Comparisons with the measured data in **Figure A- 101** lead to an assessment of the transport equations on their applicability to predict the morphology of the sandy bed of the Chosui River. The best equations, in the order of better agreements with the measured data, are: Wu (2000), Yang (1973 and 1979), Engelund-Hansen (1974), and van Rijn (1984a). The remaining two equations, Bagnold (1980), and Ackers-White (1973), predict poorly the channel morphology of the study reach.

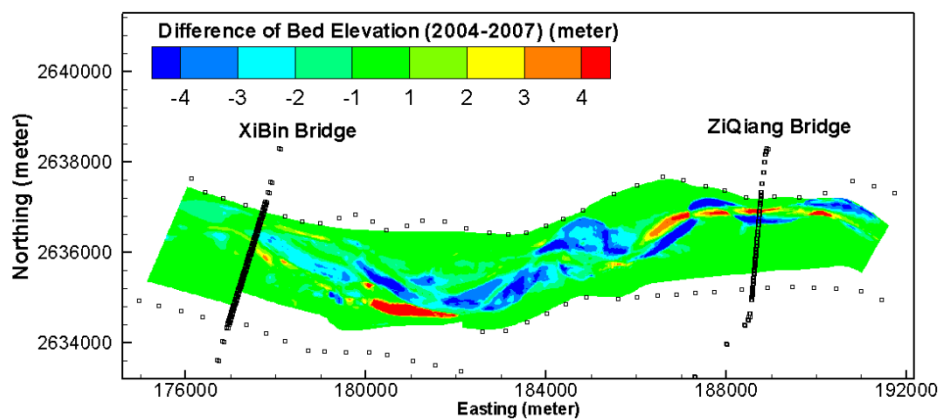


Figure A- 94. Predicted bed elevation change (m) from July 2004 to August 2007; Prediction is made with Engelund-Hansen equation.

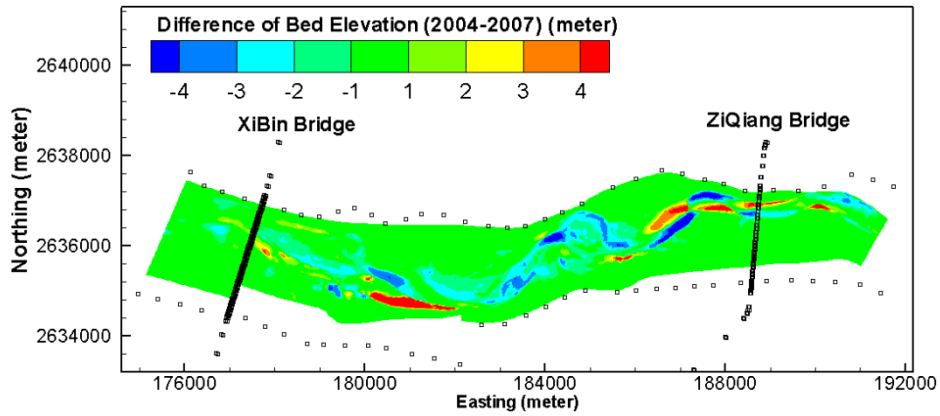


Figure A- 95. Predicted bed elevation change (meter) from July 2004 to August 2007; Prediction is made with Wu (2000) equation.

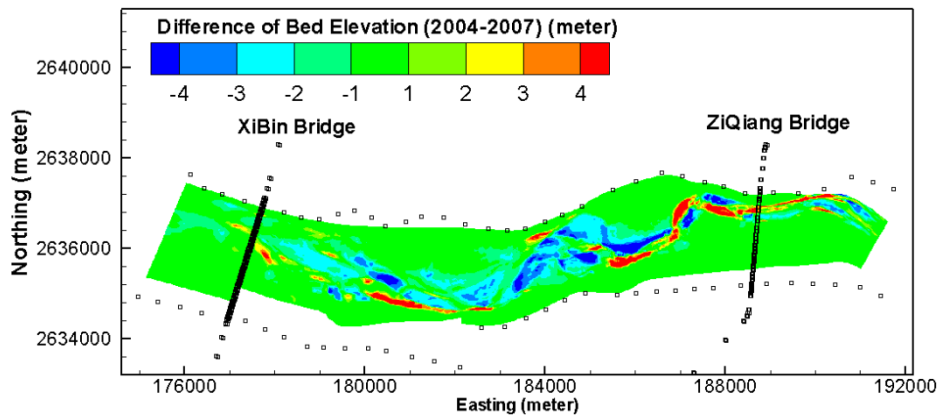


Figure A- 96. Predicted bed elevation change (m) from July 2004 to August 2007; Prediction is made with Yang (1973) equation.

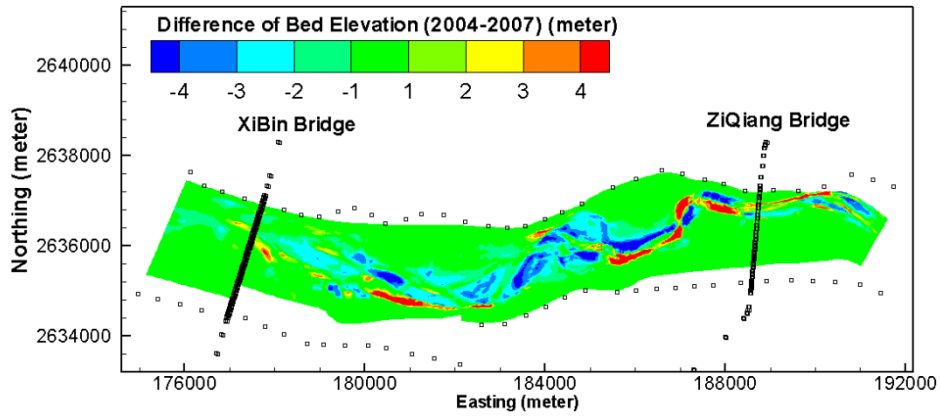


Figure A- 97. Predicted bed elevation change (m) from July 2004 to August 2007; Prediction is made with Yang (1979) equation.

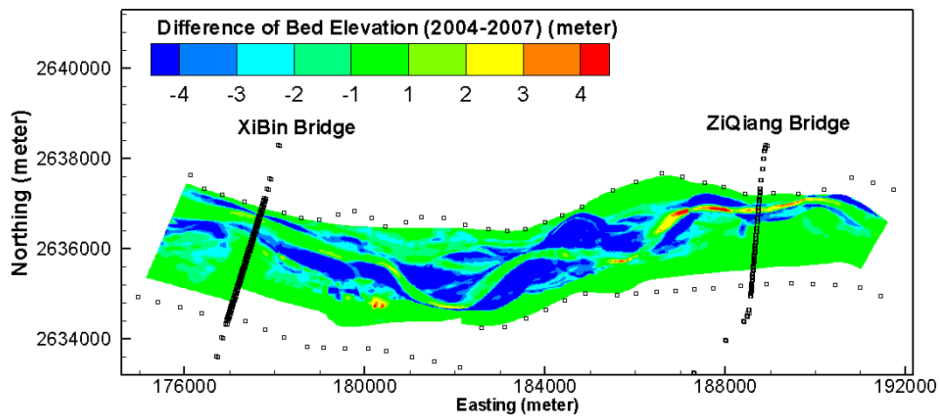


Figure A- 98. Predicted bed elevation change (m) from July 2004 to August 2007; Prediction is made with Ackers-White (1973) equation.

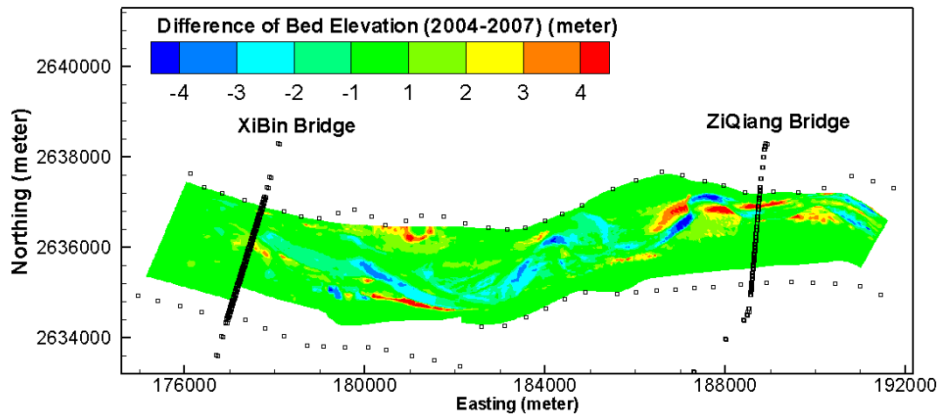


Figure A- 99. Predicted bed elevation change (m) from July 2004 to August 2007; Prediction is made with van Rijn (1984a) equation.

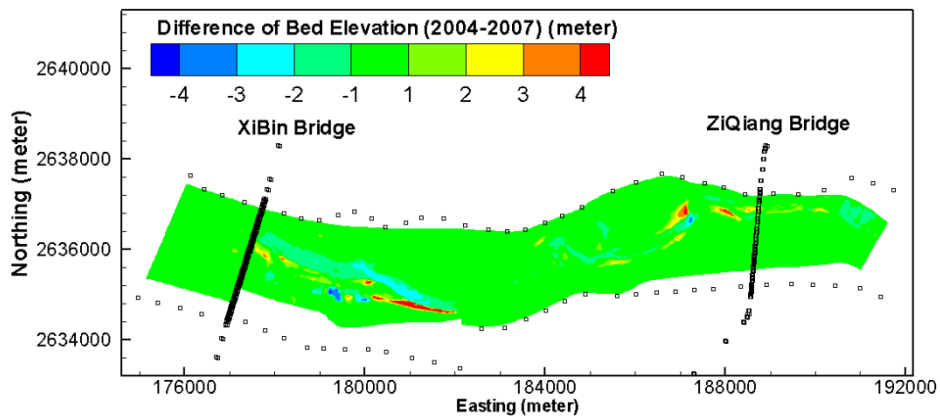


Figure A- 100. Predicted bed elevation change (m) from July 2004 to August 2007; Prediction is made with Bagnoldoint (1980) equation.

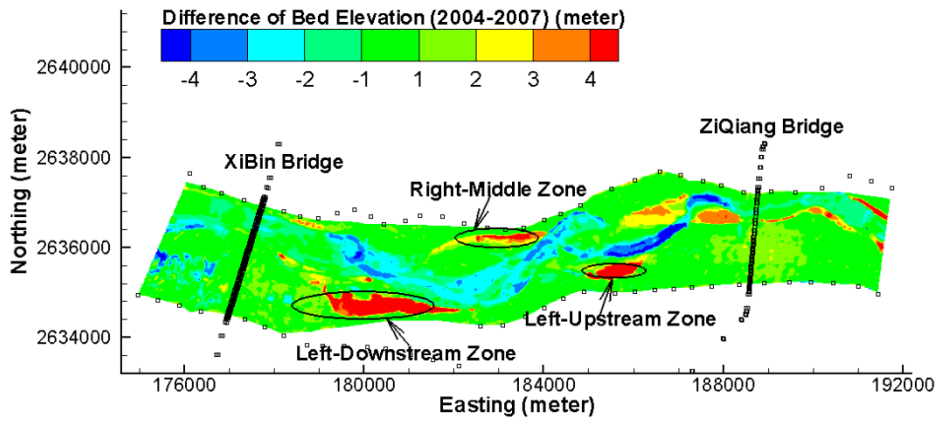


Figure A- 101. Measured bed elevation change (m) from July 2004 to August 2007.

References

- Albuquerque Area Office (AAO), (2007). Elephant Butte Reservoir Temporary Channel Maintenance Project - Biological Assessment, Bureau of Reclamation, Albuquerque Area Office.
- Ackers, P. and W.R. White, (1973). Sediment transport: new approach and analysis. *Journal of the Hydraulic Division, ASCE*, 99(11), Proceeding paper 10167, 2041-2060.
- Andrews, E.D., (2000). Bed material transport in the Virgin River, Utah. *Water Resources Research*, 36: 585-596.
- Armanini, A. and G. di Silvio, (1988). A one-dimensional model for the transport of a sediment mixture in non-equilibrium conditions, *J. Hydraulic Res.*, 26(3), 275-292.
- Ashida, K. and M. Michiue, (1971). An investigation of river bed degradation downstream of a dam, *Proc.*, 14th IAHR Congress, Paris, 3, 247-256.
- Bagnold, R.A., (1980). An empirical correlation of bedload transport rates in flumes and natural rivers. *Royal Society of London Proceedings*, A372:453-473.
- Bauer, T.R., (2007). 2007 Rio Grande Profile Data Collection. Bureau of Reclamation, Technical Service Center, Sedimentation and River Hydraulics Group, Denver, Colorado 80225.
- Baxter, R.M., (1977). Environmental Effects of Dams and Impoundments. *Annual Review of Ecology and Systematics*, by R. F. Johnston. Palo Alto, *Annual Reviews Inc.* 8: 255-283.
- Bhallamudi, S.M. and M.H. Chaudhry, (1991). Numerical modeling of aggradation and degradation in alluvial channels. *J. Hydraulic Engineering*, 117, 1145-1164.
- Blondeaux, P. and G. Seminara, (1985). A Unified Bar-Bend Theory of River Meanders, *J. Fluid Mech.*, 157, 449-470.
- Bountry, J.A., Y.G. Lai, and T.J. Randle, (2011). Sediment Impacts from the Removal of Savage Rapids Dam. 31st Annual USSD Conference, San Diego, California, April 11-15.
- Bowen, M.W. (2004). Consequences of Reservoir Drainage on Downstream Water Chemistry, Suspended Sediment, and Nutrients, Southwest Missouri. M.S. Thesis, Southwest Missouri State University.
- Briaud, J.L., H.C. Chen, Y. Li, P. Nurtjahyo, and J. Wang, (2004). Pier and contraction scour in cohesive soils. NCHRP Report 516, National Cooperative Highway Research Program,

Transportation Research Board, Washington, D.C.

- Brush, L.M. and M.G. Wolman, (1960). Knickpoint behavior in noncohesive material: A laboratory study. *Bulletin of the Geological Society of America*, 71, 59-73.
- Bullard, K.L. and W.L. Lane, (1993). Middle Rio Grande Peak Flow Frequency Study, Reclamation, Technical Service Center, Flood Hydrology Group, Denver, Colorado.
- Buffington, J.M. and D.R. Montgomery, (1997). A systematic analysis of eight decades of incipient motion studies, with special reference to gravel-bedded rivers. *Water Resources Research*, 33: 1993-2029.
- Callander, R.A., (1968). Instability and River Meanders. Ph.D. Thesis, University of Auckland.
- Cebeci, T., and P. Bradshaw, (1977). *Momentum transfer in boundary layers*. Hemisphere, Washington, D.C.
- Chien, N. and Z.H. Wan, (1983). Mechanics of sediment movement. Science Publications, Beijing (in Chinese).
- Childers, D., D.L. Kresch, S.A. Gustafson, T.J. Randle, J.T. Melena, and B. Cluer, (2000). Hydrologic Data Collected During the 1994 Lake Mills Drawdown Experiment, Elwha River, Washington. 99-4215 U.S. Geological Survey, Tacoma, Washington Water-Resources Investigations Report.
- Collins, K.L., and R. Ferrari, (2000). Elephant Butte Reservoir 1999 Reservoir Survey. Reclamation, Technical Service Center, Sedimentation and River Hydraulics Group, Denver, Colorado.
- Collins, K.L., (2006). 2006 Middle Rio Grande Maintenance Modeling: San Antonio to Elephant Butte Dam. Reclamation, Technical Service Center, Sedimentation and River Hydraulics Group, Denver, Colorado.
- Colombini M., G. Seminara, and M. Tubino, (1987). Finite-amplitude alternate bars. *J. Fluid Mech.* 181: 213-232.
- Colombini M. and M. Tubino M, (1991). Finite-amplitude free bars: a fully non-linear spectral solution. in *Sand Transport in Rivers, Estuaries and the Sea*, Soulsby R, Bettess R (eds). Balkema AA, Rotterdam: 163-169.
- Cooke, G. D., E.B. Welch, S. A. Peterson, and P.R. Newroth, (1993). Restoration and Management of Lakes and Reservoirs, 2nd Ed. Boca Raton, Florida, Lewis Publishers.
- Defina, A., (2003). Numerical experiments on bar growth. *Water Resources Research*, 39(4): ESG2-1. DOI: 10.1029/2002WR001455.

- Derrick, D.L. and G.E. Freeman, (2004). Stream Investigation, Stabilization, and Restoration Workshop, American Society of Civil Engineers.
- Doyle, M.W., E.H. Stanley, and J.M. Harbor, (2002). Channel Adjustments Following Two Dam Removals in Wisconsin. *Water Resources Research*, 39(1): 1011-1036.
- Engelund, F. and E. Hansen, (1972). *A Monograph on Sediment Transport in Alluvial Streams*, Teknisk Forlag, Technical Press, Copenhagen, Denmark.
- Gaeuman, D., (2014). High-flow gravel injection for constructing designed in-channel features. *River Research and Applications*. 30(6):685-706, doi:10.1002/rra.2662.
- Gaeuman, D., L. Sklar, and Y.G. Lai, (2014). Flume experiments to constrain bedload adaptation length. *J. Hydrol. Eng.*, 20, 06014007.
- García, M., (2008). Sediment Transport and Morphodynamics, Ch 2 of Sedimentation Engineering, ASCE Manual and Reports on Engineering Practice No. 110. Edited by M. Garcia.
- Gathard Engineering Consulting (GEC), (2006). Klamath River Dam and Sediment Investigation, Technical Report, 40031st Ave. NW, Seattle, Washington, 96 pages + Appendices A to K, November.
- Greimann, B. P., D. Mooney, D. Varyu, Y.G. Lai, T. Randle, J.A. Bountry, M.K. Tansey, C. Young, and J. Huang, (2007). Model calibration for the simulation of physical river processes and riparian habitat on the Sacramento River, California. Project Report. Reclamation, Technical Service Center, Sedimentation and River Hydraulics Group, Denver, Colorado.
- Greimann, B.P., Y.G., Lai, and J.C. Huang, (2008). Two-dimensional total sediment load model equations. *J. Hydraulic Engineering, ASCE*. 134(8): 1142-1146.
- Han, Q.W., (1980). A study on the non-equilibrium transportation of suspended load. In Proceedings of the 1st International Symposium on River Sedimentation (IRTCES) Beijing, China, 24-29.
- Han, Q.W. and M. He, (1990). A mathematical model for reservoir sedimentation and fluvial processes. *Int. J. Sediment Res.* 5: 43-84.
- Hilldale, R., (2001). Trip Report – Middle Rio Grande Drilling Operations,. Technical Report, Technical Service Center, Bureau of Reclamation.
- Holly, F.M. and J.L. Rahuel, (1990). New Numerical/Physical Framework for Mobile-Bed Modeling, Part 1: Numerical and Physical Principles, *J. Hydr. Res.*, 28(4): 401-416.

- Huang, J.V., (2011). 2010 Sediment Modeling of the Middle Rio Grande with and without the Temporary Channel: San Antonio to Elephant Butte Reservoir. Technical Report. Reclamation, Technical Service Center, Sedimentation and River Hydraulics Group, Denver, Colorado.
- Ikeda S., G., Parker, and K. Sawai, (1981). Bend theory of river meanders, Part 1 – linear development. *J. Fluid Mech.* **112**: 363-377.
- Jacoby, J.M., E.B. Welch, and J.P. Michaud, (1982). Control of Internal Phosphorus Loading in a Shallow Lake by Drawdown and Alum. Lake Restoration, Protection, and Management, Vancouver, British Columbia, Canada, United States Environmental Protection Agency.
- Jaeggi, M.N.R., (1984). Formation and effects of alternate bars. *J. Hydraulic Engineering, ASCE.* **110(2)**: 142-156.
- Komar P.D., (1989). Flow competence of the hydraulic parameters of floods. *Floods: Hydrological, Sedimentological and Geomorphological Implications*. K.Beven and Carling (eds.), John Wiley and Sons, UK, 107-134.
- Krone, R.B., (1962). Flumes studies of the transport of sediment in estuarial shoaling processes, Technical Report, Hydraulic Engineering Laboratory, University of California, Berkeley, California.
- Lai, Y.G., (1997). An unstructured grid method for a pressure-based flow and heat transfer solver, *Numerical Heat Transfer, Part B*, 32, 267-281.
- Lai, Y.G., (2000). Unstructured grid arbitrarily shaped element method for fluid flow simulation, *AIAA Journal*, 38(12), 2246-2252.
- Lai, Y.G., (2006). Theory and User Manual for SRH-W Version 1.1. Reclamation, Technical Service Center, Sedimentation and River Hydraulics Group, Denver, Colorado.
- Lai Y.G., (2008). SRH-2D version 2: Theory and User's Manual. Reclamation, Reclamation, Technical Service Center, Sedimentation and River Hydraulics Group, Denver, Colorado. <https://www.usbr.gov/tsc/techreferences/computer%20software/models/srh2d/index.html>.
- Lai, Y.G., (2009). Sediment Plug Prediction on the Rio Grande with SRH-2D Model, Technical Report No. SRH-2009-41. Reclamation, Technical Service Center, Sedimentation and River Hydraulics Group, Denver, Colorado.
- Lai, Y.G., (2010). Two-Dimensional Depth-Averaged Flow Modeling with an Unstructured Hybrid Mesh. *J. Hydraul. Eng.* 136: 12–23.
- Lai, Y.G., (2011). Prediction of Channel Morphology Upstream of Elephant Butte Reservoir on the Middle Rio Grande. Technical Report No. SRH-2011-04. Reclamation, Technical Service Center, Sedimentation and River Hydraulics Group, Denver, Colorado.

- Lai, Y.G., (2014). Advances in geofluvial modeling: Methodologies and applications. In *Advances in Water Resources Engineering, Handbook of Environmental Engineering*; Yang, C.T., Wang, L.K., Eds.; Humana Press: New York, NY, USA; Springer Science and Business Media: Cham, Switzerland; Volume 14.
- Lai, Y.G., (2017). Modeling Stream Bank Erosion: Performance for Practical Streams and Future Needs. *Water*, 9, 950; doi:10.3390/w9120950.
- Lai, Y.G. (2020). A Two-Dimensional Depth-Averaged Sediment Transport Mobile-Bed Model with Polygonal Meshes. *Water* 2020, 12(4), 1032; <https://doi.org/10.3390/w12041032>
- Lai, Y. G. and T.R. Bauer, (2007). *Erosion analysis upstream of the San Acacia Diversion Dam on the Rio Grande River*, Project Report, Technical Service Center, Bureau of Reclamation, Denver, Colorado.
- Lai Y.G., and T. Randle, (2007). Bed evolution and bank erosion analysis of the Palo Verde Dam on the lower Colorado River. Technical Report, Sedimentation and River Hydraulics Group, Technical Service Center, Bureau of Reclamation, Denver, Colorado.
- Lai, Y.G.; R. Thomas, Y. Ozeren, A. Simon, B.P. Greimann, and K. Wu, (2015). Modeling of multi-layer cohesive bank erosion with a coupled bank stability and mobile-bed model. *Geomorphology*, 243, 116–129.
- Lai, Y.G., L.J. Weber, and V.C. Patel, (2003). Non-hydrostatic three-dimensional method for hydraulic flow simulation - Part I: formulation and verification, *ASCE J. Hydraulic Engineering*, 129(3), 196-205.
- Leopold, L.B. (1996). *A view of the river*, Harvard University Press, Cambridge, Massachusetts.
- Leopold, L.B., M.G. Wolman, and J.P. Miller, (1964). *Fluvial Processes in Geomorphology*, Freeman and Company, San Francisco.
- Lewin J. (1976). Initiation of bedforms and meanders in coarse-grained sediment. *Bull. Geol. Soc. of America*. **87(2)**: 281-285.
- Ligon, F.K., W.E. Dietrich, and W J. Trush. (1995). Downstream Ecological Effects of Dams: A Geomorphic Perspective. *Bioscience* 45(3): 183-192.
- López, R. and J. Barragán, (2008). Equivalent Roughness of Gravel-Bed Rivers, *J. Hydraul. Eng.*,134(6): 847-851.
- Major, J., J. O'Connor, G. Grant, K. Spicer, H. Bragg, A. Rhode, D. Tanner, C. Anderson, and J. Wallick., (2008). Initial Fluvial Response to the Removal of Oregon's Marmot Dam, *EOS – Transactions of the American Geophysical Union*, 89(27), 24.

- Marek, M., and A. Dittrich, (2004). 3D numerical calculations of the flow in an open-channel consisting of an expansion and contraction. Proceedings of the 6th International Conference on Hydro-Science and Engineering, Vol. VI, Brisbane, Australia.
- McAnally, W.H. and A.J. Mehta, (2001). Collisional aggregation of fine estuarial sediment, Coastal and Estuarine Fine Sediment Processes, Proceedings in Marine Science 3.
- Mehta, A.J. and E. Partheniades, (1973). Depositional behavior of cohesive sediments, Technical Report No. 16, Coastal and Oceanographic Engineering Laboratory, University of Florida, Gainesville, Florida.
- Mehta, A.J., E.J. Hayter, W.R. Parker, R.B. Krone, and A.M. Teeter, (1989). Cohesive sediment transport. I: Process description," *Journal of Hydraulic Engineering*, 115(8), 1076-1093.
- Meyer-Peter, E., and R.Muller (1948). Formulas for bed-load transport. *Proc., 2nd Meeting, IAHR, Stockholm, Sweden*, 39-64.
- Morris, G.L., and Fan, J. (1998). Reservoir Sedimentation Handbook. McGraw-Hill, New York. P.15.18.
- Mosselman, E., (1998). Morphological modeling of rivers with erodible banks. *Hydrol. Processes* **12**: 1357-1370.
- Nelson, J.M. and J.D. Smith, (1989). Flow in meandering channels with natural topography. in *River Meandering*. Ikeka S, Parker G (eds), *AGU Water Resources Monograph* **12**: 69-102. Washington D.C.
- Parker, G., (1976). On the cause and characteristic scales of meandering and braiding in rivers. *J. Fluid Mech.* **76**: 457-480.
- Parker, G., (1990). Surface-based bedload transport relation for gravel rivers, *J. Hydraulic Research*, 28: 417-428.
- Partheniades, E., (1965). Erosion and deposition of cohesive soils, *Journal of the Hydraulics Division, ASCE*, Vol. 91(1), 105-139.
- Pemberton, E.L. and J.M. Lara, (1984). Computing Degradation and Local Scour, Technical Guideline for Bureau of Reclamation. Reclamation, Denver Engineering and Research Center, Denver, Colorado, 48 pp.
- Philips, B.C. and A.J. Sutherland, (1989) Spatial lag effect in bed load sediment transport, *J. Hydraulic Res.*, 27(1), 115-133.
- Phillip Williams and Associates, Ltd (PWA), (2009). A River Once More: Restoring the Klamath River Following Removal of the Iron Gate, Copco, and J. C. Boyle Dams, California State Coastal Conservancy and California Department of Fish and Game.

- Pizzuto, J. (2002). Effects of Dam Removal on River Form and Process. *Bioscience* 52(8): 683-691.
- Pohl, M.M. (2002). Bringing Down Our Dams: Trends in American Dam Removal Rationales. *Journal of the American Water Resources Association* 38(6): 1511-1519.
- Rahuel, J.L., F.M., Holly, J.P., Chollet, P.J., Belleudy, and G. Yang, (1989). Modeling of riverbed evolution for bedload sediment mixtures. *J. Hydraulic Engineering, ASCE*, 115(11), 1521-1542.
- Reclamation, (2002). Sediment Transport Modeling of the Rio Grande and Temporary Channel with Environmental Features from San Marcial railroad to Elephant Butte Reservoir. Reclamation, Technical Service Center, Sedimentation and River Hydraulics Group, Denver, Colorado.
- Reclamation, (2011). Hydrology, Hydraulics, and Sediment Transport Studies for the Secretary's Determination on Klamath River Dam Removal and Basin Restoration, Technical Report No. SRH-2011-02. Prepared for Mid-Pacific Region, Reclamation, Technical Service Center, Denver, Colorado.
- Rodi, W., (1993). Turbulence Models and Their Application in Hydraulics, 3rd ed.; IAHR Monograph: Rotterdam, The Netherlands.
- Seminara G. and M. Tubino, (1989). Alternate bars and meandering: free, forced and mixed interactions. in *River Meandering*.
- Shields, F.D. Jr., A. Simon, and L.J. Steffen, (2000). Reservoir Effects on Downstream River Channel Migration. *Environmental Conservation* 27(1): 54-66.
- Soni, J.P., (1981). Laboratory study of aggradation in alluvial channels. *J. Hydrology*, 49, 87-106.
- Stillwater Sciences, (2008). Klamath River dam removal study: sediment transport DREAM-1 simulation. Technical Report. Prepared for California Coastal Conservancy, 1330 Broadway, 13th Floor, Oakland, California, 94612, 73 pages, October 2008.
- Stillwater Sciences, (2009a). Dam Removal and Klamath River Water Quality: A Synthesis of the Current Conceptual Understanding and an Assessment of Data Gaps. Technical report. Prepared for State Coastal Conservancy, 1330 Broadway, 13th Floor, Oakland, California, 94612, 86 pages, January 2009.
- Stillwater Sciences, (2009b). Effects of sediment release following dam removal on the aquatic biota of the Klamath River. Technical Report. Prepared by Stillwater Sciences, Arcata, California for State Coastal Conservancy, Oakland, California. January 2009. 185 pp.
- Struiksma, N., (1983). Results of movable bed experiments in the DHL curved flume. Report on Experimental Investigation, TWO Rep. No. R657-XVIII/M1771, Delft Hydraulics

Laboratory, Delft, The Netherlands.

Struiksmas, N., (1985). Prediction of 2-D bed topography in rivers, deformation in curved alluvial channels. *J. Hydraulic Engineering, ASCE*. 111(HY8): 1169-1182.

Struiksmas, N. and A. Crosato, (1989). Analysis of a 2D bed topography model for rivers, in *River Meandering*, S. Ikeka and G. Parker (eds), *AGU Water Resources Monograph 12*, 153-180.

Struiksmas, N., K.W. Olsen, C. Flokstra, and H.J. De Vriend, (1985). Bed Deformation in Curved Alluvial Channels, *J. Hydraul. Res.*, 23(1), 57-79.

Talmon, A.M., M.C.L.M. Van Mierlo, and N. Struiksmas, (1995). Laboratory measurements of the direction of sediment transport on transverse alluvial-bed slopes, *J. Hydraul. Res.*, 33, 495-517.

Tetra Tech, Inc., (2008). Sediment Transport Analysis Total Load Report. SO-1470.5 and EB-10 Lines, Tetra Tech Project No. T22541. Reclamation, Albuquerque Area Office, Albuquerque, New Mexico, USA. June 2008.

Thuc, T., (1991). Two-dimensional morphological computations near hydraulic structures, Dissertation, Asian Inst. Of Technology, Bangkok, Thailand.

U.S. Environmental Protection Agency (EPA), (1977). Lake Drawdown as a Method of Improving Water Quality. EPA 600/3-77-005 Ecological Research Series. EPA, Corvallis, Oregon.

U.S. Interagency Committee on Water Resources, Subcommittee on Sedimentation. (1957). *Some fundamentals of particle size analysis*, Report No. 12.

van Rijn, L. C. (1984a). Sediment Transport, Part I : bed load transport. *Journal of Hydraulic Engineering, ASCE*, 110(10), 1431–1456.

van Rijn, L. C. (1984b). Sediment Transport, Part II : suspended load transport. *Journal of Hydraulic Engineering, ASCE*, 110(11), 1613–1641.

van Rijn, L.C. (1984c). Sediment transport, Part III: Bed forms and alluvial roughness. *J. Hydraulic Engineering, ASCE*, 110(12), 1733-1754.

van Rijn, L.C., (1993). Principles of sediment transport in rivers, estuaries, and coastal seas, Aqua Publications, Amsterdam, The Netherlands.

Vanoni, V.A., (2006). Sedimentation Engineering: ASCE Manual and Reports on Engineering Practice No. 54. Reston, Virginia, American Society of Civil Engineers, 418 p.

- Vasquez, J.A. and Millar, R.G. (2005). Two-dimensional morphological simulation in transcritical flow. *River, Coastal and Estuarine Morphodynamics: RCEM 2005*, Parker & Garcia (eds), Talor & Francis Group, London, ISBN 0415392705.
- Weise, S., (2002). Verifikation eines zweidimensionalen Feststofftransportmodells anhand von hydraulischen Versuchen. Diplomarbeit. Fachhochschule für Technik, Wirtschaft und Kultur, Leipzig (in German).
- Wilcock, P.R. and J.C. Crowe, (2003). Surface-Based Transport Model for Mixed-Size Sediment. *Journal of Hydraulic Engineering*, 129: 120-128.
- Wong, M. and G. Parker, (2006). Reanalysis and correction of bed-load relation of Meyer-Peter and Muller using their own database. *J Hydraulic Engineering, ASCE*, 132(11), 1159-1168.
- Wu, W., (2004). Depth-averaged two-dimensional numerical modeling of unsteady flow and nonuniform sediment transport in open channels, *J. Hydraulic Engineering*, 130(10), 1013-1024.
- Wu, W., and S.S.Y. Wang, (1999). Movable bed roughness in Alluvial rivers. *H Hydraulic Engineering, ASCE*, 125(12), 1309-1312.
- Wu, W., S.S.Y. Wang, and Y. Jia, (2000a). Nonuniform sediment transport in alluvial rivers. *Journal of Hydraulic Research*, 38(6), 427-434.
- Wu, W., Rodi, W., and T. Wenka, (2000b). 3D numerical modeling of flow and sediment transport in open channels. *J. Hydraulic Engineering, ASCE*, 126(1), 4-15.
- Yang, C.T., (1973). Incipient motion and sediment transport. *Journal of the Hydraulics Division, ASCE*, 99(10), Proceeding Paper 10067, 1679-1704.
- Yang, C.T., (1979). Unit Stream Power Equations for Total Load. *Journal of Hydrology*, vol.40, pp.123-138.
- Yang, C.T., (1984). Unit Stream Power Equation for Gravel, *J. Hydraul. Engrg., ASCE*, 110(12), pp.1783-1798.
- Yang, C.T. and F.J.M. Simoes, (1998). Simulation and prediction of river morphological changes using GSTARS 2.0. 3rd International Conference on Hydro-Science and Engineering, Cottbus/Berlin, Germany, Aug. 31-Sep. 3.
- Yanenko, N.N., (1971). *The method of fractional steps*. Springer, New York, New York.